



# Relationship between the adhesive properties and the rheological behavior of fresh mortars

Van-Tien Phan

## ► To cite this version:

Van-Tien Phan. Relationship between the adhesive properties and the rheological behavior of fresh mortars. Other. École normale supérieure de Cachan - ENS Cachan, 2012. English. NNT : 2011DENS00YY . tel-00802664

**HAL Id: tel-00802664**

**<https://theses.hal.science/tel-00802664>**

Submitted on 20 Mar 2013

**HAL** is a multi-disciplinary open access archive for the deposit and dissemination of scientific research documents, whether they are published or not. The documents may come from teaching and research institutions in France or abroad, or from public or private research centers.

L'archive ouverte pluridisciplinaire **HAL**, est destinée au dépôt et à la diffusion de documents scientifiques de niveau recherche, publiés ou non, émanant des établissements d'enseignement et de recherche français ou étrangers, des laboratoires publics ou privés.



## PHD THESIS

Presented at:  
ECOLE NORMALE SUPERIEURE DE CACHAN

Specialty:  
Civil Engineering

By:  
Mr. PHAN VAN TIEN

For obtaining the degree of:  
DOCTOR OF ENS CACHAN

Subject of the thesis:

# RELATIONSHIP BETWEEN THE ADHESIVE PROPERTIES AND RHEOLOGICAL BEHAVIORS OF FRESH MORTARS

Defended on 22/10/2012 before the jury composed of:

Mr. Abdelhafid KHELIDJ,  
Mr. Rafael G. PILEGGI,  
Mr. Guillaume RACINEUX,  
Mr. Abdelhak KACI,  
Mr. Mohend CHAOUCHE,

President of jury  
Reviewer  
Reviewer  
Examiner  
Thesis supervisor

Laboratory of Mechanic and Technology  
E.N.S. de Cachan / C.N.R.S.  
61, avenue du Président Wilson – 94235 Cachan Cedex (France)

# *Acknowledgements*

This study is carried out in the Laboratory of Mechanic and Technology (LMT) of the Ecole Normale Supérieure of Cachan.

First, I want to express my thank to Dr. Chaouche Mohend, research director at CNRS LMT Cachan, my thesis advisor, for giving me a chance to do research at LMT. I have learned a lot and I noted his great knowledge and his availability.

I also thank to Abdelhak Kaci for his supporting during my stage of Master II, continued by my three years worked in LMT and corrected my thesis report.

My gratitude also goes to the technical staff of LMT for using their effective and invaluable collaborations to me in the performing of the experiments. I express my gratitude and friendship with great pleasure.

I would not forget Fatiha Bouchelagem, Professor of Paris 6 University, for her encouragement and heartfelt remarks about my report.

Last but not least, I want to express my thanks to all my family who have been supporting me in 4 years doing research in France.

Contents	
Acknowledgements .....	i
Contents .....	ii
List of Figures .....	v
List of Tables .....	xii
 <b>GENERAL INTRODUCTION .....</b>	 <b>1</b>
 <b>CHAPTER 1. LITERATURE REVIEW .....</b>	 <b>4</b>
<b>1.1. Industrial mortars.....</b>	<b>5</b>
1.1.1. Composition .....	6
1.1.2. Mortar types .....	10
1.1.3. Method of test for fresh mortar .....	13
<b>1.2. Adhesive properties .....</b>	<b>15</b>
1.2.1. Basic notions of adhesives of fresh materials .....	16
1.2.2. Mechanism of adhesion.....	17
1.2.4. Pull-off test and the determinations of the adhesive parameters.....	20
<b>1.3. Rheology of pastes and granular materials.....</b>	<b>23</b>
1.3.1. Basic notions of Rheology .....	24
1.3.2. Constitutive equations of rheological models .....	27
1.3.3 Rheological measurements .....	30
 <b>CHAPTER 2. EXPERIMENTAL TECHNIQUES .....</b>	 <b>32</b>
<b>2.1. Apparatus and Materials .....</b>	<b>33</b>
2.1.1. Apparatus .....	33
2.1.2. Material used.....	36
2.1.3. Mortar formulations .....	40
<b>2.2. Experimental procedures.....</b>	<b>42</b>
2.2.1. Probe Tack test.....	42
2.2.2. Vane-cylinder test .....	44



<b>CHAPTER 3. CELLULOSE ETHER FIBER.....</b>	<b>47</b>
<b>3.1. Effect of fiber on the adhesive properties.....</b>	<b>48</b>
3.1.1. Tack test results.....	48
3.1.2. Adhesive strength.....	51
3.1.3. Cohesion force .....	52
3.1.4. Adherence force .....	53
3.1.5. Adhesive failure energy .....	54
<b>3.2. Effect of fiber on rheological properties.....</b>	<b>55</b>
3.2.1. Flow curves .....	55
3.2.2. Rheological parameters.....	57
<b>3.3. Compare the adhesive properties to the rheological behavior .....</b>	<b>58</b>
<b>3.4. Conclusion .....</b>	<b>60</b>
 <b>CHAPTER 4. THICKENING AGENTS.....</b>	 <b>62</b>
<b>4.1 Effect of organic additives, case of Methocel .....</b>	<b>63</b>
4.1.1 Effect of Methocel on the adhesive properties.....	63
4.1.2. Effect of Methocel on the rheological behavior.....	70
4.1.3. Compare the adhesive properties to the rheological behavior .....	74
<b>4.2 Effect of mineral additives, case of bentonite .....</b>	<b>75</b>
4.2.1 Effect of bentonite on the adhesive properties.....	75
4.2.2 Effect of bentonite on the rheological behavior.....	81
4.2.3 Compare the adhesive properties to the rheological behavior .....	84
<b>4.3 Comparison between organic and mineral thickeners.....</b>	<b>85</b>
4.3.1. Adhesive properties.....	85
4.3.2. Rheological properties .....	85
<b>4.4 Conclusion .....</b>	<b>86</b>
 <b>CHAPTER 5. HYDROXYETHYL METHYL CELLULOSE (HEMCs) .....</b>	 <b>88</b>
<b>5.1. Effect of HEMCs type A .....</b>	<b>89</b>

5.1.1. Effect of A on the adhesive properties .....	89
5.1.2. Effect of A on the rheological behaviors .....	96
5.1.3. Compare the adhesive properties to the rheological behavior .....	100
<b>5.2. Effect of HEMCs type B.....</b>	<b>102</b>
5.2.1. Effect of B on the adhesive properties .....	102
5.2.2. Effect of B on the rheological behaviors .....	107
5.2.3. Compare the adhesive properties to the rheological behavior .....	111
<b>5.3. Effect of HEMCs type C .....</b>	<b>112</b>
5.3.1. Effect of C on the adhesive properties .....	112
5.3.2. Effect of C on the rheological behaviors .....	117
5.3.3. Compare the adhesive properties to the rheological behavior .....	120
<b>5.4. Comparison the effects of three types of HEMCs .....</b>	<b>122</b>
<b>5.5. Conclusion .....</b>	<b>130</b>
 <b>CHAPTER 6. REDISPERSIBLE POLYMER POWDER .....</b>	 <b>132</b>
<b>6.1. Effect of Vinnapas on the adhesive properties.....</b>	<b>133</b>
6.1.1. Tack test results.....	133
6.1.2. Adhesive strength.....	136
6.1.3. Cohesion force .....	136
6.1.4. Adherence force .....	137
6.1.5. Adhesive failure energy .....	138
<b>6.2. Effect of Vinnapas on the rheological behavior.....</b>	<b>139</b>
<b>6.3. Compare the adhesive properties to the rheological behavior .....</b>	<b>142</b>
<b>6.4. Conclusion .....</b>	<b>143</b>
 <b>GENERAL CONCLUSION &amp; PERSPECTIVES.....</b>	 <b>147</b>
 <b>APPENDIX .....</b>	 <b>148</b>
 <b>REFERENCES .....</b>	 <b>158</b>

# *List of Figures*

Figure 1. 1. Some types of fiber reinforced for mortar .....	8
Figure 1. 2. Influence of air-entraining agents on mortar.....	9
Figure 1. 3. Tile adhesive mortar spreading on a wall before covered with ceramic tiles .....	11
Figure 1. 4. Tile grout.....	12
Figure 1. 5. Render/Plaster machine.....	13
Figure 1. 6. Flow-table consistency measurement .....	14
Figure 1. 7. Vicat apparatus for identifying the setting time of fresh mortar.....	15
Figure 1. 8. (a): liquid droplets making a high and low contact angle on a flat, solid surface.	17
Figure 1. 9. Surface forces in physical absorption .....	18
Figure 1. 10. Chemical bonding theory .....	18
Figure 1. 11. Diffusion adhesion theory .....	19
Figure 1. 12. Positive and negative electrical charge at the material joints .....	19
Figure 1. 13. Mechanical interlocking between an adhesive and the substrate.....	20
Figure 1. 14. Parallel plate geometry.....	21
Figure 1. 15. Analysis of the tack test results.....	22
Figure 1. 16. Remaining mortar on the mobile plate in Probe tack test, refers to as the adherence force .....	22
Figure 1. 17. Schematically of adhesive failure energy calculated in the probe tack test data, obtained for the case of fresh mortar .....	23
Figure 1. 18. Simple schematic of shear rate.....	24
Figure 1. 19. Simple schematic of Viscosity .....	25
Figure 1. 20. Determination of static / dynamic yield stress .....	27
Figure 1. 21. Rheological behavior models.....	29
Figure 1. 22. Measuring based structure in vane cylinder test [66].....	30
Figure 1. 23. Dimension of Vane-Cylinder in Vane method .....	31
 Figure 2. 1. The rheometer used for the experiments.....	 33
Figure 2. 2. Balances .....	35

Figure 2. 3. Vertical axis mixer .....	36
Figure 2. 4. Probe Tack test.....	42
Figure 2. 5. Tack geometries .....	43
Figure 2. 6. Square grooves on the two plates surfaces.....	43
Figure 2. 7. A typical evolution of recorded normal force versus time obtained in the probe tack test.....	43
Figure 2. 9. Measuring protocol for Vane configuration.....	45
Figure 2. 10. Typical flow curves of mortar with the addition of 0.29% of polymer .....	45
Figure 3. 1. Evolution of the stretching force versus time as a function of pulling velocities (in $\mu\text{m/s}$ ) for different contents of fibers .....	49
Figure 3. 2. Nominal stress versus nominal strain for varying pulling velocity at certain contents of fiber .....	50
Figure 3. 3. Evolution of the adhesive force as a function of the pulling velocity for different fiber contents.....	51
Figure 3. 4. Evolution of the adhesive force as a function of the fiber content for different pulling velocities .....	52
Figure 3. 5. Evolution of the cohesion force versus fiber content.....	53
Figure 3. 6. Evolution of the adherence force as a function of fiber content for different pulling velocities .....	53
Figure 3. 7. Adhesive energy as a function of the separation rate for different fiber contents	54
Figure 3. 8. Adhesive energy as a function of the fiber content for different pulling velocities .....	55
Figure 3. 9. Flow curves of the mortars for different fiber contents .....	55
Figure 3. 10. Evolution of the apparent viscosity versus fiber content for different shear-rates .....	56
Figure 3. 11. Influence of the fiber content on the rheological parameters of the mortar: Yield stress, consistency coefficient and fluidity index .....	57
Figure 3. 12. Comparison between the yield stress in tension and in shear for varying fiber contents .....	59
Figure 3. 13. Difference between the yield stress in tension and in shear for varying fiber content.....	60

Figure 4. 1. Force versus time curves obtained in Probe Tack test for different polymer contents.....	64
Figure 4. 2. Nominal stress versus nominal strain curves for varying pulling velocities, case of using Methocel .....	65
Figure 4. 3. Evolution of the adhesion force as a function of pulling velocity and of cellulose ether contents.....	66
Figure 4. 4. Evolution of the cohesion force with polymer content .....	67
Figure 4. 5. Evolution of the adherence force as a function of pulling velocity and polymer dosage rate .....	69
Figure 4. 6. Adhesive energy as a function of the separation rate for different polymer contents.....	70
Figure 4. 7. Adhesive energy as a function of the polymer content for different pulling velocities.....	70
Figure 4. 8. Flow curves obtained in the stress-controlled mode using different polymer contents: (a) Linear plot; (b) Logarithmic representation .....	71
Figure 4. 9. Flow curves obtained in the shear rate controlled mode using different polymer contents - (a) Linear plot; (b) Logarithmic representation .....	72
Figure 4. 10. Influence of the cellulose-ether content on the rheological parameters of the mortar: Yield stress, Consistency and Fluidity index.....	73
Figure 4. 11. Comparison of the yield stress in tension and shearing condition for different Methocel contents.....	74
Figure 4. 12. Difference between the yield stress in tension and in shear for different Methocel contents.....	75
Figure 4. 13. Force versus time curves obtained in the Tack test for different bentonite contents.....	76
Figure 4. 14. Nominal stress vs. nominal strain curves for varying bentonite content. ....	77
Figure 4. 15. Evolution of the adhesion force as a function of the pulling velocity for varying bentonite contents .....	78
Figure 4. 16. Evolution of the cohesion force with bentonite content.....	79
Figure 4. 17. Adherence force of the mortar in formulation with bentonite .....	79
Figure 4. 18. Adhesive energy as a function of the separation rate for different bentonite contents.....	80
Figure 4. 19. Adhesive energy as a function of the bentonite content for different pulling velocities.....	81

Figure 4. 20. Flow curves obtained in rheological measurements of mortars in formulation with bentonite: (a) Linear scale; (b) Logarithmic presentation .....	82
Figure 4. 21. Rheological flow curves in low shear rate, case of bentonite .....	82
Figure 4. 22. Evolution of the yield stress with bentonite content .....	83
Figure 4. 23. Evolution of consistency and fluidity index with the variation of bentonite contents .....	83
Figure 4. 24. Comparison of the yield stress in tension and in shear condition for different bentonite contents .....	84
Figure 4. 25. Difference between the yield stress in tension and in shear for different bentonite contents .....	85
Figure 5. 1. Force versus time curves obtained in the tack test for different contents of A .....	90
Figure 5. 2. Nominal stress and strain curves for varying content of A .....	91
Figure 5. 3. Evolution of the adhesion force as a function of pulling velocity (left) and of polymer contents (right), case of A .....	92
Figure 5. 4. Performing of the best fit of the adhesion force versus polymer content, case of A .....	93
Figure 5. 5. Evolution of cohesion force of polymer content, case of A .....	94
Figure 5. 6. Evolution of the adherence force as a function of pulling velocity and polymer content, case of A .....	95
Figure 5. 7. Evolution of the adhesion energy for variation contents of A .....	96
Figure 5. 8. Flow curves obtained in rheology measurement with the variation contents of A .....	97
Figure 5. 9. Loading flow curves with the variation contents of A .....	98
Figure 5. 10. Perform the best fit of flow curves to Herschel-Bulkley models in variation of polymer content, case of A, in which $m_1$ = yield stress, $m_2$ = consistency, $m_3$ = fluidity index .....	98
Figure 5. 11. Rheological parameters of mortar in variation content of A .....	100
Figure 5. 12. Comparison of the yield stress of mortar in tension and in shear with the variation contents of A .....	101
Figure 5. 13. Difference between the yield stress in tension and in shear for the variation contents of A .....	101
Figure 5. 14. Force versus time curves obtained in tack tests for different contents of B .....	102
Figure 5. 15. Nominal stress and strain curves for variation content of B .....	103

Figure 5. 16. Evolution of the adhesion force of mortar in formulation with B.....	104
Figure 5. 17. Evolution of cohesion force with the variation contents of B.....	105
Figure 5. 18. Evolution of the adherence force as a function of pulling velocity and polymer content, case of B .....	106
Figure 5. 19. Evolution of the adhesion energy for various contents of B.....	106
Figure 5. 20. Flow curves obtained in controlled stress mode with the variation contents of B .....	108
Figure 5. 21. Comparison of the loading curves obtain in rheological measurement for different contents of B .....	108
Figure 5. 22. Yield stress of mortar for different content of B.....	109
Figure 5. 23. Rheological parameters of mortar for different content of B.....	110
Figure 5. 24. Comparison of the yield stress of mortar in tension and in shear with the variation contents of B.....	111
Figure 5. 25. Force versus time curves obtained in Probe tack tests for different contents of cellulose ether type C .....	112
Figure 5. 26. Nominal stress versus nominal strain for different contents of C.....	113
Figure 5. 27. Evolution of the adhesion force as a function of pulling velocity (left) and of polymer contents (right) in case of C .....	114
Figure 5. 28. Evolution of the cohesion force with the variation of the content of cellulose ether type C.....	115
Figure 5. 29. Evolution of the adherence force as a function of pulling velocity and polymer content, case of C .....	116
Figure 5. 30. Evolution of the adhesion energy as a function of dosage rate of cellulose ether type C.....	117
Figure 5. 31. Flow curves obtained in controlled stress mode with the variation content of C .....	118
Figure 5. 32. Rheological flow curve, with the variation of C, plotted in normal scale and semi-logarithm scale to highlight the behavior at low shear rate .....	119
Figure 5. 33. Rheological parameters of mortar in variation content of C.....	120
Figure 5. 34. Comparison between the yield stresses of mortar in tension and in shear with different contents of C .....	121
Figure 5. 35. Difference between the yield stress in tension and in shear for different contents of C .....	121

Figure 5. 36. Comparison of the evolutions of adhesion force with the variation of polymer contents, case of A, B and C, under different tack speeds.....	123
Figure 5. 37. Influence of molecular weight on the adhesive force of the mortar at low polymer contents for different tack speeds.....	124
Figure 5. 38. Evolution of the adhesive force as a function of molecular weight at high polymer contents for different tack speeds.....	125
Figure 5. 39. Comparison of the evolutions of the cohesion force with the variation of polymer contents.....	126
Figure 5. 40. Influence of molecular weight on the cohesive stress of the mortar at low and high polymer contents.....	127
Figure 5. 41. Comparison of the evolutions of adhesive failure energy with the variation of polymer contents, case of A, B and C, at different tack speeds.....	128
Figure 5. 42. Evolution of yield stress in shear for the variation of polymer content (a) and molecular weight (b).....	129
Figure 5. 43. Evolution of the consistency of mortar pastes as a function of polymer content and molecular weight .....	130
Figure 6. 1. Force versus time curves obtained in the Tack test for different polymer content, case of Vinnapas.....	134
Figure 6. 2. Nominal stress vs. nominal strain curves obtained in the Tack test for different Vinnapas content .....	135
Figure 6. 3. Evolution of the maximum normal force versus the polymer content, case of Vinnapas .....	136
Figure 6. 4. Evolution of the cohesion force versus the polymer content, case of Vinnapas.	137
Figure 6. 5. Evolution of the adherence force versus the polymer content, case of Vinnapas .....	138
Figure 6. 6. Evolution of the adhesive failure energy versus polymer content, case of Vinnapas and pulling velocity .....	139
Figure 6. 7. Loading and unloading curves of different content of Vinnapas.....	140
Figure 6. 8. Yield stress obtained in shearing condition of mortar in case of adding Vinnapas .....	141
Figure 6. 9. Consistency coefficient and fluidity index of mortar.....	142
Figure 6. 10. Comparison between the yield stress in tension and in shear for different polymer content, case of Vinnapas.....	142



Figure 6. 11. Difference between the yield stress in tension and in shear for varying Vinnapas content .....	143
Figure A. 1. Evolution of the stretching force versus time as a function of pulling velocities (in $\mu\text{m/s}$ ) for different contents of fibers .....	147
Figure A. 2. Nominal stress versus nominal strain for varying pulling velocity at certain contents of fiber .....	147
Figure B. 1. Force versus time curves obtained in the Tack test for different bentonite contents .....	148
Figure C. 1. Force versus time curves obtained in Probe tack test for different content of A	149
Figure C. 2. Force versus time curves obtained in Probe tack test for different content of B	150
Figure C. 3. Force versus time curves obtained in Probe tack test for different content of C	151
Figure C. 4. Flow curves obtained in rheology measurement with the variation contents of A .....	152
Figure C. 5. Flow curves obtained in rheology measurement with the variation contents of B .....	152
Figure C. 6. Flow curves obtained in rheology measurement with the variation contents of C .....	153
Figure C. 7. Evolution of the adhesive force as a function of molecular weight at high polymer contents for different tack speeds.....	153
Figure D. 1. Force versus time curves obtained in the Tack test for different contents of Vinnapas .....	154
Figure D. 2. Nominal stress vs. nominal strain curves obtained in the Tack test for different Vinnapas content .....	154
Figure D. 3. Loading and unloading curves of different content of Vinnapas .....	155

# *List of Tables*

Table 2. 1. Specifications of AR2000ex.....	34
Table 2. 2. The size distribution of standard sand CEN ISO.....	37
Table 2. 3. Typical physical characteristic of three types of walocel.....	38
Table 2. 4. Typical general characteristic of Vinnapas 5010n .....	39
Table 2. 5. Specification data of Vinnapas 5010n.....	39
Table 2. 6. Fiber-reinforced mortar formulation .....	40
Table 2. 7. Polymer-modified mortar formulation, case of Methocel.....	40
Table 2. 8. Polymer-modified mortar formulation, case of Vinnapas.....	41
Table 2. 9. Polymer-modified mortar formulation, case of HEMC .....	41

# *General Introduction*

Nowadays, with the development of the construction industry, mortars are produced in factory by specifically designed dry-mix plants, in which mineral binders and aggregates are mixed together in the appropriate way. These dry-mix mortars (ready to use) are characterized by a very complex formulation involving various constituents. In addition to the basic components (cement, lime, sand), different additives and admixtures are often added in the mortar formulations to improve their characteristic and to achieve different technical properties. Indeed, when applying an adhesive mortar, the product must adhere to the application support instead of to the working tool. Depend on their application purposes, the usage of these additives and admixtures must be fully investigated in order to observe the most effective contributions.

Based on current standards, the adhesive properties of cement-based mortars are often measured at the early age. However the adhesive properties of mortar is usually said to be open in a relatively short duration (several hours) depending on the type of the mortar used. It is therefore necessary to examine the evolution of adhesive properties in the fresh state as well as the rheological properties with the variation of polymer concentrations.

An adhesive mortar in fresh state can be considered as a granular suspension in a complex fluid. The study of the rheological behavior of such materials involves the rheology of complex fluids, including granular suspensions, colloidal dispersions, etc. Many scientific questions still exist in this domain, for example: the problem of shear localization and interpretation of the corresponding rheological measurements. The investigation of these problems in the variation of different types of additives and admixtures help answer these questions.

To characterize the rheological behavior of an adhesive mortar, in quasi-static regime, we use a three-parameter behavior law that includes a yield stress, a viscosity coefficient and a fluidity index. The adhesiveness of the mortar can be characterized by identifying the evolution of the adhesive force, the cohesive stress and the adherence force.

The objective of this thesis is to determine the roles of various additives of organic origin (cellulose ethers, re-dispersible resins powders) and/or mineral (clays, silica fume, etc.) on the

fresh state properties of these mortars, including their adhesive properties and rheological behaviors.

We have studied the influence of different admixtures on the properties of fresh mortar by considering the experimental views. Different types of mortars (coating, adhesive, etc.) are formulated in the laboratory. The mortars are characterized by a commercial rheometer from TA instruments series, which is equipped with different geometries for different kinds of rheological experiments. In present thesis, we use plane-plane geometry for the Probe Tack test, which is used to determine the adhesiveness of materials. The rheological property of mortar is investigated using Vane-Cylinder geometry. We examine in detail the influence of polymer additives on the adhesive properties as well as the rheological behavior of mortar in fresh state.

This thesis is presented in 6 chapters, in which:

Chapter 1 introduces the adhesive properties and rheological behavior of complex fluids, including fresh mortar. The definitions of the adhesive parameters, including cohesion, adhesion and adherence, have been given, as well as their determination methods. In the presentation of the rheology, besides the basic notions, we have discussed about the rheological models, which are used to perform flow curves' fittings to determine the rheological parameters. The Vane-Cylinder method, a popular method for characterizing the rheological properties of cement-based materials, is presented in detail.

Chapter 2 shows the experimental apparatus and the materials used in this thesis. The procedures of the experiments, including tack test and Vane-cylinder experiment, are presented as well as the method to obtain high accuracy related parameters.

Chapter 3 discusses about the effect of cellulose ether to the properties of fresh adhesive mortar. It is found that the increasing of fiber content have significant influence on the properties of mortar in fresh state, and a difference between the used fiber-reinforce mortar in tension and in shear conditions had also been observed.

Chapter 4 gives a comparison of the effect of the thickening agents, including cellulose ether-based polymer and sodium bentonite clay to the properties of fresh mortar, with a basic formulation. The result expects that the water-soluble polymers can be used to modify the viscosity and the adherence properties, while the mineral additives can be used to control yield stress and cohesion of fresh mortar. These two additives may reveal complementary regarding the placement properties of mortar.

Chapter 5 analysis the effect of three types of hydroxyethyl methyl celluloses (HEMCs). These cellulosic polymers are commercial water-soluble polymers, which have different

viscosities and molecular weights. Both the effect of each type of cellulosic polymer and the influence of the molecular weight on the properties of fresh mortar are discovered.

Chapter 6 studied the effect of a commercial re-dispersible polymer powder with the trade name “Vinnapas 5010n”, in combination with a cellulose ether polymer, on the adhesive properties and rheological behavior of fresh mortar. It is found that the combination between these two polymers does not influence on the properties of fresh mortar.

## CHAPTER 1

# *Literature review*

### Contents

<b>1.1. Industrial mortars .....</b>	<b>5</b>
1.1.1. Composition .....	6
1.1.2. Mortar types .....	10
1.1.3. Method of test for fresh mortar .....	13
<b>1.2. Adhesive properties .....</b>	<b>15</b>
1.2.1. Basic notions of adhesives of fresh materials .....	16
1.2.2. Mechanism of adhesion.....	17
1.2.4. Pull-off test and the determinations of the adhesive parameters.....	20
<b>1.3. Rheology of pastes and granular materials.....</b>	<b>23</b>
1.3.1. Basic notions of Rheology .....	24
1.3.2. Constitutive equations of rheological models .....	27
1.3.3 Rheological measurements .....	30

Mortar is a building material, which is used for joining the building elements together, provide the stability of the whole structure and fill the gaps between the building blocks. In general, mortar consists of cement or lime, sand, water and additives.

In this chapter, I present some general information on the composition of modern industrial mortars, which are going to be investigated herein. Different types of mortar and their main characteristics such as workability, setting, and removal are also introduced.

Some basic notions on the adhesive properties and rheological behaviors of fluid concretes and cement-based mortars in fresh state are presented in followed sections. In this part, the popular measurement methods, which are used to measure these properties, are also described.

In details, this chapter includes 3 main sections.

Section 1.1 gives general knowledge on the modern industrial mortars and their classifications. These types of mortars will be studied in the variation of different additives and admixtures in this thesis. Popular testing methods, applied for fresh mortar, are also presented.

Section 1.2 introduces the basic notions of the adhesive properties of complex fluids and their basic chemistry. 5 different adhesion mechanisms, which are able to explain the adhesion, have also been presented. It is then followed by the presentation of the measurement methods and the calculation of the adhesive failure energy of the adhesion.

Section 1.3 recalls basically knowledge on the rheology of materials in fresh state, in which the basic notions of rheology and the constitutive equations of rheological models are presented as well as their measurement methods.

## **1.1. Industrial mortars**

In any structure, it is essential to bring together the various elements (concrete blocks, bricks, precast concrete, etc.) using mortar that is designed to:

- Obtain the solidarity of the construction blocks together;
- Ensure the stability of the whole structure;
- Fill in the gaps between the building blocks.

The mortar is obtained by mixing a binder (cement or lime), sand, water and possibly additions. Multiple compositions of mortar can be obtained by adjusting the various parameters: binder (type and dosage), additive and admixtures, water dosage. With respect to the binder, for the cases of cement and lime, the work that mortar will be performed and its surrounding environment determine their choice and dosage rate.

Industrial mortar has been significantly developed in recent years. There are many recently invented additives and admixtures that need to be investigated for better contributions. These components were used to obtain some requirements related to the mortar properties in fresh state (pump-ability, workability, adhesive, cohesive, etc.), in hardened state (open-time, cracking resistance, mechanical properties, etc.) and their long-time behavior (durability, water-proof resistance, etc.).

In this section, the general characteristic of these mortar constituents will be presented as well as their classification and advantages. Some specific types, which are widely used, are highlighted.

### 1.1.1. Composition

Mortar can be quite different from each other depending on the type and the proportions of the components, the mixing, the implementation and the cure. We focus herein on the standard definitions and requirements of these main constituents.

**Binder** has a very important role in forming the strength of the mortar both in fresh and hardened states. It sticks various particles together and forms the adhesive properties of the mortar to the substrate. Generally, one can use standardized cement (white or gray), special cement (aluminous, prompt, etc.), masonry binder, and lime.

Nowadays, concrete mortar is the most widely used. In our studies, two types of Portland cements were used: CEM I 42,5N and CEM I 52,5N.

**Sand** gives volume, stability, resistance to wear or erosion, and other desired physical properties to the finish structure. Typically, we use a commercial product called normalize sand. It consists of fine, medium and coarse grained. The fine grained will arrange themselves to fill the gaps between the coarse grains. It helps to reduce the volume variation, the released heat, and also the price of the whole structure.

The maximum diameter of grains of sand used for mortars is:

- Extra-fine: up to 0.8 mm;
- Fine: >0.8 – 1.6 mm;
- Medium: >1.6 – 3.15 mm;
- Coarse: >3.15 – 5 mm.

**Additives** are chemical products that are used in the case of concrete. They modify the properties of concretes and mortars in which they were added in a small proportion (about 5% by weight of cement). In general, the additives used for mortar may be classified into:

- Plasticizers (water-reducer);



- Air – entraining agents;
- Modifiers of the setting process (retarders, accelerators);
- Water repellents.

**Admixtures** which are used in mortars are:

- Pozzoland fine powders (ash, silica fume, etc.);
- Fibers of different types;
- Dyes (natural or synthetic);
- Polymers

There are many types of additives and admixtures which need to be studied in order to have a better understanding on their effects. In the following, we will introduce several additives and admixtures which were studied in present thesis. They include fiber, sodium bentonite clay, cellulose ether polymer, and air entraining agent.

***a) Cellulose ether***

The term “cellulose ether” refers to a wide range of commercial products and differs in terms of substituent, substitution level, molecular weight (viscosity), and particle size. The most widespread cellulose ethers used in dry mortars as admixtures are the methyl cellulose (MC), methyl-hydroxyethyl cellulose (MHEC) and methyl-hydroxypropyl cellulose (MHPC) [Bayer 2003].

According to their properties, cellulose ethers are used in various industrial fields, including food industry, pharmaceutical industry, in paints and adhesives, etc. They significantly modify the properties of materials even if they are introduced in small amounts (0.02-0.7 % [Bayer 2003]). They are used to control the viscosity of a medium, as thickeners or gelling agents. In mortar, cellulose can be added before or during the mixing as thickening and water retaining agents. The effect of cellulose ethers on the mortar in fresh state was not fully studied. For example, there are few studies on the effect of methyl-hydroxyethyl cellulose (MHEC) on the adhesive properties and rheological behavior of fresh mortar. Therefore a comparison of the effects of three different types of MHEC on the properties of fresh mortar has been carried out and is discussed in chapter 5.

In building industry, modified cellulose ethers are often blended with other additives to improve desired properties and/or to reduce undesirable properties and/or to add new properties, including sag-resistance, stickiness, water retention, air-content, etc. We have also studied the effect of a combination between a cellulose ether type with a re-dispersible polymer powder to the adhesive and rheological properties of fresh mortar. The results are

presented in chapter 6.

**b) Fibers**

Fibers are often added in the mortar formulation in order to avoid creeping in the fresh state and to improve the mortar properties in the hardened state, in particular to reduce cracking. For rendering mortars, which tend to be thin coating, having a long surface area, the biggest problems are moisture loss and subsequent cracking; the polypropylene fibers are usually used to protect it against plastic shrinkage cracking.



*Figure 1. 1. Some types of fiber for reinforced mortars (source: asiafiberhk.com)*

Fibers can be classified into two groups depend on their average length: long fibers with the higher aspect ratio among 200 to 500, are mainly used for reinforcement of mortars; short fibers, which have a general aspect ratio among 20 to 60, are used in influence wet-mortar properties and water demand. Long fibers, typically over 40 mm's length are also called macro fibers. A typical dosage of macro fiber is 3-8 kg/m<sup>3</sup>. Whereas micro fibers are normally 6-12 mm's length with a typical dosage is 0.6-1.0 kg/m<sup>3</sup>. Macro fibers are primarily used to enhance the toughness of a render or screed.

Figure 1.1 shows some types of fibers, which can be used for reinforcement of mortars, including polypropylene fiber, cellulose fiber, etc.

In general fibers are added in cementitious materials, including mortar, in order to improve their mechanical properties in hardened state, and this has been studied by numerous authors [Wang 1990, Song 2005, Perez-Pena 1994]. On the other hand, the effect of fiber addition on the fresh properties, including the rheological behavior has been much less studied [Banfill 2006, Kuder 2007, Ozyurt 2007]. Moreover, there are few reported studies on the effect of fibers on the adhesive properties of cementitious materials in the fresh state. We have studied the influence of a cellulosic fiber on the properties of fresh rendering mortar, which is discussed in chapter 3.

**c) Air entraining agent**

This is an admixture which increases workability, or allow water reduction, by incorporating during mixing a controlled quantity of small, uniformly distributed air bubbles which remain after hardening.

Air-entraining agents act physically by entraining air micro-pores in the mortar/concrete. The bubbles are introduced into the mortar/concrete by the addition to the mix of an air-entraining agent, a surfactant (surface-active substance, a type of chemical that includes detergents). The air bubbles are created during the mixing of the plastic (flowable, not hardened) mortar/concrete, and most of them survive to be part of the hardened state. The primary purpose of air entrainment is to increase the resistance of the hardened mortar/concrete; the secondary purpose is to increase work-ability of the mortar/concrete while in a plastic state. The plasticizing properties of the admixtures also result in decreased mix water demand, subsequent reduction in shrinkage.

The addition of air entraining agents also leads to a decreased wet mortar density and a higher wet mortar yield. The included air leads to better insulation against cold and heat, but also to lower strength. The air bubbles act like minute ball bearings and lubricate the mortar making it easier to work. We can observe the effect of air entraining agent in figure 1.2, in which the left sample has 0% of air entraining agent, while the right one has 0.025% by weight.

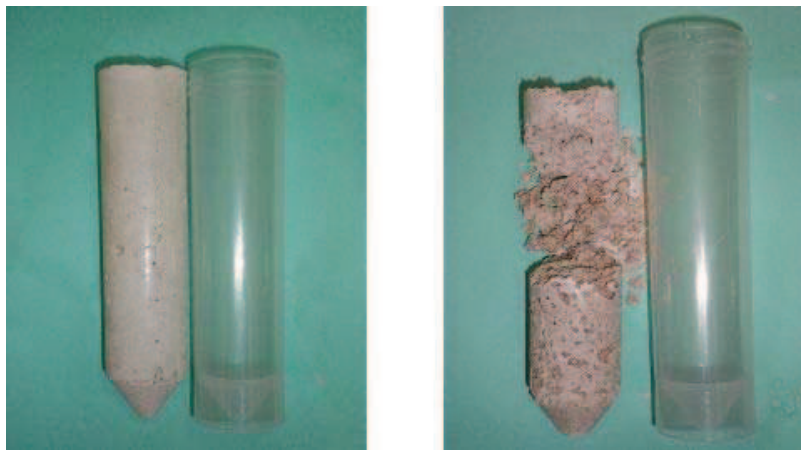


*Figure 1. 2. Influence of air-entraining agents on mortar: The right sample, in which the air entraining agent is added, contains many voids and is easily broken after removing from the mould.*

Air-entraining agents are based on powder form and mainly sodium salts of fatty acid sulfonates and sulphates. The additions rate in mortars normally varies from 0.01 to 0.06%.

d) ***Sodium bentonite clay***

Sodium bentonite is largely employed in drilling muds and retaining fluids formulations. Such additives serve as thickening agents, and must present particular rheological properties such as high yield stress to prevent sedimentation [Laribi 2005]. The effect of bentonite clay on the rheological behavior of fresh mortar has also been studied [Kaci 2011]. However, to the best of our knowledge, there are few reported studies that concern the influence of bentonite clay, which serves as a thickening agent, on the adhesive properties of mortar in fresh state.

1.1.2. Mortar types

In civil engineering, there are different types of mortars. Depending on the used binder; mortars can be classified into 3 types: cement, lime and mix mortar.

Cement mortars are highly resistant, and can harden quickly. The cement to sand ratio is usually 1:3 and the water to cement ratio is about 0.35.

Lime mortar has lower resistance compared with cement mortar. The curing duration is slower than cement mortar.

When the binder is a mixture of cement and lime, it refers to mortar mix. In general, the amounts of these two types of binder are equal, but sometimes it takes a greater or lower amount of one or the other depending on the application and the required quality.

Mortar can also be classified into many types according to their applications. In the following, we will introduce three types, including tile adhesive, tile grout and render/plaster mortar, which are going to be studied herein.

***1.1.2.1. Tile adhesive mortar***

Tile adhesive mortar is used to bond the bottom of the tile to a surface – called the setting bed (figure 1.3). In recent years, the improvements in adhesives mortar make it easier for people to lay tile themselves, without contracting the job out to a professional. There are numerous types of tile adhesives (ceramic, wall, porcelain, granite, etc.) and each has a specific application.



*Figure 1. 3. Tile adhesive mortar spreading on a wall before covered with ceramic tiles*

Typical basic formulations for a standard and a high quality flexible tile adhesive mortar are given in Table 1.1, in which A corresponds to standard formulations; B corresponds to flexible, high-quality polymer-modified tile adhesives. Different types of additives are added if required for special performance.

Tile adhesive mortar must fulfill technical requirements such as good workability characteristics, good water-retention capability, long open time, etc. After curing, the mortar must provide good adhesive and cohesive bond strength.

*Table 1.1. Typical formulation of tile adhesive [Bayer 2003]*

<b>Adhesive type</b>	<b>A</b>	<b>B</b>
Portland cement	45	35
Sand (0.05-0.5 mm)	53.1-51.6	59.6-57.6
Cellulose ether (viscosity ca 40 000 mPa s	0.4	0.3
Redispersible powder	0-4	5-10

#### **1.1.2.2. Tile grouts (joint mortar)**

Grout is a building material which is used to connect sections of pre-cast concrete, fill in the voids, embed reinforcing steel in masonry wall, and seal the joints. In general, grout composes of water, cement, sand and other additives, including color tint, sometimes fine gravel. According to their applications; grout can be classified into tiling grout, flooring grout, structural grout, and some specific types for distinct tasks. Among them, the grout is most applied for tiling application, which is used to fill the joints between tiles or natural stones laid on walls or floors (figure 1.4).



Figure 1. 4. Tile grout

Tile grout must provide an attractive surface and must perform technical requirements. It must be capable of neglecting the harmful influences of water penetrating into the whole construction and protect the materials and layers under the tiles against mechanical damage. Thus a tile grout must provide good adhesion, toughness and cohesion properties. Moreover, tile grout must also have low shrinkage, low water absorption, and low stickiness.

According to their applications, tiles grout can be classified into two main types: standard (A) and high quality, pigmented, smooth-surface tile grout (B) for interior and exterior use. Typical formulations are given in Table 1.2.

Table 2.2. Typical formulation of tile grout [Bayer 2003]

Tile grout type	A	B
Portland cement	25-30	20-25
High-alumina cement	0-10	0-10
Pigment	0-5	
Filler (Silica sand and/or carbonate filler)	75-56.9	79-51.9
Cellulose ether	0-0.1	0-0.1
Redispersible powder	0-2	1-5
Additives for workability	0-1	0-3

#### 1.1.2.3. Rendering and plaster (mortar)

Plaster is a coating material applied to walls or ceilings in one or more layers in different thickness. There are different types of render and plaster, classified according to their basis of the type of binder used, such as cement render and gypsum plaster.

Plaster must provide a range of physical tasks, such as protect against weathering or chemical or mechanical actions. Plasters are widely used for bathrooms and other rooms where



moisture occurs. In order to satisfy these requirements, cement or lime-cement is often used.



*Figure 1. 5. Render/Plaster machine*

Render and plaster must provide good water vapor permeability and must be suitable for painting and hanging heavy papers. While cement renders are used for exterior tasks and wet rooms, gypsum renders are used exclusively for interior walls.

Nowadays, with the development of the construction technique, one can choose either manually applied or a machine-applied render/plaster (figure 1.5). Accordingly, the render/plaster for machine application must provide the additional requirements. For instance, the consistency must be high enough for the render/plaster to remain stickiness on the construction, but also not too high that the pumping process may be impacted. It must also provide high water retention. In Europe, the trends of using machine-applied render/plaster are very common, and next to this trend, there is also a tendency of using more lightweight plasters.

### 1.1.3. Method of test for fresh mortar

The production and application of new mortars, admixtures and similar materials has proven the need of sophisticated test apparatus which are capable of performing different tests and procedures on numerous material samples. There has been many commercial apparatus which are used for those requirements. The objective of this section is to give the most popular apparatus and testing method in the case of fresh mortar, each determines one characteristic of mortar, including consistency, water retention, setting time, open time, etc.

In general, mortar testing is undertaken for controlling or monitoring the consistency of a product, examining their performance under specific conditions, investigating problems and for evaluating conformity with a specification or Standard. In fresh state, the consistency and the setting time of mortar are the most important parameters. The measurement methods of

these two parameters will be introduced herein.

There are many approaches when identifying the consistency and the setting time of the mortars. In the following, we will refer to several popularly laboratory measurement methods. However, in our studies, the consistency and the workability of the mortar is considered in both tension and shearing conditions, by a different test, performed on a commercial rheometer which will be introduced in the next chapter.

### 1.1.3.1. Consistency

The dry mortar is mixed with a certain amount of water before applying to a support. The sufficient amount of water leads to the desired application consistency. A higher or lower amount of water causes unexpected properties of the mortar. Therefore the controlling of the mortar consistency acts an important role in the construction. For the mortar in fresh state, the consistency is identified using flow-table apparatus (ASTM C270 - figure 1.6), in which a mortar sample is first placed in a conical mould, and then the mould is removed before applying a mechanical drop to the whole table. The frequency of the table shocks is often taken 15 times in 15 seconds.

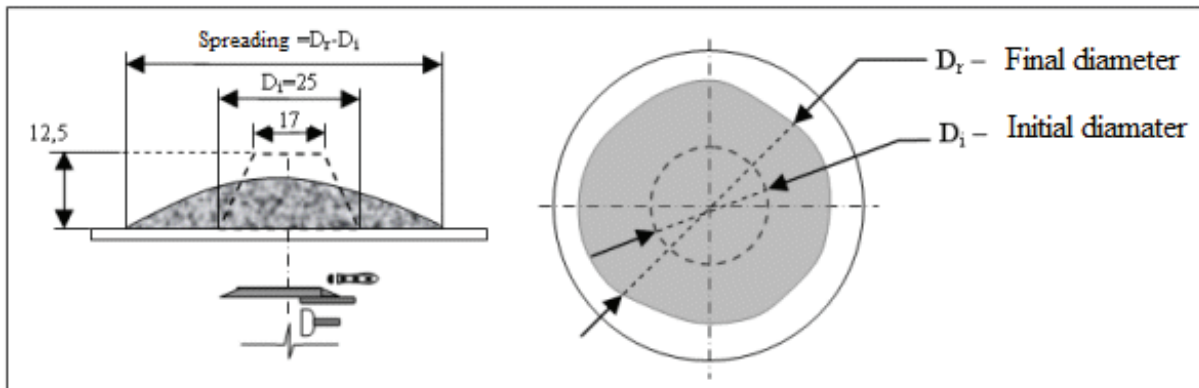


Figure 1. 6. Flow-table consistency measurement

The final diameter of the mortar after shocked is compared with the initial diameter, resulted in the spread of the mortar sample, given by the formula:  $E(\%) = 100 \frac{D_r - D_i}{D_i}$ , in which  $D_r$

is the final diameter, and  $D_i$  is the initial diameter of the mortar sample.

This method is not used to identify the mortar consistency at the site because it is not suitable to their wetter consistency.

### 1.1.3.1. Initial setting time (workability)

The initial setting time / workability measurement of cement pastes and mortars is an important parameter for the quality inspection and verification. For fresh cement paste and



mortar, Vicat apparatus, illustrated in figure 1.7, is often used.

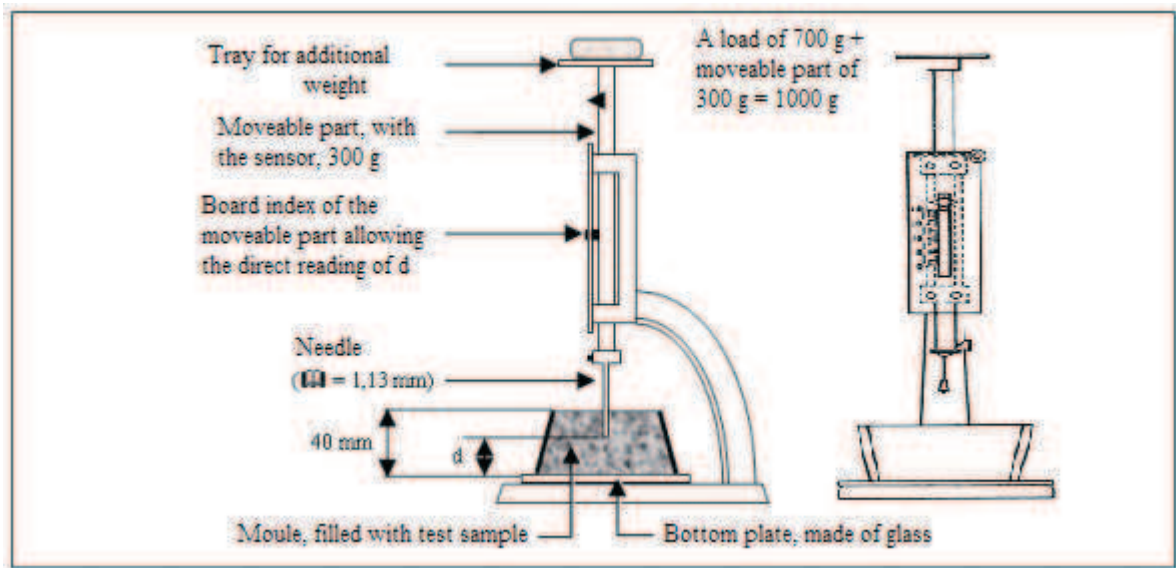


Figure 1. 7. Vicat apparatus for identifying the setting time of fresh mortar

This apparatus include a tray for an addition weight, often 700 grams, a moveable part with sensor, and a standard needle. These parts are installed as in figure 1.7. A test sample of 300 grams is taken. It is mixed with an amount of water, which is 0.85 times that of standard consistency, in within 3 to 5 minutes, then fill the Vicat mould completely with the cement paste made and smooth off the surface of the mould. The mould is placed under the needle, which is then lowered gently to touch the surface of the sample. The needle will be released and dropped down to penetrate into the test sample. This procedure is repeated until the needle penetrate the test block by  $d = 5 \pm 0.5$  mm from the bottom of the mould. The time started from the mixing of water to the cement to the time when the needle fails to penetrate the test sample by  $5 \pm 0.5$  mm is described as the initial setting time.

This method is often applied to identify the initial setting time of fresh mortar in laboratory.

## 1.2. Adhesive properties

An adhesive is a material used for holding two surfaces together. For a material to perform as an adhesive, it must wet the surfaces, adhere to the surfaces, develop strength after it has been applied, and remain stable. Therefore the adhesive property must be considered in at least 3 stages; including fresh, plastic and hardened state. However, to the best of our knowledge, the measurement of adhesive property is often performed in plastic and hardened state. There are few publications that deal with the adhesive property of fresh mortar.

Adhesive properties of fresh mortars pastes are considered in two points of view. Firstly, it must fulfill the requirement during the application process, including pumping, casting,

smoothing, etc. The adhesion strength must be sufficient to stay on the support, but it must also be limited in order to avoid excessive sticking to the working tool, or in order to avoid blockages during the pumping process. Secondly, the quality of the adhesion between fresh mortar pastes and the support plays an important role in forming the final strength of the hardened product, as well as the efficiency of the bonding.

Depending on the objective of the application, different parameters will be considered. For example, in case of preventing the mortar from the blockage during the pumping, the thixotropy of the material is considered [Kaci 2010].

In the following, we will firstly present some basic notions of the adhesives properties of fresh materials, including adhesion, cohesion and interface adherence. After that, the different models, which have been defined for explaining the adhesion mechanisms, will be introduced. This part is continued by the presentation of the three popular measurement methods of the adhesion.

### 1.2.1. Basic notions of adhesives of fresh materials

Cohesion refers to the tendency of similar or identical particles / surfaces to cling to one another, which usually refers to the strength of the materials with which the particles attract to each other. In fresh state materials, cohesion is used to characterize the resistance of materials to flow initiation under various conditions, including shearing and tension. Cohesion force related to the yield stress of the material [Kaci 2009].

Reversely, adhesion is described as the tendency of particles of different substances to cling to one another, which usually refers to the strength with which a material forms a good bonding with the others. In construction, the adhesion of fresh mortar is an important characteristic that decided the strength of the interaction between the mortar and the substrates. The substrate can be steel, cement, glass with various physical and chemical characteristics.

Adhesion strength comprises both cohesion strength and viscous dissipation, and can be employed to characterized adhesion properties under flow conditions [Kaci 2009].

Interface adherence is defined as “the force that must provide the adhesive system to separate two adherence components” [Lamure]. It expresses the product’s ability to stand on its support.

In the area of fresh mortars applied on a support, the adhesion is related to several factors:

- adhesiveness, which give the ability to create the interaction forces between the support and the mortar,
- the surface and the nature of the support (porosity, roughness, absorptive, cleanliness),

- Wet-ability affects the ability of the mortar to create a contact with the support on which it is applied.

When an adhesive is brought into contact with a substrate, it must establish a continuous contact between the adhesive and the surface. This process is known as “wetting”. The efficiency of an adhesive in this “wetting” process is determined by contact angle measurements. The smaller contact angle observed, the better “wetting” occurs. When the contact angle is 0 deg, the material spreads uniformly over the substrate to form a thin sheet as illustrated in figure 1.8 [Comyn 1997]. Different authors have studied the influence of the wetting process [Winnefeld 2012, Jenni 2006, Maranhao 2011]. So does the influence of the additives and admixtures on the adhesiveness of mortars [Ray 1994, Izaguirre 2011, Jenni 2005]. However, these investigations are mostly performed with plastic and/or hardened state mortars. Kaci *et al.* are among the first authors to deal with mortar in fresh state [Kaci 2009, Kaci 2011]. Our work is to continue this research by considering influence of various other additives and admixtures.

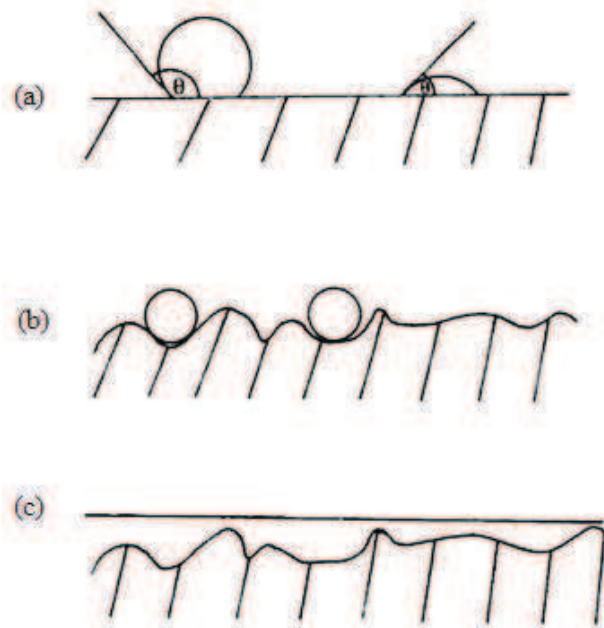


Figure 1. 8. (a): liquid droplets making a high and low contact angle on a flat, solid surface

(b): high contact angle-no spreading on surface wetting

(c): zero contact angle-complete substrate [Comyn 1997]

### 1.2.2. Mechanism of adhesion

The mechanism of adhesion has been studied for years. In order to provide an explanation for adhesion phenomena, several theories have been proposed. However, no unifying theory that

describes all adhesive bonds in general in comprehensive ways.

The bonding of an adhesive to a substrate includes numerous mechanical, physical, and chemical forces that influence each other. As it is impossible to separate these forces from each other, it can be divided into 5 different adhesion mechanisms, including mechanical, electrostatic, adsorption, chemisorptions and diffusion theory.

#### 1.2.2.1. Physical absorption

The adhesion results from the molecular contact between two materials and these two materials are held together by the “van de Waals” forces (figure 1.9). These are weakest forces that contribute to the adhesive bonding, but are quite sufficient to make strong joints [Comyn 1997].

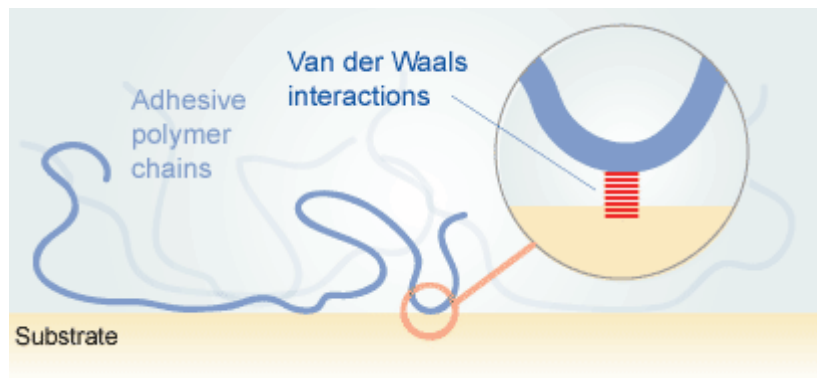


Figure 1. 9. Surface forces in physical absorption

#### 1.2.2.2. Chemical bonding

The chemical bonding adhesion is attributed to the formation of either covalent, ionic or hydrogen bonds across the interface. Two materials form a compound at the joint by swapping electron (ionic bonding), sharing electron (covalent bonding) or the hydrogen atoms are attracted to an atom of nitrogen, oxygen or fluorine (hydrogen bonding).

Chemical bonds are strong and have significantly contribution to the interior adhesion.

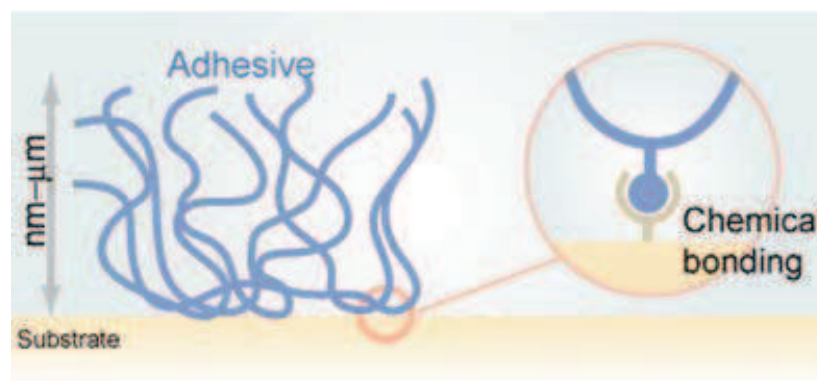


Figure 1. 10. Chemical bonding theory

### 1.2.2.3. Diffusion adhesion

Adhesion of polymeric materials is attributed to interpenetration of chains at the interface. This theory requires both the adhesive and the substrate are polymers, which are both mobile and can be soluble in each other.

Figure 1.11 illustrates the interface between an adhesive and the substrate before and after merged by diffusion. When a polymer adhesive and the substrate are pressed together and heated, atoms diffuse from one particle to the neighbors. This creates the adhesion.

The diffusion adhesion is affected by the contact time, the temperature, molecular weights of polymers and their physical form (liquid, solid).

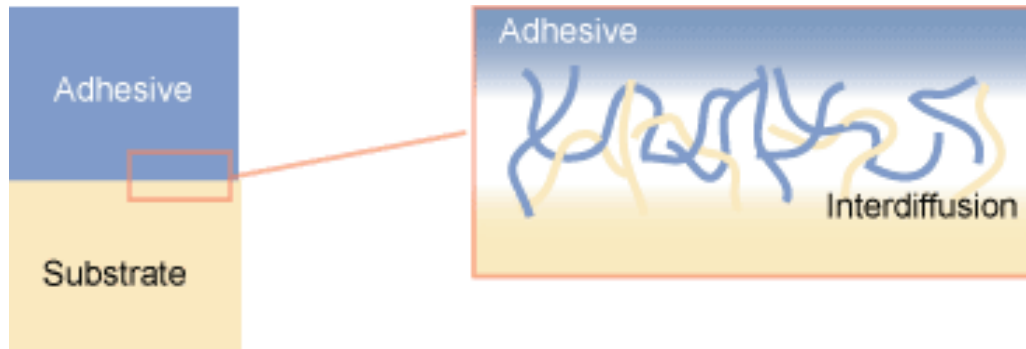


Figure 1. 11. Diffusion adhesion theory

### 1.2.2.4. Electrostatic theory

Electrostatic adhesion theory invokes the forming of a difference in electrical charge at the interface between two materials, in which electrons transfer from one to another. That gives a force of attraction between these materials, which contribute to the resistance to the separation of the adhesive and the substrate.

Figure 1.12 illustrates an electrical double layer appeared when an adhesive is brought into contact with a substrate.

This theory can not be applied if either one or both materials are insulators.

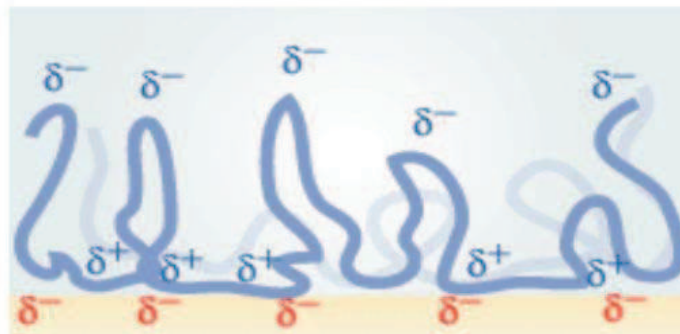


Figure 1. 12. Positive and negative electrical charge at the material joints

#### 1.2.2.5. Mechanical adhesion

The mechanical interlocking theory of adhesion states that good adhesion occurs only when an adhesive penetrates into the pores, holes and crevices and other irregularities of the adhered surface of a substrate, and locks mechanically to the substrate. The adhesive must not only wet the substrate, but also have the right rheological properties to penetrate pores and openings in a reasonable time.

As illustrated in figure 1.13, one surface is never completely smooth. It always consists of a numerous of peaks and valleys. According to this theory, when an adhesive is brought in contact with the substrate, it must penetrate the cavities on the surface, displace the trapped air at the interface, and establish a mechanical interlocking with the interface. It means that the adhesive must not only wet the surfaces, but also have the right rheological properties to fill in the cavities and to be opened in a reasonable duration.

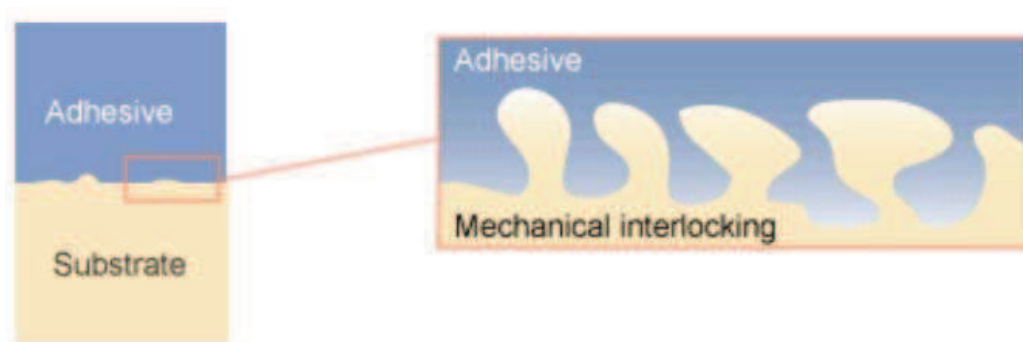


Figure 1. 13. Mechanical interlocking between an adhesive and the substrate

The surface roughness helps to increase the total contact area that the adhesion force can develop. That will increase the total energy of surface interaction, which leads to a higher resistance to separation of the joint. However, the adhesive must wet the substrate well in order to have an efficiently joint.

#### 1.2.4. Pull-off test and the determinations of the adhesive parameters

A popularly used method for measuring the adhesive properties of materials in fresh state is the pull-off test, in which two solid surfaces are brought in contact between which an adhesive layer is inserted, and after certain duration, pulled away at a fixed speed. The force versus separating distance (or time) is then recorded, from which we can calculate the adhesion force, cohesion, the interface adherence and other parameters, i.e., the total adhesion energy.

This method has been largely employed during formulation of polymer pastes [Creton 1996,



Zosel 1985] and more recently to investigate the normal force and possible failure modes of smectite muds [Chaouche 2008]. However, to the best of our knowledge, there are few authors who had performed the pull-off test for the cases of fresh mortar. This method allows dissociating several aspects of practical interest, related to adhesive properties of fresh mortar, which have been introduced in previous section, including cohesion, adhesion and interface adherence [Kaci 2009]. A simple illustration of this method is shown in figure 1.14, in which two solids, separated by a layer of material, are moved away from each other following the perpendicular direction to their surfaces. Such process implies the creation of new interfaces, but in general the required energy is much higher than typical surface energies [Barral 2010]. This means that the separating process involves the deformation or flow of the inserted material between the two moving solid plates.

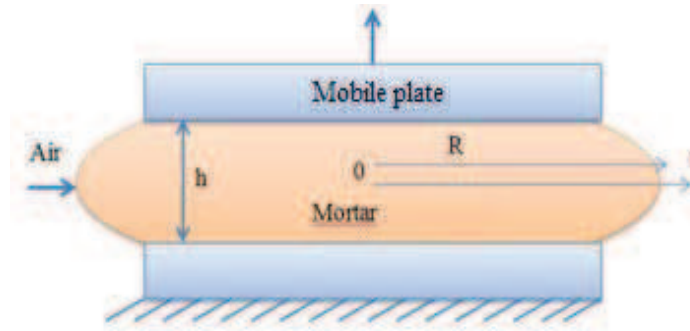


Figure 1. 14. Parallel plate geometry

The force curves, which are recorded in the separation step, are represented in figure 1.15. This curve can be divided into three zones. The force first increase (zone 1), passes through a maximum  $F_{max}$  and then decreases (zone 2) reaching finally a plateau (zone 3). In zone 1 the mortar displays mainly elastic and then viscous-elastic behaviors. The force peak is related to the adhesive strength of the material. In zone 2 one has irreversible rupture and inward flow of the material towards the plates centre. Analysis of the force decay in this zone allows characterizing rupture dynamics of the mortar. Mortar displays viscous-plastic behavior in this zone. Zone 3 starts as soon as the rupture process is completed. The average value of the force plateau is related to the amount of material remind stuck onto the mobile plate. This gives the adherence strength of the mortar relative to the surface of this plate.

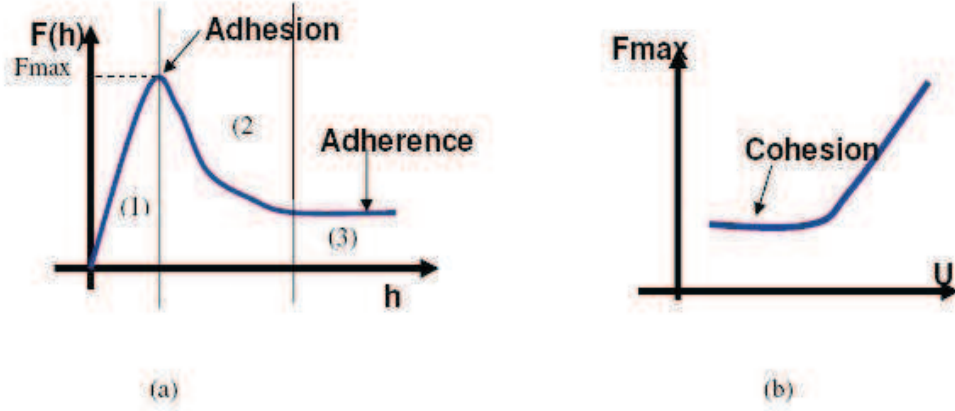


Figure 1. 15. Analysis of the tack test results – (a) General shape of the tack force curve; (b) Evolution of the peak force versus pulling velocity

The value of force peak  $F_{max}$  is related to both viscous dissipation (dynamic property) and cohesion strength (static property) whose origin includes in particular intermolecular and capillary forces. To infer the cohesion component from the adhesion strength, the force peak is represented as a function of the stretching velocity. The cohesion force is then taken to be the value of the force peak when the velocity tends to zero (figure 1.15 b).

The adherence force is identified by the quantity of the mortar remain stuck on the upper plate at the end of the experiment. Figure 1.16 shows the mortar remaining on the upper plate at the end of one tack experiment, which is referring to as the adherence force.

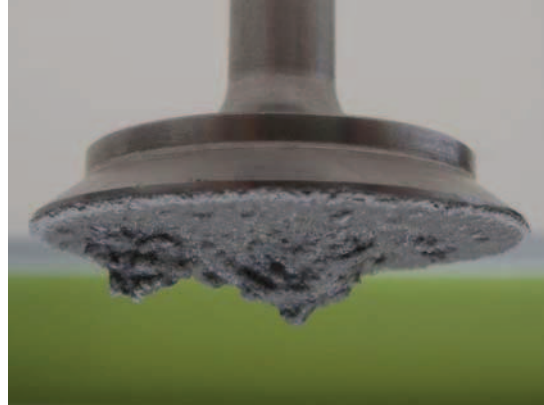


Figure 1. 16. Remaining mortar on the mobile plate in Probe tack test, refers to as the adherence force

The energy needed for completing the pull-off test is calculated by the following equation:

$$W = \int_{h_b}^{h_a} F dh \quad (1.11)$$

where  $h_a$  and  $h_b$  are respectively the gap distance at the beginning and that at the finishing of the separation process.



It can be rewritten as:

$$W = \int_{t_2}^{t_1} F.vdt \quad (1.12)$$

where  $v$  is the separation velocity and  $F$  is the recorded normal force during the separation process which starts at  $t_1$  and lasts for  $t_2 - t_1$  (second). The moment of  $t_2$  corresponds to the finishing of the separating process.

Figure 1.17 represents the calculation of the adhesive failure energy in experiment. In general, it is determined by the area formed by the force curve obtained in the test and the horizontal axis.

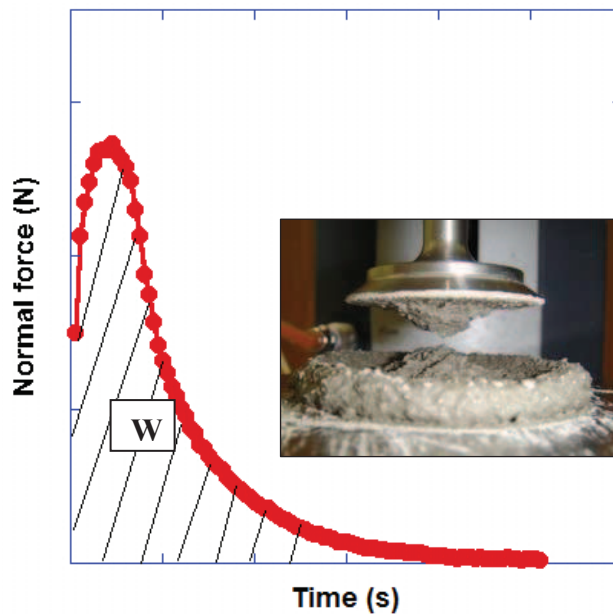


Figure 1. 17. Schematically of adhesive failure energy calculated in the probe tack test data, obtained for the case of fresh mortar

### 1.3. Rheology of pastes and granular materials

Rheology is the study of the deformation and flow of material under the influence of an applied stress, which might be, for example, a shear stress. It concerns the relationships between shear stress, shear strain and time. It deforms when exerted to a force, results in the change of the shape and dimensions of the material. We say that the element is flowing if the degree of deformation changes with time.

The rheological behavior of a volume element of a body is how these deformations correspond to the stresses imposed on the body. The aim of the study of rheological behavior is to estimate the system of forces to cause specific deformation, or the prediction of deformation caused by a system of specific forces. Ideal systems are described by simple, linear equations as, for example, Hooke's Law for ideal solids or Newton's Law for ideal

liquids.

In this section, some basic notions of rheology and constitutive models, which are used to characterize the complex fluids, like mortar, will be introduced. The Vane-Cylinder test, used for investigate the rheological properties of mortar paste, is also presented.

### 1.3.1. Basic notions of Rheology

In this section, we wish to recall the some basic definitions of the rheological science, without particular reference to mortar. These are basic definitions of the parameters involved in the rheometry, including shear stress, shear rate, viscosity, yield stress and fluidity index.

#### 1.3.1.1. Shear stress $\tau$ (Pa)

A shear stress, denoted  $\tau$ , is defined as a stress, which is applied parallel or tangential to a face of a material, as opposed to a normal stress, which is applied perpendicularly. In particular as shown in figure 1.18, it will result in a strain, or deformation, changing the square into parallelogram.

The formula to calculate average shear stress is:

$$\tau = \frac{F}{A} \quad (1.15)$$

where  $\tau$  is the shear stress, F is the force applied and A is the cross sectional area.

#### 1.3.1.2. Shear rate $\dot{\gamma}(s^{-1})$

Consider a volume material as a set of parallel molecular layers kept between two parallel planes with the distant h between them as described in the figure1.18. One of the planes is fixed, and the other is displaced by a distance dx at a constant speed  $V_0$ .

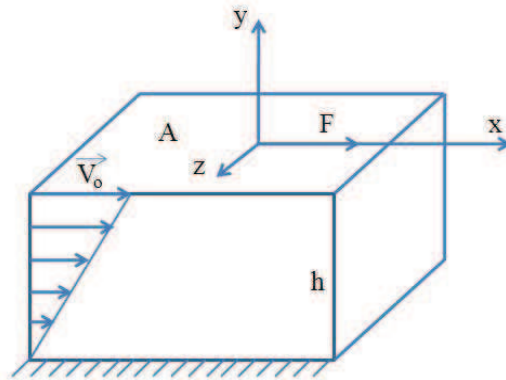


Figure 1. 18. Simple schematic of shear rate

Under the effect of tangential forces, the upper molecular layers move at the same speed. The

lower layers will move in the same direction but with smaller and smaller velocities. They create a gradient of velocity between the two planes.

The displacement between two planes is defined as the deformation of the volume material, denoted  $\gamma$ , follows the relation:

$$\gamma = \frac{dx}{dz} \quad (1.16)$$

The standard constant velocity gradient across the sample is defined as the shear rate.

Also called strain rate or shear rate, it is the strain rate between two adjacent layers of the sheared fluid. It is often presented as the derivative versus time of the deformation:

$$\dot{\gamma} = \frac{d\gamma}{dt} = \frac{d}{dt} \left( \frac{dx}{dz} \right) = \frac{d}{dz} \left( \frac{dx}{dt} \right) = \frac{dv}{dz} \quad (1.17)$$

### 1.3.1.3. Viscosity (Pa.s)

Viscosity is the fluid resistance to shear or flow. It is a measurement of the adhesive/cohesive or frictional property of fluid which is being deformed, i.e., by a shear stress. The fluid's resistance to flow is caused by intermolecular friction exerted when layers of fluids attempt to slide by one another.

The knowledge of viscosity is needed for proper design of required temperatures for storage, pumping or injection of fluids. There are two related measures of fluid viscosity - known as dynamic (or absolute) and kinematic viscosity.

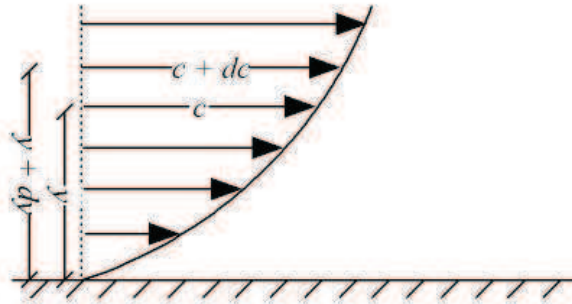


Figure 1. 19. Simple schematic of Viscosity

- *Dynamic viscosity*  $\mu$  is the tangential force per unit area required to move one horizontal plane with respect to the other at unit velocity when maintained a unit distance apart by the fluid. It can be expressed as following:

$$\tau = \mu \frac{dc}{dy} \quad (1.18)$$

and

$$\mu = \frac{\tau}{\frac{dc}{dy}} = \frac{\tau}{\dot{\gamma}} \quad (1.19)$$

in which,  $\tau$  is the shearing stress,  $\mu$  is the dynamic viscosity.

In conclusion, the dynamic viscosity (sometimes referred to as Absolute viscosity) is obtained by dividing the Shear stress by the rate of shear strain. The unit is Force/Area x Time = Pa.s.

- *Kinematic viscosity* is the ratio of absolute or dynamic viscosity to density - a quantity in which no force is involved. Kinematic viscosity can be obtained by dividing the absolute viscosity of a fluid with its mass density:

$$\nu = \frac{\mu}{\rho} \quad (1.20)$$

in which  $\rho$  is the mass density,  $\nu$  is the kinematic viscosity and  $\mu$  is the dynamic viscosity of fluid.

#### 1.3.1.4. Yield stress $\tau_0$ (Pa)

The yield stress is defined as the minimum applied shear stress that we observed a fluid flow in the materials. When the applied shear stress is lower than this value, the material shows the solid-like behavior (no flow, no permanent deformation). Pass through this threshold, there will be a transition from solid-like to liquid-like behavior. The material will be sheared.

There are different methods to measure the yield stress which sometimes lead to different physical notions, using different types of rheometer.

The most commonly used method for obtaining the value of yield stress is to shear the testing sample over a range of applied shear stresses, plot the shear stress as a function of shear rate and fit the curve (using various available models) through the data points (see figure 1.20).

There are two approaches to determine the yield value. The first approach is to start with the sample in its at-rest state (no permanent deformation) and incrementally increase the stress until we identify a value at which it starts to flow. It means that the fluid sample goes from solid-like behavior to liquid-like behavior. This value is called a static yield stress - the stress at which we initiate flow.

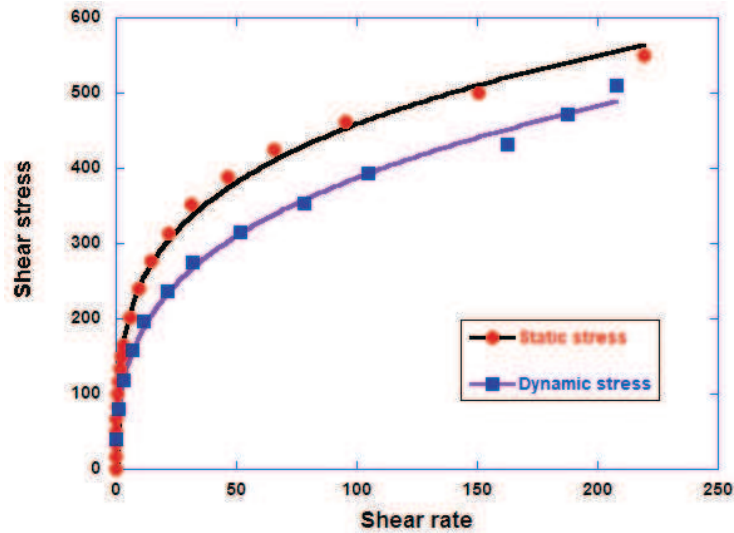


Figure 1. 20. Determination of static / dynamic yield stress; The data points obtained in case of using the base mortar formulation as: 5% Vinnapas®5010N 0, 22% Methocel 21% water

Another approach is to look at the sample in motion (i.e. under shear) and try to investigate from this how it behaves when not in motion. The so-called dynamic yield stress is the value at which the fluid sample goes to solid-like behavior from the initial liquid-like behavior.

In figure 1.20, we have performed the calculation of the yield stress by fitting the curves through the data in case of fresh mortar, using the formulation of 5% of Vinnapas® 5010N; 0, 22% of Methocel and 21% of water. The intersection with the stress axis is taken as the yield stress. It is then assumed that any applied stress below that is insufficient to cause a flow inside the mortar sample. Static yield stress is considerably higher than its dynamic yield stress for any given product.

In order to characterize a product, one can use either static or dynamic yield stress depending on the application purpose. The dynamic yield stress is used in investigating the mortar properties after pumping. In the present study, we use the static yield stress combined with other parameters, including the consistency coefficient and fluidity index, to characterize the rheological properties of adhesive mortar in fresh state.

### 1.3.2. Constitutive equations of rheological models

Rheological properties of fresh cement pastes were calculated from the resulting flow curves, using various rheological models. In this section, the mathematical equations of these models will be presented.

The rheological behavior of fluids flow can be classified into Newtonian and non-Newtonian fluids based on the relationship between the shear stress and shear rate. If this relationship is linear, the fluid is Newtonian. Otherwise, it is non-Newtonian. Typical flow curves of shear

stress versus shear rate for different rheological behavior models are shown in figure 1.21.

At the fresh state, mortars (complex fluid) can be characterized by its rheological parameters at the stationary state like yield stress, plastic viscosity, etc. We assume that there is no time-dependent behavior (thixotropy, creep, etc.).

The Bingham fluids, which exhibit a linear behavior of shear stress against shear rate and has a yield stress value, is given by the following formula:

$$\tau = \tau_0 + \mu_0 \dot{\gamma} \quad (1.26)$$

where  $\tau$  is the shear stress applied to the material,  $\tau_0$  is the Bingham yield stress, describing the stress needed to initiate flow,  $\mu_0$  is the Bingham plastic viscosity, which is the resistance of the material to flow, and  $\dot{\gamma}$  is the shear strain rate.

Bingham model is used to characterize the fluids which have a constant viscosity value. For fluids which have a shear-dependent viscosity, shear thinning and shear thickening, the Bingham model is generalized to Herschel-Buckley, in which the shear stress experienced by the fluid is related to the shear rate is a non-linear way.

$$\tau = \tau_0 + K \dot{\gamma}^n \quad (1.27)$$

The consistency coefficient  $K$ , the fluidity index  $n$ , and the yield stress  $\tau_0$  are three parameters characterize Herschel-Buckley fluids. The consistency  $K$  is a simple constant of proportionality, while the flow index  $n$  measures the degree to which the fluid is shear-thinning or shear-thickening. We see that in the equation 1.27, when  $n=1$  and  $\tau_0 \neq 0$ , the fluid behavior is Bingham. When  $n=1$  and  $\tau_0=0$ , the fluid is Newtonian. By variation of  $n$  and the yield stress  $\tau_0$ , we can express the shear thinning as well as the shear-thickening fluids.

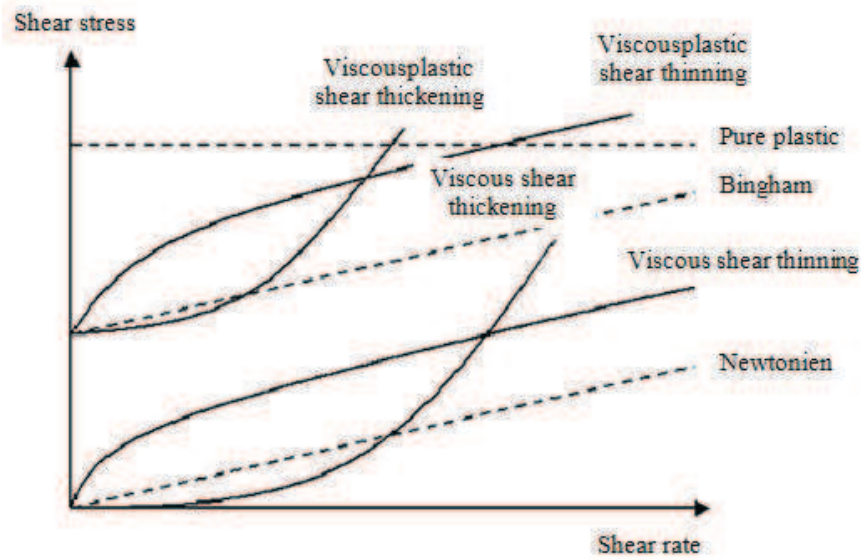


Figure 1. 21. Rheological behavior models

Some other models were commonly used in characterizing rheological behavior of cement pastes are listed in table 1.3 in the following.

Table 1. 3. Commonly used rheological models and their applications

Models	Constitutive equation
Casson	$\sqrt{\tau} = \sqrt{\tau_0} + \sqrt{\mu_p} \sqrt{\dot{\gamma}}$
Modified Bingham	$\tau = \tau_0 + \mu_p \dot{\gamma} + c \cdot \dot{\gamma}^2$
Sisko	$\mu = \mu_\infty + K \cdot \dot{\gamma}^{n-1}$
Williamson	$\mu = \frac{\mu_0}{1 + (K \dot{\gamma})^n}$
Vom-Berg	$\tau = \tau_0 + a \sinh^{-1} \left( \frac{\dot{\gamma}}{b} \right)$
Robertson-Stiff	$\tau = a(b + \dot{\gamma})^c$
Briant	$\tau = \mu_\infty \dot{\gamma} \left( 1 + \frac{\tau_\infty}{a \mu_\infty \dot{\gamma}} \right)^a$

The various models were fitted to measured flow curves using rheological data analysis software [61], which also estimate the standard error for the various rheological models using the equation 1.35. This standard error will be used as a scale for measuring the relative level of accuracy of the different rheological models. The calculation of standard error is based on the standard deviation normalized by the difference between the maximum and minimum

measured values multiplied by 1000 as follows:

$$S.E. = \frac{1000 \cdot [\sum (X_m - X_c)^2 / (n - 2)]^{1/2}}{\text{Range}} \quad (1.35)$$

Here,  $X_m$  = measured value,  $X_c$  = calculated value,  $n$  = number of data points and Range = maximum value of  $X_m$  - minimum value of  $X_m$  [60].

Fresh mortar is a yield stress fluids, it can behave as a Newtonian or non-Newtonian fluid with yield. Thus, in order to estimate the yield stress, model Bingham and Herschel-Bulkley are normally used.

### 1.3.3 Rheological measurements

The aim of rheological tests is to select the correct type and dosage rate of constituents in order to improve placement (or processing) characteristics of the materials.

A mortar can be considered to be a fresh concrete without the coarse aggregate and its testing has attractions for the study of the effects of ingredients at small scale [59]. Banfill has described the use of the Viskomat as a small calibrated mixer for mortar testing [Banfill 1994]. More recently, E.Bauer 2007 used a rheometer equipped with Vane-cylinder geometry to investigate the rheological properties, including yield stress, of non-Newtonian fluids (figure 1.22). It was concluded that the Vane system is an efficient method to measure the yield stress of non-Newtonian fluids [Bauer 2007].

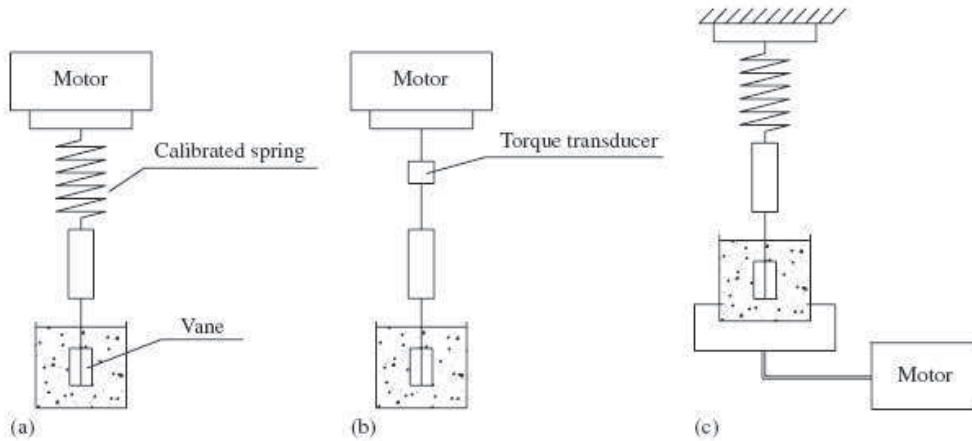


Figure 1. 22. Measuring based structure in vane cylinder test [66]

In the Vane method, the yield stress were obtained by rotating the vane slowly at a constant shear rate/shear stress to detect the yielding moment when the testing sample inside the cylinder changes from the solid-like state to liquid-like state. Once flow starts, the resulting viscosity at a given shear rate can describe the smoothness of the mortar. The existence of a



yield point value means the destruction of a structure to induce flow into the system. Today, commercial rheometers are available that can apply a lower shear stress than the existing yield stress.

In the present work, the rheological properties of the mortars are determined using the rheometer AR2000ex from TA Instruments, equipped with 4-blade vane geometry (figure 1.23). Vane geometry is recognized to be suitable for granular pastes like mortars since with this system wall-slippage is minimized (the material is sheared in volume) [Bauer 2007, Stokes 2004]. The gap thickness (distance between the periphery of the vane tool and the outer cylinder) is taken 8.3 mm, which is more than an order of magnitude higher than the maximum size of the grains (0.5 mm). Then, the measurements may not be sensitive to the discrete aspect of the mortar composition. On the other hand, since the gap thickness is not sufficiently smaller than the vane tool diameter, the variation of the shear rate and shear stress throughout the gap space cannot be neglected. Therefore the fundamental rheological quantities cannot be determined straightforwardly from the measured torque and the rotational velocity of the vane tool. A calibration method, which is described in details in [Bousmina 1999], is then used.

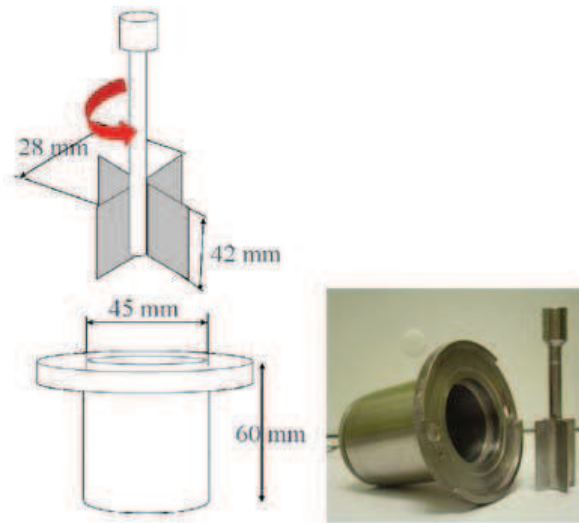


Figure 1. 23. Dimension of Vane-Cylinder in Vane method

The determination of a yield stress as a true material parameter in any system is difficult as the measured value is usually dependent on the measurement technique and apparatus, and/or the model used to evaluate rheological data. Therefore, there is not an accepted standard procedure for determining the yield stress, and there are many differing views on the concept of a yield stress. The yield stress is indirectly determined using rheological models. In this study, we use the model of Herschel-Buckley to fit with the flow curves.

## CHAPTER 2

# *Experimental techniques*

### Contents

<b>2.1. Apparatus and Materials .....</b>	<b>33</b>
2.1.1. Apparatus.....	33
2.1.2. Material used.....	36
2.1.3. Mortar formulations .....	40
<b>2.2. Experimental procedures .....</b>	<b>42</b>
2.2.1. Probe Tack test.....	42
2.2.2. Vane-cylinder test.....	44

The experimental program is presented herein. Firstly, we introduce some general information about our rheometer, together with other apparatus, including a balance and a mixer. The mixing procedure is also given here. This part is then followed by the presentation of the materials used and the formulation of the mortar. And then, in the next section, we show the experimental procedures, Probe tack test and Vane-Cylinder test, which were used for characterizing the adhesive properties and rheological behavior of fresh mortars.

## 2.1. Apparatus and Materials

### 2.1.1. Apparatus

In our study, we have used a rheometer, a mixer and two balances for investigating the properties of mortar in fresh state. These apparatus will be introduced herein.

#### 2.1.1.1. Rheometer AR2000ex

To measure rheological properties of mortars, flow tests were performed using a high-accuracy rheometer (figure 2.1), a commercial rheometer called AR2000ex of TA instrument series.

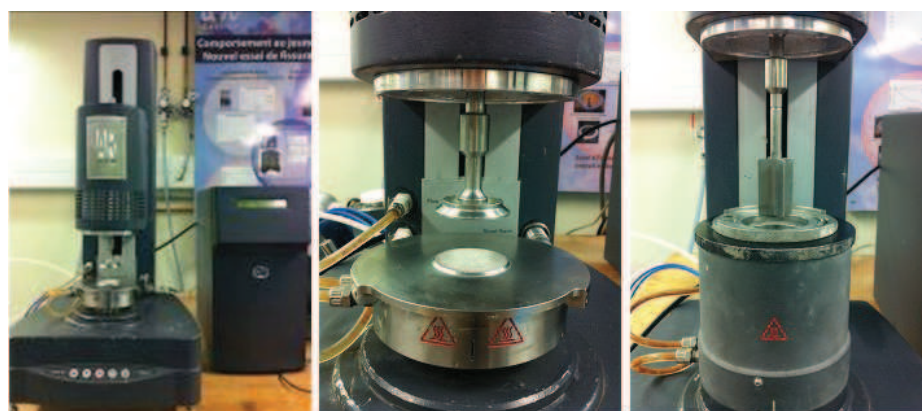


Figure 2. 1. The rheometer used for the experiments - (a) The AR2000ex machine of TA instrument series; (b) Schematic used for “Tack test”; (c) Schematic used for “Rheology”

This rheometer includes a unique ultra-low inertia drag cup motor and porous carbon air bearings for outstanding controlled stress, direct strain and controlled rate performance. The high resolution optimal encoder, high stiffness low inertia design make the AR2000ex extremely versatile and appropriate for a wide variety of applications including characterization of delicate structures in fluids of any viscosity, polymer melts, solids, and reactive materials.

This rheometer is capable of continuous shear rate sweep, stress sweep and strain sweep. The capabilities of the device regarding shear rate, shear stress, torque, angular velocity

sweep and other parameters are listed in table 2.1.

Table 2. 1. Specifications of AR2000ex

Minimum Torque Oscillation CR	0.3 $\mu$ N.m
Minimum Torque Oscillation CS	0.1 $\mu$ N.m
Minimum Torque Steady CR	0.05 $\mu$ N.m
Torque Range Steady Shear CS	0.1 $\mu$ N.m
Maximum Torque	200 mN.m
Motor inertia	15 $\mu$ N.m.s
Angular velocity Range CS	0 to 300 rad/s
Angular velocity Range CR	1 E <sup>-8</sup> to 300 rad/s
Displacement resolution	40 nrad
Step change in velocity	25 ms
Step change in strain	60 ms
Normal / Axial force Range	0.005 to 50 N

The temperature of the specimen is kept constant during the entire time span of the experiments through a water circulation system around the sample container [60]. Here, the temperature is kept at room temperature, 25°C (to within 0.1°C). In order to minimize water evaporation the cup of the measurement system was sealed.

Rheometer AR2000ex can be used for characterizing cement pastes in fresh state. Different geometries are used to test for rheological properties by simply changing fixtures. In this study, parallel plates and coaxial cylinders (vane and cylinder) were used, represented in figure 2.1. Parallel plates are used for investigating the behavior of mortar in tension (tack test), while vane-cylinder is used for characterizing fresh mortar in shearing condition.

#### 2.1.1.2. Balances & Mixer

##### ❖ Balances

We used the two balances shown in figure 2.2. The left one is a high accuracy balance, which is used for measuring the quantity of the polymer and other additives used in small quantities. In our study, for investigating the effect of one type of additive, its dosage rate must be varied. In some cases, the minimum content by weight is taken 0.05%. It means that for a mix of 300 grams, we need an amount of 0.15 grams of polymer. A balance with a precision of 0.001 gram will be useful in these cases. The maximum capacity of this balance is 120 grams.

For measuring the quantity of other constituents, which are used at high percentages, i.e. sand, another balance is used. The precision of this balance is 0.1 gram and the maximum capacity is around 300 grams. This balance is used for measuring the weight of sand, lime, cement and water.



*Figure 2. 2. Balances*

#### ❖ Mixer

After the preparation of the mortar components in prescribed quantity, dry-mortar was blended with water by a vertical axis mixer. This mixer is capable of preparing the cement pastes in the laboratory (figure 2.3). Mortar is mixed at room temperature to within 0.1° (25° C).

The mixing has an important role in obtaining a homogeneous cement pastes. In order to have a reliable investigation of the fresh mortar, a uniform mixing procedure must be made. In our study, he mixing procedure includes the following steps:

- (1) Mixing of the dry components at low speed (60 rpm) for 30s
- (2) Addition of the required quantity of water
- (3) Mixing at low speed for 30s
- (4) Stop the mixer in 30s. During this time, the material is mixed by hand to recover the sticking material to the container's wall
- (5) Mix at high speed (125 rpm) for 60s.

In order to minimize the difference between the obtained mortars pastes, the above step (4) must be paid attention that the action of hand mixing is almost the same for all cases. This ensures that mortars pastes in the same state will be obtained in all cases.

The mortar sample was poured into the rheometer after 5 minutes resting from the end of mixing to start the experiments. The measurements were performed during the induction

period, characterized by a very low hydration rate, which may not influence the properties of the test material.

In the tack measurement, the weight of mortar for each experiment is taken very small (0.27N). Therefore each mixture can be used to perform many experiments. Between experiments, the mortar must be sealed to prevent it from drying, which influence the properties of mortar.

In order to obtain a homogeneous mortar paste, the minimum weight of the dry mortar must be 300g for each mix.



*Figure 2. 3. Vertical axis mixer*

### 2.1.2. Material used

The mortar formulation is chosen depending on the objectives of the study. However, in general, the constituents of the mortar include cement and/or lime, sand, and admixtures. The admixtures can be a combination of several types of polymers.

The binder comprises a Portland cement (CEM I 52.5 N CE CP2 NF from Teil-France) and a hydraulic lime (NHL 3.5 Z).

We use standard sand CEN EN 196-1 ISO 679 in order to minimize phase separation. The CEN standard sand (sand ISO standard) is natural sand, silica especially in its finer fractions. It is clean; the grains are isometric and rounded shape generally. It is dried, screened and prepared in a modern workshop with all guarantees of quality and consistency. Table 2.2 shows its particle size determines by sieving complies with standards EN 196-1 and ISO 679. It indicates that the cumulative refusal of the sand remaining on the sieve size of 1.6 mm is  $7 \pm 5$  %, whereas the remaining sand on the sieve size of 2 mm is 0 %. This explains the choice of the tested mortar layer that the taken thickness must be sufficient for the mortar to

flow during the experiments. It is chosen 3 mm in tack tests and 8 mm in rheological measurements.

Table 2. 2. The size distribution of standard sand CEN ISO

Sieve opening of meshes (mm)	Cumulative refusal (%)
0.08	99 ± 1
0.16	87 ± 5
0.50	67 ± 5
1.00	33 ± 5
1.60	7 ± 5
2.00	0

We have investigated the effect of five types of admixtures, including fibers, cellulose ethers (Methocel), hydroxyethyl methyl cellulose (walocel), bentonite and re-dispersible polymer powder (Vinnapas 5010n). The physical characteristic of these admixtures will be introduced in the following.

❖ **Fibers:**

As having discussed in the section 1.1.1, fibers are often included in the mix-design to avoid creeping in the fresh state and improve the mortar properties in both the fresh and hardened state. In the present study, we use a modified cellulose fibers, which included both high-performance fibers (aramids and high-modulus high-strength polyethylene) and low-cost fibers (polypropylene). The average length of the fibers is about 1 mm and their average diameter on the order of 10  $\mu\text{m}$ .

❖ **Cellulose ether:**

Methocel (from Dow Chemicals company) is used as thickeners, binders, film formers, and water-retention agents. In this thesis, we have investigated the fresh state properties of mortar using a particular type with the trade name 'Methocel 10-0353'. The typical viscosity of it in a certain condition of (Brookfield RVT, 20 rpm, 20°C, 2% in water) is 15.000 mPa.s. This is advised to use for base plaster, absorbent substrate and decorative render by the producer. Methocel helps increasing the workability and the consistency of the used mortar.



❖ **Hydroxyethyl methyl cellulose:**

Cellulose ethers such as hydroxyethyl methyl cellulose (HEMC) is a common admixtures in factory made mortars for various applications including cement spray plasters, tile adhesives, etc. It has been published many researches of the influence of HEMC in the case of various application fields, such as biological macromolecules [Jiang 2011, Angadi 2010, Percin 2011], carbohydrate polymers [Said 2006, Stefan 2005, Chen 2010], etc. However, there are few published studies concerning the influence of HEMCs on the fresh state properties of cementitious materials including cement grouts [Sigh 2003, Pourchez 2006], cement-based mortars [Patural 2011]. In this study, we have studied the effect of three types of HEMCs whose trade names are MKW20000 PP01 (denoted A), MKW30000 PP01 (denoted B) and MKX70000 PP01 (denoted C). They are commercialized by Dow Chemical. Typical physical characteristics of A, B and C are introduced in Table 2.3. It indicates that these three polymers have different molecular weights. Therefore a discussion on the effect of molecular weight to the fresh state properties of mortar will also be implemented.

Table 2. 3. Typical physical characteristic of three types of walocel

Properties	MKW20000 PP01 (A)	MKW30000 PP01 (B)	MKX70000 PP01 (C)
Form	Powder	Powder	Powder
Solubility	Water soluble	Water soluble	Water soluble
Viscosity <sup>(1)</sup> , mPA.s	20000	30000	70000
pH (2% solution)	Neutral	Neutral	Neutral
Molecular weight	600.000	680.000	1.000.000

(1) solution in water, Haake Rotovisko RV 100, shear rate  $2.55 \text{ s}^{-1}$ ,  $20^\circ\text{C}$

A and B are designed for cement spray plaster applications, such as one- or two-coat cement-based plaster and cement-based lightweight plaster, while C is designed for cement-based applications such as cement-based tile adhesives. A and B impart well-balanced properties, including high standing strength and stabilization of air voids, while C imparts well-balance properties, including open time, adhesion and shear strength. These three types of HEMCs also add good workability and enhance water retention.

❖ **Vinnapas 5010n**

Vinnapas (also from Dow) has been widely used in tile adhesives, grouts, mineral plasters,



sealing slurries, gypsums, repair mortars, exterior insulation and finish systems (EIFS), self-leveling compounds and powder paints. A commercial product in the Vinnapas system, 5010n, has been used. Vinnapas 5010n is a copolymer powder of vinyl acetate and ethylene latex. It is dispersible in water and has good saponification resistance. Typical characteristic of this polymer powder is presented in table 2.4 and 2.5.

Table 2. 4. Typical general characteristic of Vinnapas 5010n

Property	Inspection method	Value
Film properties of the redispersion	specific method	cloudy, tough-elastic
Minimum film forming temperature	DIN ISO 2115	4°C
Particle size	DIN EN ISO 4610	Max. 4°C over 400 µm
Predominant particle size at redispersion	specific method	0.5-8 µm
Protective colloid / emulsifier system	specific method	Polyvinyl alcohol

Table 2. 5. Specification data of Vinnapas 5010n

Property	Inspection method	Value
Bulk density	DIN EN ISO 60	490.0-590.0 kg/m <sup>3</sup>
Ash content	specific method	9.0-13.0 %
Solids content	DIN EN ISO 3251	98.0-100.0 %

❖ **Bentonite clay:**

Sodium bentonite clay, which is in particular employed in drilling mud and retaining fluids formulations [Grim 1978, Menezes 2010], is used. Such additives serve as thixotropic and thickening agents, and must present particular rheological properties such as a high yield stress to prevent sedimentation [Laribi 2005].

❖ **Air entraining agent:**

A certain dosage rate of a commercial air-entraining agent, which is named NANSA LSS, is used to guarantee moderate rheological properties within the resolution range of our rheometer.

### 2.1.3. Mortar formulations

#### 2.1.3.1. Fiber reinforcement

The formulation of fiber-reinforced mortar is represented in table 2.6. The fiber percentage by weight is varied between 0 and 0.82%. The water dosage rate is fixed to 30 % by weight for all the mortar pastes considered. Other constituents' contents are also fixed as represented in table 2.6.

The influence of fiber reinforcement on the properties of mortar is discussed in chapter 3.

Table 2. 6. Fiber-reinforced mortar formulation

Constituent	Cement	Sand	Fibers	Methocel	Water
% (by weight)	30	70	Varied (0-0.82)	0.22	30

#### 2.1.3.2. Cellulose ether

The only variable formulation parameter is the amount of polymer additives. In the present study, the high molecular weight water-soluble polymer is a commercial cellulose ether-based polymer (*METHOCEL*<sup>TM</sup> 0353, named here Methocel), available in powder form and usually employed to formulate industrial mortars, similarly to the Walocel grades. Methocel and Walocel are similar polymers (associative polymers). The polymer content is varied according to the following proportions:  $C_e = [0.05; 0.1; 0.15; 0.2; 0.25]$  % by weight.

Table 2. 7. Polymer-modified mortar formulation, case of Methocel

Constituent	Cement	Lime	Sand	Air entraining	Methocel	Water
% (by weight)	15	5	80	0,01	Varied	16

The water dosage rate is fixed to 16% by weight for all the investigated pastes. A certain dosage of air training agent (0.01%) is always used to guarantee the moderate rheological properties within the resolution range of our rheometer.

The mortar composition corresponds actually to a basic version of commercially available render mortars.

#### 2.1.3.3. Sodium bentonite

We consider the formulation given in table 2.7 and we set a cellulose-ether content equal to 0.05 %. We will focus on their rheological and adhesive effects when added to mortars. The bentonite content has been varied in the following range: [0.05; 0.2; 0.5; 0.8; 1; 2] % by weight, while the percentages of the other constituents remained unchanged (table 2.7).

The results, which concern the influence of cellulose Methocel and of bentonite clay, are discussed in chapter 4.

#### 2.1.3.4. Vinnapas 5010n

The combination of inorganic and polymer binders in dry-mix mortars is essential to modern construction techniques. In this part of study, we will see the influence of the combination of organic additives (cellulose-ether) and a dispersible polymer powder, Vinnapas 5010n, in fresh state.

The formulation of test mortar is shown in table 2.8, in which the cellulose-ether content was set equal to 0.22 %. We have varied the content of Vinnapas 5010n, which is supplied by Parex Lanko Company. The typical general characteristic and specification data of Vinnapas 5010N are shown in table 2.4 and 2.5. The dosage was varied in the following range: [1; 2; 3; 4; 5] % by weight. The water content remained unchanged at 21 %. The content of other constituents such as cement, lime and sand are shown in table 2.8.

Table 2. 8. Polymer-modified mortar formulation, case of Vinnapas

Constituent	Cement	Lime	Sand	Methocel	Vinnapas	Water
% (by weight)	15	5	80	0,22	Varied	21

The results concern the influence of Vinnapas 5010n is then presented in chapter 6.

#### 2.1.3.5. Hydroxyethyl methyl celluloses (HEMCs)(Walocel)

The weight proportion of each constituent of the mortar is represented in table 2.9.

Table 2. 9. Polymer-modified mortar formulation, case of HEMC

Constituent	Cement	Lime	Sand	Air entraining	HEMC	Water
% (by weight)	15	5	80	0,01	Varied	19

The Walocel content in the mortar formulation is varied according to the following proportions:  $C_e = [0.19; 0.21; 0.23; 0.25; 0.27; 0.29; 0.31]$  % by weight. The water dosage rate is fixed to 19% by weight for all the investigated pastes.

The results obtained by the tack test and rheology measurement of mortar formulated by this formulation are presented in chapter 5.

## 2.2. Experimental procedures

### 2.2.1. Probe Tack test

The experimental set-up is represented in figure 2.4. The rheometer is equipped with a two-parallel-plates geometry. The mortar pastes are inserted between two parallel plates with rough surfaces (to minimize wall-slippage) (figure 2.6), and then squeezed out at a given velocity ( $500 \mu\text{m/s}$ ) to reach an initial gap thickness of 3 mm (illustrated in figure 2.5) before separating them at different applied velocities.

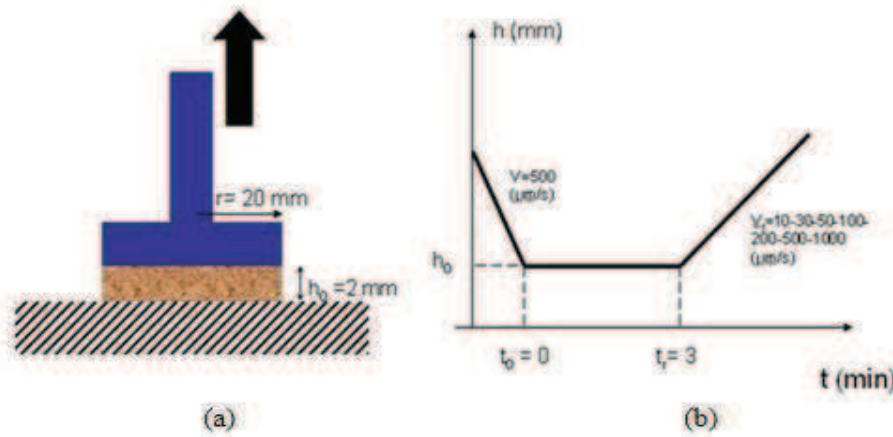


Figure 2. 4. Probe Tack test - (a) Experimental set-up; (b) Test procedure

The diameter of the mortar sample, which is equal to that of the two plates' surfaces, is 40 mm. Since the initial gap thickness (3mm) is much smaller than the diameter of the sample, one can assume that, at least in the beginning of the stretching test, the flow is a priori dominated by the shear component. The lubrication-type approach may then apply.

The initial weight of the tested sample must be taken the same for all the experiments. In our study, it was taken 0.27N. It helps to determine the weight of the material that remains stuck on the upper plate (which gives the adherence strength).

The experiment procedure has 3 steps: Firstly, the mortar sample is compressed to the gap thickness of 3mm. In the second step, the material is left to relax for 3 minutes for erasing eventual memory effects. By recording the evolution of the normal force, it is checked that a steady state is actually reached within this period of time. Tack measurement takes place in the third step. In this step, the material is stretched with different pulling velocities until the sample has totally separated. The experiment has to be stopped correctly on time, when there is no connection through material between two parallel plates. This helps the accurate determination of the adherence force.

The pulling velocity is varied between two orders of magnitude (between 10 and 1000  $\mu\text{m/s}$ ). At least 3 different runs are performed for each freshly prepared sample.

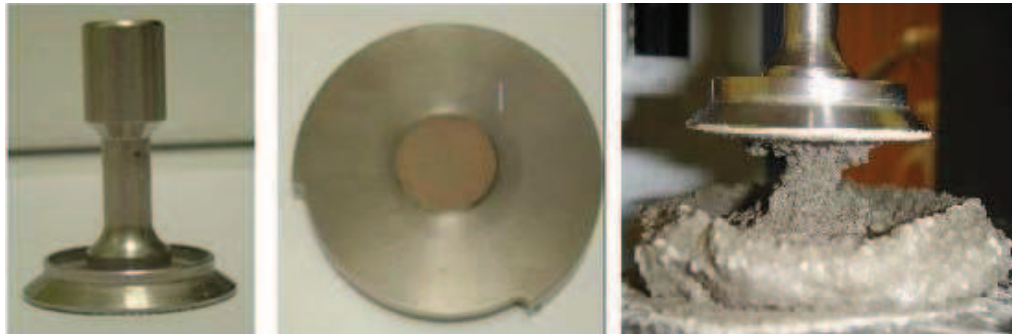


Figure 2. 5. Tack geometries - (a) Upper plate; (b) Bottom plate; (c) A tack test in process

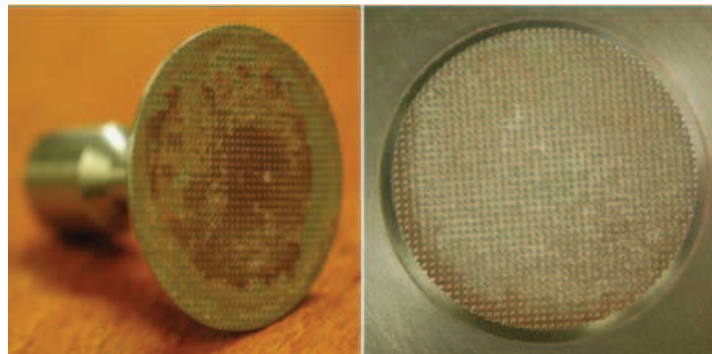


Figure 2. 6. Square grooves on the two plates surfaces

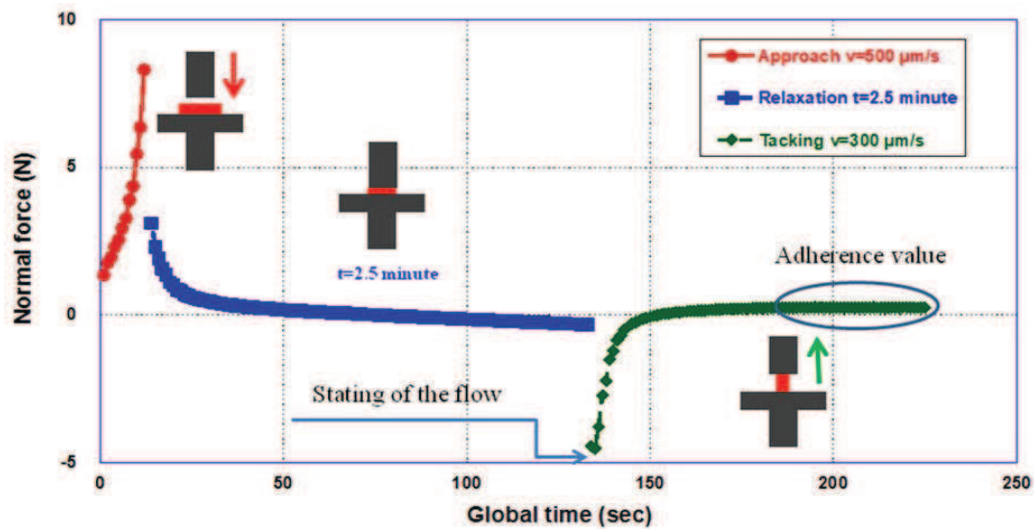


Figure 2. 7. A typical evolution of recorded normal force versus time obtained in the probe tack test

A typical pulling curves obtained in the tack experiment is illustrated in figure 2.7. The relaxation time was taken to be 2.5 minutes and the separation velocity was 300  $\mu\text{m/s}$ . Although there are three steps in the experiment, we are interesting in studying the third step that corresponds to the adhesive properties of the material. From these obtained force curves, the adhesive parameters, including adhesion force, cohesion force, interface adherence, and the adhesive failure energy, will be determined.

In all the tack experiment, the initial weight of the test sample is taken to be 0.27 N.

### 2.2.2. Vane-cylinder test

As introduced in the previous chapter, for characterizing the rheological properties of the mortars by minimizing slippage, the rheometer is equipped with 4-blade vane geometry (figure 1.23). Yet, with this geometry the tested material is not subjected to a uniform shear rate. This condition is usually required in rheological measurements in order to measure actual material properties, and to have an analytical relationship between the measured torque/rotational velocities and shear rate/shear stress. Nevertheless, vane geometry has been retained since it is appropriate for high yield stress fluids such as dense granular suspensions, including mortars [Kaci 2010], as slippage can be avoided and the material can be sheared in volume.

The yield stress is measured with the vane-cylinder geometry in stress controlled mode in which a "ramp" of steps of increasing stress levels is applied to the vane immersed in the material, and the resulting shear rate is measured as a function of applied stress. The yield value is determined from the critical stress at which the material starts to flow. Between two successive steps there is no pre-shear or rest. The measurement point duration is set and assumed that equilibrium reached at each stress condition to obtain a flow curve. In the present study, the point duration is set 1-2 minute depending on the mortar formulation.

Depending on each specific experiment, we have to perform the test at least three times to determine the best possible procedure. In the first run, the interval between two successive steps must be chosen large enough to reduce the duration of the test. The yield stress is determined, but with a low precision. And then, for the latter runs, the measuring points must be increased around the determined yield point. That would help to determine a high accuracy yield stress of the test sample.

The measuring procedure is shown in figure 2.8, in which both increasing and decreasing ramps of shear stress were imposed to the material. The applied stress is slowly increased until a threshold deformation, at which the sample starts changing from solid-like to liquid-like behavior. This value is considered to be the yield stress of the testing mortar. Below this value, the shear rate is almost equal to zero and the behavior of the mortar is viscoelastic, while beyond the yield stress the shear rate increases quite rapidly from zero and the behavior of the mortar has liquid-like behavior.



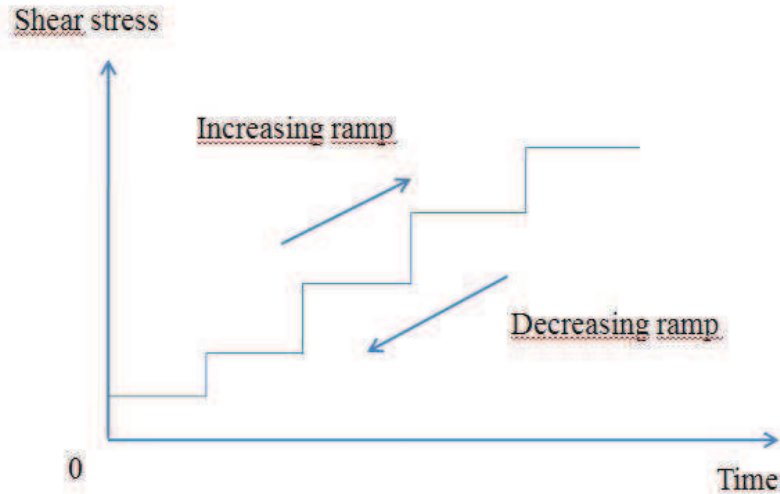


Figure 2. 8. Measuring protocol for Vane configuration

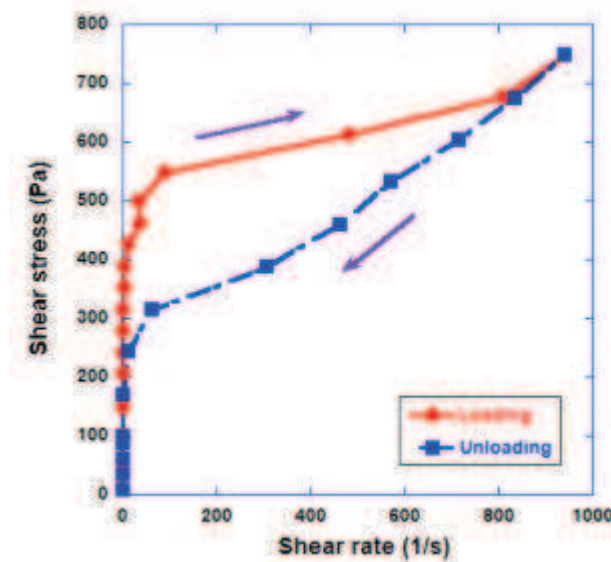


Figure 2. 9. Typical flow curves of mortar with the addition of 0.29% of polymer

A typical curve obtained in the rheology test, which consists of a loading and an unloading curve, is presented in figure 2.9. The yield stress is determined by the critical stress at which we observe the transition from solid state to liquid state of the material. However, in actual experiments, almost all cases, the transition from solid to liquid state is occurred gradually and is hard to detect. Therefore, it is difficult to determine the exact value of the yield stress. So, different models have been developed in order to determine the value of the yield stress as well as other rheological parameters by fitting the flow curves' data with the model's equation. In this study, we use the most general models for concentrated suspensions, that is Herschel-Bulkley's, which is characterized by the equation 1.27. In some cases the use of Herschel-Bulkley model leads however to non-physical values of the yield stress (negative), this parameter is then determined by the applied stress at which we obtained a finite shear rate

( $0.01 \text{ s}^{-1}$ ). These tests led to the determination of three rheological parameters, including yield stress, consistency coefficient and fluidity index. The influence of various types of admixtures on the shear properties was investigated through these three rheological parameters.



CHAPTER 3

Cellulose Fibers

Contents

3.1. Effect of fiber on the adhesive properties ..... 48

    3.1.1. Tack test results ..... 48

    3.1.2. Adhesive strength ..... 51

    3.1.3. Cohesion force ..... 52

    3.1.4. Adherence force..... 53

    3.1.5. Adhesive failure energy..... 54

3.2. Effect of fiber on rheological properties..... 55

    3.2.1. Flow curves ..... 55

    3.2.2. Rheological parameters..... 57

3.3. Compare the adhesive properties to the rheological behavior ..... 58

3.4. Conclusion..... 60

In this chapter, the influence of cellulose fibers on the adhesive and rheological properties of mortars in fresh state is investigated. The mortar formulation has been given in Table 2.6. The Probe tack test and vane-cylinder measurement have been used. In Probe tack test, the pulling velocity was varied between 10 and 1000  $\mu\text{m/s}$ . The normal force during the pulling process was recorded as a function of time. From these data, the adhesive properties of the mortar pastes, including adhesion strength, cohesion, and adherence will be investigated.

The rheology tests were performed under stress-controlled mode, in which the applied stress was increased step by step, and the measured shear rate was recorded. This resulted in a shear stress versus shear rate evolution curves. These curves were used to determine the rheological parameters of the mortar pastes, including yield stress, consistency and fluidity index as discussed in chapter 2.

This chapter consists of 4 sections. The first section introduces the effect of fiber on the adhesive properties of fresh mortars. The rheological measurements for mortar pastes with varying fiber concentration will be discussed in section 3.2. This section is then followed by the comparison between the adhesive and rheological behavior of mortar pastes in the presence of fiber reinforcement. The last section gives the conclusion of the chapter.

### **3.1. Effect of fiber on the adhesive properties**

#### **3.1.1. Tack test results**

The evolution of the recorded normal force versus time is plotted in a semi-logarithmic scale for different applied pulling velocities at 3 percentages of fibers in figure 3.1. Each figure corresponds to a given dosage rate of fibers, including 0.13; 0.55 and 0.82%. Other results for additional fiber contents are represented in appendix A.1. These flow curves were taken from the “pulling-out” steps with different applied pulling velocities, including 10, 30, 50, 100, 200, 300, 500 and 1000  $\mu\text{m/s}$ .

The force curves have roughly the general shape represented schematically in figure 2.8a. It rises, passes through a maximum and monotonically decreases to a plateau. Each curve consists of 3 different zones. However, at high velocities the “viscous-elastic” zone (increasing part of the force curve) is difficult to be observed. In particular at 1000  $\mu\text{m/s}$  it was not possible to observe this part of the force curve. This is due to the limited rate of data acquisition of our experimental set-up (1 measure per second).

From these data, the different parameters, including adhesive strength, cohesion force, adherence force and adhesive failure energy of the separation process, will be considered. In the following, the evolution of these parameters with the variation of the fiber dosage rate will be discussed.

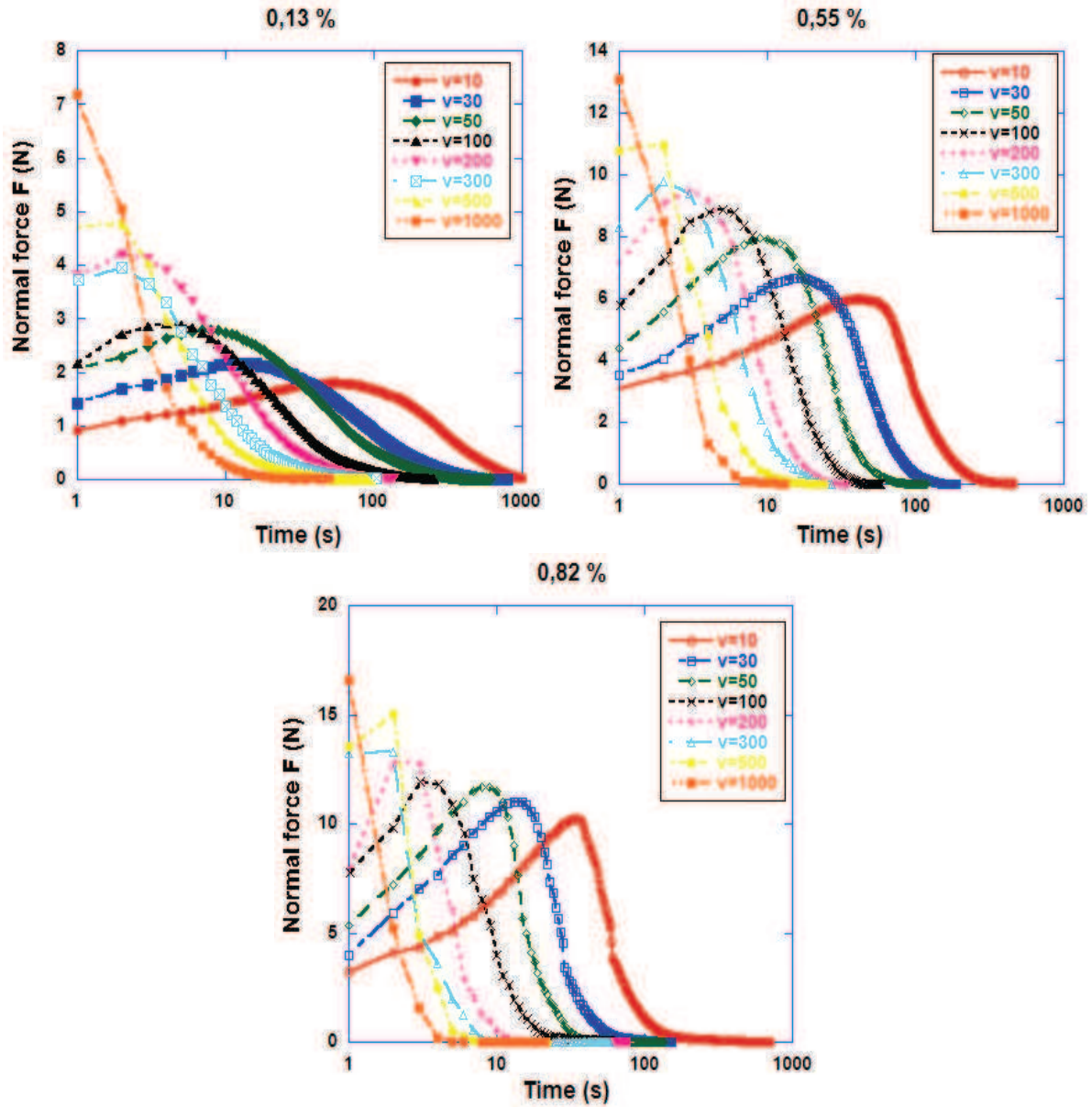


Figure 3. 1. Evolution of the stretching force versus time as a function of pulling velocities (in  $\mu\text{m/s}$ ) for different contents of fibers

In order to investigate further the dependency of the adhesion of mortar on the pulling velocity, the evolution of the nominal stress versus nominal strain needs to be considered. First, let us recall the calculation of these values.

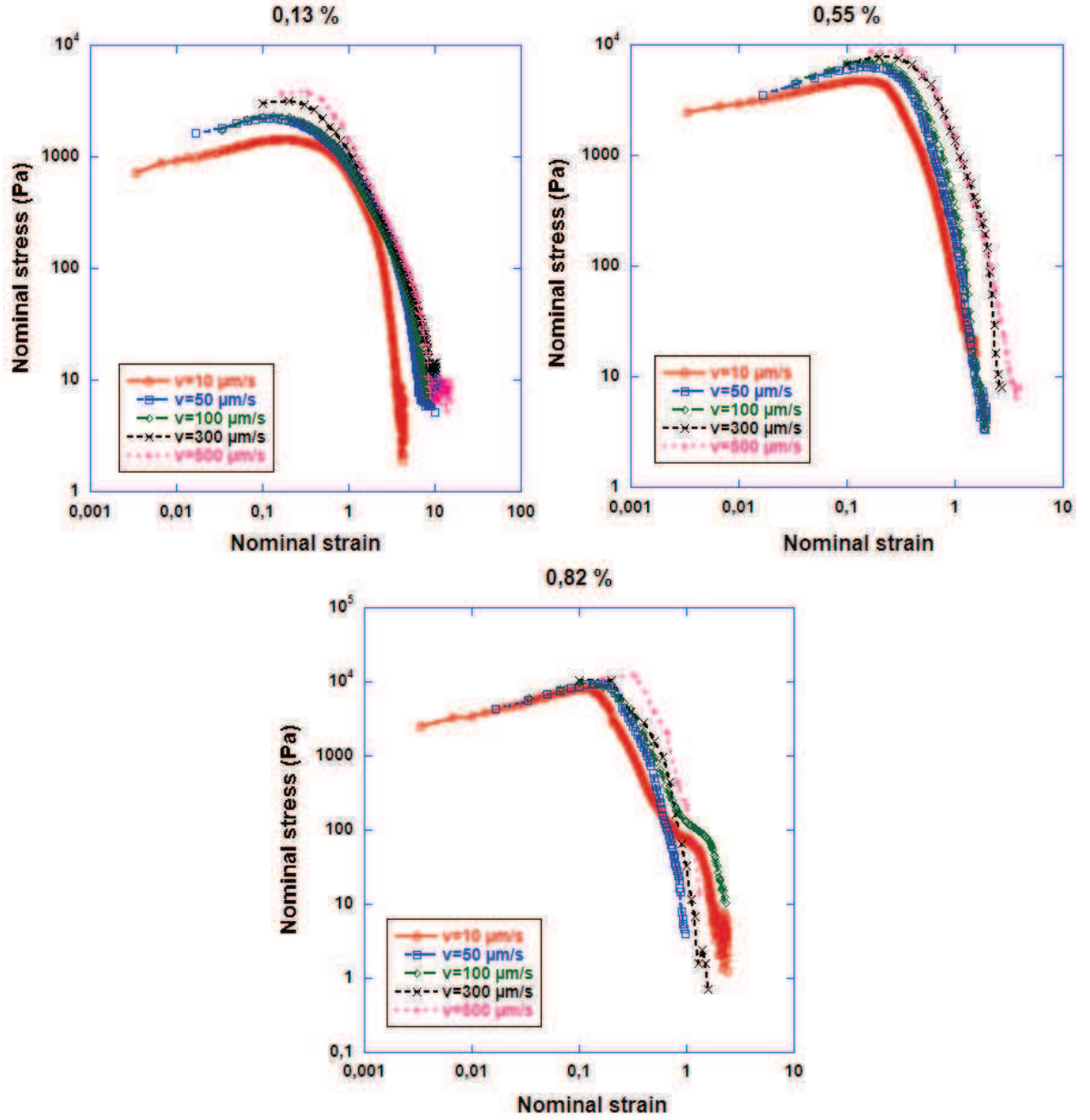


Figure 3. 2. Nominal stress versus nominal strain for varying pulling velocity at certain contents of fiber

Nominal stress presents an average stress ( $\sigma_{avg}$ ) over the area, assuming that the stress in the cross section is uniformly distributed. It is calculated by the following equation:

$$\sigma_{avg} = \frac{F_n}{A} \quad (3.1)$$

in which A is the cross-sectional area. In the Probe tack test, we use two parallel circular plates with the diameter of the two plates is 40 mm, so  $A = \pi \cdot r^2 = 0.001257 \text{ m}^2$

The engineering normal strain or nominal strain of a material axially loaded is defined as the change in length per unit of the initial length of the element. In the probe tack test, the testing sample is stretched, the nominal strain is positive. We have  $e = \frac{\Delta L}{L_0}$ , in which e is the nominal

strain,  $L$  is the initial length of the two plates,  $L=3\text{mm}$ .  $\Delta L$  is the displacement between the upper plate and the lower plate which is fixed;  $\Delta L = v \cdot t$ ;  $v$  is the pulling velocity and  $t$  is the time at which we calculate the nominal strain  $\epsilon$ .

After calculating the nominal stress and nominal strain of the testing material at different pulling velocities at each content of fiber, we plotted the nominal stress as a function of nominal strain in the figure 3.2. This figure presents only 3 percentages of fiber additions. The curves corresponding to remaining fiber contents are represented in the appendix A.2.

It can be noticed that the peak nominal strain (around 0.5) does not depend on the pulling velocity, while the peak nominal stress increase with the pulling velocity. The nominal strain corresponds to the starting of the inward flow towards the center of the plates. This suggests that the process of progressive inward flow and rupture of the material is not much affected by the pulling velocities.

### 3.1.2. Adhesive strength

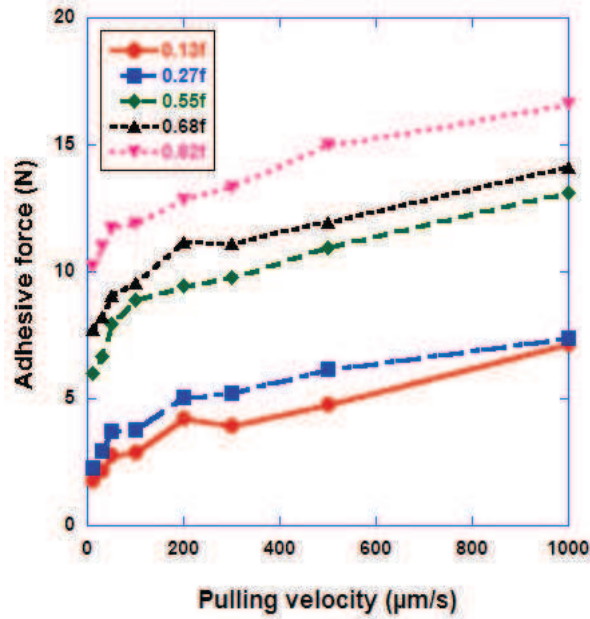


Figure 3. 3. Evolution of the adhesive force as a function of the pulling velocity for different fiber contents – (a) 0.13%; (b) 0.27%; (c) 0.55%; (d) 0.68%; (e) 0.82%

From the measurements represented in figure 3.1, the evolution of the maximum normal force (also referred to as the adhesive force, the starting point of the flow) as a function of the pulling velocity can be determined for each mortar formulation corresponding to a given fiber content. The results are represented in figure 3.3. For each given fiber content, the adhesive force increases with the pulling velocity. Moreover, the sensitivity of the adhesive force to the pulling velocity is almost unchanged. This quantity is independent on the fiber content,

represented by parallel evolution curves in figure 3.3.

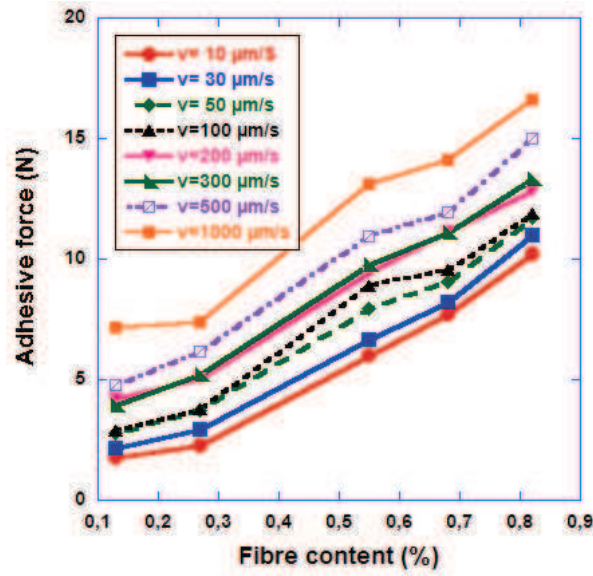


Figure 3. 4. Evolution of the adhesive force as a function of the fiber content for different pulling velocities

The evolution of the adhesive force as a function of fiber content for different pulling velocities is represented in figure 3.5. Up to 0.3% there is only a small increase of the adhesive force. Beyond that dosage rate, the adhesive increases then almost linearly with fiber content. It can be noticed that the slope of the curves is almost independent of the pulling velocity. This behavior will be related to the rheological properties further on.

### 3.1.3. Cohesion force

As it has been discussed above, the adhesive force comprises both viscous effects, which are velocity dependent, and cohesion, which is related to the strength of the interactions between the material components at rest. The paste cohesion can be then determined from the adhesive force at zero-velocity. In the present study, the lowest pulling velocity is  $10 \mu\text{m/s}$ . This is low enough to be considering as zero. Thus the cohesive force of the material is taken as the adhesive force at the pulling velocity of  $10 \mu\text{m/s}$ .

The evolution of the cohesion force versus fiber dosage rate is represented in figure 3.6. Similarly to the adhesive force, we can observe a significant increase of the cohesion when increasing fiber content. Moreover, there seems to be a critical fiber content (located between 0.27% and 0.55%) above which we obtain a huge increase of the cohesion strength. Below this content, the dependence of the paste cohesion to the fiber content is less significant.



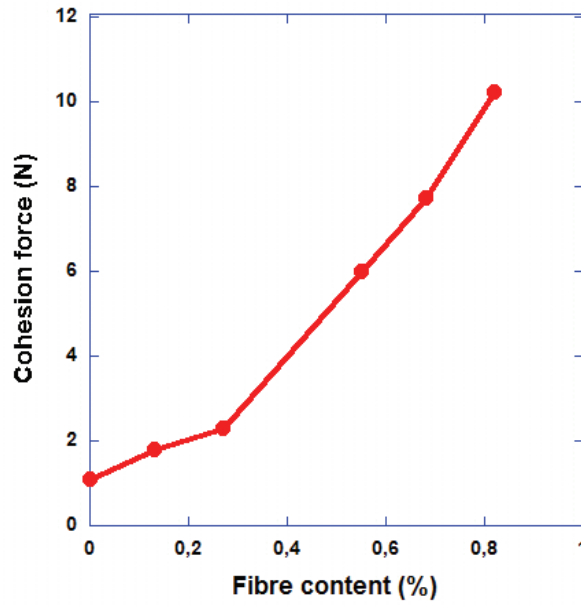


Figure 3. 5. Evolution of the cohesion force versus fiber content

#### 3.1.4. Adherence force

We remind that the adherence force is assumed be equal to the weight of the mortar that remains stuck on the moving plate at the end of the tack test. This is determined from the force curve plateau. The evolution of the adherence force versus fiber content for 3 different pulling velocities is represented in figure 3.7.

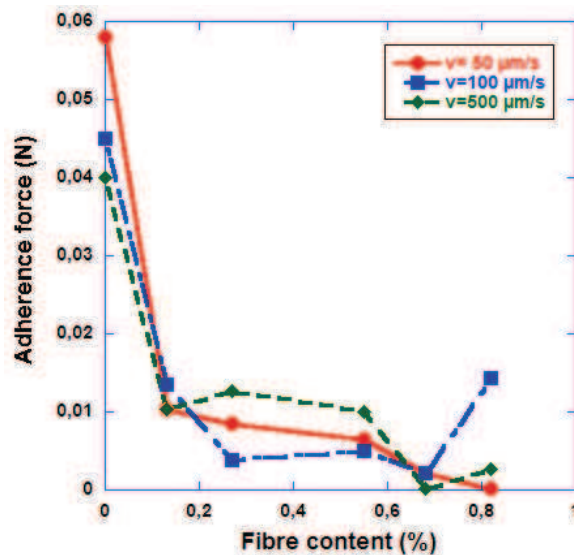


Figure 3. 6. Evolution of the adherence force as a function of fiber content for different pulling velocities

Although the adherence force values are quite small (the accuracy of the force measurement is 1 mN), one can observe a dramatic decrease of adherence when increase the dosage rate of fibers in the formulation. At high fiber content (0.82%), the adherence force is vanishingly

small. It means that there is almost no-mortar remains stuck on the upper plate. This may have important practical implications. The decrease of adherence with fiber content can be related to the evolution of the rheological properties when adding fibers as it is discussed below.

### 3.1.5. Adhesive failure energy

As it has been discussed in the previous section, the adhesion energy is calculated by the equation 1.12. From the experimental data, we can calculate the adhesive failure energy by integrating the normal force versus time data. The calculated adhesion energy is then plotted as a function of fiber dosage rate (figure 3.9) and separation velocity (figure 3.8). Figure 3.8 shows that the adhesion energy decreases with the applied pulling velocity in the separation process. It can be explained that when a high pulling velocity is applied, the layer of mortar between two plates are broken immediately so that there is no time for the particles to rearrange. Inversely, at low pulling velocity, i.e.  $10 \mu\text{m/s}$ , the particles have enough time to rearrange their structure against the separation process. Thus it takes more energy to finish the tack. A.Zosel found similar results in his research in 1985 that the adhesive failure energy is dependence on the rate of separation in the case of elastomeric adhesives [Zosel 1985].

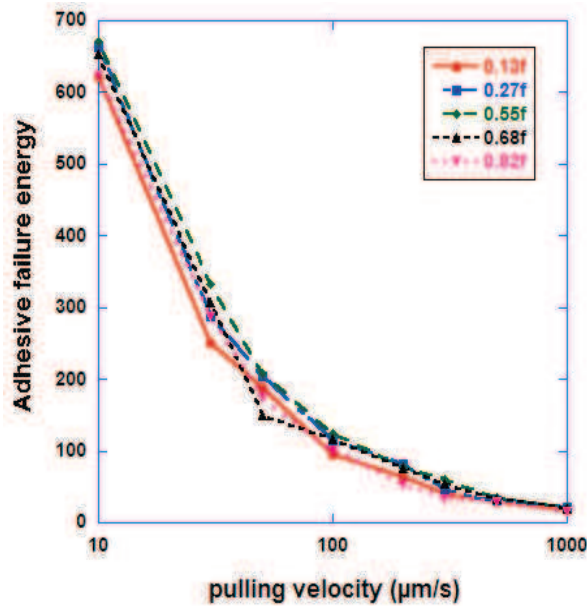


Figure 3. 7. Adhesive energy as a function of the separation rate for different fiber contents

From the evolution of adhesion energy with the variation of fiber content in the figure 3.9, we can see that the adhesion energy is not affected by the variation of fiber dosage rate. Thus we can conclude that the adhesive failure energy of fresh fiber reinforced mortar is independent on the fiber content but is dependence of the rate of separation.



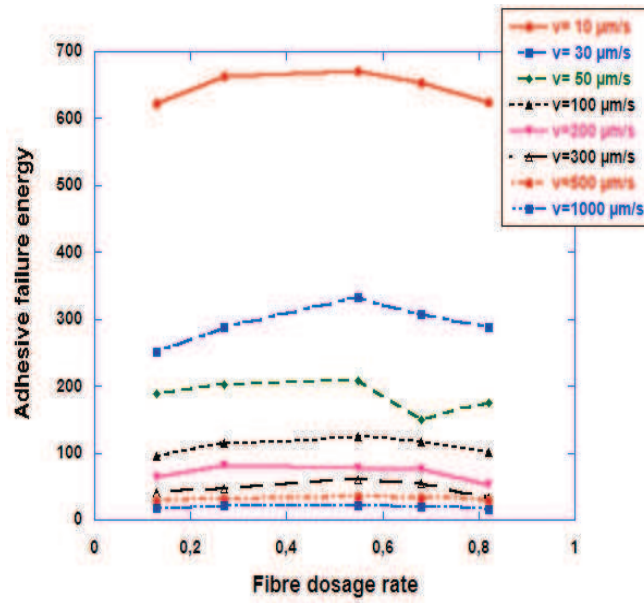


Figure 3. 8. Adhesive energy as a function of the fiber content for different pulling velocities

## 3.2. Effect of fibers on rheological properties

### 3.2.1. Flow curves

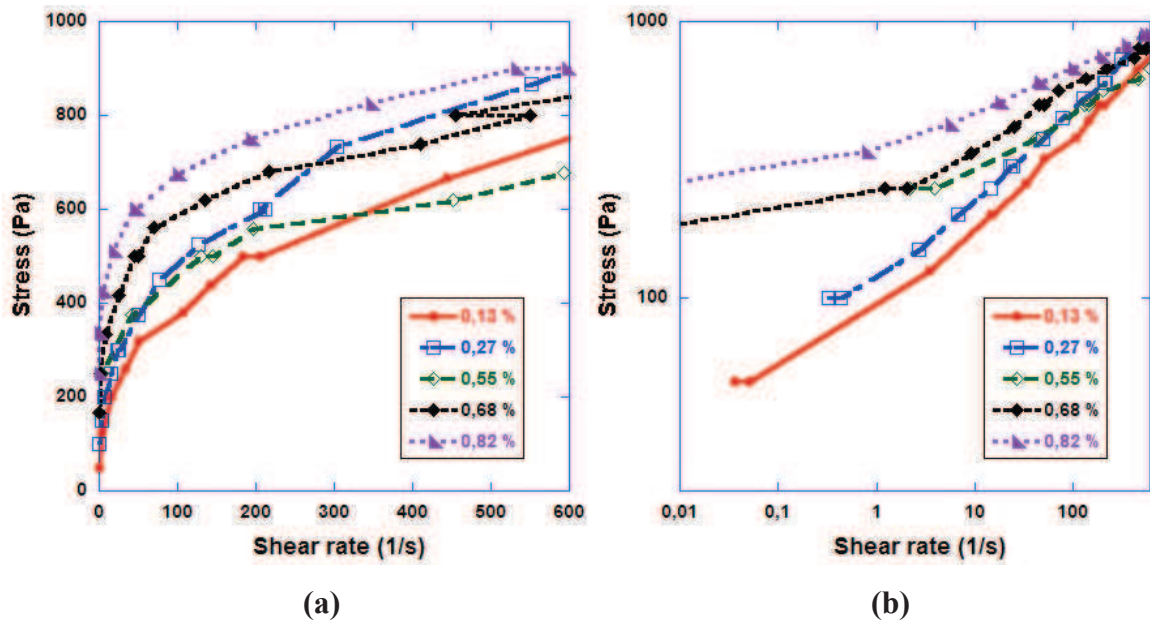


Figure 3. 9. Flow curves of the mortars for different fiber contents  
(a) Linear plot; (b) Logarithmic representation

The flow curves of the mortar pastes for different fiber contents are represented in figure 3.10. These curves were determined at controlled stress mode. Figure 3.10a represents the flow curves in a linear scale to display the overall form of the curves and figure 3.10b represents

the corresponding Log-Log plot in order to highlight the rheological behavior at low shear-rates.

The general form of the flow curves indicates that the mortars behave as Herschel-Bulkley shear-thinning fluids for all the investigated fiber concentrations. Therefore the corresponding rheological parameters are determined by performing the best fit of the experiment data to Herschel-Bulkley model. The evolution of these parameters will be discussed further.

Examining the flow curves, we can observe an expected phenomenon: the flow curves cross over. This means that for some shear-rates and fiber concentration intervals, the apparent viscosity (stress divided by shear-rate) may decrease with fiber content. To the best of our knowledge, this phenomenon has never been reported in the literature.

Figure 3.11 shows the evolution of the apparent viscosity versus fiber content for 3 different shear-rates (low, intermediate and high).

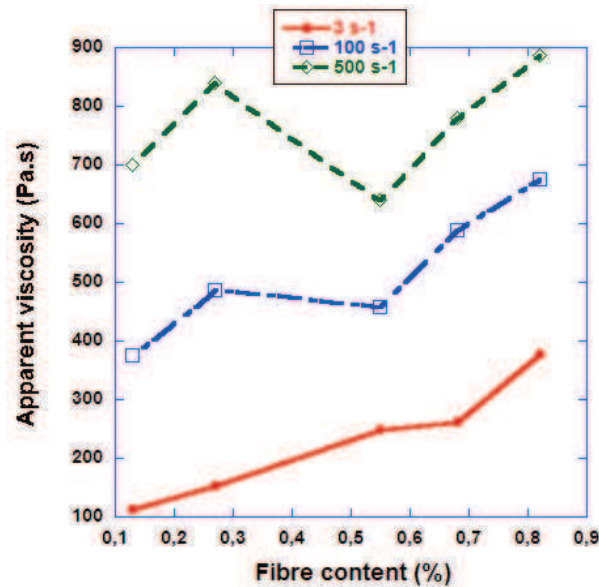


Figure 3. 10. Evolution of the apparent viscosity versus fiber content for different shear-rates

At high shear-rates we can observe a minimum for the apparent viscosity for a fiber concentration of 0.55%. This minimum disappears at low shear-rates. A possible physical origin of the presence of these extremes in the evolution of the apparent viscosity versus fiber content may be the following. The presence of the fibers in the mortar may lead to two different antagonistic effects: on one hand they will increase the viscous dissipation since they resist flow gradients experienced by the liquid phase, but on the other hand they will locally increase the flow-gradient and then decrease the viscosity of the mortar since it is shear-thinning. Then depending upon the value of shear-rate the presence of the fiber may lead to either increase or decrease of the global viscous dissipation (apparent viscosity). There is

another possible explanation for local minima in the viscosity curves: cellulose fibers may increase air-entrainment. The increase of air content will decrease the apparent viscosity and eventually compensate for the fiber effect.

### 3.2.2. Rheological parameters

Rheological parameters, including the yield stress, consistency coefficient and fluidity index, were determined by performing the best fit of the experimental results with the Herschel-Buckley model, which is characterized by the equation 1.27. The evolutions of these parameters are represented in figure 3.12.

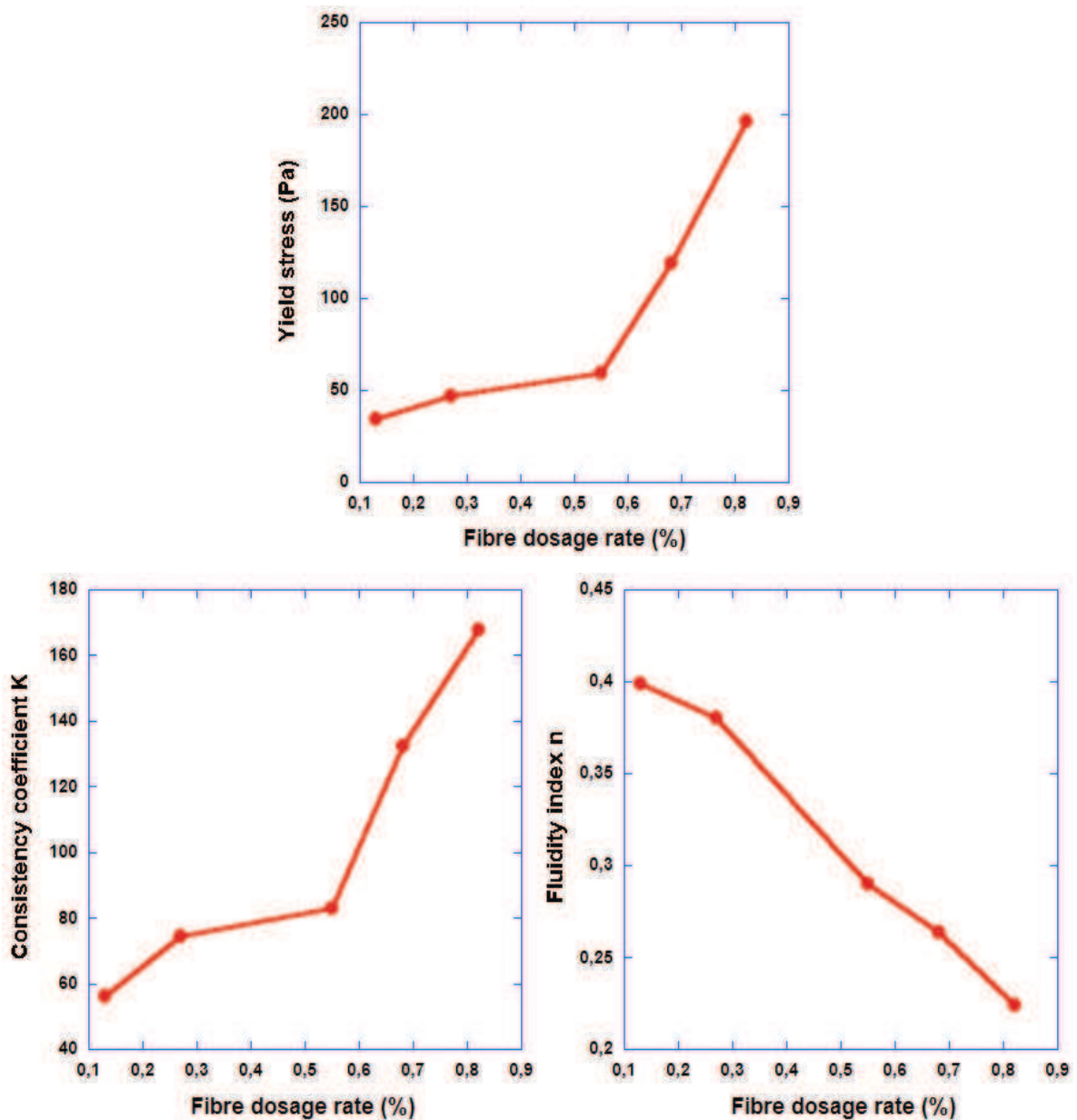


Figure 3. 11. Influence of the fiber content on the rheological parameters of the mortar: Yield stress, consistency coefficient and fluidity index

The yield stress is measured directly by determining the applied stress for which we have a finite shear-rate. As expected the yield stress increases with fiber content. However this increase is not monotonous. Below a certain value of fiber content (around 0.55%) the yield stress has only a moderate dependence upon this additive. Beyond this critical content we obtain a huge increase of the yield stress. The existence of this critical value of fiber concentration may be related the appearance of a significant entanglement of the fibers leading to an interlocking and then a resistance to an initiation of the flow. If this is actually the case the critical concentration will then depend upon the geometry of the fibers (in particular their aspect ratio). A rheological investigation with different fiber sizes is needed in order to check this hypothesis.

The behavior of the consistency is very similar to that of the yield stress. A similar physical interpretation may be then put forward. The monotonous increase of the consistency of mortar pastes reflects the increase of the viscous drag effects with the increase of fiber content.

The fluidity index decreases with fiber content, indicating that the material becomes more and more shear thinning when adding fibers. The increase of the sensitivity of the stress to the shear-rate may be due to the flow induced de-flocculating of fiber aggregates [Chaouche 2001].

### 3.3. Comparing the adhesive properties to the rheological behavior

In the probe tack tests, the instantaneous distance between the plates is small compared to the sample diameter, in particular in the first zone (see figure 2.8) of the tack curves. We can then use the lubrication approach, in which one assumes that the flow is dominated by the shear component, to determine the adhesive force ( $F_{max}$ ). For Herschel-Buckley fluids, this calculation has already been performed in the literature [Meeten 2002].

$$F_{max} = \frac{2\pi R^3 \tau_0}{3h_m} + \frac{2\pi k}{n+3} \left( \frac{2n+1}{n} \right)^n \frac{R^3}{h_m} \left( \frac{RV}{h_m} \right)^n \quad (3.2)$$

in which, R is the mortar sample radius, R=40 mm;  $h_m$  the instantaneous distance between the plates corresponding to  $F_{max}$  and V the pulling velocity. The relationship 3.6 can be used to link the adhesive properties as determined with a tack test to the rheological parameters.

As we have discussed in the previous section, the cohesion force is taken to be the value of the force peak  $F_{max}$  when the pulling velocity tends to zero. It means that from expression (1) we can infer the cohesion force by setting the pulling velocity to zero, which gives:

$$F_{coh} = \frac{2\pi R^3 \tau_0}{3h_m} \quad (3.3)$$

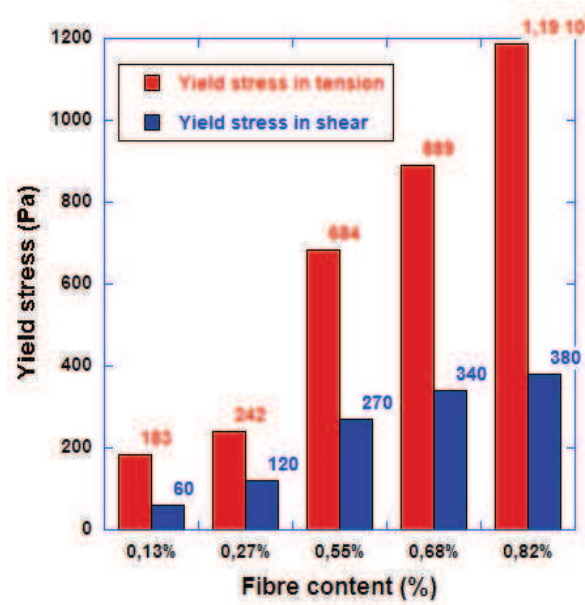


Figure 3. 12. Comparison between the yield stress in tension and in shear for varying fiber contents

In figure 3.13 the cohesive stress (calculated from equation 3.7) is compared to the yield stress for different dosage rates of fibers. These results indicate that the resistance of mortars with fibers is significantly higher in extension than in shear. This can be understood as the following: In shear flow the fiber tend to be orientated in the flow direction, perpendicular to the flow gradient. Consequently they exert quite low resistance to flow. On the other hand in an extensional flow (tack test) the fibers tend to be orientated in the direction of the extensional-gradient and may then contribute significantly to flow resistance.

We cannot go farther and make a comparison between the dynamic rheological properties, including the consistency and the fluidity index, as determined in shear flows and those corresponding to the tack tests. Indeed, in the tack tests the flow-gradients involved are actually very low. The highest shear-gradient can be estimated as  $V_{max}/h_{min} = (1mm/s)/(3mm) = 0.33s^{-1}$ , where  $V_{max}$  is the highest pulling velocity considered in the tack tests and  $h_{min}$  the minimum value of the gap (initial value).

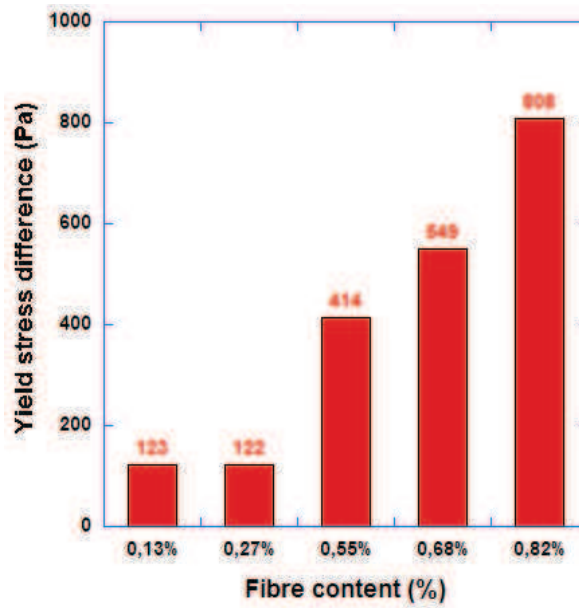


Figure 3. 13. Difference between the yield stress in tension and in shear for varying fiber content

Figure 3.14 represents the difference between the cohesion stress obtained in the tack test and the yield stress determined from the rheology test. At low fiber content, including 0.13 % and 0.27 %, this difference is identical. We observe a plateau of this difference value at low fiber contents. Beyond 0.27 %, we observe a significantly increase in this difference. This can be explained by the change of the concentration regimes of fiber from dilute, through semi-dilute to concentrated regime. When the fiber dosage rate increases, the transition from dilute regime (low dosage rate) to semi-dilute regime and concentrated regime (high dosage rate) occurs. At low fiber content, including 0.13% and 0.27%, each fiber can freely rotate without strong interactions (we have mainly far field hydrodynamic interactions) with the others. Therefore, the adhesive properties and rheological parameters such as adhesion strength, cohesion, consistency and yield stress in shearing condition are lowest at these fiber contents. At high fiber content, there is probably the entanglement and interlocking between fibers and other particles (close contact interactions). That probably leads to the significant decreasing of the resistance difference between tension and shearing conditions, as obtained in figure 3.14.

### 3.4. Conclusion

Adhesive properties of mortars containing different dosage rates of cellulose ether based fibers were studied using the probe tack test. From the measured tack force curves various adhesive quantities were determined, including adhesion, cohesion, adherence and adhesive failure energy. It was found that the evolution of these properties versus fiber content was in

general non-monotonous, comprising low and high increase regimes. Such behavior was attributed to a probable transition to fiber entanglement and interlocking when increasing fiber content. More investigation, in particular by taking into account the fiber geometry, is needed in order to achieve quantitative interpretation of the tack test results.

The adhesive failure energy is independent on the fiber dosage rate, and decreases as the applied rate of separation increases.

Finally, a comparison between adhesive and rheological properties was presented. The results showed that the resistance of the mortars was significantly larger in tension than in shear. The result was similar with the consistency. This was attributed to the difference between the induced orientation of the fibers in extension and shear.

## CHAPTER 4

# *Thickening agents*

### Contents

<b>4.1 Effect of organic additives, case of Methocel.....</b>	<b>63</b>
4.1.1 Effect of Methocel on the adhesive properties .....	63
4.1.2. Effect of Methocel on the rheological behavior .....	70
4.1.3. Compare the adhesive properties to the rheological behavior.....	74
<b>4.2 Effect of mineral additives, case of bentonite .....</b>	<b>75</b>
4.2.1 Effect of bentonite on the adhesive properties.....	75
4.2.2 Effect of bentonite on the rheological behavior .....	81
4.2.3 Compare the adhesive properties to the rheological behavior.....	84
<b>4.3 Comparison between organic and mineral thickeners .....</b>	<b>85</b>
4.3.1. Adhesive properties.....	85
4.3.2. Rheological properties .....	85
<b>4.4 Conclusion .....</b>	<b>86</b>



In this chapter, an investigation on the effect of two types of thickening agents on the adhesive properties and rheological behavior of mortars is presented. An organic additive, Methocel, cellulose ether-based polymer, and a mineral one, sodium bentonite are used. The mortar formulation has been introduced in section 2.1.3.2 and 2.1.3.3.

The fresh properties of the mortars are investigated using the Probe tack test and vane-cylinder measurement. The experimental procedures are similar to those with fibers, and described in section 2.2.

This chapter consists of 4 sections. The effects of two types of thickening agents are discussed separately in the two first sections. In each section, the effect of each additive on both the adhesive properties and rheological behavior is discussed. A comparison between these two properties is also performed. The section 4.3 shows the comparison between the effects of these two additives. In this section, we discussed the influence of organic and mineral additives on the properties of mortar: the similarity and the difference between these additives. The last section is the conclusion of the chapter.

## **4.1 Effect of organic additives, case of Methocel**

### **4.1.1 Effect of Methocel on the adhesive properties**

#### ***4.1.1.1 Tack test results***

Figure 4.1 represents the evolutions of the recorded normal force, under varying velocities and for the formulation with various contents of Methocel. Each graph corresponds to a given polymer content, including 0.1; 0.15; 0.2 and 0.25 %. These flow curves were taken from the tack measurement with different pulling velocities, including 10, 50, 100, 300 and 500  $\mu\text{m/s}$ .

A plot in semi-logarithmic scale has been performed to highlight the behavior around the peak. The force curves are all qualitatively similar. Each curve has roughly the general shape represented in figure 2.8a and consists of three zones. From each measurement, various adhesive quantities can be inferred straightforwardly, including the adhesive strength, cohesive stress, adherence and adhesive energy as will be presented in the following sections.

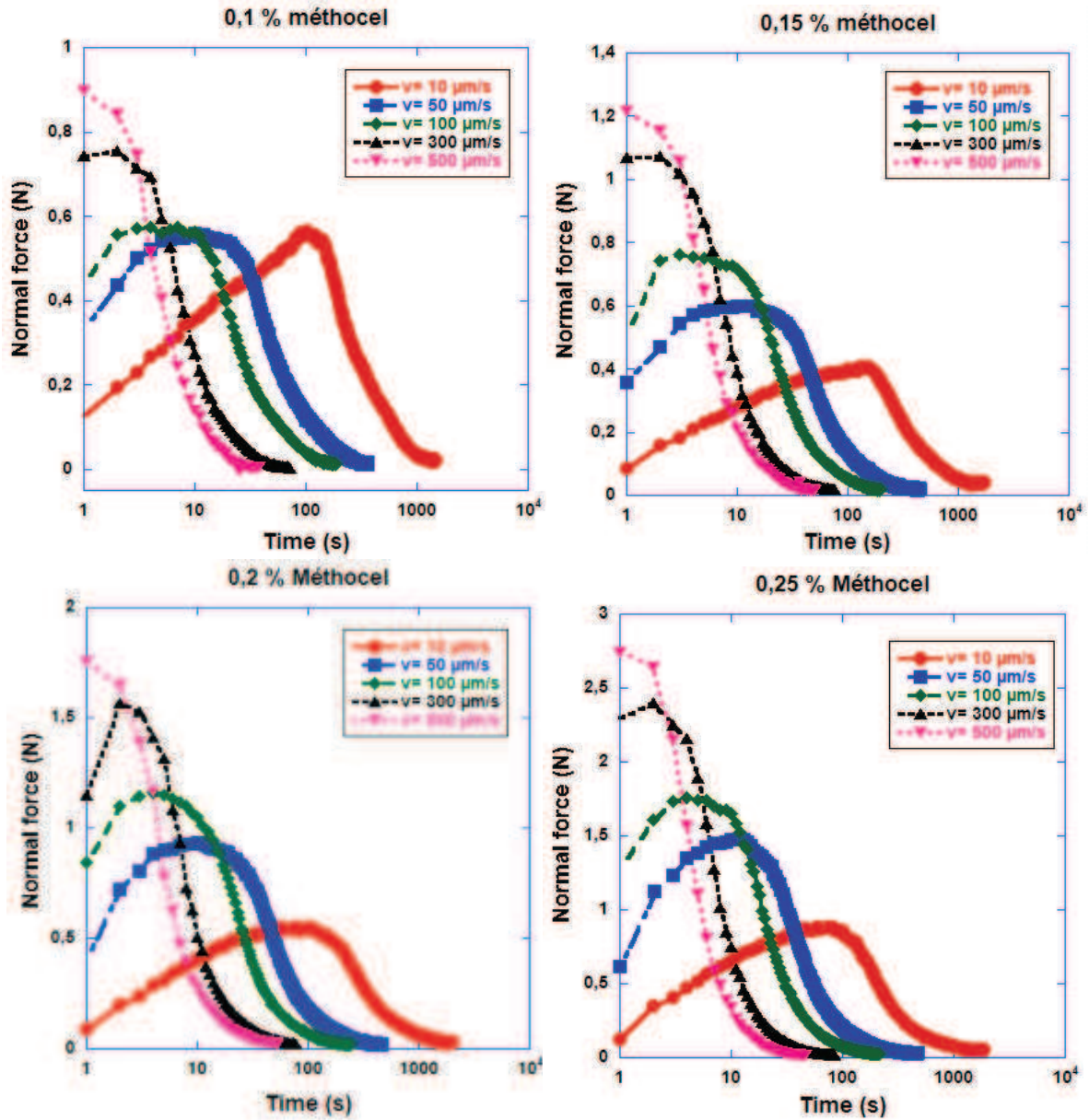


Figure 4. 1. Force versus time curves obtained in Probe Tack test for different polymer contents

We have also represented in figure 4.2 the nominal stress (normal force divided by the nominal surface area of the plate) evolution with the nominal strain (vertical displacement divided by the initial gap), in order to investigate further the dependency on pulling velocity. From figure 4.2, it appears clearly that the peak nominal strain (around 0.5) does not depend on the pulling velocity, while the peak stress increases with the pulling velocity (only for the highest velocities in the case of low dosage). It is similar to the observations of Kaci *et al.*, [Kaci 2009] concerning the influence the same types of additive to the fresh properties of joint mortars. This suggests that the process of progressive inward flow and rupture of the material is not affected by the pulling velocity, and appears rather as characteristic of the paste formulation.

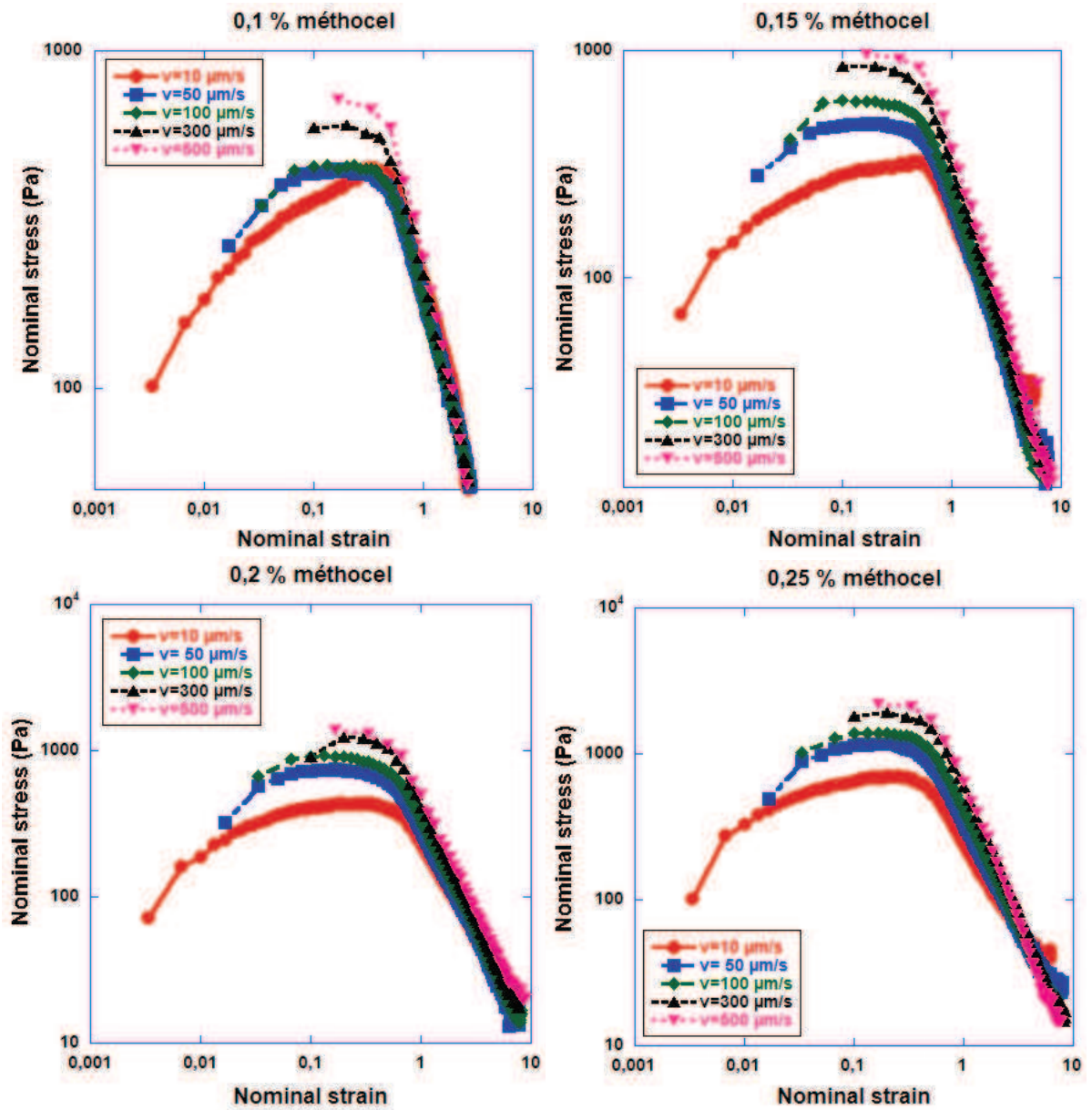


Figure 4. 2. Nominal stress versus nominal strain curves for varying pulling velocities, case of using Methocel

#### 4.1.1.2 Adhesive strength

Figure 4.3a shows the variations of the maximum normal force (referred hereafter as the adhesive force, which characterizes the adhesive strength), with pulling velocity for varying polymer contents. As it is expected, the adhesive force increases with the pulling velocity for all the investigated mortar pastes. Moreover the sensitivity of the adhesive force to the pulling velocity variation significantly increases with polymer concentration. For polymer contents between 0.15% and 0.25%, a strong dependency of adhesion force on pulling velocity is noticed, while for low polymer contents (0.05-0.1%) the force increase is much less

significant. This more marked dependency of adhesion force on velocity, observed for high polymer contents, is expected and can be attributed to an increase of the viscous contribution to the adhesive force with polymer content, which can overshadows the air-entraining and hydrodynamic lubrication effects of the polymer [97].

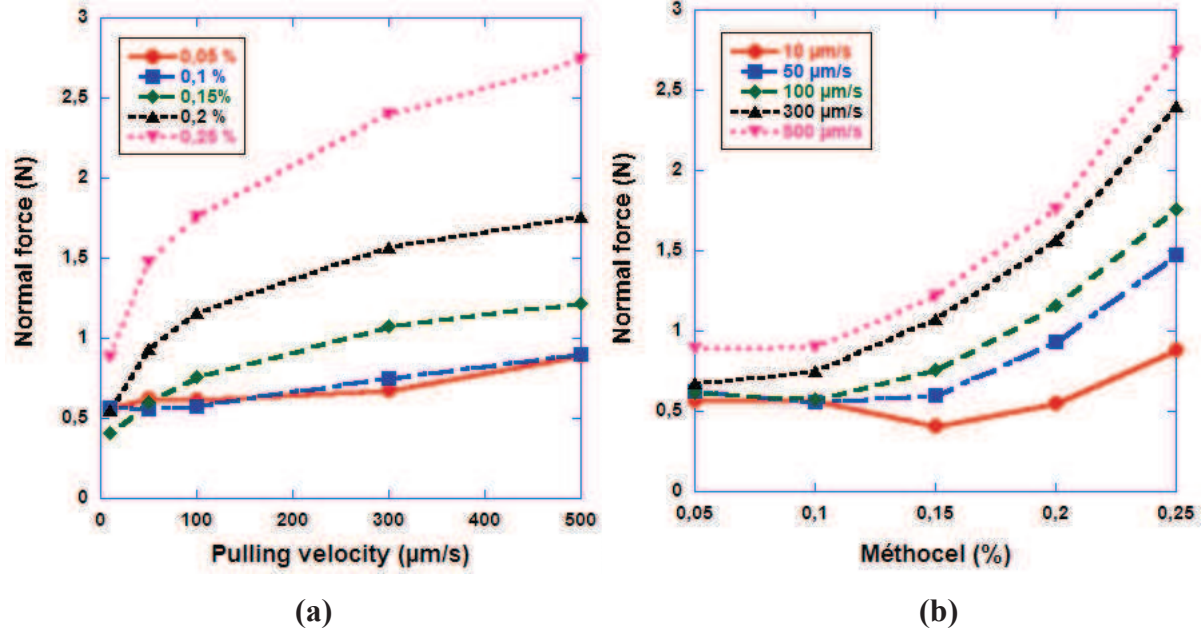


Figure 4. 3. Evolution of the adhesion force as a function of pulling velocity (a) and of cellulose ether contents (b)

This observation is similar to a published research, concerning the influence of a cellulose ether-based polymer on the fresh properties of mortar joints, by A. Kaci *et al.* [Kaci 2009].

From a practical point of view, the latter results highlights the essential difference of behavior between render mortars (which are formulated with  $C_e < 0.1\%$ ), and adhesives mortars characterized by  $C_e$  values higher than 0.2%, which can sustain higher normal stress levels (high tchiness).

The evolution of the adhesive force as a function of polymer content is represented in figure 4.3b. At small pulling velocity, 10  $\mu\text{m/s}$ , we observe a minimum value of adhesive force at 0.15 %. Increasing the pulling velocity this minimum value disappears and then reappears at a smaller polymer concentration: 0.05 % for the velocity 300  $\mu\text{m/s}$  and 0.1 % for other velocities. This observation can be attributed to the interplay between several effects of the polymer in the presence of the solid particles (induced dispersion, lubrication, increase of pore solution viscosity, etc.).

#### 4.1.1.3 Cohesion force

The cohesion force can be identified as the adhesion force corresponding to the lowest value of pulling velocity that can be attained with our rheometer (10  $\mu\text{m/s}$ ) and the evolution of the paste cohesion as a function of polymer content are represented in figure 4.4.

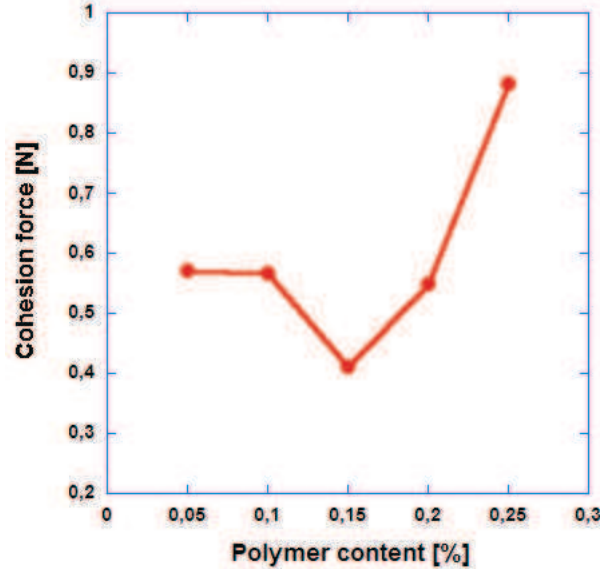


Figure 4. 4. Evolution of the cohesion force with polymer content

Similarly to the adhesion force, the influence of polymer content on the paste cohesion depends qualitatively on the concentration interval considered. The cohesion force evolution with varying polymer content is non-monotonic. For low polymer contents, including 0.05% and 0.1%, the paste cohesion is almost unchanged, represented by a plateau in the above figure. Beyond this content, increasing the polymer concentration first leads to a decrease of cohesion force to a minimum at 0.15%, then followed by a significantly increase of the paste cohesion. The presence of such a minimum has also been reported by Kaci *et al.* for the case of joint mortars [Kaci 2009].

For high percentages in cellulose ether, the observed cohesion strength increase could either be attributed to viscous effects originating from the finite value of velocity employed, or to cohesive effects related with the formation of a polymer gel. If the first assumption is valid, the cohesion should decrease with the pulling velocity employed for its identification. From figure 4.3, we notice that the adhesion force displays an important decrease at low velocities and for high cellulose ether contents. By extrapolating the results to lower values of velocity, we can conclude that the cohesion effort identified at a velocity of 10  $\mu\text{m/s}$  is likely to be over-estimated, and there is no firm evidence that the polymer will increase the true cohesion. At low pulling velocities, we also observe a local minimum in adhesion, which is around 0.15



%. Cohesion variations will be discussed further in relation with the yield shear stress identified from rheological tests.

#### 4.1.1.4 Adherence force

The adherence force is taken to be equal to the weight of material that remains stuck on the upper plate at the end of the tack test. Its weight may be used to characterize the strength of adherence of the material onto the plate's surface. It corresponds to the residual value of the stretching force after completion of the rupture process. Although the adherence force is clearly not a material property, from a practical point of view it will determine the tackiness for render mortars and the effective bonding between masonry elements for adhesive mortars. Figure 4.5 represents the evolution of the adherence force as a function of pulling velocity, and of polymer content, separately.

For low cellulose ether contents ( $C_e < 0.1\%$ ) and high values of pulling velocity, the adherence force is vanishingly small. Above that content, one can observe an increase of the adherence force with the increase of polymer content. This increase is more significant at low pulling velocity ( $10\text{ }\mu\text{m/s}$ ).

Kaci *et al.* have also observed the quasi-monotonic decreasing of the adherence force with pulling velocity for mortar joints [Kaci 2009]. This has been interpreted in relation with the occurrence of various debonding modes. In particular, it has been shown that such mortar pastes display debonding patterns intermediate between a liquid and an elastomeric adhesive, depending on pulling velocity and polymer concentration. For a liquid, rupture occurs through an ax-symmetric flow towards the center of the sample, while an elastomeric adhesive may display either an adhesive rupture at the material-plate interface in which most of the material remains on the lower plate or a cohesive rupture for which a certain fraction of material remains stuck on the surface.

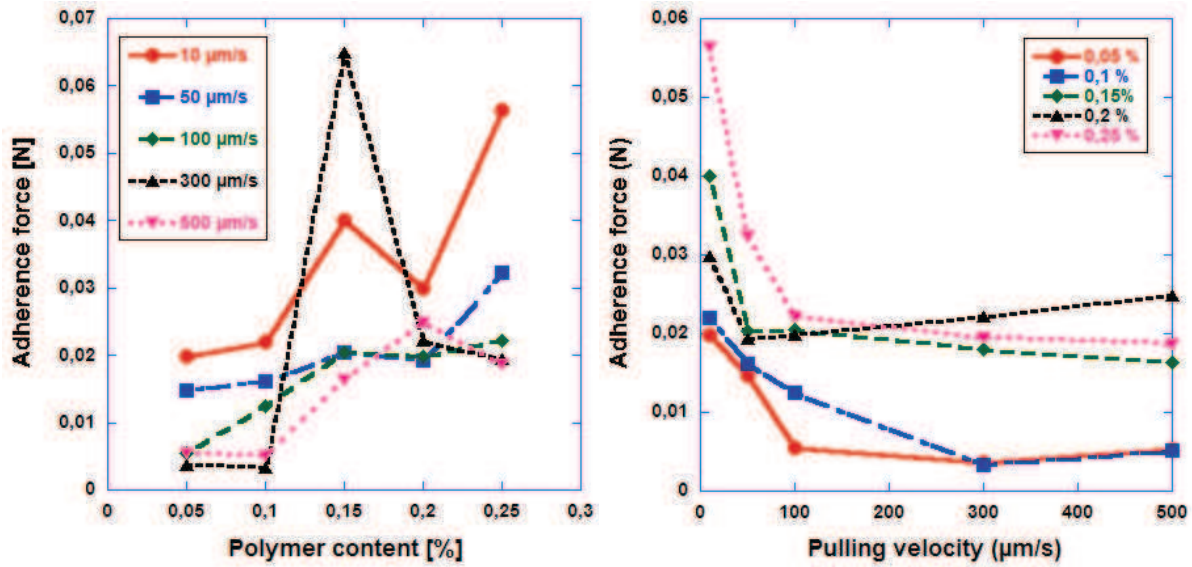


Figure 4. 5. Evolution of the adherence force as a function of pulling velocity and polymer dosage rate

#### 4.1.1.5 Adhesive failure energy

The adhesive failure energy is calculated by equation 1.12. The evolution of the pastes' adhesive failure energies is then plotted as a function of the pulling velocity and of the polymer content in figure 4.6 and figure 4.7.

From figure 4.6, we can observe a significant decrease of the adhesive energy as the pulling velocity increases. This is expected and has been interpreted by the blockage of the mortar constituents at high pulling velocities. At low velocity, the mortar constituents have time to re-arrange, which would lead to higher extensional deformation before rupture and then higher adhesive failure energy. Inversely at high pulling velocities the failure is more abrupt, and even if the adhesion force is higher the total failure work is smaller.

Figure 4.7 highlights the evolution of the adhesive failure energy as a function of polymer content for 4 different pulling velocities. For any given velocity, the increase of the polymer concentration first leads to only slightly increase of the adhesive energy. Beyond a critical content, around 0.15%, the increase becomes more significant. Again, these results highlight the difference from the point of view of tackiness between render mortars, which are usually formulated with low polymer contents  $C_e < 0.1\%$ , and adhesive mortars, which has higher polymer contents ( $C_e > 0.15\%$ ).

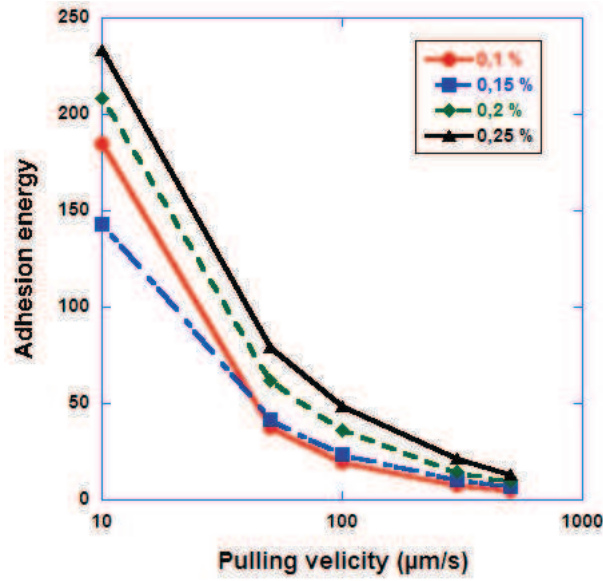


Figure 4. 6. Adhesive energy as a function of the separation rate for different polymer contents

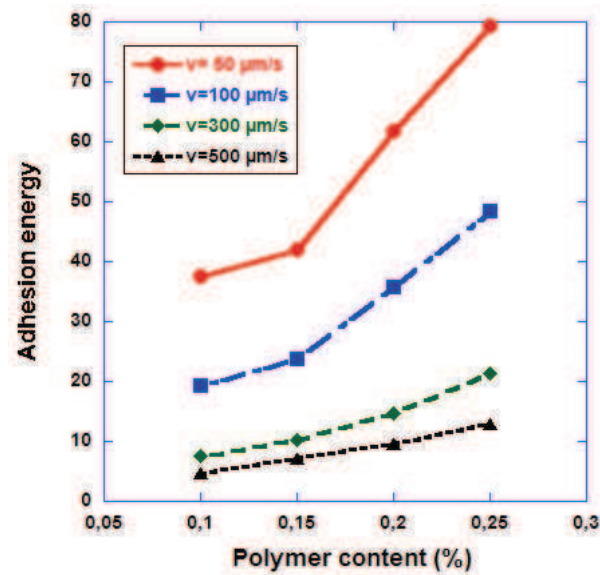


Figure 4. 7. Adhesive energy as a function of the polymer content for different pulling velocities

#### 4.1.2. Effect of Methocel on the rheological behavior

Figure 4.8 and 4.9 represent the flow curves of the mortar pastes for different polymer concentrations. These flow curves were determined at controlled stress and controlled shear rate respectively. Figure 4.8a and 4.9a display the rheological behavior at low shear rates (in linear scale) and figure 4.8b and 4.9b highlights the behavior around the yield points (in semi-logarithmic scale).



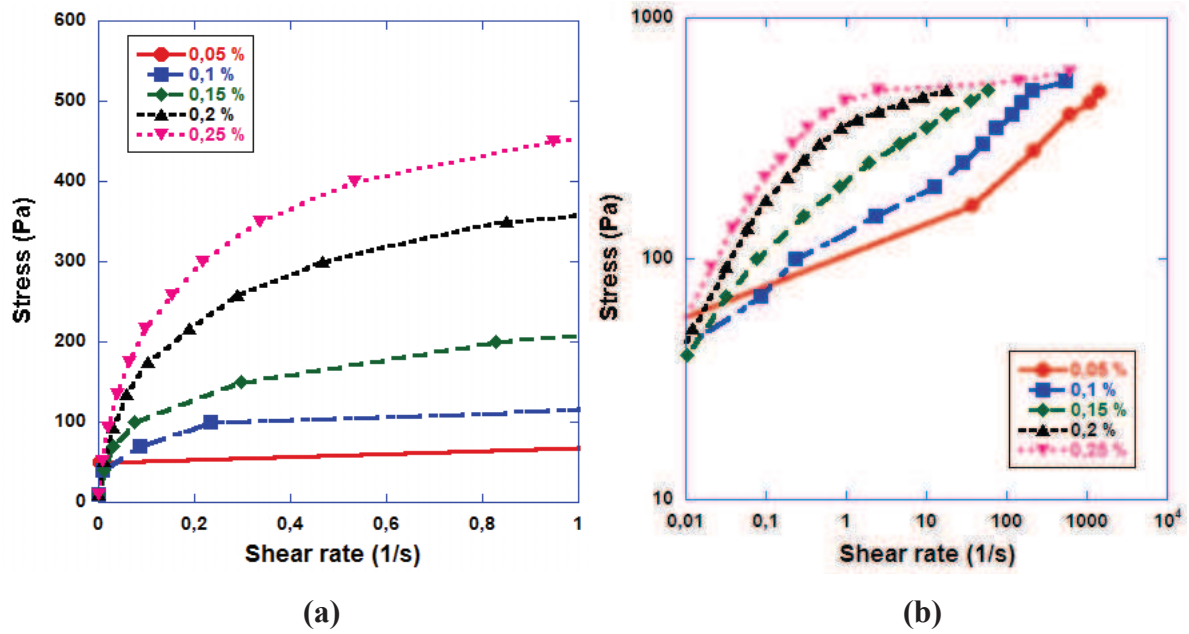


Figure 4. 8. Flow curves obtained in the stress-controlled mode using different polymer contents: (a) Linear plot; (b) Logarithmic representation

The flow curves in the stress-controlled mode, displayed in figure 4.8, allow determining in particular the yield shear stress that characterizes the onset of fluid flow. With the employed vane geometry, the smallest measurable shear-rate value is about  $0.01\text{s}^{-1}$ , and will therefore serving as the lower bound for fluid flow. At low polymer content (0.05%) and low shear-rates, the behavior is elastic-perfectly plastic: below the yield stress, the shear rates is vanishingly small, and above the yield stress the measured stress is independent of the applied shear rate. At higher polymer contents the viscous effects increase.

From figure 4.8, we observe a qualitative change of the rheological behavior with increasing polymer contents and shear-rates. At low shearing rates (figure 4.8a), we observe a gradual transition from viscous-plastic behavior to a shear-thinning behavior. At high shearing rates (figure 4.8b), the material is shear thickening at low cellulose ether contents, but remains shear thinning for high cellulose ether contents. We observed the same rheological behavior of the mortar in the shear rate controlled mode (figure 4.9).

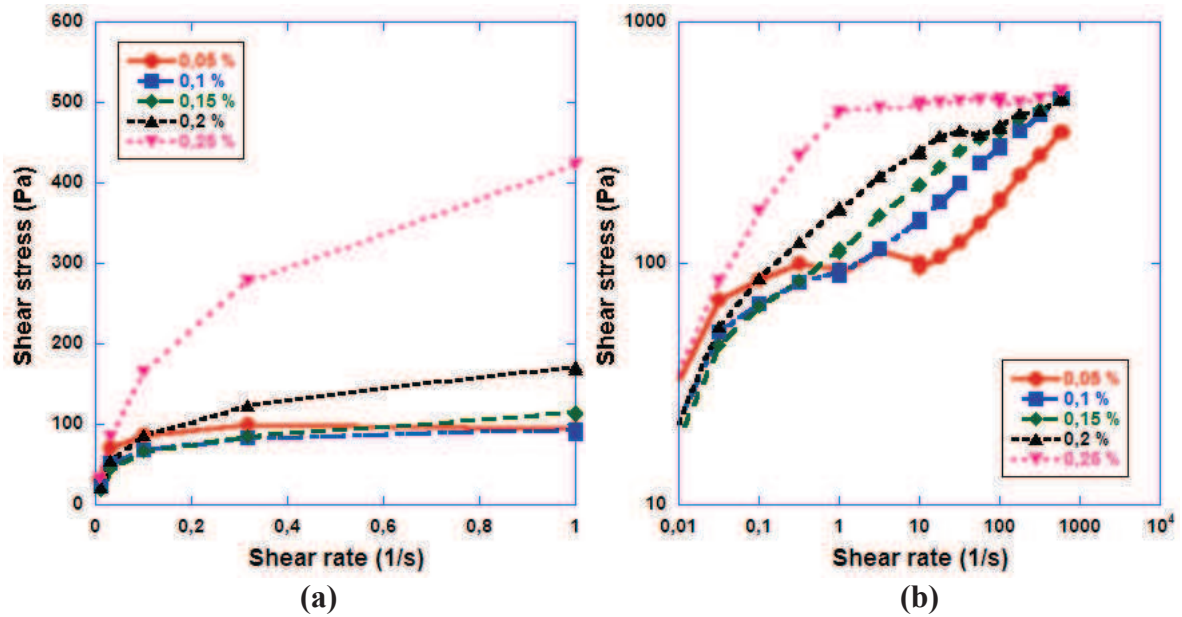


Figure 4. 9. Flow curves obtained in the shear rate controlled mode using different polymer contents - (a) Linear plot; (b) Logarithmic representation

The yield stress is identified as the applied shear stress corresponding to a finite shear rate value equal to  $0.01\text{s}^{-1}$ . The yield stress evolution with polymer content is represented in figure 4.10. The yield stress is related with the cohesion of the material, and should therefore be correlated to the cohesion strength identified during tack tests. Similarly to the cohesion force obtained from the tack tests (figure 4.4) the yield stress displays a minimum value at  $C_e=0.15\%$ . The presence of such a minimum of the yield stress has already reported in the literature concerning other types of mortars [39, 44, Kaci 2009, 98, and 99]. This has been explained by the interplay between opposing effects caused by the air-entraining effects of the cellulosic ether polymers. These effects consist of the increasing of the yield stress due to capillary forces of the air bubbles, and the decrease of the yield stress due the lubricating effect of the polymer that decreases granular friction. The competition between these effects would lead to the appearance of extrema values.

Two other rheological parameters, including fluidity index and consistency coefficient, were determined by performing the best fit of the experimental results with the Herschel-Buckley model, which is characterized by equation 1.27. The evolution of the consistency and fluidity index versus polymer content is then reported in figure 4.10.

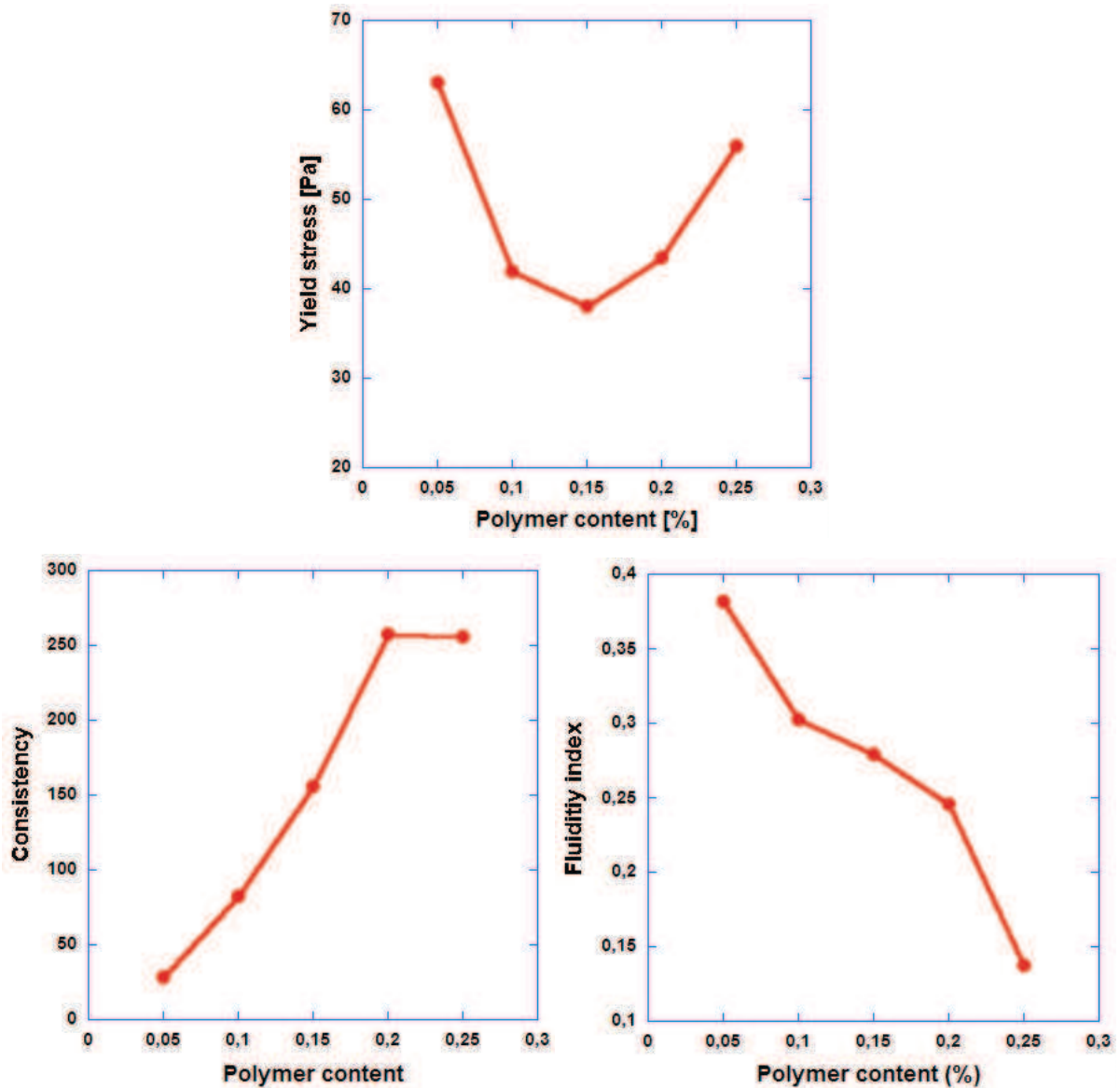


Figure 4. 10. Influence of the cellulose-ether content on the rheological parameters of the mortar: Yield stress, Consistency and Fluidity index

The fluidity index decreases with the increase of cellulose-ether content, which indicates that the mortar becomes more and more shear thinning when adding polymer. This could already be seen in the flow curves above. The evolution of the consistency of the mortars is in contrast to that of the fluidity index: As the polymer content increases, the mortar consistency coefficient increases. We can observe a significant increase (almost linear) of the consistency and it seems to reach a plateau value at the polymer content of 0.2%. The evolution of the consistency of the mortar indicates a monotonic increase when increasing the polymer concentration, reflecting the increase of the viscous drag effects with polymer content. Such huge effects of the polymer on the viscosity may be attributed to its associative property. The same observation on the mortar's consistency, with the variation of the same type of polymer, has also been reported [Kaci 2009].

#### 4.1.3. Comparing the adhesive properties to the rheological behavior

The yield stress of the mortar in extension is calculated from the Tack test results as have been discussed in section 3.3. In figure 4.11, the yield stress obtained in the two tests, including Probe tack test and rheology test, is plotted. In contrast with fiber reinforced mortars (chapter 3), the yield stress of the mortar in shearing condition is much higher than that in extension. The difference between the two values for different cellulose-ether contents is represented in figure 4.12. We obtain a minimum of yield value in both shear and extension at 0.15% of cellulose ether. The minimum yield stress measured in tack test is around 6.12 Pa, which is much smaller compared with 38 Pa measured in shear.

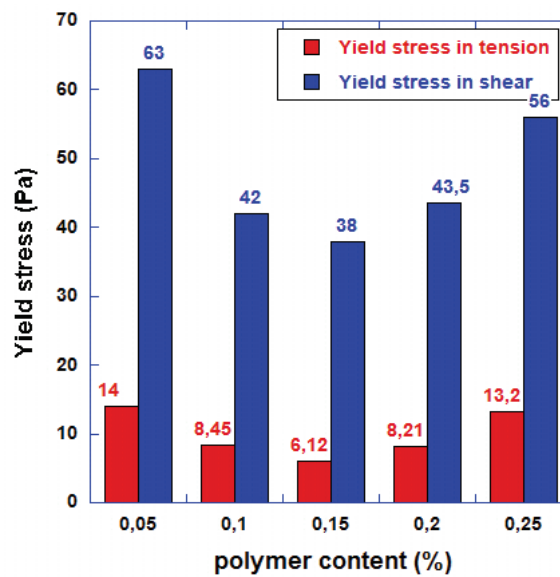


Figure 4. 11. Comparison of the yield stress in tension and shearing condition for different Methocel contents

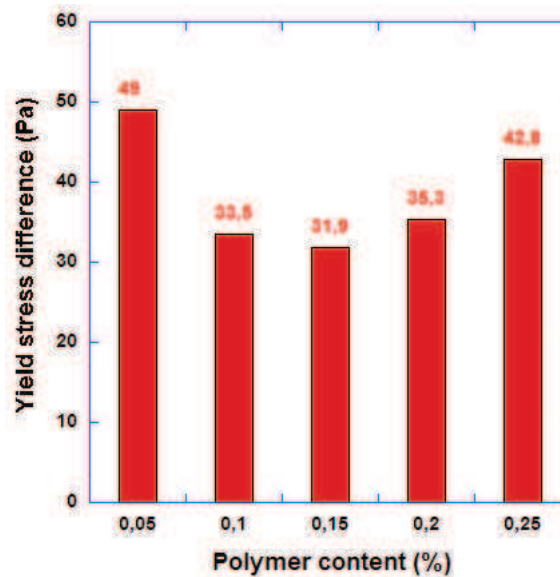


Figure 4. 12. Difference between the yield stress in tension and in shear for different Methocel contents

## 4.2 Effect of mineral additives, case of bentonite

### 4.2.1 Effect of bentonite on the adhesive properties

#### 4.2.1.1 Tack test results

Recorded force as a function of displacement (time) curves obtained in the probe tack test for different contents of bentonite is plotted in figure 4.13. Each graph corresponds to a given dosage rate of bentonite, including 0.05; 0.5; 1 and 2 %. Flow curves related to 2 other dosage rates of bentonite are presented in appendix B.1. The force curves are approximately similar to the general shape represented in figure 2.8a. These curves also consist of three zones. At high pulling velocities, for example at  $v=500 \mu\text{m/s}$ , the mortar has started flow since beginning of the tack test so that the viscous-elastic zone of the force curve is almost disappeared (according to the maximum data acquisition rate of our set-up). In these cases, we assumed that the first recorded normal force is referring to as the adhesive strength of the mortar in tension.

The flow curves, which are presented in figure 4.13, have similar form. At each applied separation velocity, the peak normal force only slightly increases with the increase of bentonite content. It can be suspected that the viscosity of the mortar is not much affected by the variation of bentonite content. We will come back to this issue when discussing rheological results.

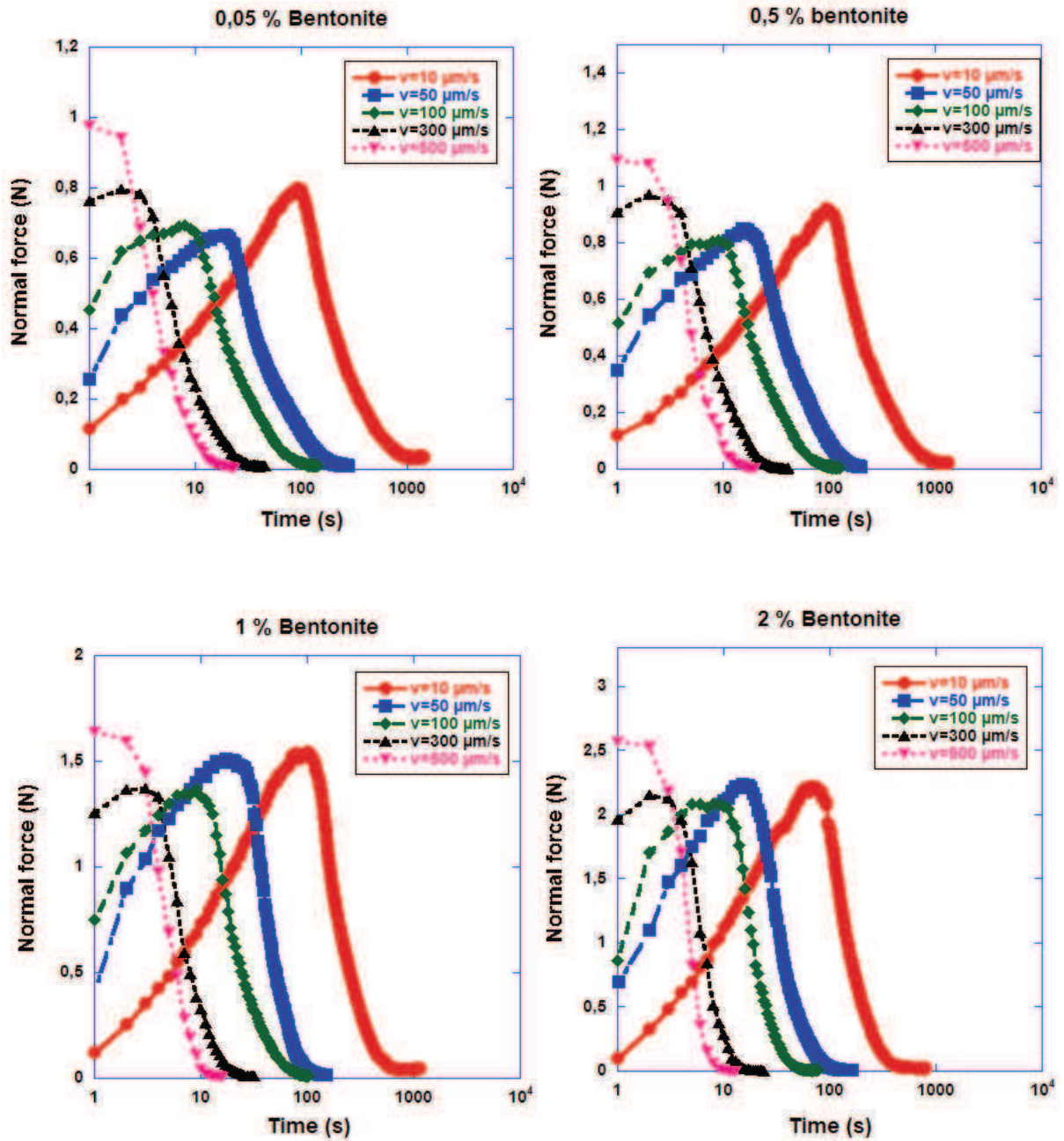


Figure 4. 13. Force versus time curves obtained in the Tack test for different bentonite contents

We have also represented in figure 4.14 the nominal stress (normal force divided by the nominal surface area of the plate) evolution with the nominal strain (vertical displacement divided by the initial gap), in order to investigate further the dependency on pulling velocity. From figure 4.14, it appears clearly that the peak nominal strain (around 0.5) does not depend on the pulling velocity, and the peak stress slightly increases, but only slightly, with the increasing of bentonite content. For a given bentonite content, this peak stress value does not depend so much on the pulling velocity.



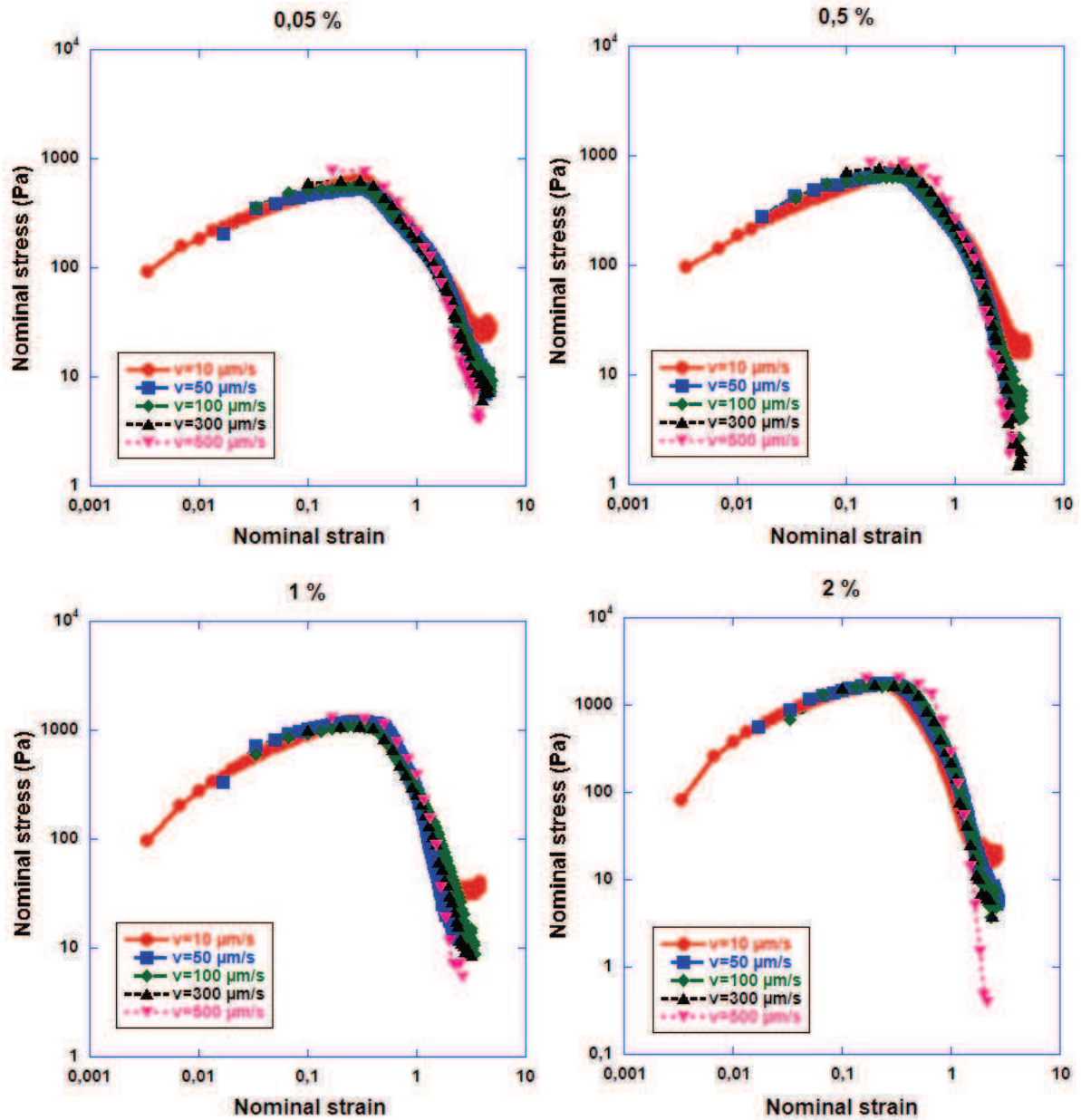


Figure 4. 14. Nominal stress vs. nominal strain curves for varying bentonite content.

#### 4.2.1.2 Peak force

The maximum pulling force (adhesion force) as function of velocity is represented in figure 4.15. The curves are qualitatively different from those of bentonite muds [50]. The peak force is almost independent on the tack velocity. We can observe a minimum of the force at around  $100 \mu\text{m/s}$ .

Figure 4.15 represents also the evolution of the peak force versus bentonite content for different pulling velocities. At a certain pulling velocity, the relationship between adhesion force and bentonite content is approximately linear, which can be related with the fact that bentonite additions increase mostly the yield stress and not the viscosity as it can be shown

from the rheological measurements presented below.

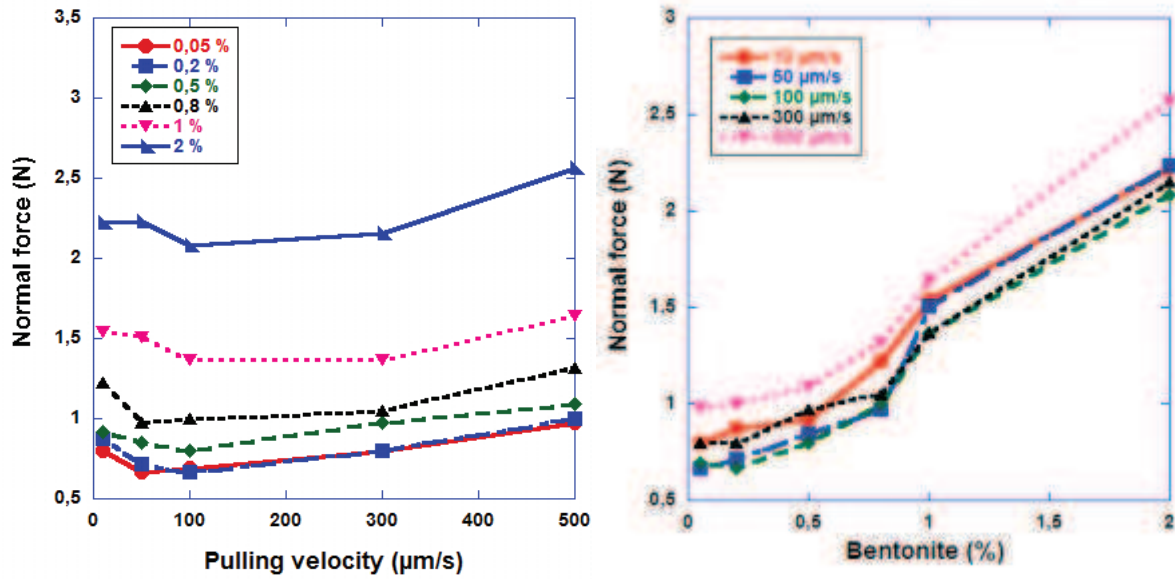


Figure 4. 15. Evolution of the adhesion force as a function of the pulling velocity for varying bentonite contents

#### 4.2.1.3 Cohesion force

The cohesion force is taken to be the value of the force peak when the velocity tends to zero. In our case we took the value of the peak force for the lowest pulling velocity, that is 10  $\mu\text{m/s}$ . From the force curves obtained from the tack test, we plot the evolution of the cohesion force as a function of bentonite content as shown in figure 4.16.

Similarly to the adhesion force, the evolution of the paste cohesion shows a linear increasing with the increasing of bentonite concentration. We will come back to this discussion when considering the rheological properties of the mortar.



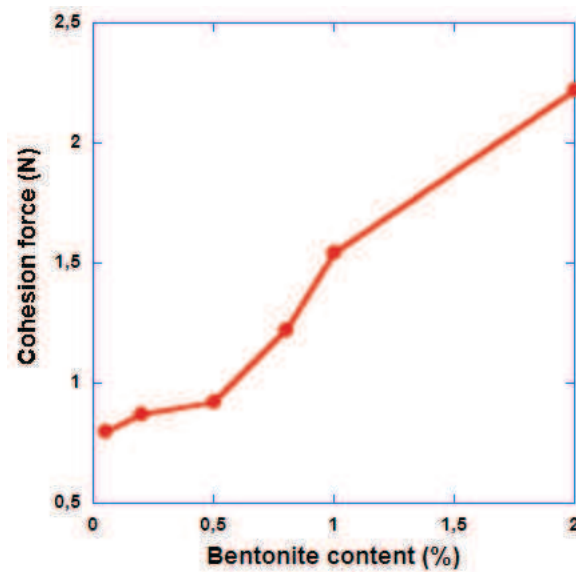


Figure 4. 16. Evolution of the cohesion force with bentonite content

#### 4.2.1.4 Interface adherence

Adherence force is related to the weight of the mortar which remains stuck on the mobile plate after the completion of the tack process. The evolution of the adherence force as a function of bentonite content for different velocities and its evolution with pulling velocity for different bentonite contents are represented in figures 4.17a and 4.17b respectively.

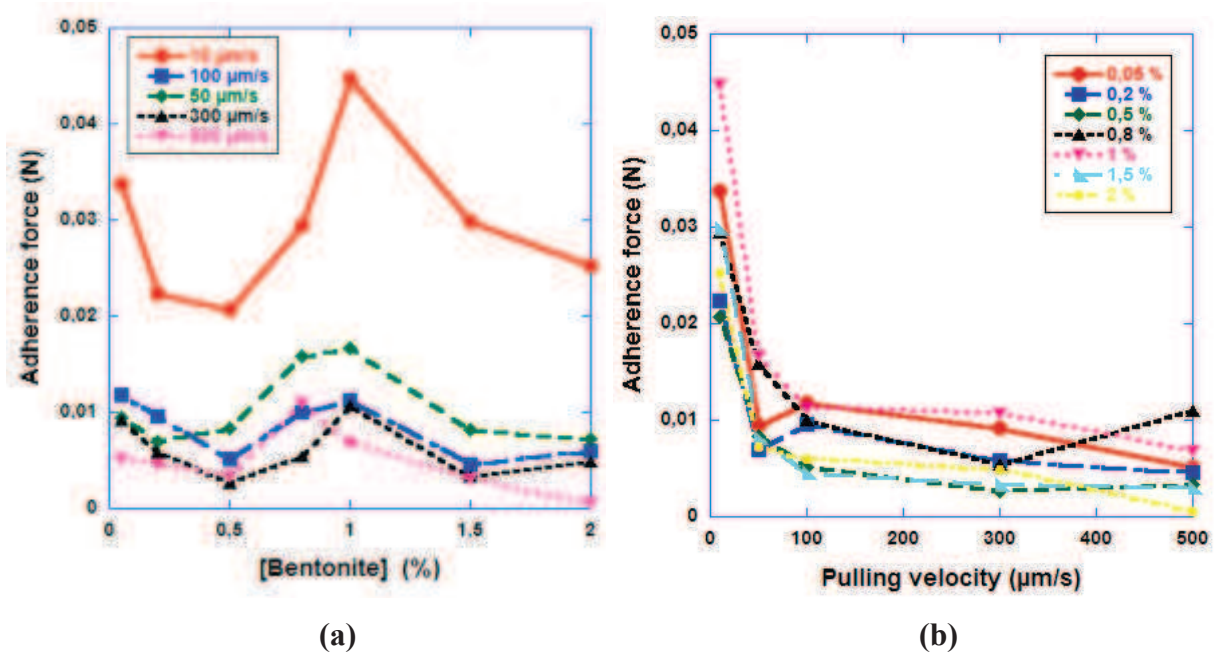


Figure 4. 17. Adherence force of the mortar in formulation with bentonite  
(a) as a function of bentonite concentration; (b) as a function of pulling velocity

The observed behavior is unexpectedly complex. For each given velocity, the adhesion force decreases at first when bentonite is added to the mixture. A minimum in adhesion is reached at 0.5% bentonite content, and then adherence increases to a maximum value at 1% bentonite content, and decreases afterwards.

In order to investigate the influence of adherence force of the pulling velocity, we have plotted the adherence force as a function of pulling velocity at various bentonite contents in figure 4.17b. We have observed a good adherence for lowest pulling velocities and adherence decreases abruptly for higher velocities. Starting from the pulling speed of 50  $\mu\text{m/s}$ , the adherence force is almost unchanged. This observation can be related to the difference between rupture modes in the solid-like and the liquid-like mortar pastes [Kaci 2009].

#### 4.2.1.5 Adhesive failure energy

The evolution of adhesive failure energy as a function of separation velocity, represented in figure 4.18, is similar to the previous results obtained with cellulose-ether (figure 4.6).

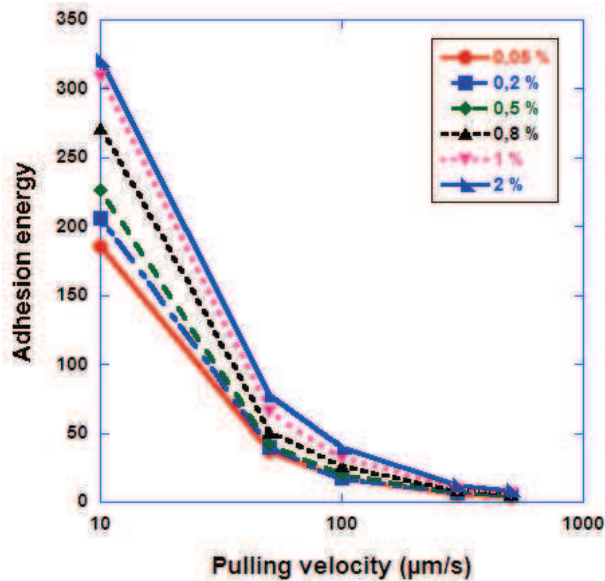


Figure 4. 18. Adhesive energy as a function of the separation rate for different bentonite contents

The faster separating velocity applied, the less energy required. The adhesion energy is around 250 (mJ) at the lowest pulling velocity (10  $\mu\text{m/s}$ ), decreases to around 50 (mJ) as the pulling velocity increases to 50  $\mu\text{m/s}$ , and is almost zero at highest velocity (1000  $\mu\text{m/s}$ ).

Figure 4.19 represents the evolution of adhesive failure energy as a function of bentonite concentration. It is found that the adhesive energy increases with bentonite content at low velocities, but the increase is much lower at high velocities. We can notice a similarly form of

these curves to that of the cohesive force evolution, represented in figure 4.16. The fact that the tack energy is small at high velocities may be related to the fact that the total deformation decreases when increasing the velocity (more abrupt failure) while the tack force is almost independent upon the velocity (or even decreases) (see figure 4.15).

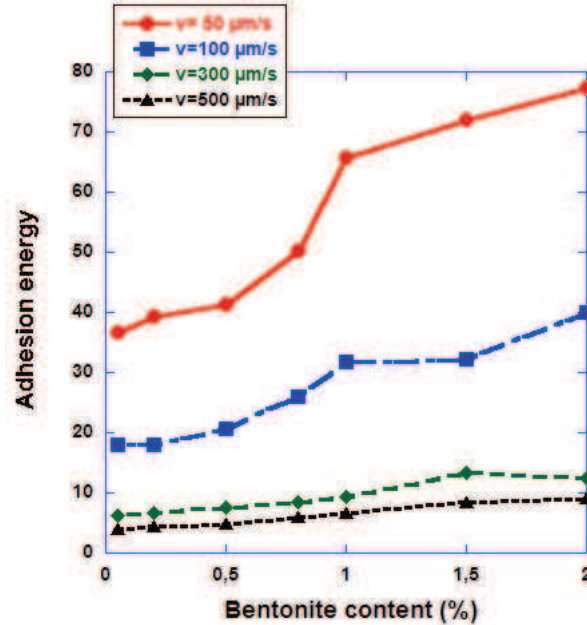


Figure 4. 19. Adhesive energy as a function of the bentonite content for different pulling velocities

#### 4.2.2 Effect of bentonite on the rheological behavior

The flow curves obtained under shear stress controlled mode are displayed in figure 4.20 for varying bentonite contents. These curves are plotted in both linear and logarithmic scales in order to highlight the evolution of shear stress versus shear rate at low shear rates.

We can see in the linear plots that there are two qualitatively different rheological behaviors depending of the bentonite content: shear-thinning behavior at low contents of bentonite and Bingham fluid at high bentonite contents.

To see this more clearly, the flow curves are zoomed in at the low shear rates in figure 4.21. At low content of bentonite, the flow curve is that of a shear-thinning fluid with a yield stress (Herschel-Bulkley fluid). As it can be clearly seen, at high bentonite content, e.g. 0.8 %, after the applied stress exceed the yield value, the relationship between the shear stress and shear rate is almost linear with a low slope. It can be considered that the viscosity is constant and the mortar behaves as a Bingham fluid. We observe the same behavior at 1, 1.5, 1.7 and 2%.

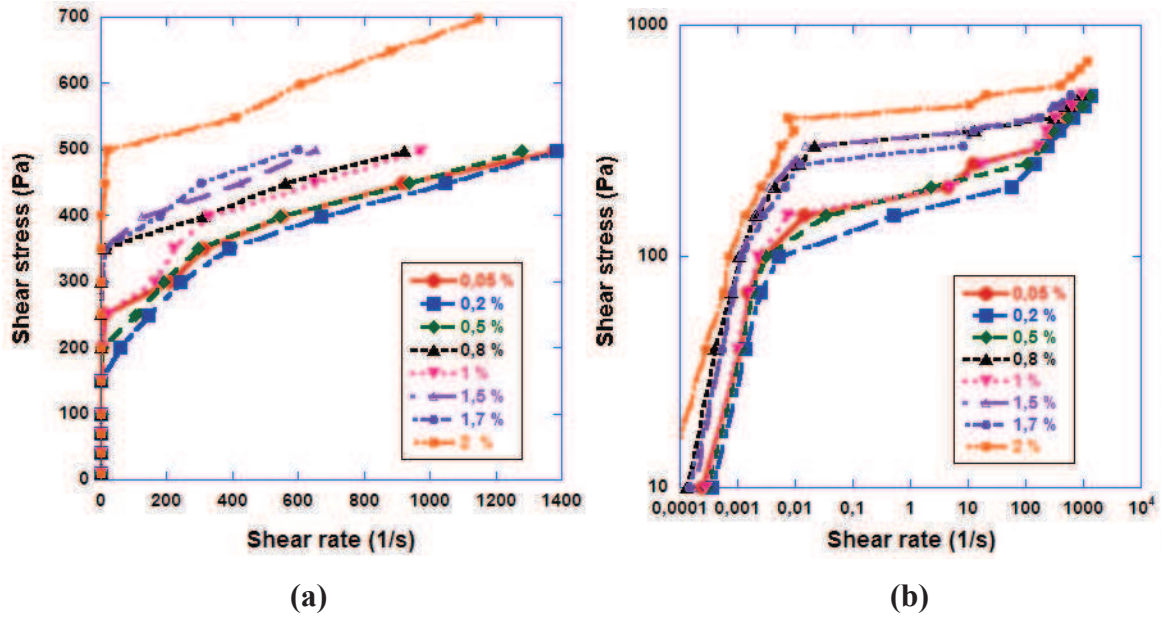


Figure 4. 20. Flow curves obtained in rheological measurements of mortars in formulation with bentonite: (a) Linear scale; (b) Logarithmic presentation

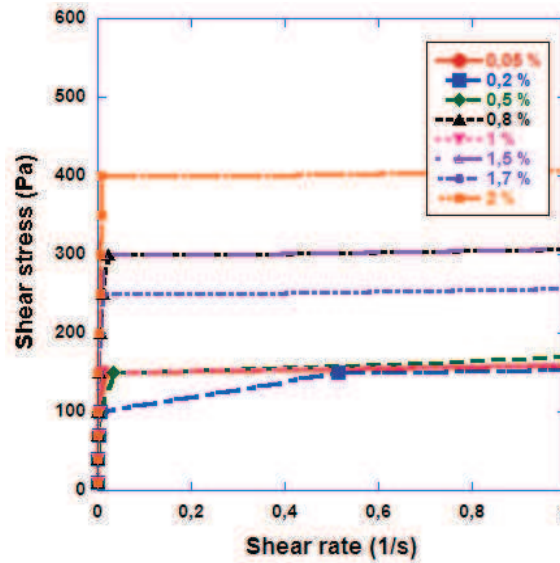


Figure 4. 21. Rheological flow curves in low shear rate, case of bentonite

The yield stress is identified as the applied shear stress corresponding to a finite shear rate value equals to  $0.01\text{s}^{-1}$ . The evolution of the yield stress with bentonite content is shown in figure 4.22. It indicates that increasing the bentonite concentration first decreases the yield stress. We observed a minimum at 0.2 %. It is to be noted that this minimum is not an artifact since the test has been repeated three times. This is followed by a significantly increase of the yield stress with bentonite concentration. We see that the yield stress and the cohesion force evolutions with bentonite content are fairly similar (see figure 4.16).

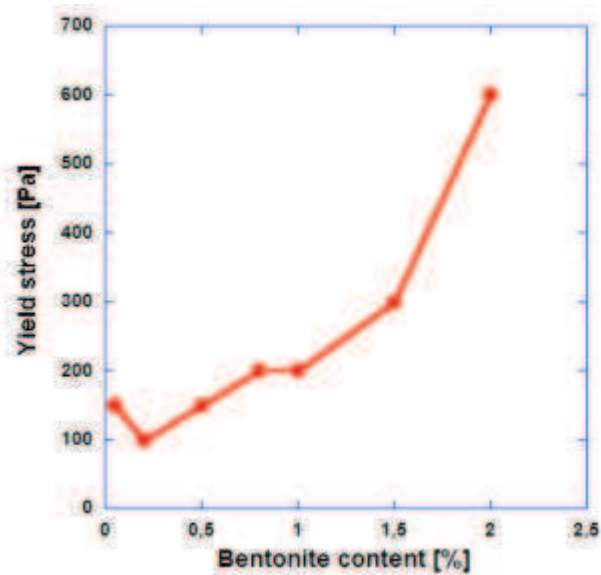


Figure 4. 22. Evolution of the yield stress with bentonite content

Two other rheological parameters, including the consistency and the fluidity index, were determined by performing the best fit with the Herschel-Bulkley model, as it has been discussed in the previous section. The evolutions of consistency coefficient and fluidity index versus bentonite concentration are represented in figure 4.23. The consistency of the mortars decreases with the increasing bentonite content. This decreasing is monotonic and reflects the decrease of the viscous drag effects with bentonite content.

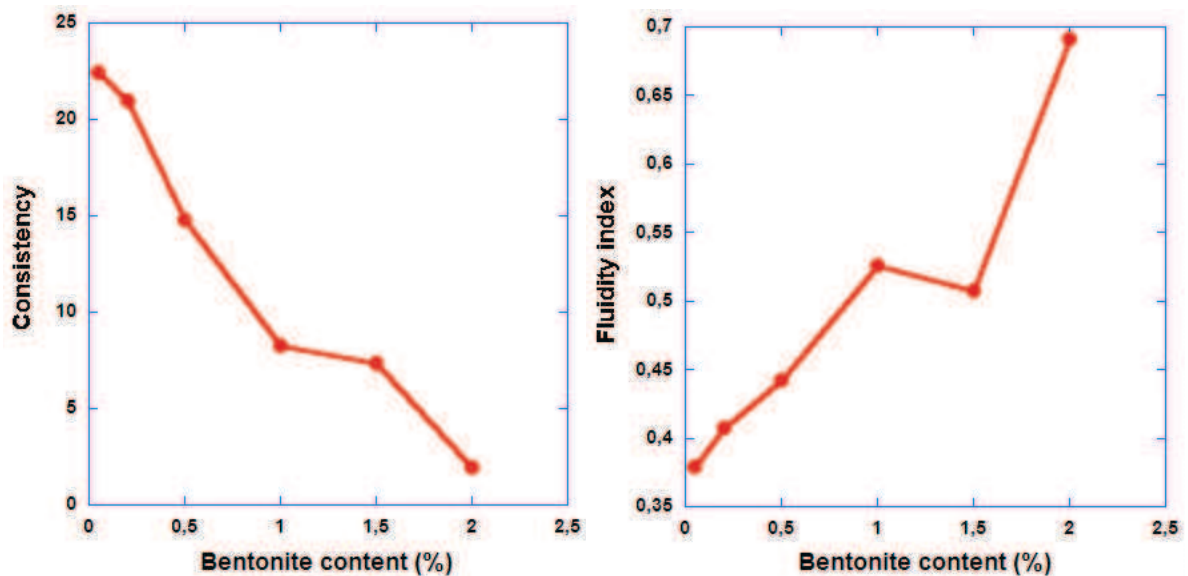


Figure 4. 23. Evolution of consistency and fluidity index with the variation of bentonite contents

The fluidity index first increases with the increasing of bentonite content. We observed a maximum at 1 %, followed by a minimum at 1.5 %. However the gap between these two

quantities is small. Overall, we can see that we have increase of the fluidity index of the mortar with bentonite content. This evolution means that the mortar becomes less shear thinning at higher bentonite content. At 2%, the value of fluidity index approach 1, at which the mortar behaves like a Bingham elasto-plastic fluid.

#### 4.2.3 Comparing the adhesive properties to the rheological behavior

The yield stress in extension is calculated by equation 3.3 as performed in previous cases. The figure 4.24 shows the yield stresses obtained in tension and in shearing conditions for various bentonite contents, while figure 4.25 represents the difference between these two quantities. It shows that in both tension and shearing conditions, the yield stress increases with the increasing of bentonite content. The results also indicate that the resistance of the mortar in shearing conditions is significantly higher than that in tension conditions.

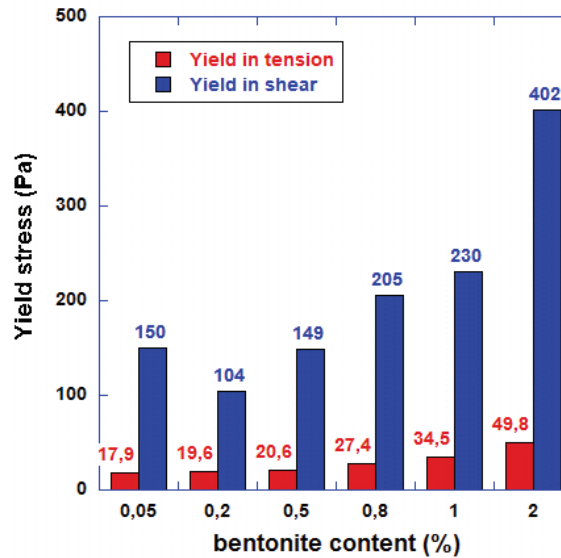


Figure 4. 24. Comparison of the yield stress in tension and in shear condition for different bentonite contents



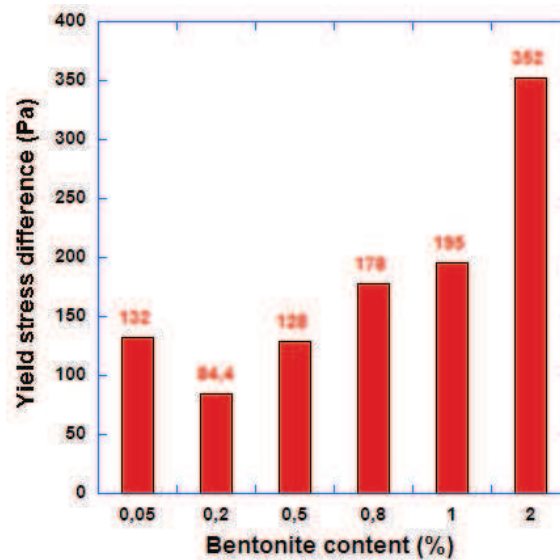


Figure 4. 25. Difference between the yield stress in tension and in shear for different bentonite contents

### 4.3 Comparison between organic and mineral thickeners

#### 4.3.1. Adhesive properties

The difference in the evolutions of the adhesive strength with varying polymer and bentonite contents indicates that both two additives improve the adhesive strength of the mortar. However, the adhesive quantities that are increased are different. Bentonite increases mainly the cohesion component while cellulose ether increases adherence and adhesion strength. This is related to the fact that bentonite decreases the viscosity of the mortar and increases its yield stress, while cellulose ether significantly increases the viscosity of the mortar without significant change in its yield stress (or even decreases it). In practice one can use cellulose ether to increase tackiness and bentonite to increase cohesion and eventually to moderate tackiness effects of cellulose ethers.

#### 4.3.2. Rheological properties

Similarly to the cohesion force, the measured yield stress displays a pronounced local minimum at 0.15% polymer content, while the yield stress mostly increases with bentonite additions. It is also interesting to notice that the yield stress is about ten times higher with bentonite additions as compared to polymer-based mortars.

Although the viscosity evolution has not been represented, we observe from the flow curves that the apparent viscosity increases with the polymer content, for shear rates below  $80 \text{ s}^{-1}$ .

For higher shear rates, a reverse tendency is obtained; the apparent viscosity decreases with polymer content. This feature, which has been observed in [97] on polymer-based cement pastes, has been attributed to the competition between the fluid phase's viscosity (which increases with polymer concentration) and the hydrodynamic lubrication, which efficiency increases with polymer concentration, and consequently limits the direct inter-granular friction.

With bentonite additions, the corresponding rheograms are much more irregular and complicated to interpret at low shearing rates, if we compare to the corresponding rheograms obtained in figure 4.8 using polymer additions. Globally, at low shear rates, viscosity increases with bentonite contents lower than 1%, and decreases for higher bentonite contents. As for polymer-based mortars, this shows that the rheological behavior of cement pastes is determined by lubricated inter-granular contacts and direct inter-granular contacts, which are partly controlled by the viscosity of the inter-granular fluid.

#### **4.4 Conclusion**

In the present study, we have undertaken a systematic study of the properties of fresh mortars that can be derived from tack tests and rheological experiments. Starting with a reference mortar paste, the effect of polymer or bentonite additions has been investigated. The experimental investigation has displayed quite different patterns of evolution for the reference mortar with bentonite or with polymer additions, during tack tests and rheological experiments as well.

With polymer additions, case of cellulose ether, we observe a marked dependency of adhesion on pulling velocity, and a non-monotonous variation with polymer content during tack tests and yield stress measurements. A strong dependency of adhesion is noticed at high content of polymer (0.15-0.25 %), and it is less dependency at low polymer content ( $<0.15\%$ ). A similar observation is obtained with the dependency of the adhesive, cohesive and also the adhesive failure energy. The adhesive behavior of polymer-modified mortar, case of cellulose ether, is insignificant at polymer content lower than 0.15% (render mortars), and significant at high polymer content (adhesive mortars).

With bentonite additions, the dependency with respect to pulling velocity is less important. The peak normal force, the cohesion force and the yield stress all monotonically increase with bentonite content, while the adherence force and viscosity's evolutions with bentonite content are more complex. Several mechanisms have been proposed to interpret the observed results; in particular the role of the viscosity of the fluid phase should be investigated further by



performing viscosity measurements for the suspending fluid alone.

The comparison between debonding tests and rheological measurements has shown that the cohesion force can be related to the yield stress identified on flow curves, while the viscosity correlates well with the interface adherence. In both case of using cellulose ether or bentonite in the mortar formulation, the yield stress obtained in tension condition is much smaller than that obtained in shearing conditions.

By comparing the two types of thickeners it can be expected that water-soluble polymers and mineral additives may reveal complementary regarding the placement properties of mortars. The former can be used to adjust viscosity and adherence properties while the latter can be included to control yield stress and cohesion.

## CHAPTER 5

# *Hydroxyethyl methyl celluloses (HEMCs)*

### Contents

<b>5.1. Effect of HEMCs type A.....</b>	<b>89</b>
5.1.1. Effect of A on the adhesive properties.....	89
5.1.2. Effect of A on the rheological behaviors.....	96
5.1.3. Compare the adhesive properties to the rheological behavior.....	100
<b>5.2. Effect of HEMCs type B.....</b>	<b>102</b>
5.2.1. Effect of B on the adhesive properties.....	102
5.2.2. Effect of B on the rheological behaviors.....	107
5.2.3. Compare the adhesive properties to the rheological behavior.....	111
<b>5.3. Effect of HEMCs type C.....</b>	<b>112</b>
5.3.1. Effect of C on the adhesive properties.....	112
5.3.2. Effect of C on the rheological behaviors.....	117
5.3.3. Compare the adhesive properties to the rheological behavior.....	120
<b>5.4. Comparison the effects of three types of HEMCs .....</b>	<b>122</b>
<b>5.5. Conclusion.....</b>	<b>130</b>

In this chapter, we investigated the effects of three types of hydroxyethyl methyl cellulose ethers (HEMC), symbolized as A, B and C. Their physical characteristics have been introduced in section 2.1.2.3, in which their viscosity and the molecular weights are:

- A: MKW 20000 PP01, viscosity 20000 mPas,  $M_w=600$  kDa
- B: MKW 30000 PP01, viscosity 30000 mPas,  $M_w=680$  kDa
- C: MKX 70000 PP01, viscosity 70000 mPas,  $M_w=1.000$  kDa

The above mentioned viscosity is the average value, measured with 2% solution in water using a Haake rotational rheometer, under the shear rate  $2.55s^{-1}$  and  $T=20^{\circ}C$ .

The adhesive and rheological properties of mortars have been investigated using two experimental methods, represented in chapter 2, including probe tack test and vane cylinder test.

The results are presented in 5 sections. In the first three sections, each section introduces the effect of one type of polymer on the adhesive and rheological properties of mortars. In the fourth section, a comparison between the effect of molecular weight on the properties of mortars will be considered. The last section is the conclusion of chapter.

## 5.1. Effect of HEMCs type A

### 5.1.1. Effect of A on the adhesive properties

#### 5.1.1.1. Tack test results

The polymer content is varied according to the following proportions:  $C_e = [0.19; 0.21; 0.23; 0.25; 0.27; 0.29; 0.31]$  % by weight. Figure 5.1 represents the flow curves for four polymer dosage rates. Additional results which correspond to the remaining polymer contents, including 0.21; 0.25 and 0.29 % are presented in appendix C.1. A semi-logarithmic plot has been performed to bring out the behavior around the peak value of the flow curves.

The force curves are all qualitatively similar. The curve rises, passes through a maximum and monotonically decreases to a steady state value. These curves have roughly the general shape which is represented schematically in figure 2.8b and consisting of 3 different zones. However, at the highest pulling velocity ( $500 \mu m/s$ ), there is no “viscous-elastic” zone because of the limited rate of data acquisition of our experimental set-up (1 measure per second) and the mortar has started de-structuring since the beginning of the tack experiment.

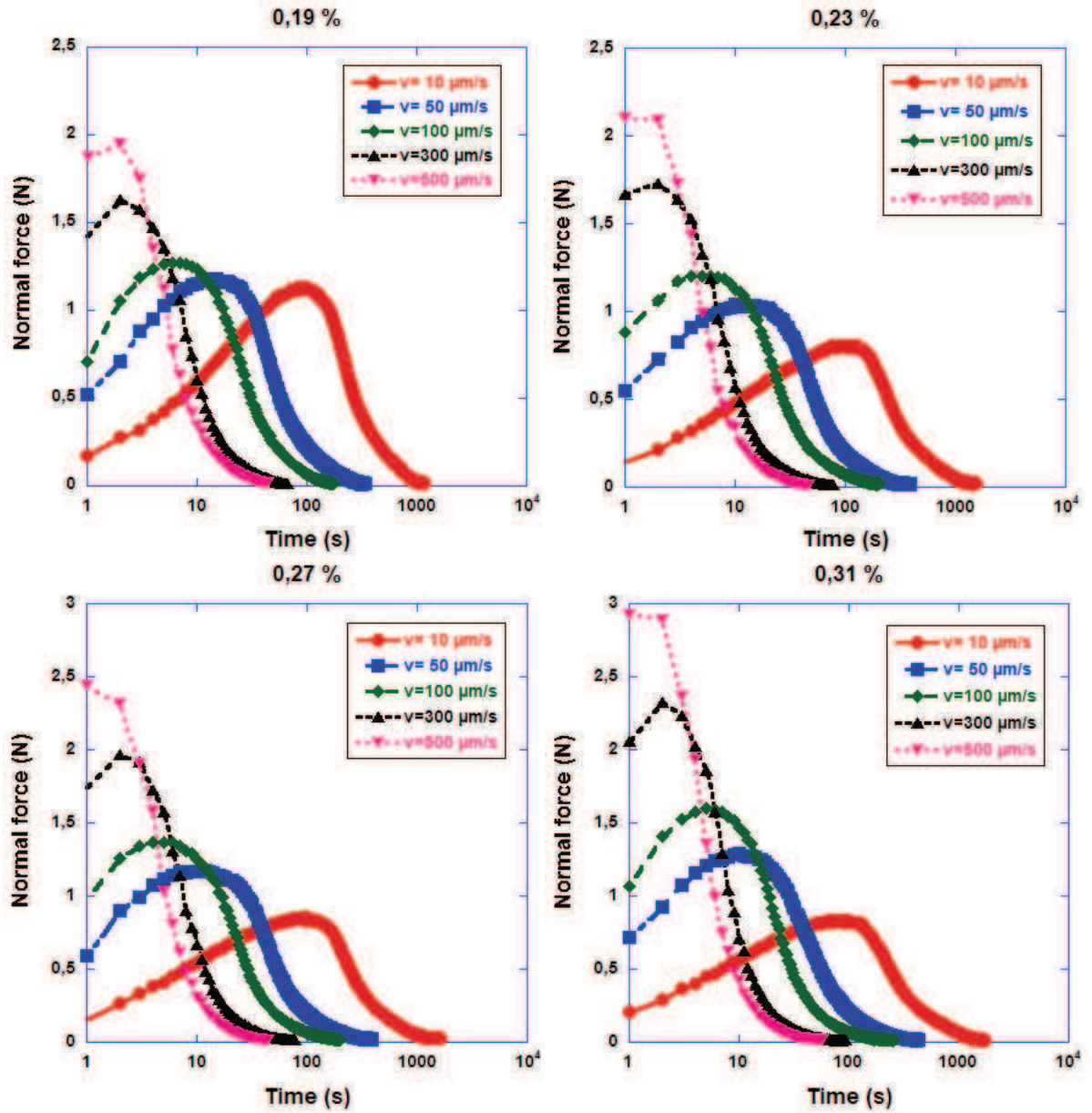


Figure 5. 1. Force versus time curves obtained in the tack test for different contents of A

The corresponding nominal stress, calculated as described in section 3.1.1, are plotted in figure 5.2. It can be seen that the peak nominal strain is almost independent on the pulling velocities, while the peak nominal stress increases with the increase of pulling velocity. This observation is similar to that in case of using fiber reinforcement (section 3.1.1) and suggests that the separation velocity has an important effect of the process, and the mortar rupture would be governed by a progressive inward flow.

Considering the variation of the peak nominal stress, figure 5.2 shows that it is independent on the variation of the content of A. It can be assumed that the variation of A almost has no effect on the adhesion strength of the mortars. This feature will be verified further in the following sections.

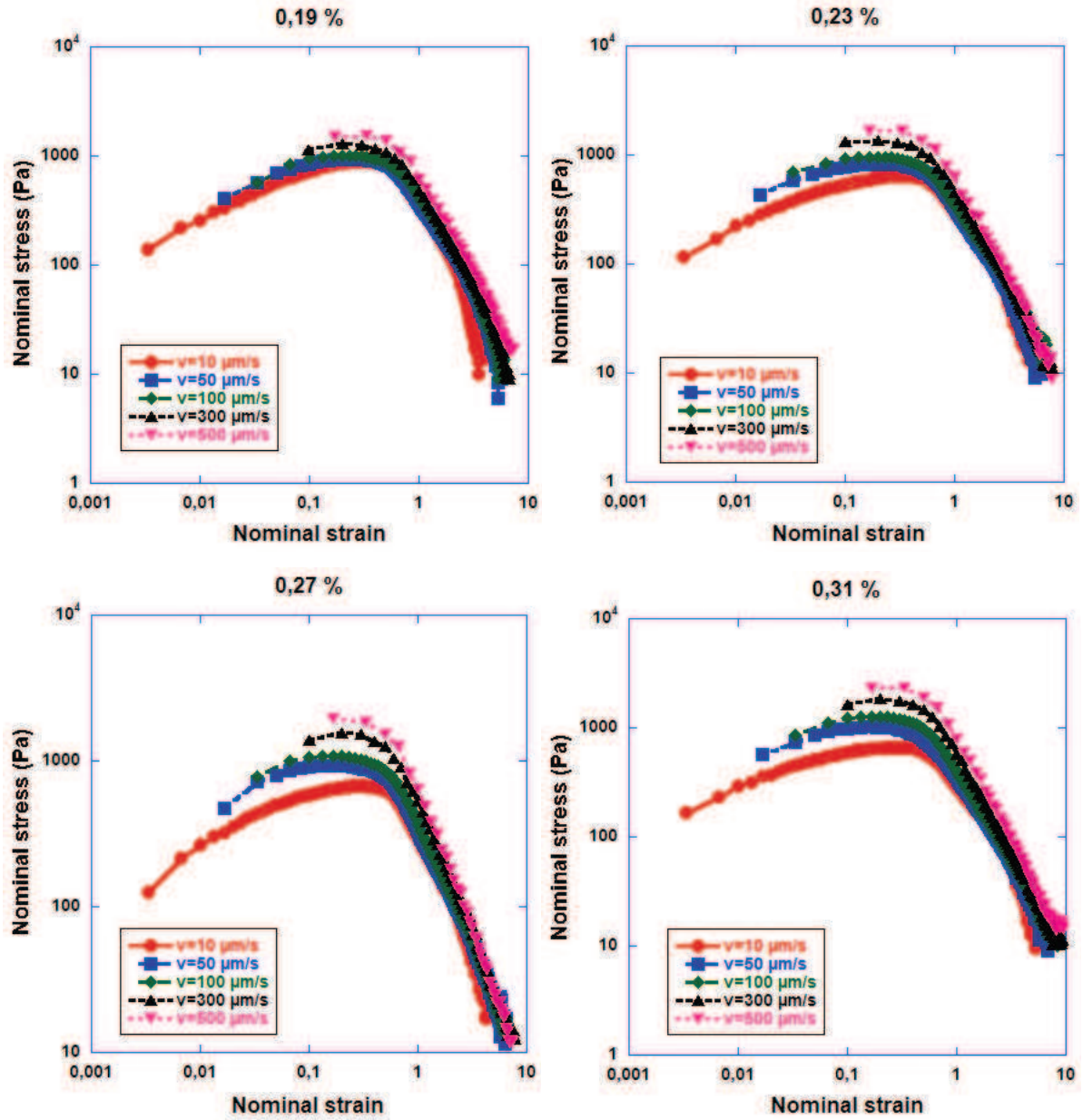


Figure 5. 2. Nominal stress and strain curves for varying content of A

#### 5.1.1.2. Adhesive strength

Figure 5.3 shows the variation of the peak normal force, or adhesion force, with pulling velocity as a function of A content.

As expected the adhesion force increases with pulling velocity. This is expected since we deal with an associative polymer which is expected to significantly increase the viscosity of the pore solution.

Figure 5.3 also shows that the sensitivity of the adhesive force to the variation of tack speed is almost unchanged with polymer concentration, which is represented by the parallelism of the curves. This differs from the previous observation on the effect of cellulose ether; discussed in

chapter 4, figure 4.3, which demonstrated that the viscous distribution to the adhesive force increases with polymer content. This difference will be discussed further.

In the figure 5.3 we represent the evolution of adhesion force versus A dosage for different velocities. The adhesion strength depends only slightly on the polymer dosage. We can observe different extreme, which are artifacts since they are approximately reproducible. The evolutions of adhesion force versus polymer content are almost similar, independently on the tack velocity. We observe a maximum of the adhesion force at 0.21%. Beyond this value, the adhesion force decreases to a minimum value at 0.23%, followed by a maximum value at 0.25%, and continued by reaching another minimum at 0.29%. The differences of the obtained adhesive forces between these extremes are however relatively small.

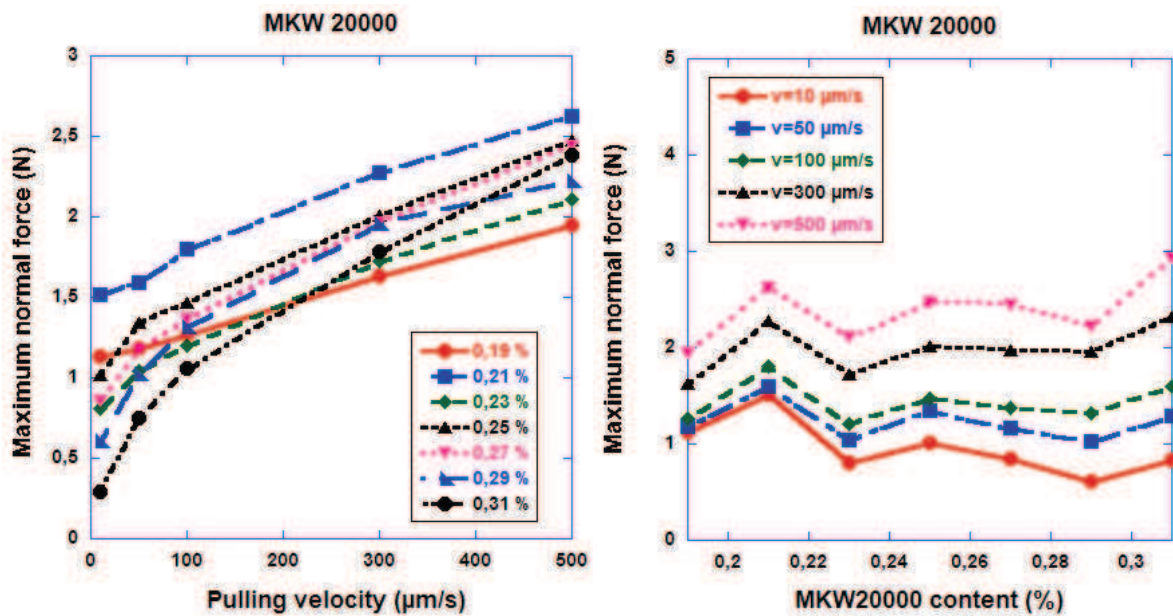


Figure 5. 3. Evolution of the adhesion force as a function of pulling velocity (left) and of polymer contents (right), case of A

The non-monotonous evolution of the adhesion force with polymer concentration can be attributed to the interplay between different effects of the polymer, which would lead to both the increase and decrease of the adhesive force. First, polymer both increases the viscous dissipation of the liquid phase and decreases the granular contribution to the dissipation due to the lubrication effects. Second, cellulosic ether polymers have strong air-entraining effects [44]. The air bubbles would lead to the increase of the adhesive force due to the capillary forces. On the other hand, the presence of air bubbles decreases the viscosity of the mortar, which would decrease the adhesive strength.



Considering the overall behavior of the curves on the right part of figure 5.3, we can notice the following. At low pulling velocity, i.e. 10  $\mu\text{m/s}$ , the adhesion force decreases slightly with the increase of the polymer content. However, this decreasing disappears at high velocities. At  $v = 100 \mu\text{m/s}$ , the adhesion force is almost unchanged. At  $v = 500 \mu\text{m/s}$ , we observe an increase of the adhesion force with the increase of polymer content. The best fits of the evolution curves have been performed, and shown in figure 5.4. This highlights the above remarks. This low sensitivity of the adhesion strength of the mortar on the polymer concentration in the case of A, will be considered in relation to two other polymers in following sections.

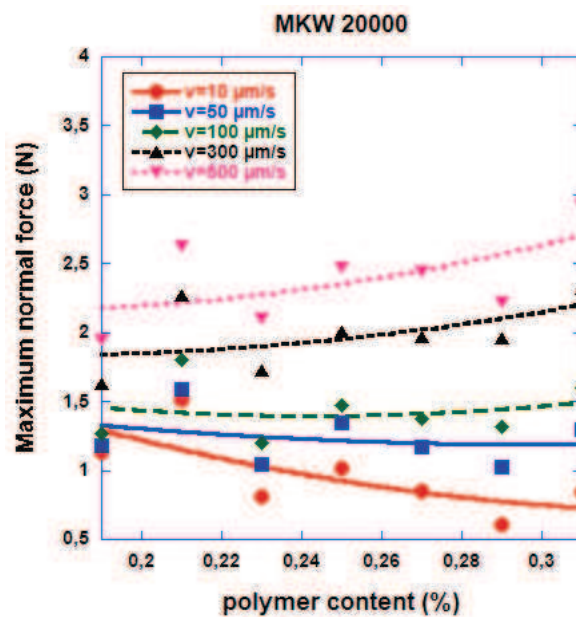


Figure 5. 4. Performing of the best fit of the adhesion force versus polymer content, case of A

#### 5.1.1.3. Cohesion force

The evolution of the cohesion force is represented in figure 5.5. We can see that below a certain value of polymer content (around 0.25%), increasing polymer content leads to a significant decrease of the paste cohesion. Beyond this content, the cohesion force remains almost constant when we increase polymer content.

The decrease of the cohesion force can be attributed to air-entrainment effects of the polymer and/or originating from the finite value of velocity employed. It means that the addition of A makes improving the viscosity of the mortar at low percentages. We will resume the discussion of these results when comparing them to the shear rheological properties.

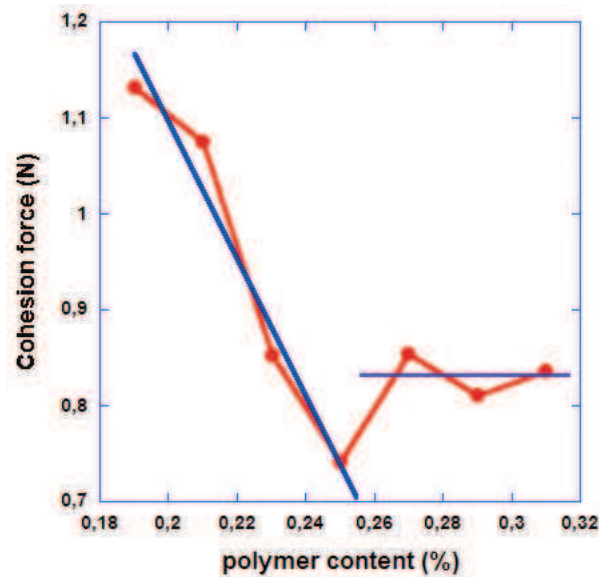


Figure 5. 5. Evolution of cohesion force of polymer content, case of A

#### 5.1.1.4. Interface adherence

The evolution of the adherence force of the mortar with the variation of polymer content is plotted in figure 5.6. The results indicate that the adherence force of the mortar is always the highest at the polymer content of 0.25%, independently of the pulling velocity. This dosage seems then to represent an optimum value regarding interface adherence. For both higher and lower polymer concentrations, the adherence force is almost unchanged. It is important to be noted that the same experiments have been performed at least 3 times with freshly prepared samples. Therefore, the local maximum in the adherence force is physical. The maximum values are less significant at low pulling velocities. This observation has practical implication. It indicates that there is an optimum dosage of A when dealing with interface adherence of mortars.

Considering the evolution of the adherence force with pulling velocity for different polymer concentrations, we observe a similar form of the curves compared with those with fibers, Methocel and bentonite (see right of Figure 5.6). The adherence is the highest at lowest pulling velocity, 10  $\mu\text{m/s}$ . A huge decrease of the adherence force can be observed with ease as a higher pulling velocity is applied. The decrease of the adherence force as a function of the pulling velocity has also been reported by A. Kaci et al [44] in the case of mortar joints.



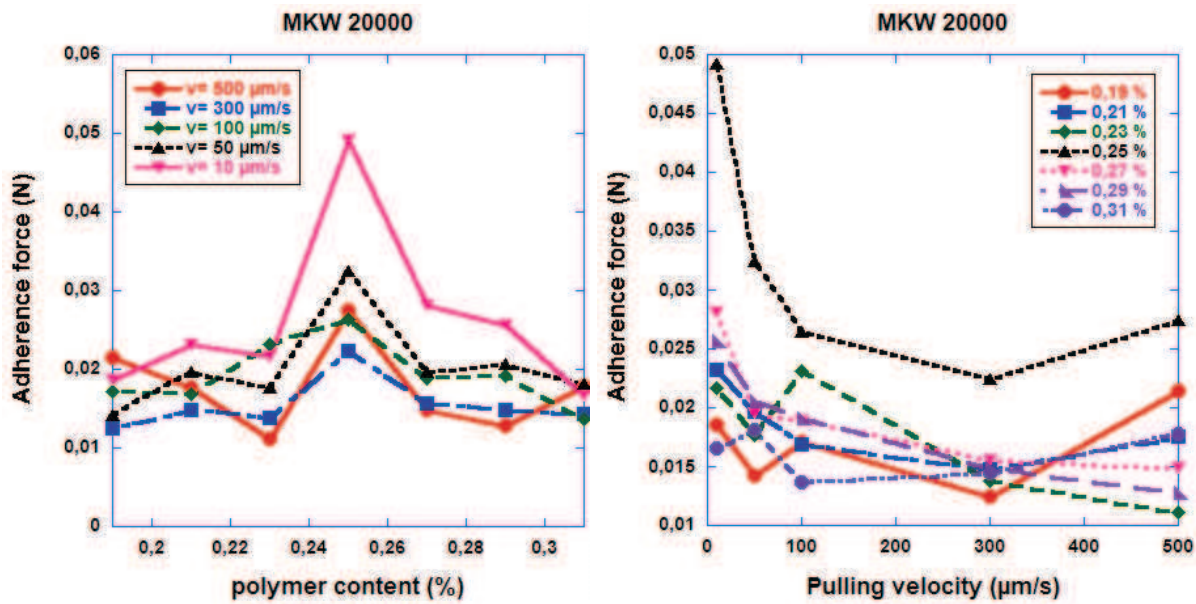


Figure 5. 6. Evolution of the adherence force as a function of pulling velocity and polymer content, case of A

#### 5.1.1.5. Adhesive failure energy

The adhesive failure energy is calculated using equation 1.12. Its evolution versus polymer content for different pulling velocities is plotted in figure 5.7. The adhesive energy is almost independent of the polymer content. We can notice however a significant influence of the tack velocity. There is a big difference between the adhesion energy at lowest pulling velocity, that is 50  $\mu\text{m/s}$ , and the remaining velocities. At high velocity, i.e. 300  $\mu\text{m/s}$ , the adhesion energy is quite small compared with that obtain at low pulling velocity (50  $\mu\text{m/s}$ ). These results are similar those obtained in previous cases concerning the effects of other types of thickening agents.

For any given pulling velocity, the evolution of the paste's adhesive energy versus polymer content is similar to the adhesion force's evolution, represented in figure 5.3. Increasing the polymer content leads to quite low change of the adhesion energy. We have several local extrema (although small) that appear and that may be attributed as previously to the different antagonist effects of the cellulose ether: enhancement of air-entrainment, lubrication, dispersion, hydrophobic association, etc. Again, these extrema are not measurement artifacts since they are reproducible. The amplitude of the extrema are relatively significant at low velocity and almost disappear at higher pulling velocities.

The similarity between the evolutions of the adhesion force and the adhesive failure energy

can be explained by the calculation of the adhesive energy itself (equation 1.12). The same interpretation may be applied.

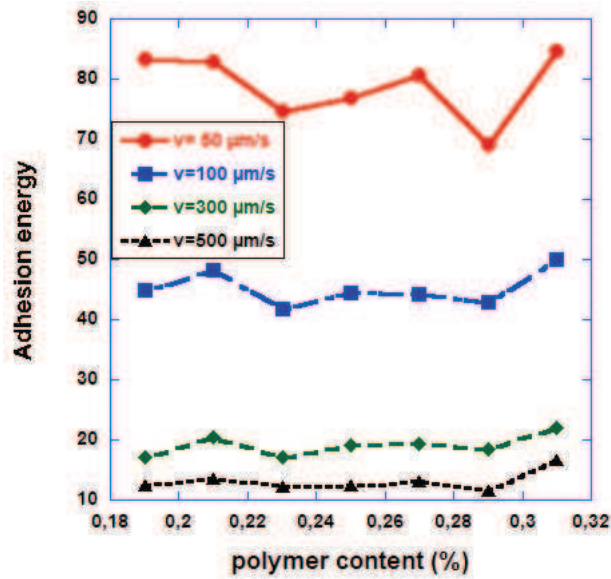


Figure 5. 7. Evolution of the adhesion energy for variation contents of A

### 5.1.2. Effect of A on the rheological behaviors

The shear rheological characterization of the mortar pastes have been performed at 5 different contents of A, including 0.21; 0.23; 0.25; 0.27 and 0.29 % by weight. Figure 5.8 represents the flow curves obtained in the rheology measurements at 3 percentages. The 3 remaining contents are represented in the appendix C.4. The mortar was investigated under stress-controlled mode. Each flow curve includes loading and unloading branches. In the present studies, we are interested in the static yield stress of the mortar, determined from the loading curves.

The loading-unloading curves indicate that the mortar pastes behave as a shear thinning fluid with a yield stress. In figure 5.9, a comparison of the loading flow curves corresponding to different polymer contents is presented. The graph is also represented in semi-logarithm scale to highlight the overall behavior of the curves at both low and high shear rates. From this comparison, we observe a qualitative similarity of the rheological behavior with increasing content of A. At low shear rates, the mortar represents Herschel-Bulkley shear-thinning behavior for all the investigated concentrations. This behavior remains shear thinning at high shear rates.

The evolution of the shear stresses as a function of shear rates in the loading curves indicates that: At certain applied stress, the recorded shear rates of mortar pastes decreases with the increase of polymer concentration. Considering the flow curves in figure 5.8 for 3 different polymer concentrations, at an applied stress of 600 Pa, the shear rates are about  $80 \text{ s}^{-1}$  for 0.21 %, and about  $45 \text{ s}^{-1}$  for 0.25 % and 0.29 %. This observation may be attributed in particular to the air-entraining effects of A.

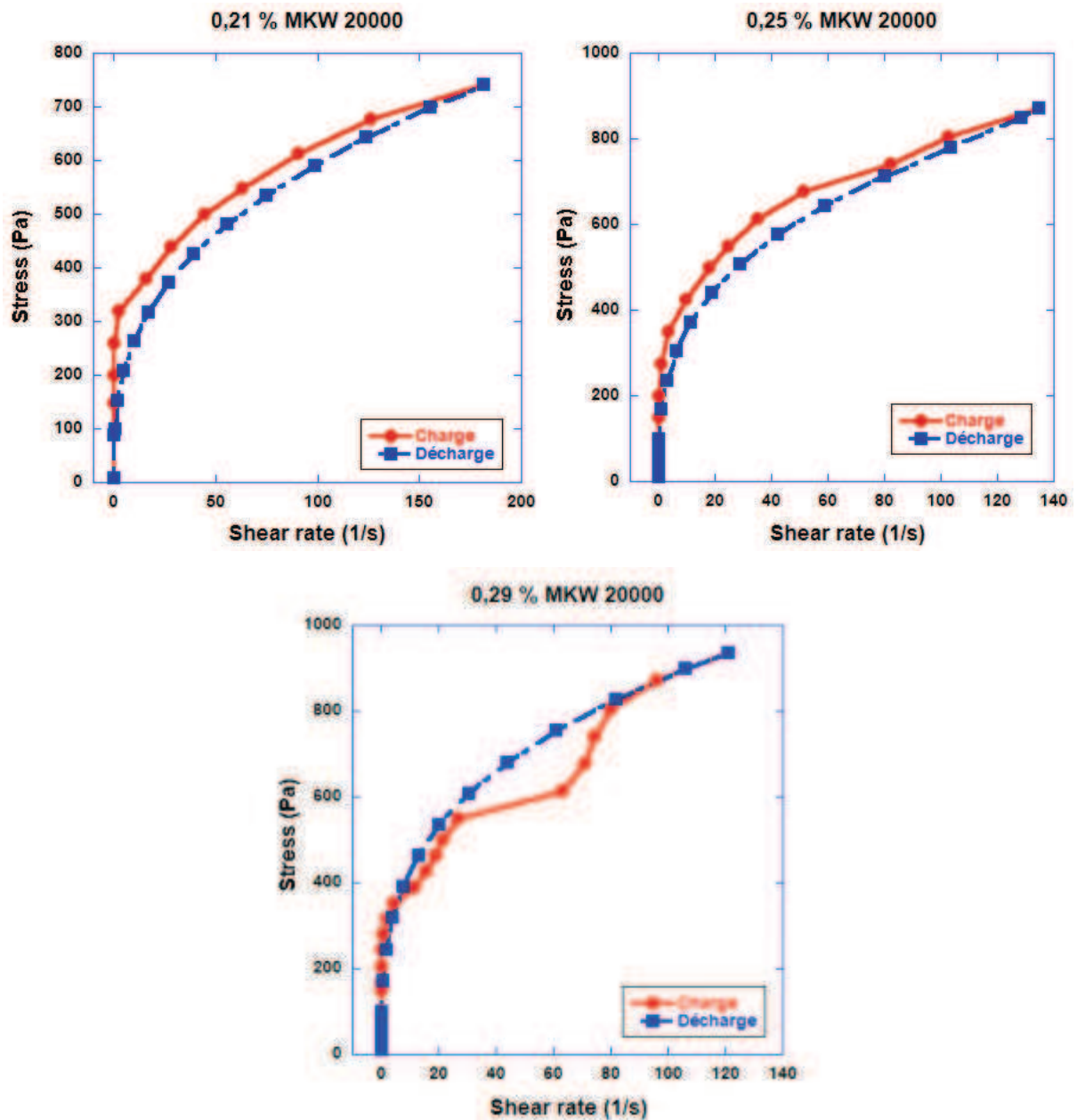


Figure 5. 8. Flow curves obtained in rheology measurement with the variation contents of A

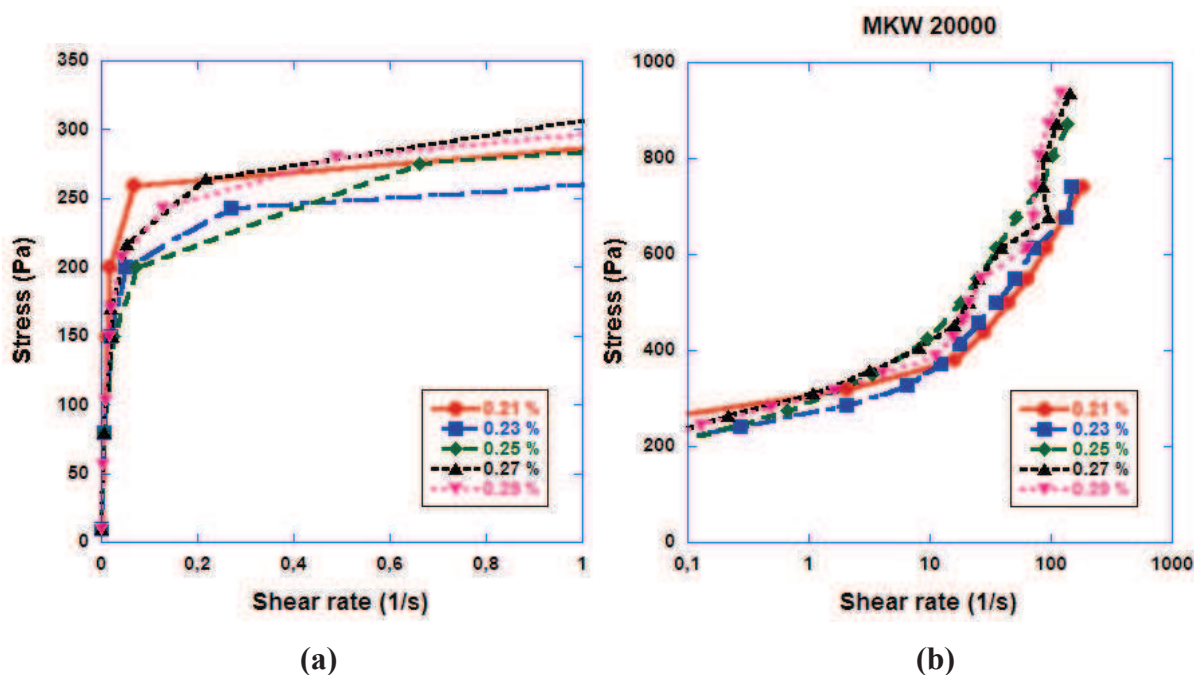


Figure 5. 9. Loading flow curves with the variation contents of *A*  
(a) Linear scale; (b) Semi-logarithmic plot

The rheological parameters are determined by performing the best fits of the loading curves with the Herschel-Bulkley model. Figure 5.10 represents all the curves fitted by the Herschel-Bulkley model.

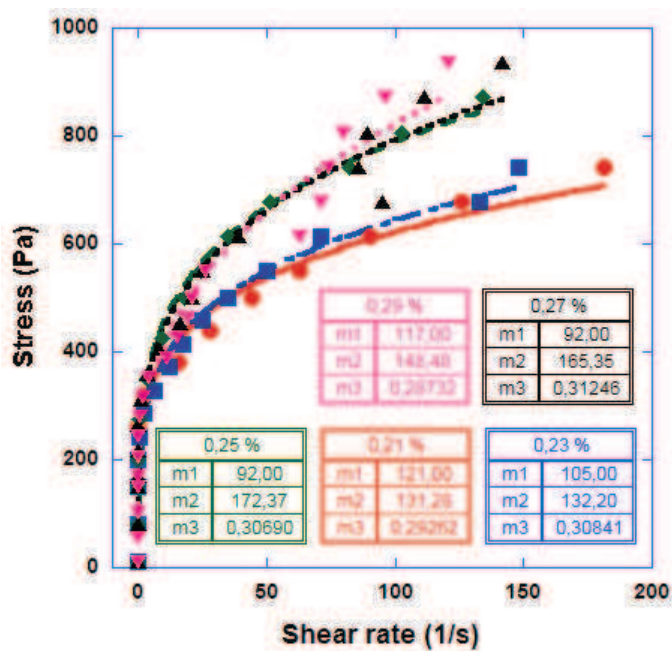


Figure 5. 10. Perform the best fit of flow curves to Herschel-Bulkley models in variation of polymer content, case of *A*, in which  $m1$  = yield stress,  $m2$ = consistency,  $m3$ = fluidity index

The evolutions of the three rheological parameters, including yield stress, consistency and fluidity index, are presented in figure 5.11. It can be seen that an optimum is observed in the evolution of the yield stress with the variation of polymer content. The yield stress reaches a minimum for a content of 0.25%. The observation of such a minimum has already reported by several authors concerning other types of mortars [39, 44, Kaci 2009, 98, and 99]. This has been attributed to the air-entraining effects of cellulosic ether polymers [39]. In fresh state, the air bubbles in the mortar may lead to an increase of the resistance to flow initiation due to capillary forces. However, these bubbles along with the lubrication effects of the polymer would decrease the resistance to flow initiation due to decrease of granular contacts. These effects have opposing impacts. The interplay between them would lead to the appearance of minimum value in the resistance to flow initiation.

The evolution of the yield stress is similar to that of the cohesion force, represented in the figure 5.5. A similar physical interpretation may be applied. The content corresponding to this minimum of cohesion and yield stress is usually selected for industrial applications, since it facilitates their application.

The evolution of the consistency with polymer content is represented in figure 5.11. The consistency reaches a maximum for a concentration of 0.25 %. In contrast of the yield stress, the consistency increases slightly, reaching a maximum at 0.25%, followed by a decrease of the consistency when increasing the polymer content. As discussed above, the interplay between increasing of pore solution viscosity, lubricating and air-entraining effects would lead to the decreasing of the viscous effects. The presence of a maximum in the evolution of the consistency can be attributed to the competition of the three effects, which lead to the increase or decrease of the viscous effects.

The evolution of the fluidity index is less significant. We observe a slightly increase of the fluidity index when increasing the polymer concentration. This is followed by an approximate plateau and for a dosage rate of 0.27%, the fluidity index decreases. This evolution of the fluidity index is similar to the observation of A.Kaci *et al.* [49] in case of mortar joints with the variation of another type of cellulose ether polymer.

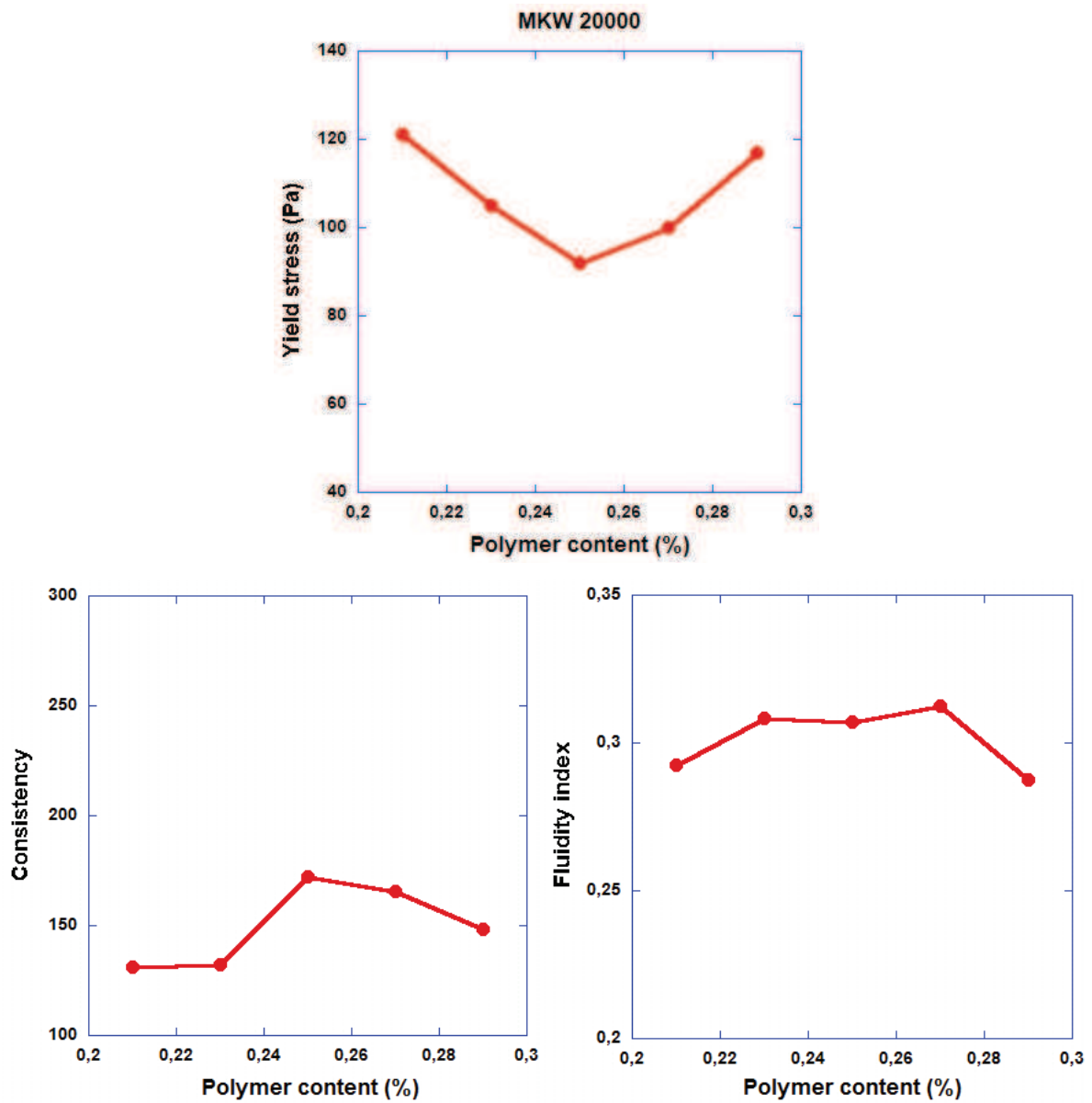


Figure 5. 11. Rheological parameters of mortar in variation content of A

### 5.1.3. Comparing the adhesive properties to the rheological behavior

The cohesion stress, also corresponding to a yield stress in tension or the resistance of the mortar for flow initiation in tension, is determined using equation 3.3. The resistance of mortar to flow initiation under shear conditions is represented by the obtained yield stress in rheological measurements. Figure 5.12 represents in diagrammatic plot a comparison between the cohesion stress and the shear yield stress for different polymer contents.



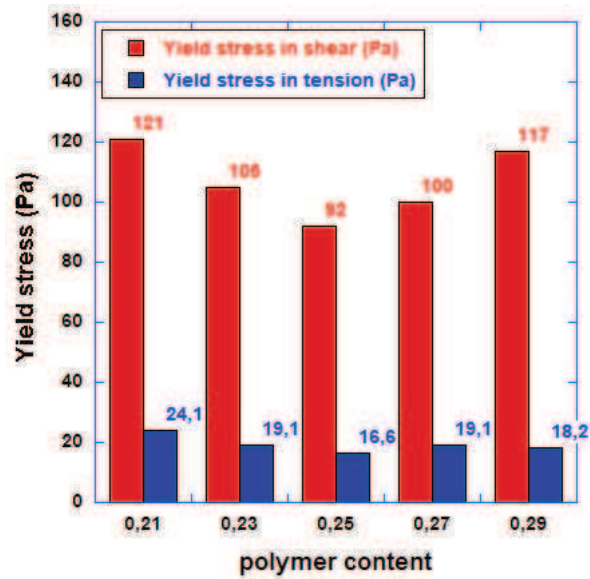


Figure 5. 12. Comparison of the yield stress of mortar in tension and in shear with the variation contents of A

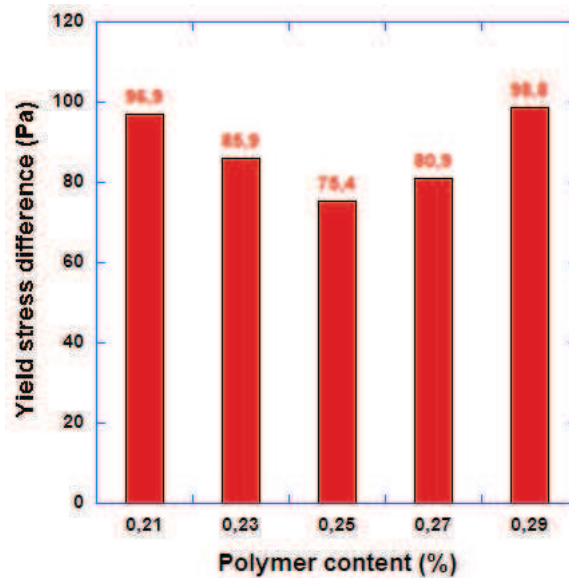


Figure 5. 13. Difference between the yield stress in tension and in shear for the variation contents of A

The results indicate that the resistance of mortars to flow initiation under varying contents of A is significantly higher in shear than in tension. For a content of 0.25%, the resistance of the mortar to flow initiation is minimum under both tension and shear conditions.

In order to have a better view on the difference between the resistance of mortar in tension and in shearing conditions with varying content of A, we have plotted the difference of these two quantities as a function of polymer content, and this represented in figure 5.13. A minimum value of this gap is also observed, around 0.25%. Whether the polymer concentration increases or decreases, the gap between two quantities increases with polymer content.



## 5.2. Effect of HEMCs type B

### 5.2.1. Effect of B on the adhesive properties

#### 5.2.1.1. Tack test results

Figure 5.14 shows the flow curves obtained in the tack measurements for different polymer contents. Additional tack curves corresponding to other contents of B are presented in the appendix C.2. The curves are represented in semi-logarithmic scale to highlight the evolution of the normal force around the peak force.

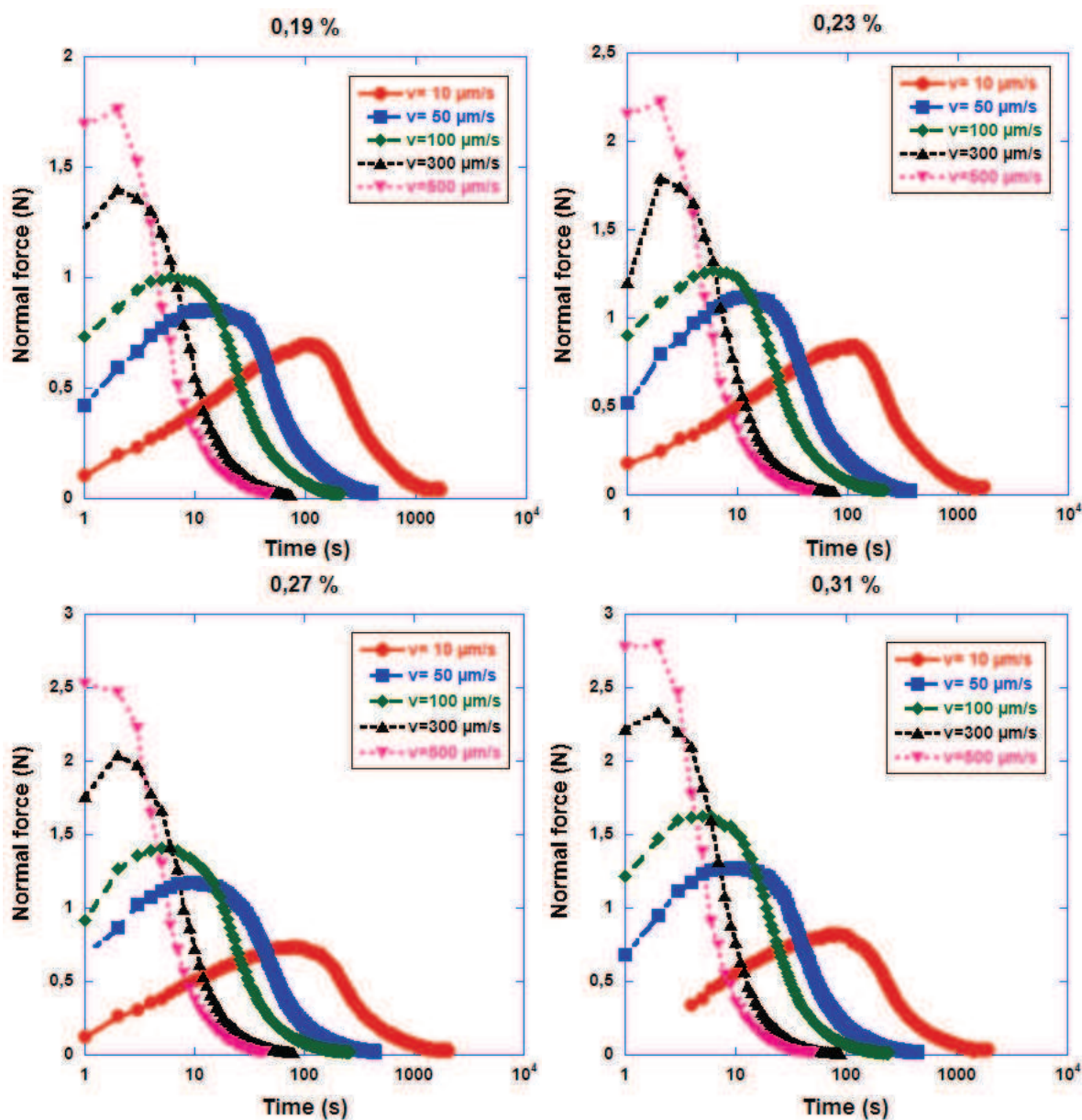


Figure 5. 14. Force versus time curves obtained in tack tests for different contents of B

We have also represented in figure 5.15 the nominal stress (normal force divided by the surface area of the plate) as a function of nominal strain (vertical displacement divided by the initial gap), in order to investigate further the dependency of the forces' evolutions versus pulling velocity. From figure 5.15, it can be observed that the nominal strain corresponding to the starting of the inward flow towards the plate's center (around 0.5) is almost independent on the pulling velocity. This observation is similar to previous cases and has also been reported elsewhere [49]. A similar physical interpretation may be then put forward.

The dependence of the peak nominal stress on pulling velocity is similar to that of the peak normal stress, which can be determined from the flow curves in figure 5.15. We discuss this issue in the following sections.

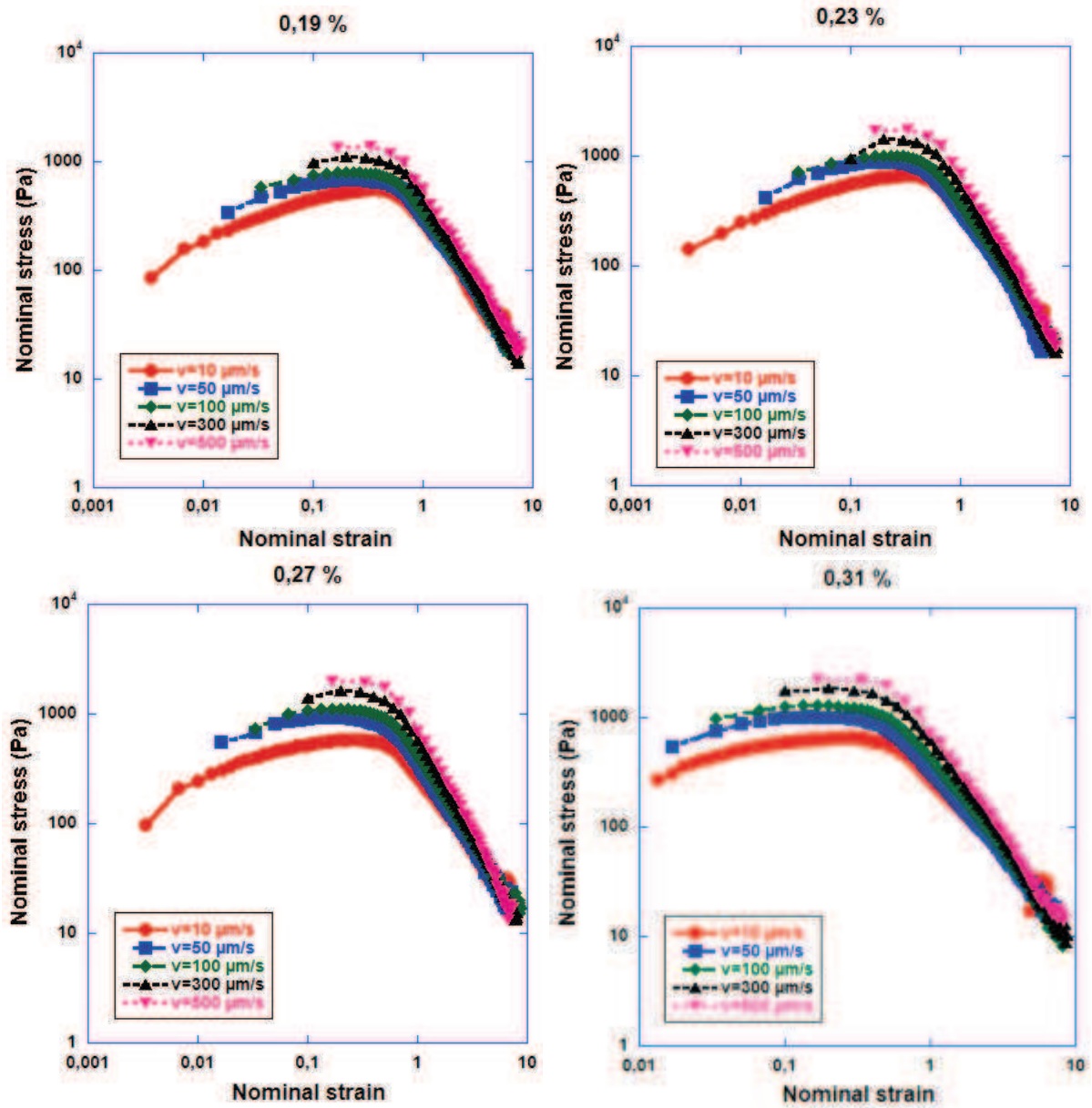


Figure 5. 15. Nominal stress and strain curves for variation content of B

### 5.2.1.2. Adhesive strength

Figure 5.16 shows the evolution of the maximum recorded normal forces, or adhesion force, with pulling velocity for different polymer contents. The results show a high dependency of the adhesion force on the pulling velocity. At each polymer concentration, the adhesion force increases with the increase of pulling velocity. Moreover, except at lowest polymer content, 0.19 %, the sensitivity of the adhesion force to the tack speed variation is independent on polymer concentration. This observation is similar to that in case of A. Therefore, a similar explanation can be put forward.

The evolution of the adhesive force versus polymer concentration is also considered in figure 5.16 for different pulling velocities. At the lowest velocity, 10  $\mu\text{m/s}$ , the dependency on polymer content is small and we observe a minimum value of adhesion at 0.29 %. Increasing the pulling velocity, the minimum value disappears and then reappears at smaller polymer content, 0.25 % at the tack speed of 300 and 500  $\mu\text{m/s}$ .

Considering the overall behavior of the evolution of the adhesion force versus polymer concentration, one can observe a qualitative change in these evolutions. The evolution appears to change gradually. At lowest tack speed, the adhesion slightly decreases with the enhancement of polymer dosage. However, starting from the tack speed of 50  $\mu\text{m/s}$ , the adhesion force increases with the increase of polymer content. This increase is more and more significant at high pulling velocities. This is one of the main differences with the case of polymer A.

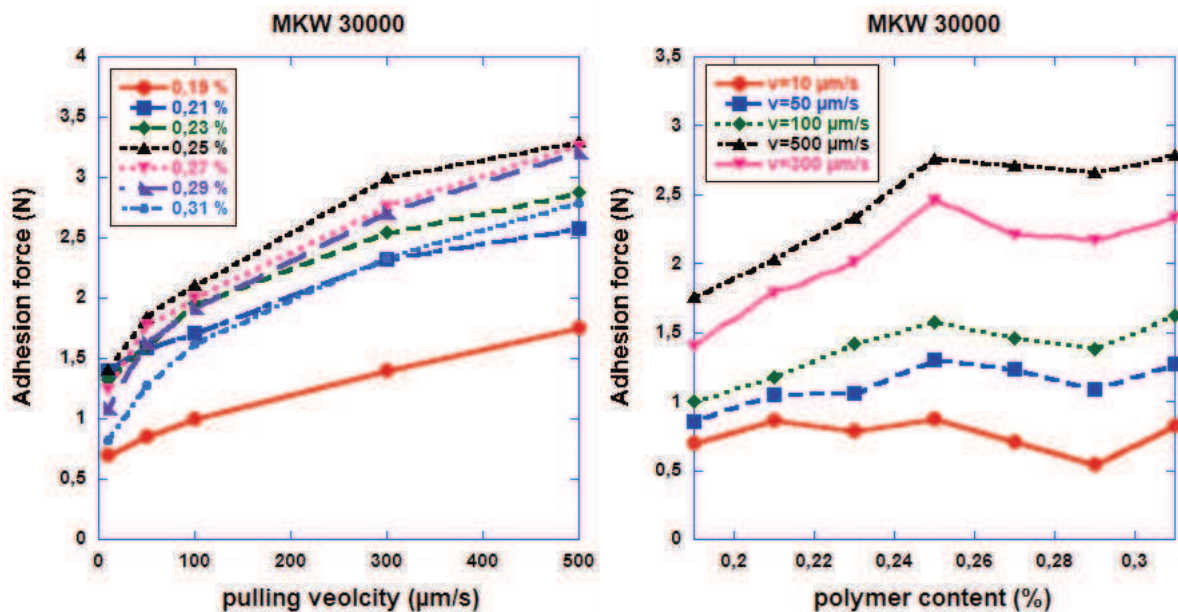


Figure 5. 16. Evolution of the adhesion force of mortar in formulation with B as a function of pulling velocity (a) and of polymer contents (b)

### 5.2.1.3. Cohesion force

The cohesion force is identified as the adhesion force corresponding to the lowest value of pulling velocity that can be applied with our rheometer (10  $\mu\text{m/s}$ ). The evolution of the cohesive force for different contents of B is plotted in figure 5.18.

The results indicate that the cohesion force is lowest at a critical content of B, around 0.27%. Below this content, the cohesion force slightly decreases when the polymer content increases. Beyond this content, 0.27%, the cohesion's evolution is reversed. The increase of polymer content seems to improve the paste cohesion. However, this increase is not significant. An average value of the cohesion force can be observed, around 0,8 N, while considering the overall behavior of the curve.

We will resume discussion about this observation when considering the rheological measurements.

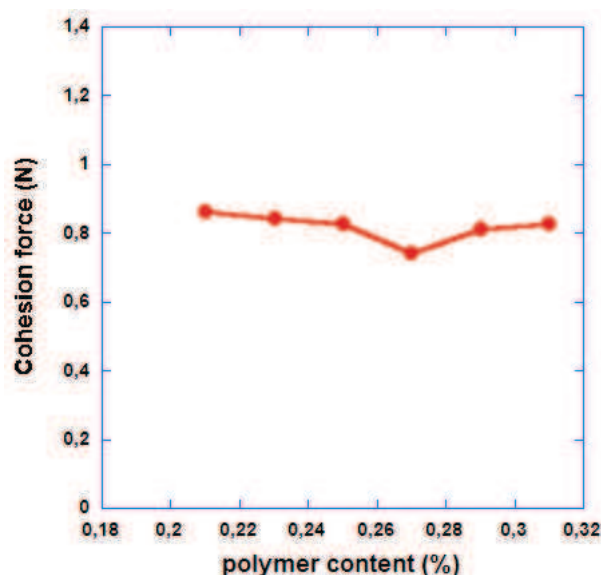


Figure 5. 17. Evolution of cohesion force with the variation contents of B

### 5.2.1.4. Interface adherence

The adherence force is plotted respectively as a function of polymer content and of pulling velocity in figure 5.19. At the lowest pulling velocity, 10  $\mu\text{m/s}$ , a peak value of adherence is observed. However, this peak force disappears at high pulling velocities. In most cases, the adherence is independent of polymer contents; it varies around a mean value (between 0.02N and 0.03N).



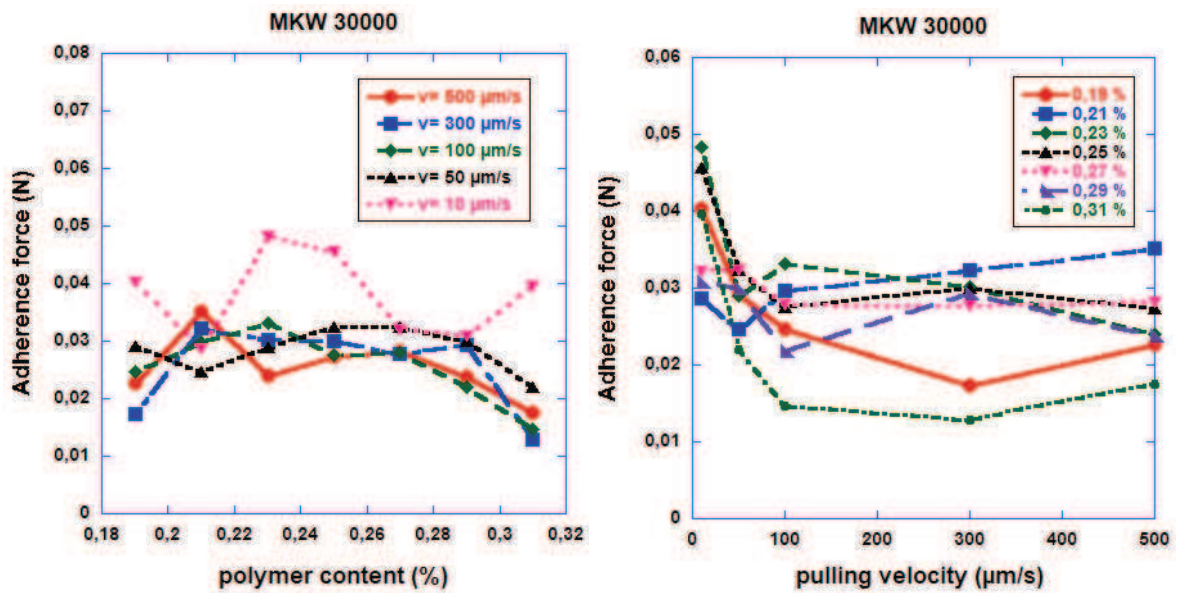


Figure 5. 18. Evolution of the adherence force as a function of pulling velocity and polymer content, case of B

The independence of the adherence force on the polymer concentration at different tack speeds indicates that the increase of B content should not influence the easiness of the mortar applicability on a given surface.

#### 5.2.1.5. Adhesive failure energy

The adhesive failure energy is calculated by equation 1.12 and its evolution for different contents of B is represented in figure 5.20.

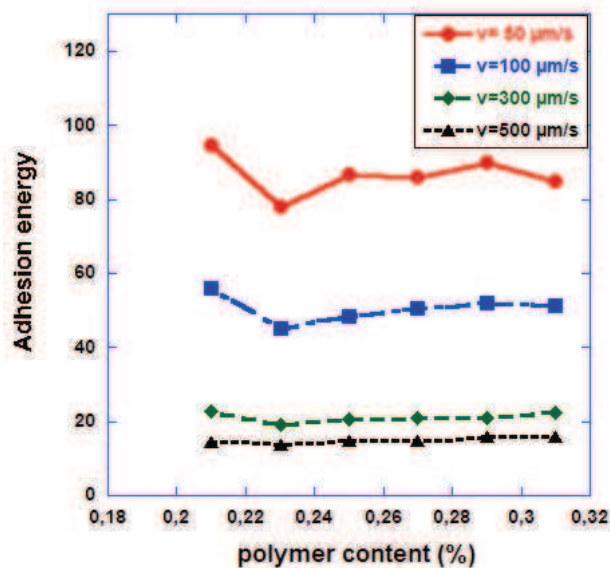


Figure 5. 19. Evolution of the adhesion energy for various contents of B

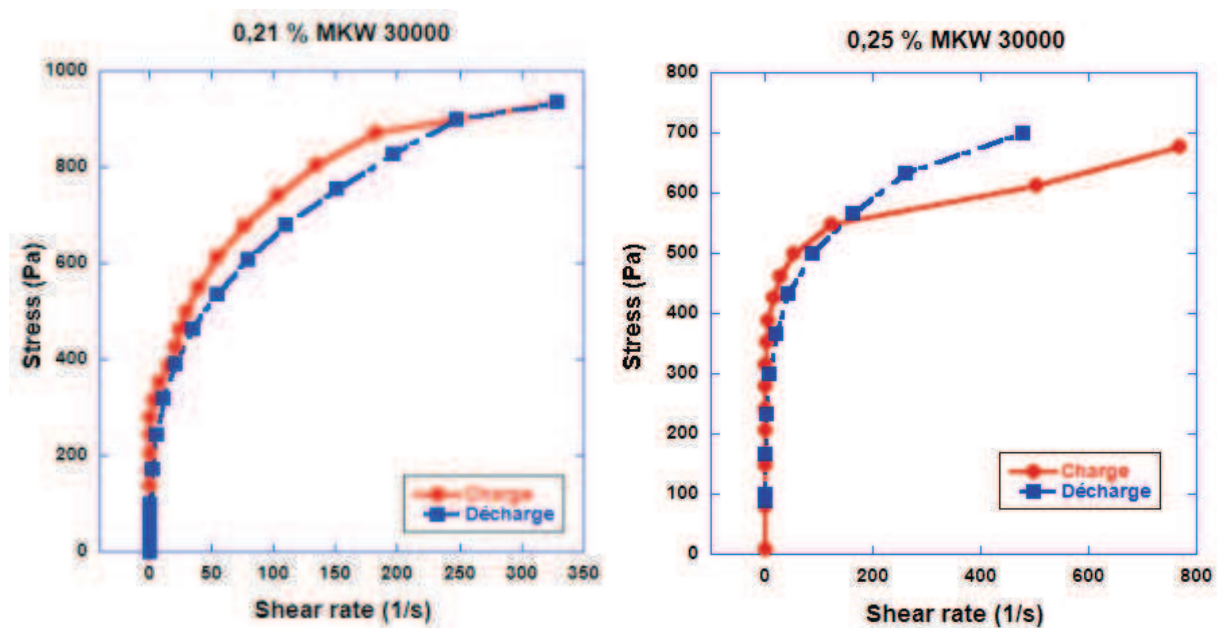
The dependence of the adhesion energy on the tack speed is found to be similar to previous cases. In particular we also observe a decrease of adhesion energy as a function of pulling velocity. At low pulling velocity, i.e. 50  $\mu\text{m/s}$ , the evolution of the adhesive failure energy is non monotonic. With the increase of polymer concentration, the adhesive energy first decreases to reach a minimum at 0.22 %. Beyond this content, the adhesive energy is almost independence on the polymer content. A mean value can be observed for each given velocity.

### 5.2.2. Effect of B on the rheological behaviors

Figure 5.21 represents the flow curves of the mortar pastes for 3 polymer concentrations. The remaining investigated flow curves are represented in appendix C.5. The flow curves were determined at controlled stress. The test samples were investigated at 5 different percentages of polymers, including 0.21; 0.23; 0.25; 0.27 and 0.29%.

We can see in the figure 5.21 that the mortars become more and more shear-thinning when we increase polymer content. We will come back this in more quantitative way below.

In order to distinguish the rheological behavior of mortar pastes at low shear rates, the comparison of the flow curves is then plotted in both linear scale at low shear rates and semi-logarithmic scale, as represented in figure 5.22. It can be seen that the mortar pastes behave as Herschel-Bulkley shear-thinning fluids for all the investigated concentrations, similarly to the mortars formulated with cellulose ether A.



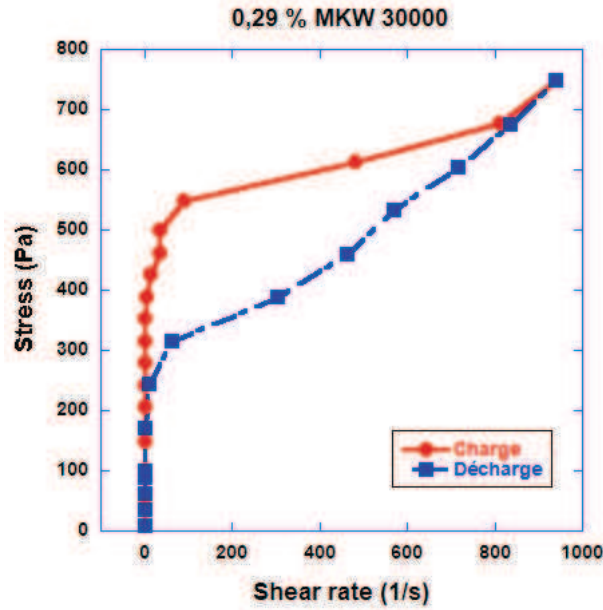


Figure 5. 20. Flow curves obtained in controlled stress mode with the variation contents of B

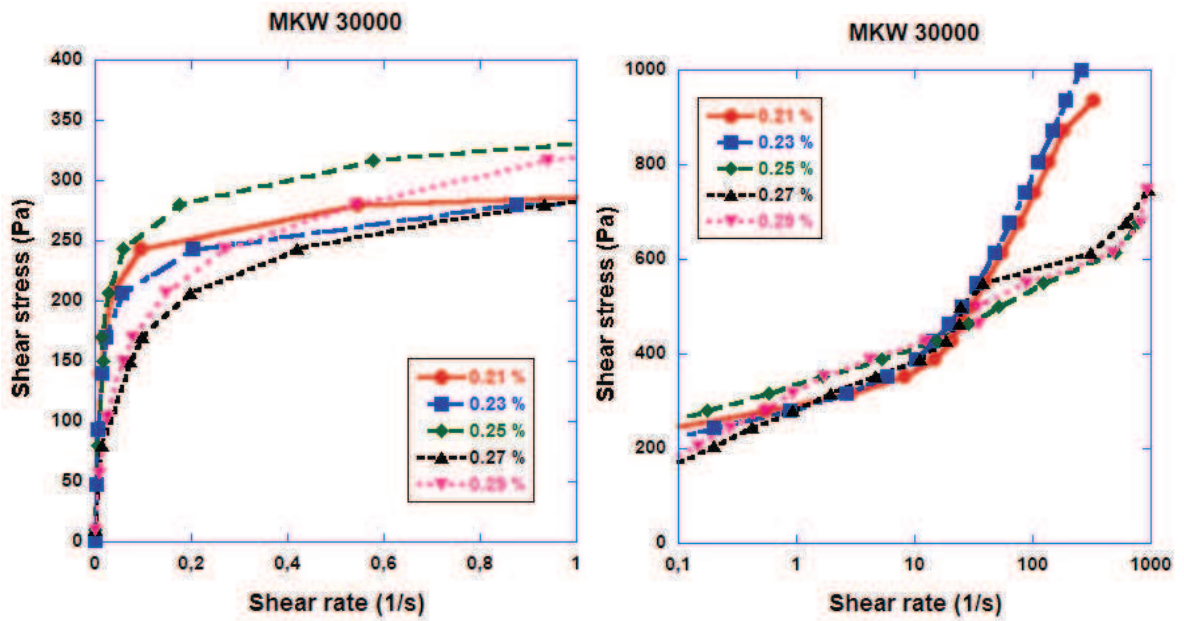


Figure 5. 21. Comparison of the loading curves obtain in rheological measurement for different contents of B

Considering the evolution of the applied stresses as a function of recorded shear rate at some given stresses and for different polymer contents of B, we can see that: At certain stress, for instance 600 Pa, the recorded shear rates are about  $60 \text{ s}^{-1}$  for 0.21%, and  $500 \text{ s}^{-1}$  for 0.25% and 0.29%. This indicates that for certain given applied stresses, the recorded shear rates increases with the increase of polymer content. This observation is inverse to that in previous



case for mortars with polymer A. The crossover of the flow curves (Figure 5.22 left) indicates that the evolution of the apparent viscosity (stress divided by shear rate) versus polymer content is dependent of the shear-rate interval considered. Here again this may be attributed to the different antagonistic effects of the polymer.

The yield stress of the mortar is determined as the shear stress value at a finite but very small shear rate ( $0.01 \text{ s}^{-1}$ ). The evolution of yield stress versus polymer concentration is shown in figure 5.23. It can be seen that once again the presence of an optimum when varying polymer content. The yield stress decreases significantly to a minimum value at 0.25%, then followed by a slightly increase of the yield stress as the polymer content increased.

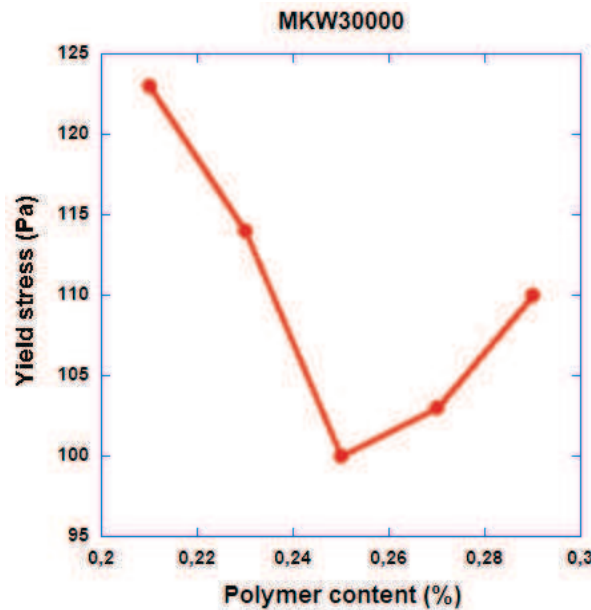


Figure 5. 22. Yield stress of mortar for different content of B

The presence of a minimum in the yield stress curves of mortar pastes seems to be a general result. This has been obtained in previous case with the use of A. It has also been reported by several authors for others types of mortar mixes [39, 44, 49] and has been attributed in particular to the air-entraining effects of cellulosic ether polymers [39].

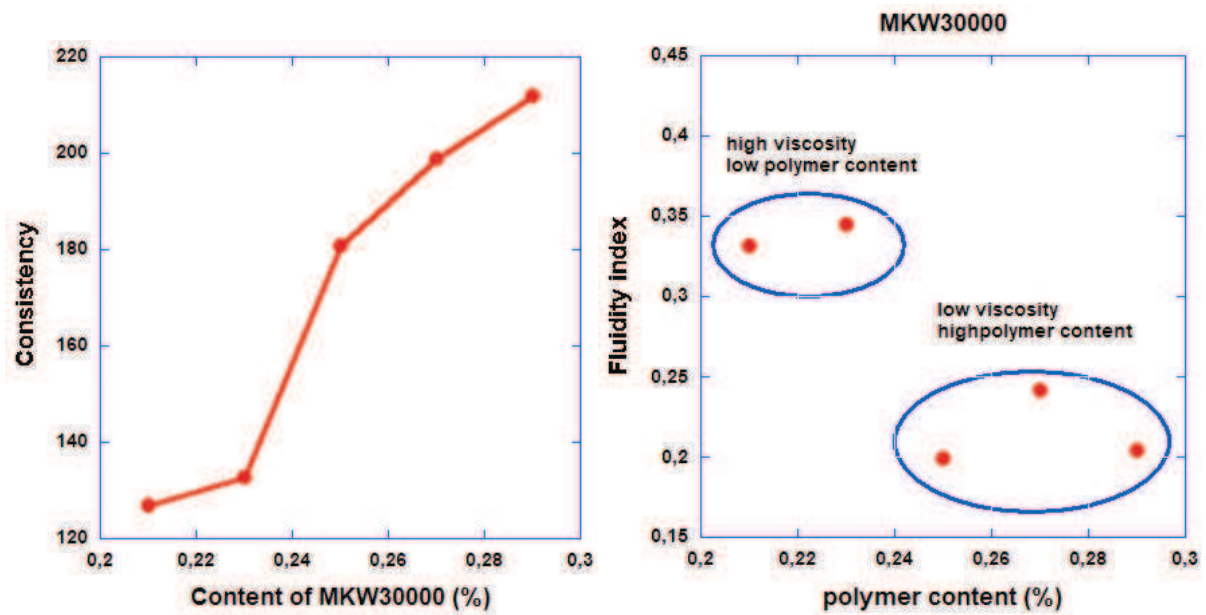


Figure 5. 23. Rheological parameters of mortar for different content of B

The two other rheological parameters, including consistency coefficient and fluidity index, are determined by performing the best fit of the flow curves with the Herschel-Bulkley model. The evolutions of these parameters are represented in the figure 5.24.

In contrast with the yield stress's evolution, we observe a monotonous increase of the consistency when increasing the polymer concentration, reflecting the increase of the viscous drag effects with polymer content. A similar observation concern the effect of another type of cellulose ether polymer on mortar joints has been reported [49]. Polymer B has much higher effect on consistency that polymer A. This is rather expected since the molecular weight of B is higher, so its effect on the viscosity of the pore solution is higher due more entanglement. A huge increase of the consistency can be observed when the polymer content is above 0.23 %. They may correspond to a transition from dilute/semi-dilute to concentrated regimes in the polymer pore solution.

The evolution of the fluidity index indicates that the fluidity (figure 5.24) of the mortar is high at low content, and significantly decreases to a small value at high polymer contents. We can recognize two areas of the fluidity index of mortar as circled in figure 5.24. At low polymer contents, including 0.21 and 0.23 %, the mean value of the fluidity index of is around 0.34, while it is around 0.21 at high polymer contents. It means that the mortar becomes more shear-thinning with increasing polymer content. The transition from high to low fluidity indexes coincides with that of low to high consistency.

### 5.2.3. Comparing the adhesive properties to the rheological behavior

The yield stresses, which are identified in extension (cohesion) and in shear conditions, are plotted as a function of polymer content in figure 5.25. The resistance of mortar to initiation of shear flow is significantly higher than that under extension.

We can see that the cohesion stress and shear yield stress of the mortars formulated with A and B are close to each other (figures 5.25 and 5.12). This issue can be explained as following: Cellulose ethers A and B are used for enhancement of water retention and for giving the material good workability. The improvement of workability means that the yield stress in shearing should be minimized without being too low in order to avoid creep. The experiment results have proved that the rheological measurement method using in this study is a complementary method for characterizing the mortar in fresh state.

Similarly to the case of polymer A (see figure 5.12), figure 5.25 shows that the resistance of the mortar to shear initiation is much larger than that in extension. Therefore these two admixtures increase the mortar creep resistance without increasing too much its stickiness. Their application is then suitable for render mortars. They are indeed used for render mortars.

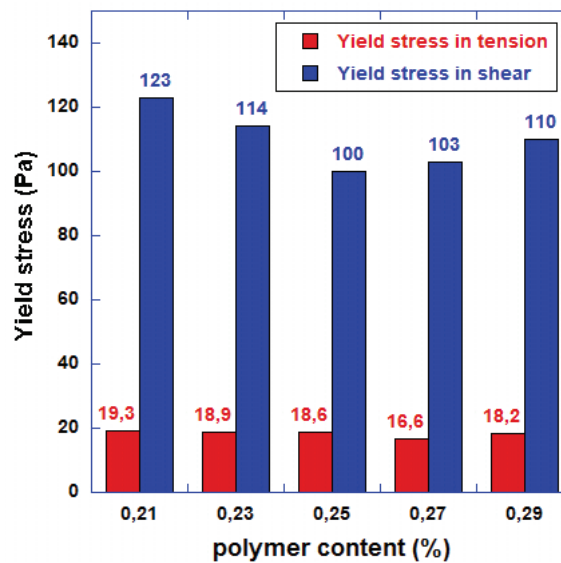


Figure 5. 24. Comparison of the yield stress of mortar in tension and in shear with the variation contents of B

### 5.3. Effect of HEMCs type C

#### 5.3.1. Effect of C on the adhesive properties

##### 5.3.1.1. Tack test results

This cellulose ether is used in practice in mortar adhesives such as tile adhesives. It is then expected to exhibit high tackiness. Let us then consider its influence on the tack properties of mortars.

Figure 5.27 represents the flow curves obtained in tack measurements for different polymer contents. Additional results are presented in appendix C.3.

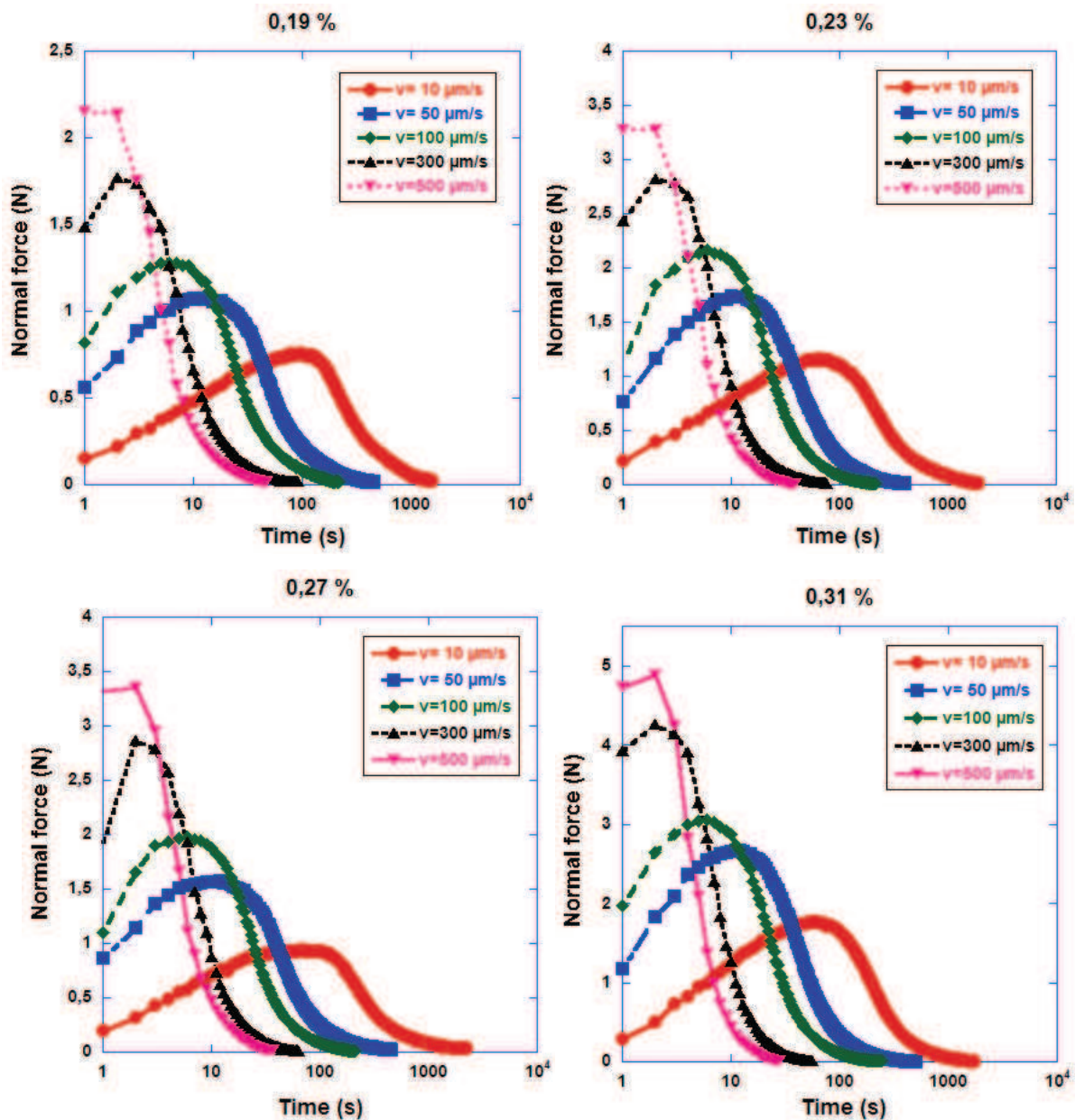


Figure 5. 25. Force versus time curves obtained in Probe tack tests for different contents of cellulose ether type C

The general forms of tack curves are fairly similar for different polymer contents and pulling velocities. The curves are also similar those of the previous mixes. However it is clear that the peak force increases with polymer content and pulling velocity. We will come back below in more details to this issue.

The nominal stress and strain, calculated as described in section 3.1.1, is presented in figure 5.28. As previously, the peak nominal strain (around 0.5) does not depend on the pulling velocity, while the peak nominal stress increase with pulling velocity. Based on the whole results presented in the present study, the value of peak nominal strain (0.5) seems to represent a universal value, being independent of the mix-design. This may indicate that for all the mixes considered here the rupture process is similar for all the mixes.

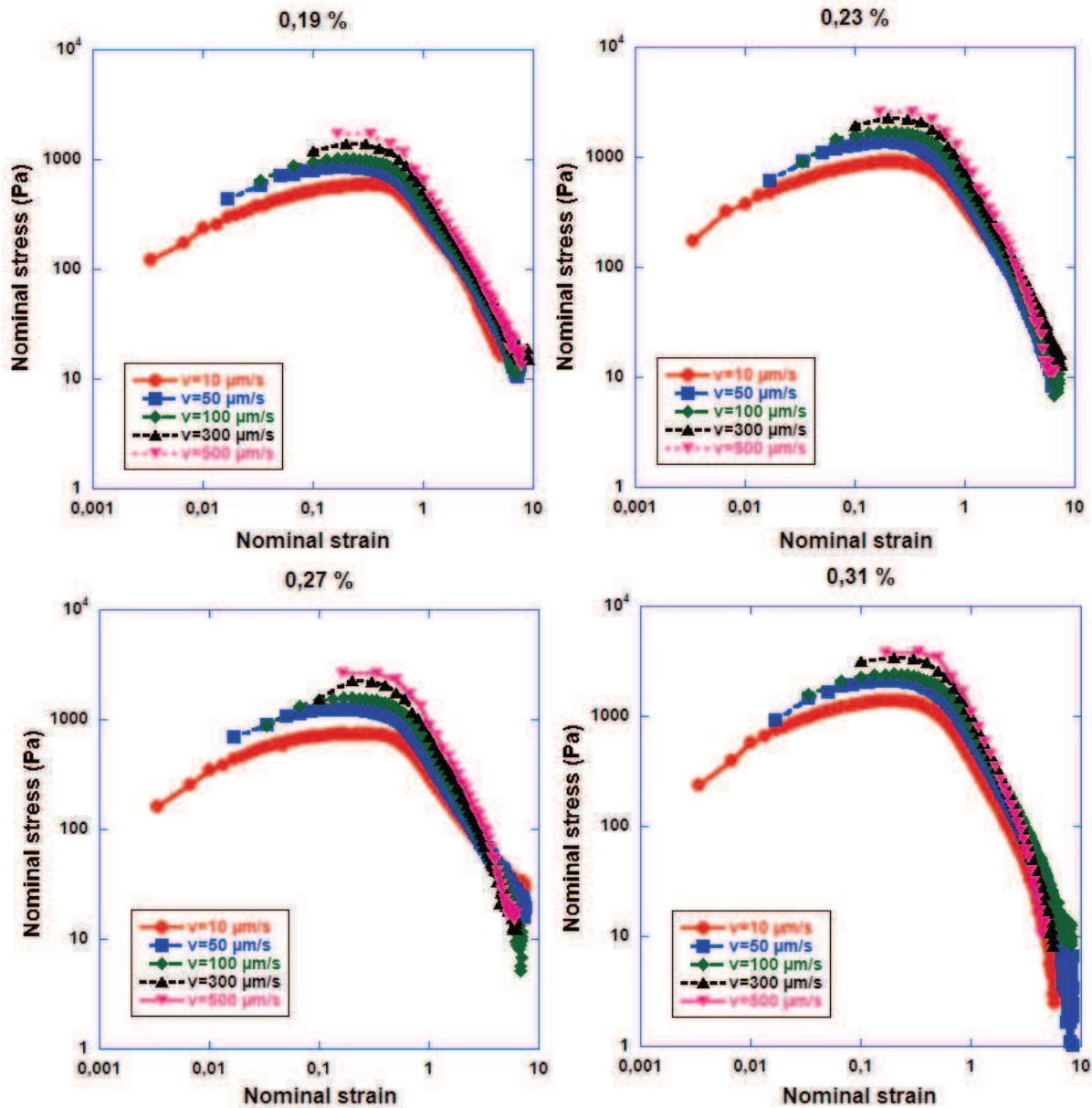


Figure 5. 26. Nominal stress versus nominal strain for different contents of C.



### 5.3.1.2. Adhesive strength

Figure 5.29 shows the evolution of the adhesive force (or peak force) with pulling velocity for polymer contents. We also represent in the same figure the evolution of the adhesive force versus polymer content for different velocities. For any given polymer concentration, the adhesion force increases with the increasing of pulling velocity. The sensitivity of the peak force to the velocity increases with polymer content. This is expected and can be attributed to the increase of the viscous contribution due to the polymer. The increase of the peak force is much higher at high pulling velocities (see right of figure 5.29). This is rather unexpected since the polymer should increase shear-thinning aspect of the mortars (see below). A possible explanation would be an extensional contribution to the peak force. In that case the polymer will indeed increase the peak force in particular at high velocity since high molecular weight polymer solutions are known to be strain-hardening in extension.

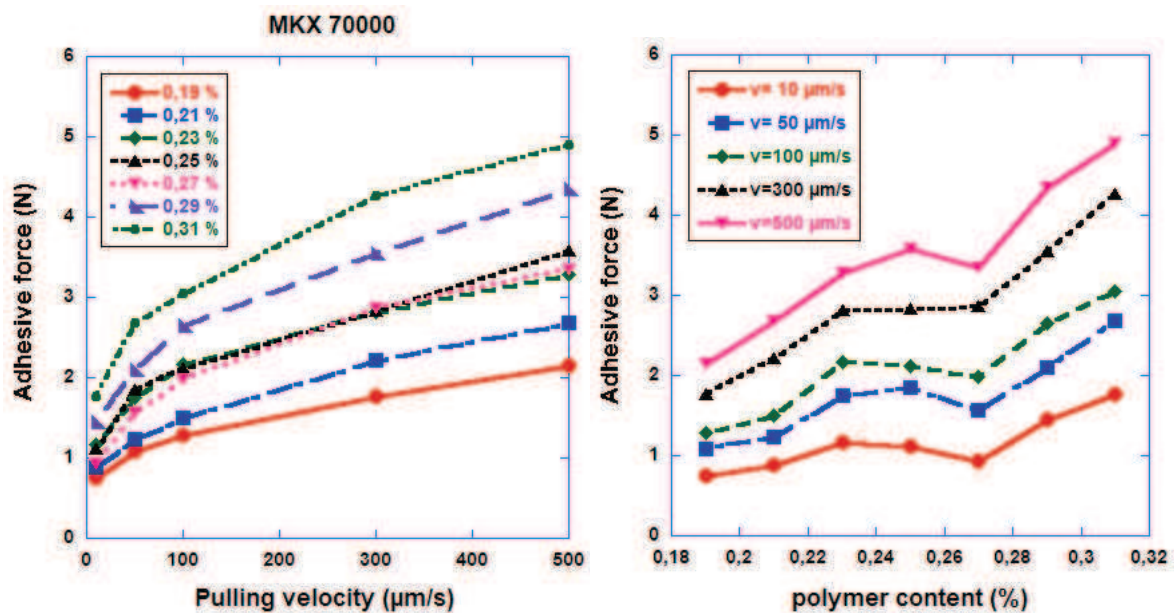


Figure 5. 27. Evolution of the adhesion force as a function of pulling velocity (left) and of polymer contents (right) in case of C

. Considering the overall behavior of the curves on the right in Figure 5.29, it can be clearly seen that the increasing of C would lead to the improvement the tackiness of the mortar paste. However, the sensitivity of the force to the polymer content variation dependent of the pulling velocity.

### 5.3.1.3. Cohesion strength

The cohesion force is assumed to be the adhesive force at the lowest pulling velocity (10

$\mu\text{m/s}$ ). The evolution of the cohesion force with the variation of polymer content is represented in figure 5.31. It can be seen that there is a significant increase of the cohesive property of mortar with increasing cellulose ether type C amount. Yet, the evolution of cohesion is non-monotonic. When the polymer content increases, the paste cohesion first increases to a maximum value at 0,23 %, followed by a decrease to a minimum at 0,27 %. Beyond this content, a significant increase of the force is observed.

The appearance of these extreme values has also been observed in two previous cases, with the variation of A and B, and has also been reported in literature by several authors concerning other types of mortars [39, 44 and 49].

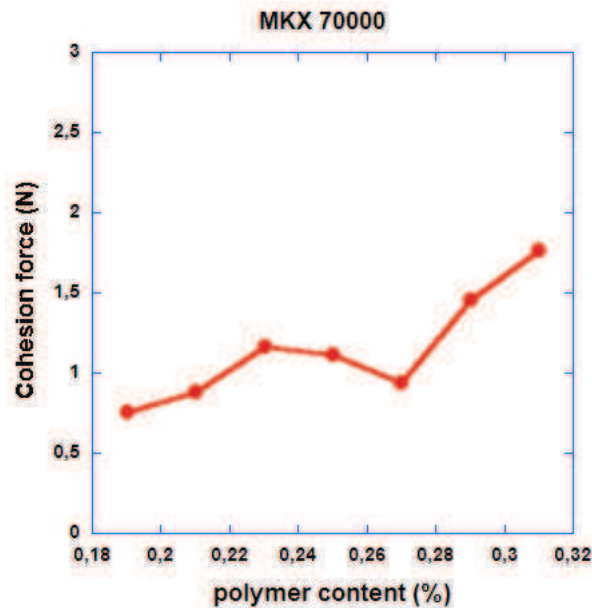


Figure 5. 28. Evolution of the cohesion force with the variation of the content of cellulose ether type C

#### 5.3.1.4. Interface adherence

The adherence force versus polymer content for different velocities and versus pulling velocity for different polymer contents is shown in figure 5.32. At relatively low dosage rates the adherence force is quite small. For a dosage rate of 0.24% the adherence force starts increasing. It passes through a maximum and then significantly decreases at high dosage rates. As in the previous mixes, the maximum adherence value is obtained at low pulling velocity. It is to be noted that the value of the typical dosage rate used for high performance tile adhesives is around 0.25%, which coincides with the dosage corresponding to the maximum of the adherence force.

The non-monotonic behavior of the adherence force (versus polymer content or pulling velocity) may be explained by an eventual competition between the bulk forces exerting



among the constituents of the material and the interfacial forces exerting between the material and the plate.

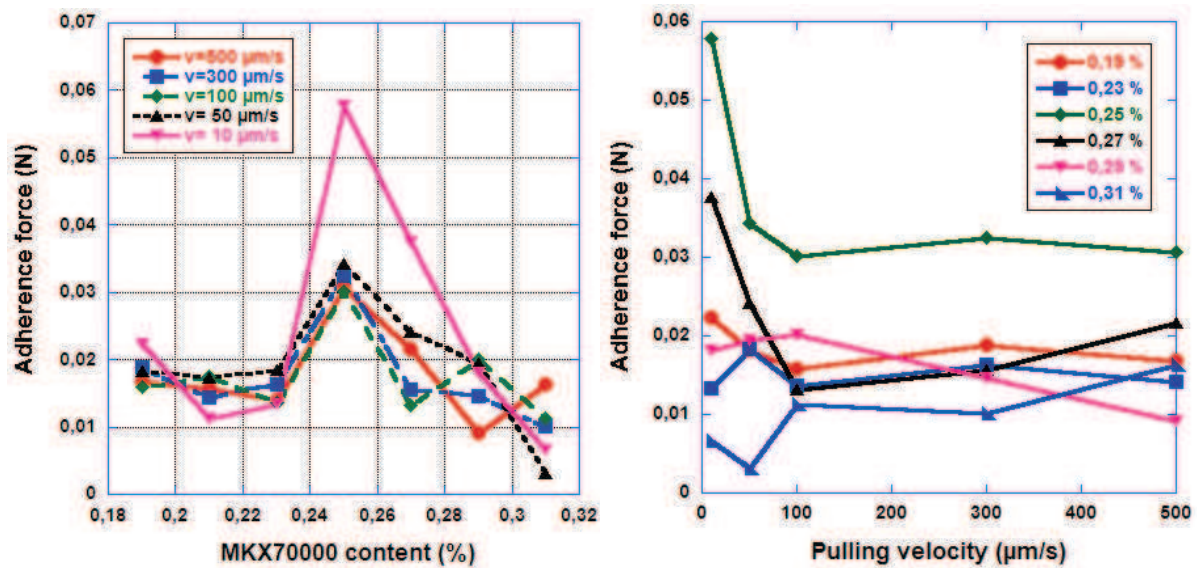


Figure 5. 29. Evolution of the adherence force as a function of pulling velocity and polymer content, case of C

#### 5.3.1.5. Adhesive failure energy

The adhesion energy is plotted as a function of polymer content in figure 5.33. We can see that the evolution of the adhesion energy at low velocity is similar to that of the cohesion force, represented in figure 5.29. The adhesive energy decreases drastically at high velocity. This also indicates that adhesion energy is related to adherence strength: both adhesive properties decrease when we increase the velocity. This may also be attributed to the strain hardening du the polymer. At high stretching velocity the resistance of the mortar to extension increases leading to it abrupt rupture at the interface. The aftermath is a low tack energy (small area under tack curve) and low adherence (amount of mortar that remains stuck on the moving plate).

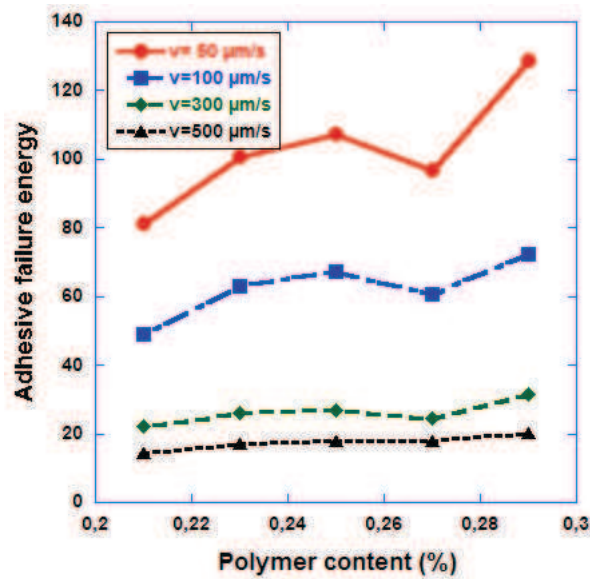


Figure 5. 30. Evolution of the adhesion energy as a function of dosage rate of cellulose ether type C

### 5.3.2. Effect of cellulose ether type C on the rheological behaviors

The flow curves obtained in the stress-controlled mode at 3 different contents of C are represented in figure 5.34. Additional investigated polymer concentrations are represented in the appendix C.6. The comparison of the loading curves is plotted in figure 5.34; both in linear and semi-logarithmic scale in order to highlight the behavior close to the yield points.

The loading curves indicate that at dosage rates of polymer C, the mortar rheological behavior is close to that of a Bingham fluid. The mortars are shear thinning at lower polymer content. However if we zoom in the flow curves around low shear rates (see figure 5.35) We can observe that the mortar behave rather as Herschel-Bulkley shear-thinning fluids for all the dosages rates.

This change in the rheological behavior of mortar pastes at low and high shear rates is also represented by the evolution of the rheological parameters, including yield stress, consistency and fluidity index, which will be discussed in the following.

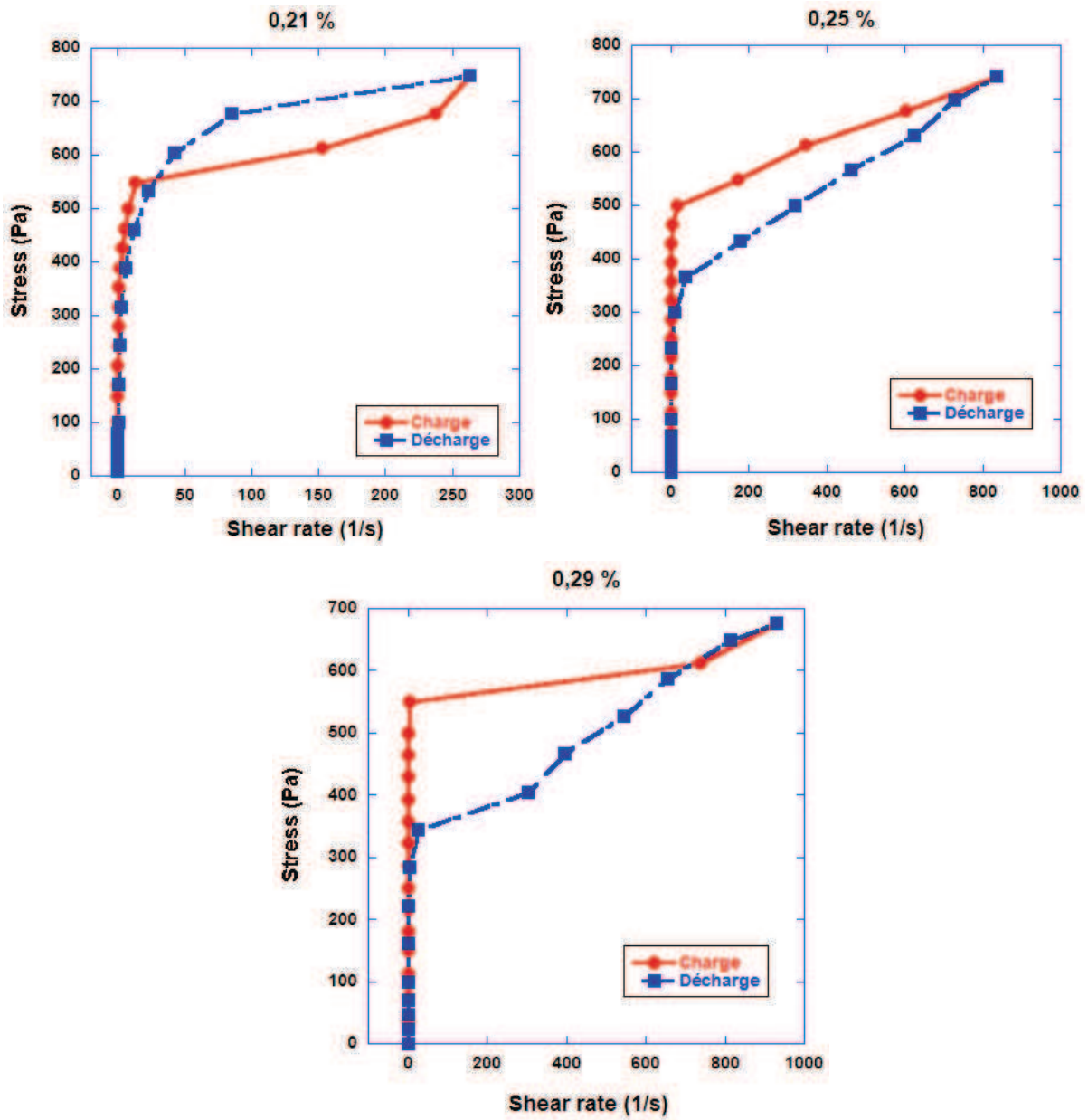


Figure 5. 31. Flow curves obtained in controlled stress mode with the variation content of C

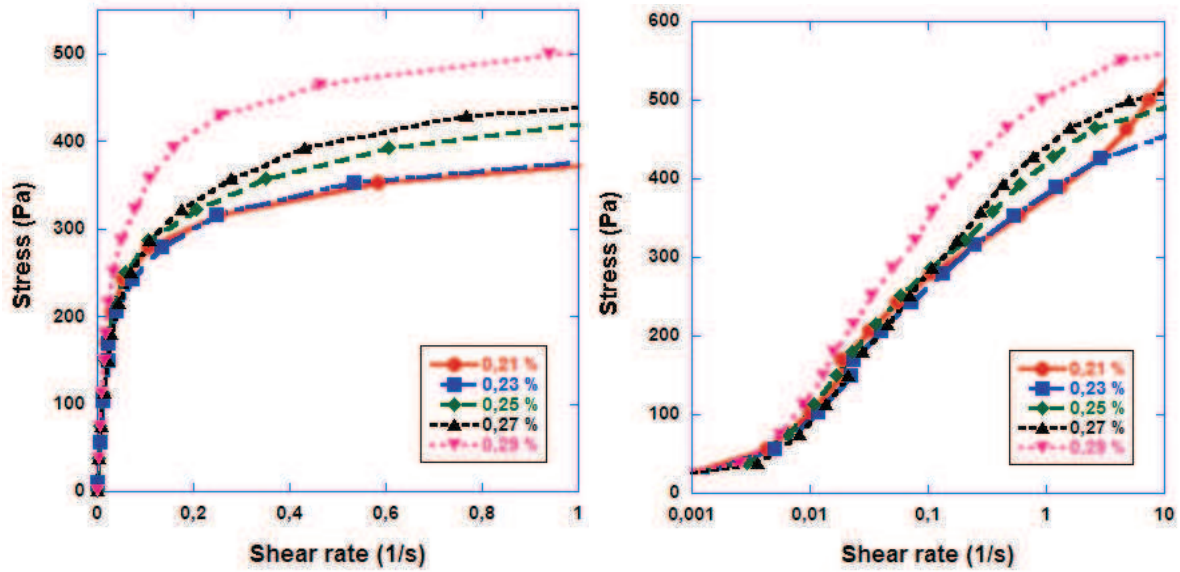


Figure 5. 32. Rheological flow curve, with the variation of  $C$ , plotted in normal scale and semi-logarithm scale to highlight the behavior at low shear rate

The yield stress is identified directly as the shear stress at which we have a finite shear rate ( $0.01 \text{ s}^{-1}$ ). The evolution of the yield stress versus polymer content is represented in figure 5.34. Similarly to the previous cases, there is a minimum value of the yield stress at 0.25 %. The same interpretation than previously can be put forward.

The two other rheological parameters, including consistency coefficient and fluidity index, are determined by performing the best fit of the flow curves with the Herschel-Bulkley model. The evolutions of these parameters for different polymer contents are also represented in figure 5.36.

In contrast with the yield stress evolution, we observe a monotonous increase of the consistency when increasing the polymer concentration, reflecting the increase of the viscous drag effects with polymer content. Similar observations on the consistency of mortar paste under the variation of another type of cellulose ether polymer on mortar joints have been reported [49], and also obtained in previous cases of A and B. The effects on the consistency of these three types of cellulose ether will be compared below.

The evolution of fluidity index of mortar pastes is similar to that of the yield with a certain lag in dosage rate. Increasing of the polymer content first leads to the decrease of fluidity index to reach a minimum value at 0.23 %. This minimum value is then followed by a significant increase of the fluidity index. The presence of a minimum value of fluidity index may result from the competition between the shear-thinning character of the addition polymer and the shear-thickening contribution of the granular phase in the suspension. In addition some

associative polymers are known to present shear-thickening at low shear-rates, and this is probably the case here.

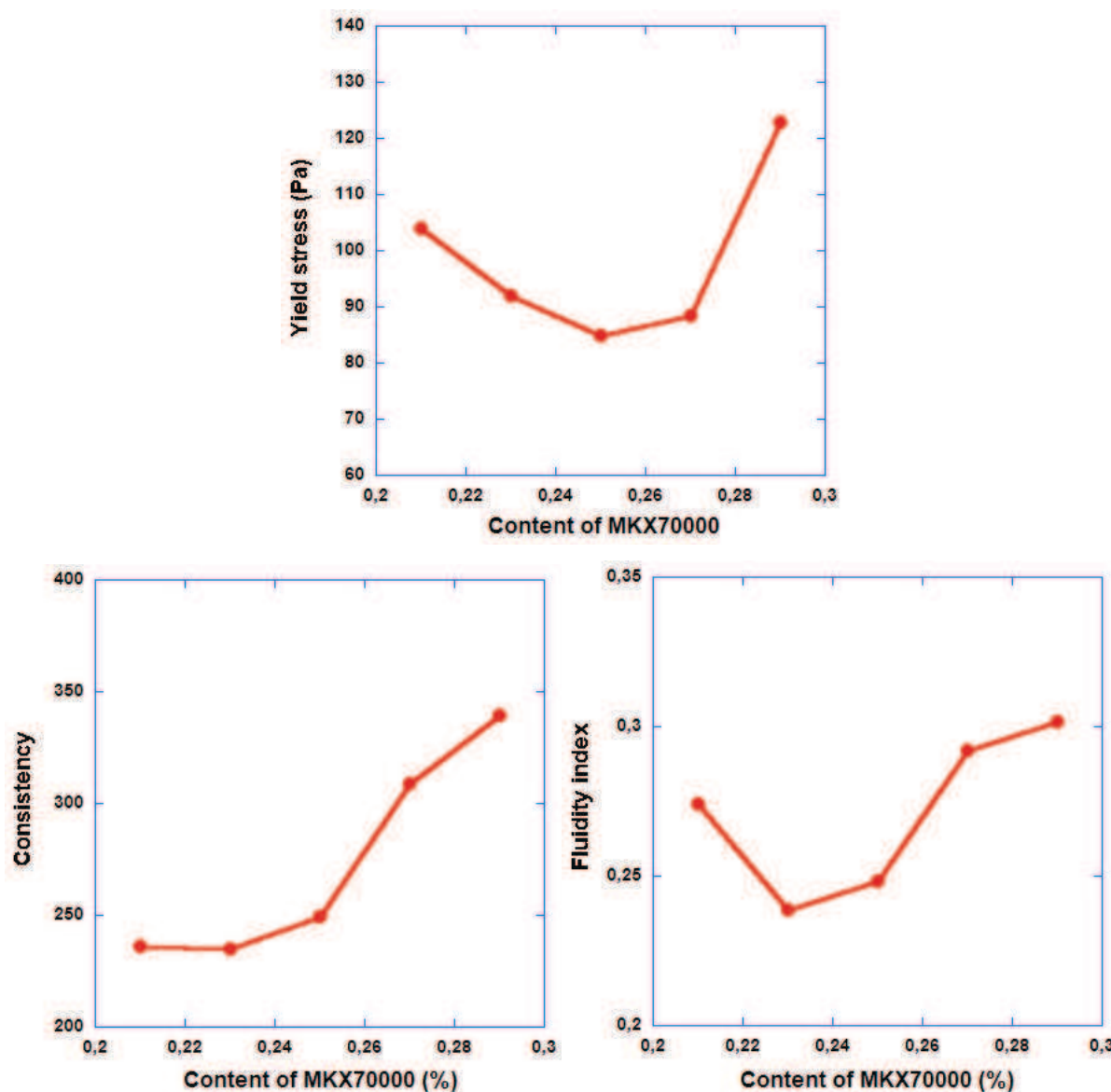


Figure 5. 33. Rheological parameters of mortar in variation content of C

### 5.3.3. Comparing the adhesive properties to the rheological behavior

The comparison of the yield stresses, calculated from tack and rheological measurements, is represented in the diagrammatic plot of figure 5.37. It indicates that the resistance of mortar in shear is much higher than in tension conditions.

We can see that the cohesion stress of mortar in this case is similar to that in cases of A and of B. The cohesion stress is almost unchanged compared with the yield stress in shearing conditions. Therefore a similar interpretation may be put forward.

In order to have a better view on the difference between the resistance of mortar in tension and in shearing conditions in the variation content of C, we have plotted the difference of these two quantities as a function of polymer content, represented in figure 5.38. It can be seen once again that there is a minimum in this difference value when varying polymer concentrations. The gap between two above quantities increases whether the polymer content increases or decreases. This observation can also be explained by the interplay between air-entraining and lubrication effects in shearing conditions.

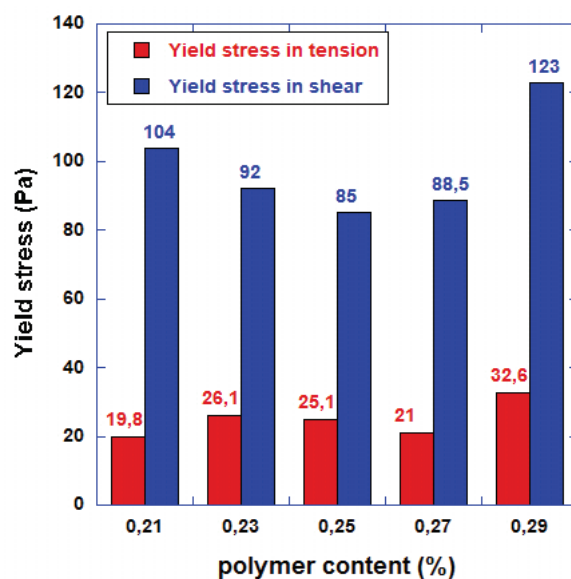


Figure 5. 34. Comparison between the yield stresses of mortar in tension and in shear with different contents of C

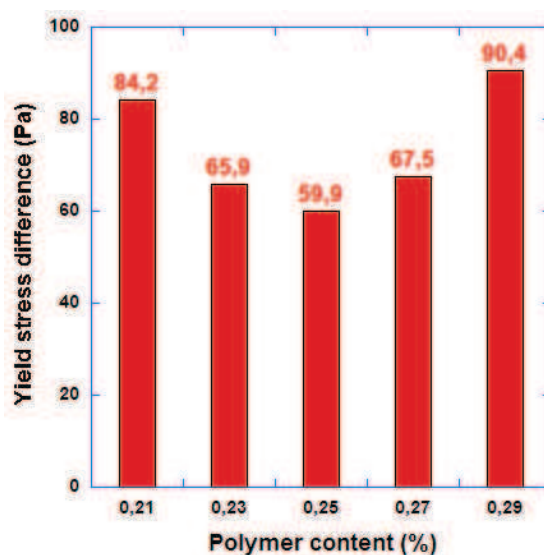


Figure 5. 35. Difference between the yield stress in tension and in shear for different contents of C



## 5.4. Comparison the effects of three types of HEMCs

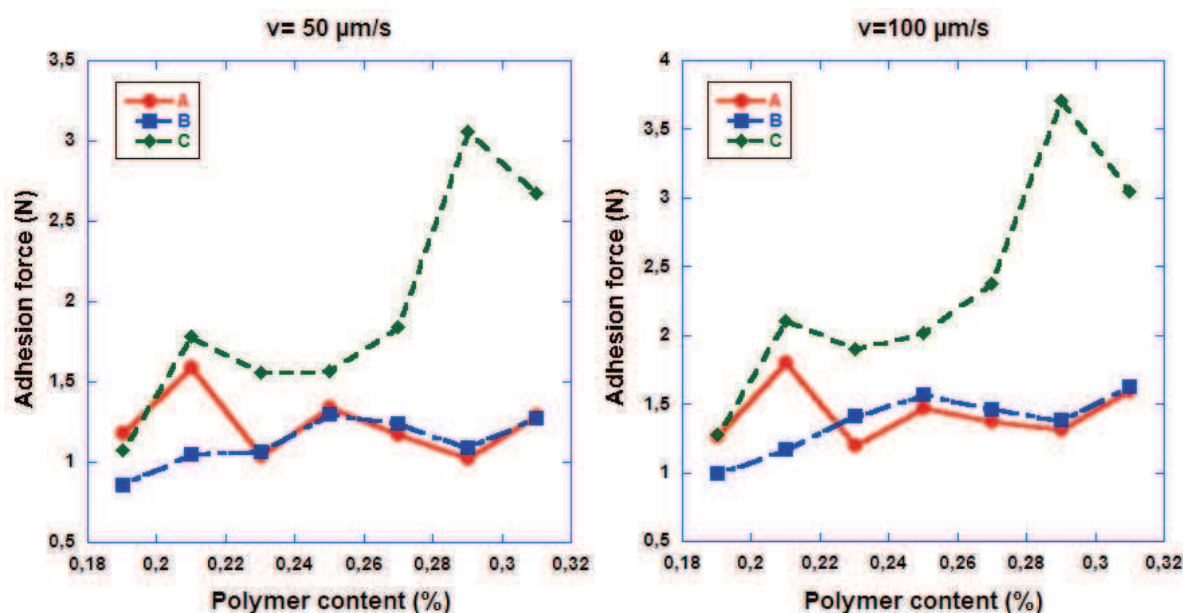
The molecular weights of three above polymers, including A, B and C, are 600 kDa, 680 kDa and 1.000 kDa, respectively. From the above tack and rheological measurements, we will investigate the influence of the molecular weight to the adhesive and rheological properties of mortar in fresh state.

### 5.4.1. Effects of HEMCs on the adhesive properties

#### 5.4.1.1. Effects of HEMCs on the adhesion force

The evolution of the adhesion force as a function of polymer content for three types of cellulose ether is re-plotted in figure 5.39 for comparison.

As it has been discussed in previous sections, the adhesive force increases with the enhancement of polymer concentration. However, one can notice the difference of the force evolution between the 3 polymers. The adhesive force of the mortar paste is always significantly higher in case of C, which has the highest molecular weight. In case of A and B, the difference between the adhesive forces are insignificant at high polymer content and at low tack speed. This difference between the adhesive forces in the two polymers becomes more significant at higher pulling velocities.





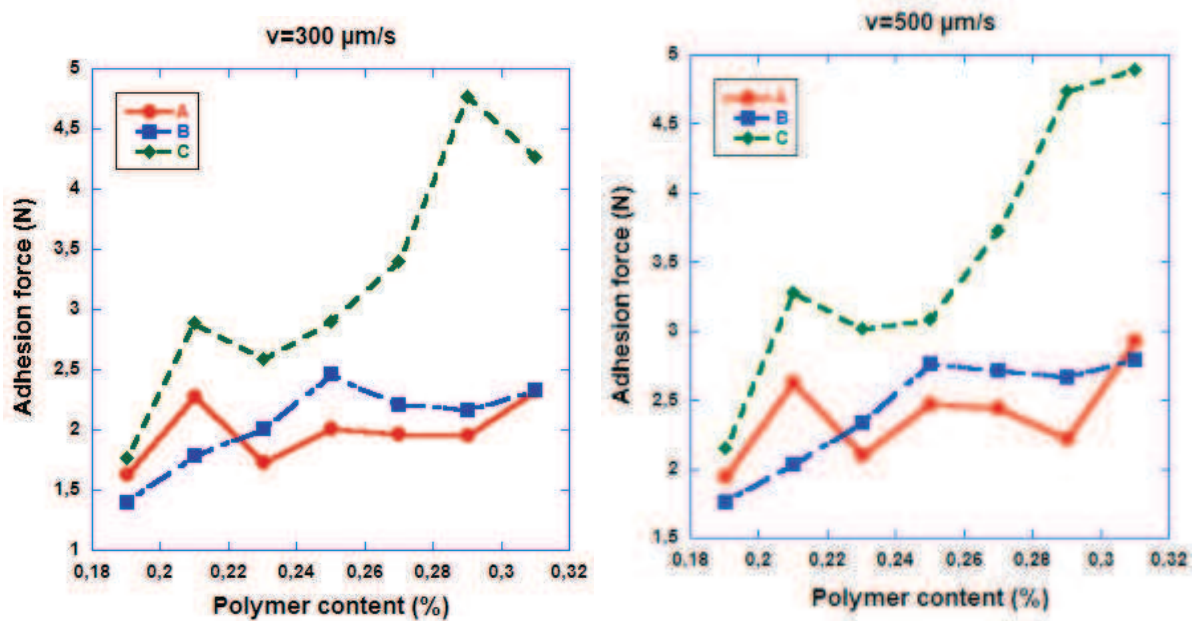


Figure 5. 36. Comparison of the evolutions of adhesion force with the variation of polymer contents, case of A, B and C, under different tack speeds.

Considering further figure 5.39 we can also notice another difference between the adhesive forces in cases of 3 types of polymers. At low polymer contents, including 0.19 % and 0.21 %, the adhesive force is higher in case of A compared with that in case of B. However, at high polymer contents, including the remaining percentages, the trend is reversed. The adhesive force is higher in case of B than that in case of A.

The net difference regarding the adhesive forces between polymer C compared to A and B justifies the fact that C is used for adhesive mortars, while A and B are rather used in mix-design of render mortars.

In figures 5.40 and 5.41, the evolutions of adhesive force as a function of the molecular weight of the polymers for different contents are presented. Figure 5.40 shows the evolution at low polymer contents, while the figure 5.41 shows the evolution at 3 higher contents, including 0.23, 0.27 and 0.31 %. The curves corresponding to the remaining contents; including 0.25% and 0.29% are represented in appendix C.7. Considering the two figures, one can observe a minimum value at the molecular weight of 680 kDa. This minimum value is significant.

At high polymer contents, the presence of this minimum value is less significant and it disappears as the pulling velocity increases. At high speed, even for a few cases, we observe a maximum.

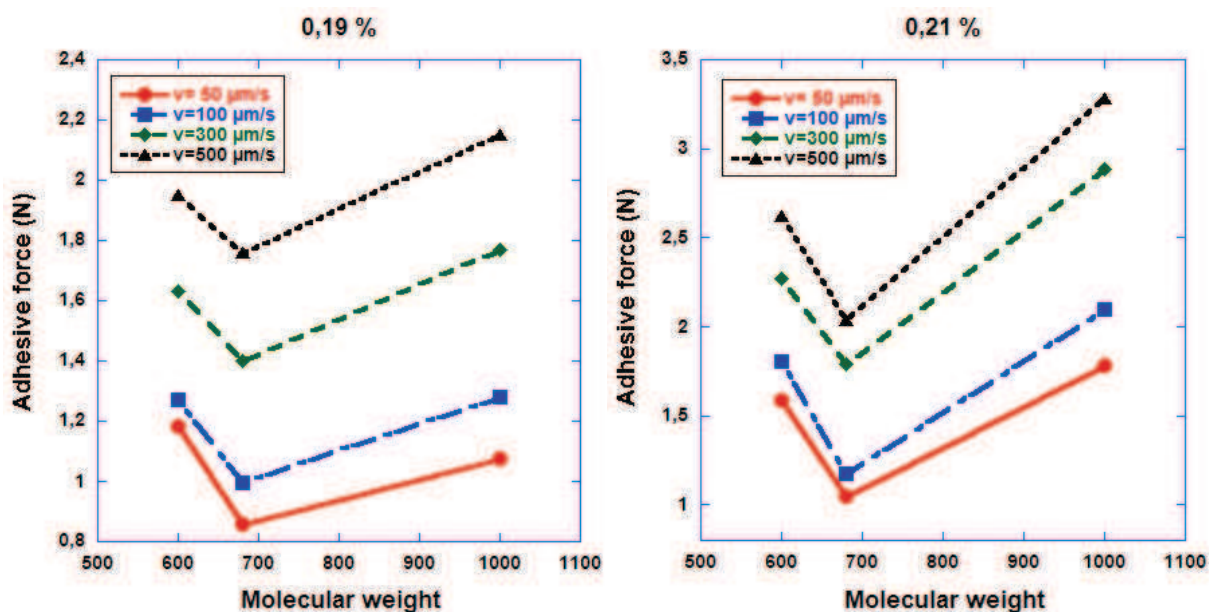
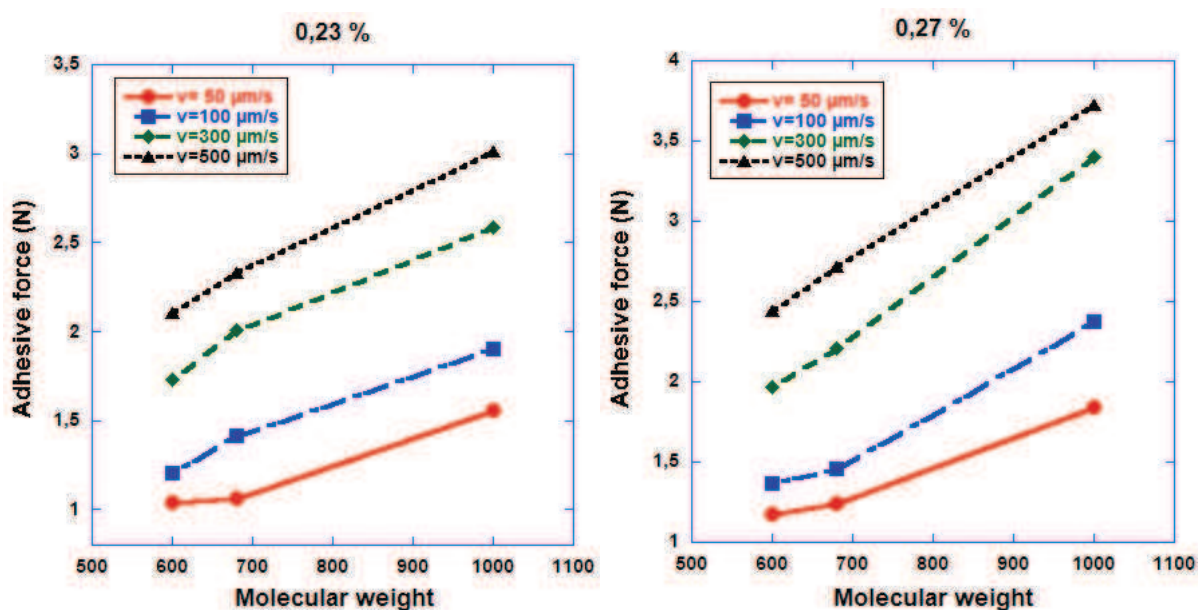


Figure 5. 37. Influence of molecular weight on the adhesive force of the mortar at low polymer contents for different tack speeds.

Although there are still extreme values of the adhesive force at high polymer contents, one can observe an increase of the adhesive force with the increase of the molecular weight. It demonstrates that the molecular weight is crucial to control the adhesion force of the mortar at high polymer contents ( $>0,23\%$ ).



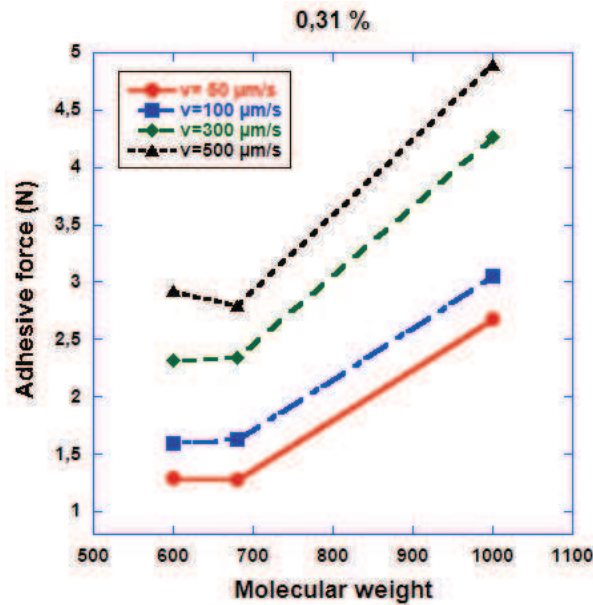


Figure 5. 38. Evolution of the adhesive force as a function of molecular weight at high polymer contents for different tack speeds.

#### 5.4.1.2 Effects of HEMCs on the cohesion force

The cohesion force is taken as the adhesion force at lowest tack speed, 10 µm/s. Therefore, the evolution of the cohesion force with the usage of three type of HEMCs, represented in figure 5.42, is similar to the observation of the adhesion forces' evolutions. However, the effect of the molecular weight of the used polymer is less significant at low molecular weight. As we can see, at high polymer contents, the cohesion force is almost similar in two cases of A and B, which have close molecular weight values. In case of C, which has the highest molecular weight, a significant increase of the cohesion stress with the enhancement of polymer is observed. As molecular weight increased, the cohesion stress was improved. This observation is attributed to the influence of molecular weight to the resistance of mortar in tension.

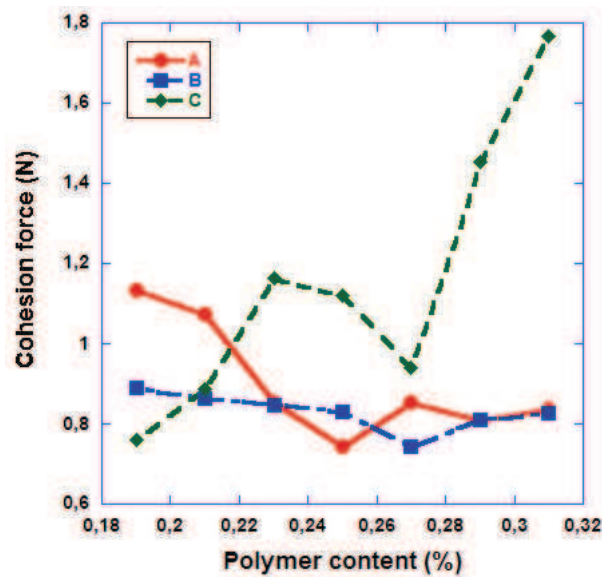


Figure 5. 39. Comparison of the evolutions of the cohesion force with the variation of polymer contents.

In order to highlight the role of molecular weight on the paste cohesion, the evolution of this quantity as a function of molecular weight is represented in figure 5.43. Two tendencies are observed. At low polymer contents, including 0,19 % and 0,21 %, the paste cohesion decreases with the increase of polymer content. This decrease of the paste cohesion has been reported by *L.Patural 2011*, in which the influence of molecular weight of different types of HEMCs on the properties of mortars has been discussed. The molecular weights of these cellulose ether polymers are in the interval of 100 and 400 kDa.

In present study, the three HEMCs have higher molecular weight ( 600, 680 and 1000 kDa). Therefore the results obtained in this research can complement the influence of molecular weight of cellulose ethers on the mortar properties.

At high polymer contents, the increase of the molecular weight leads to an increase of the paste cohesion (see figure 5.43b).

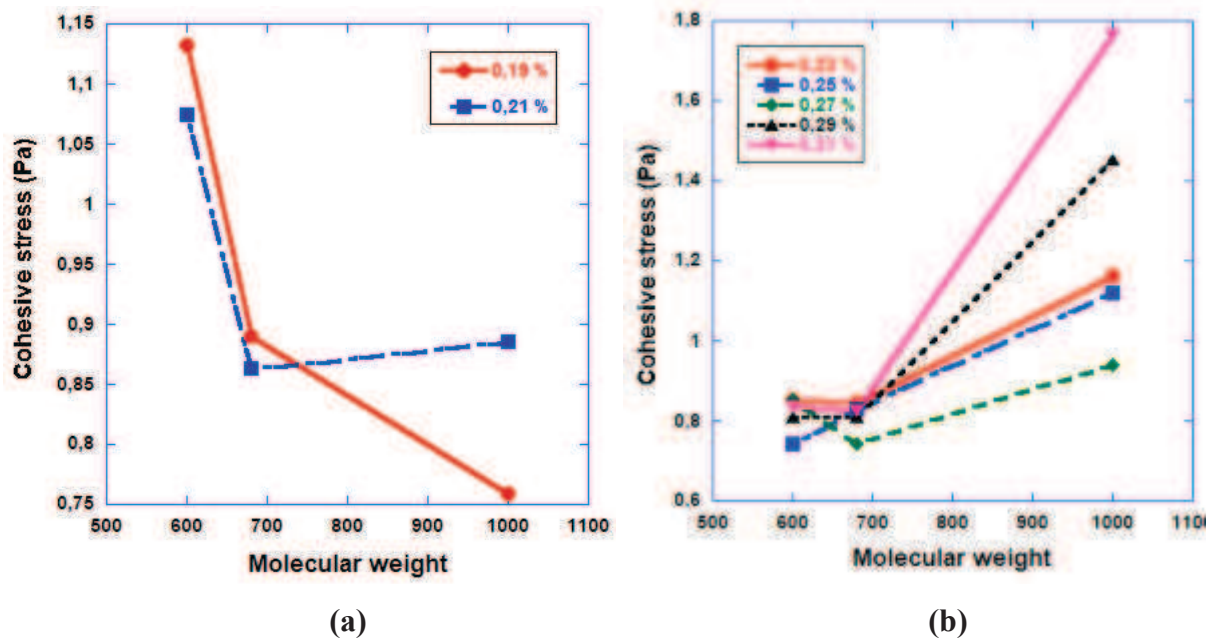


Figure 5. 40. Influence of molecular weight on the cohesive stress of the mortar at low and high polymer contents.

#### 5.4.1.3. Effects of HEMCs on the adhesive failure energy

The comparison of the influences of the three types of HEMCs on the adhesive failure energy at different tack speeds is represented in figure 5.44. We can see that the adhesive failure energy is lowest in case of A, and highest in case of C. This correlation remains the same for the all applied pulling velocities.

At low polymer contents, the difference between the values of adhesive energy is not significant. It becomes more significant as the polymer concentration increases. It demonstrates the dependence of the adhesive failure energy of mortar paste on the molecular weight. This observation is similar to the influence of molecular weight on the adhesive force of mortar paste, discussed in previous sections. Therefore a similar interpretation may be put forward. We can notice that at high dosage rates the adhesive energy in the case of polymer C is significantly higher than that with the two other polymers.



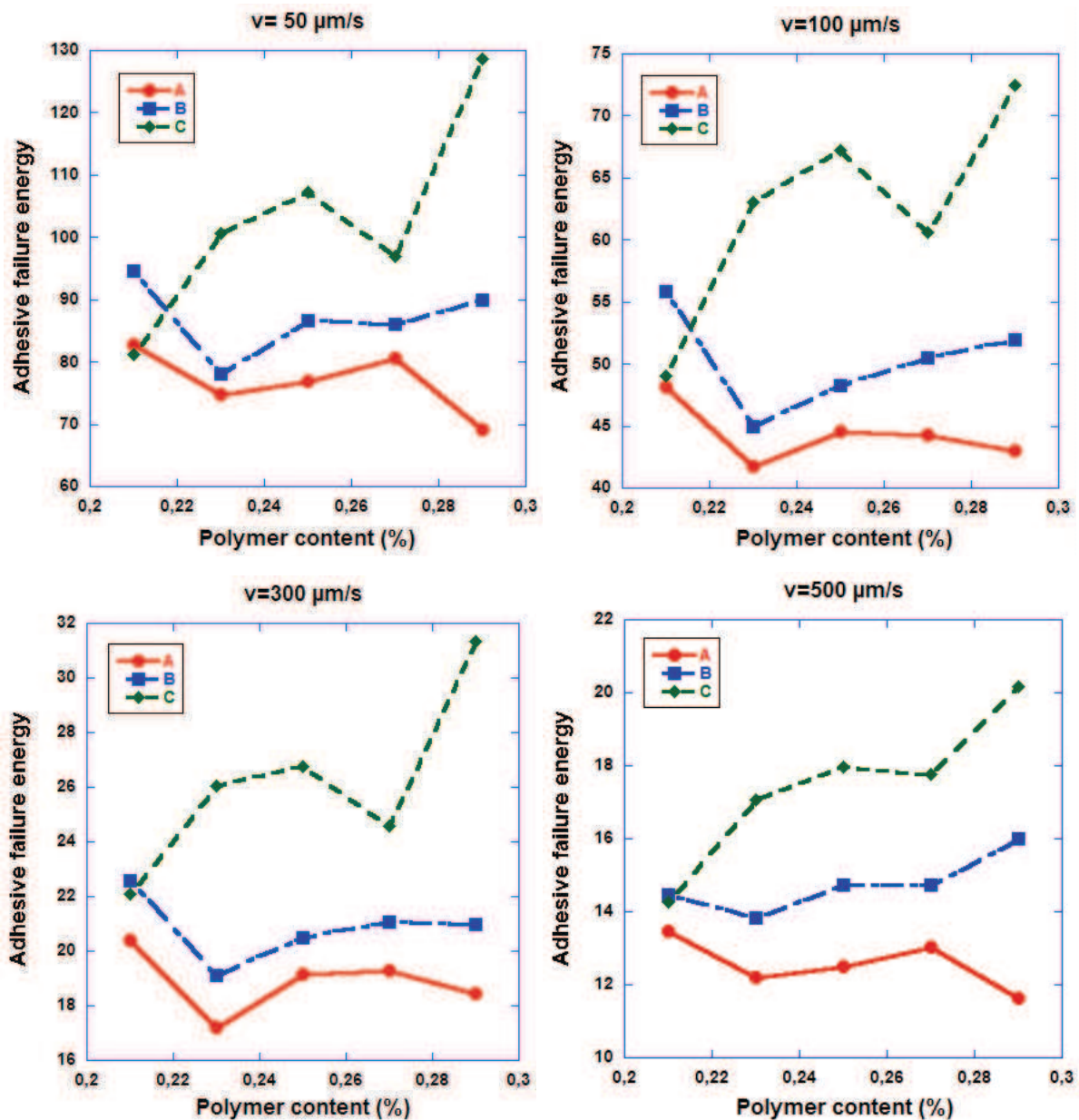


Figure 5. 41. Comparison of the evolutions of adhesive failure energy with the variation of polymer contents, case of A, B and C, at different tack speeds.

#### 5.4.1. Influence of $M_w$ on the rheological behaviors

##### 5.4.1.2. Influence of $M_w$ on the yield stress

The evolution of the yield stress, obtained in the rheological measurements, as a function of polymer content for the three molecular weights are represented in figure 5.45. The effect of molecular weight on the yield stress of the mortar is highlighted on the right graph in figure 5.45 . It can be seen that we observe an evolution with an optimum for a concentration of 0.25 % independently of the molecular weight. As discussed in the previous sections, several



authors have reported the presence of such a minimum and this has often been attributed to the air-entraining effects of cellulose ether polymers. There is no direct correlation between the depth of the minimum and the molecular weight.

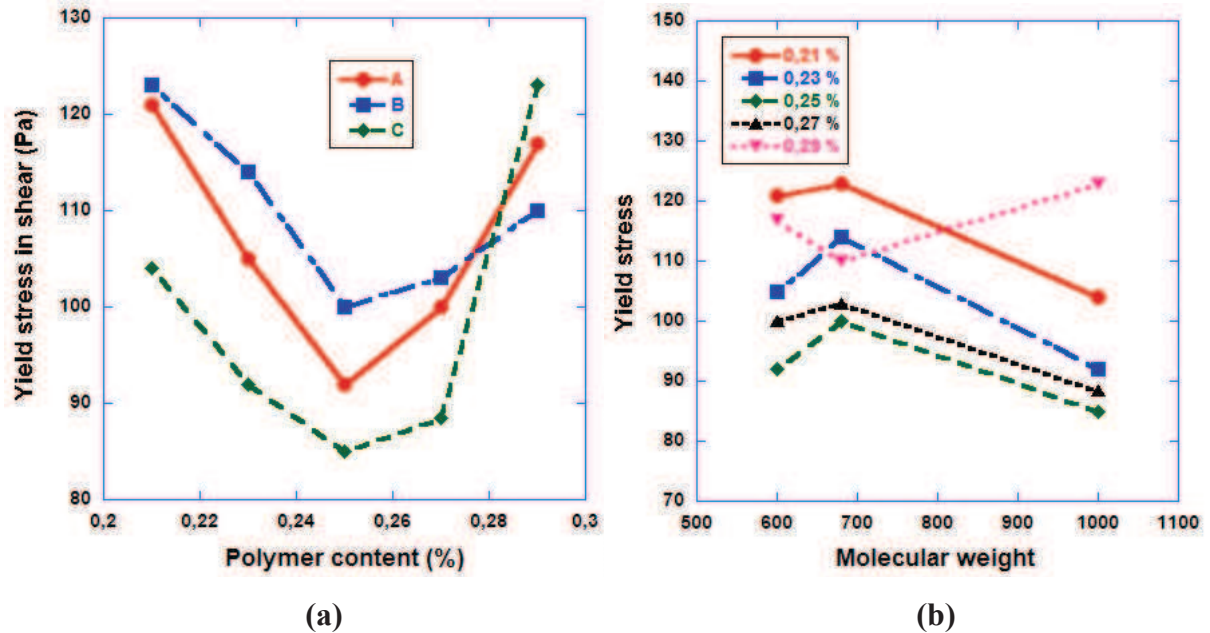


Figure 5. 42. Evolution of yield stress in shear for the variation of polymer content (a) and molecular weight (b)

The figure 5.45b shows the dependency of the yield stress on the molecular weight. Increasing the molecular weight first leads to a slightly increase of the yield stress to reach a maximum value, followed by decrease of the yield stress. These trends are observed for all the polymer concentrations expect the highest one (0.29%). For this dosage, the maximum transforms into a minimum.

#### 5.4.1.2. Influence of $M_w$ on the consistency of the mortar

The evolutions of the consistency of the mortar pastes as a function of polymer content and molecular weight are represented in figure 5.46. We can observe a significant increase of the consistency of mortar pastes when the molecular weight increases. This dependence of the consistency of mortar on the molecular weight is also in agreement with the results reported by *L.Patural (2011)* on the effect of other types of cellulose ethers on cement-based mortars. The increase of consistency with molecular weight is not surprising since the viscosity of polymer solution make up by the cellulose ether dissolved in the pore solution should increase with molecular weight.

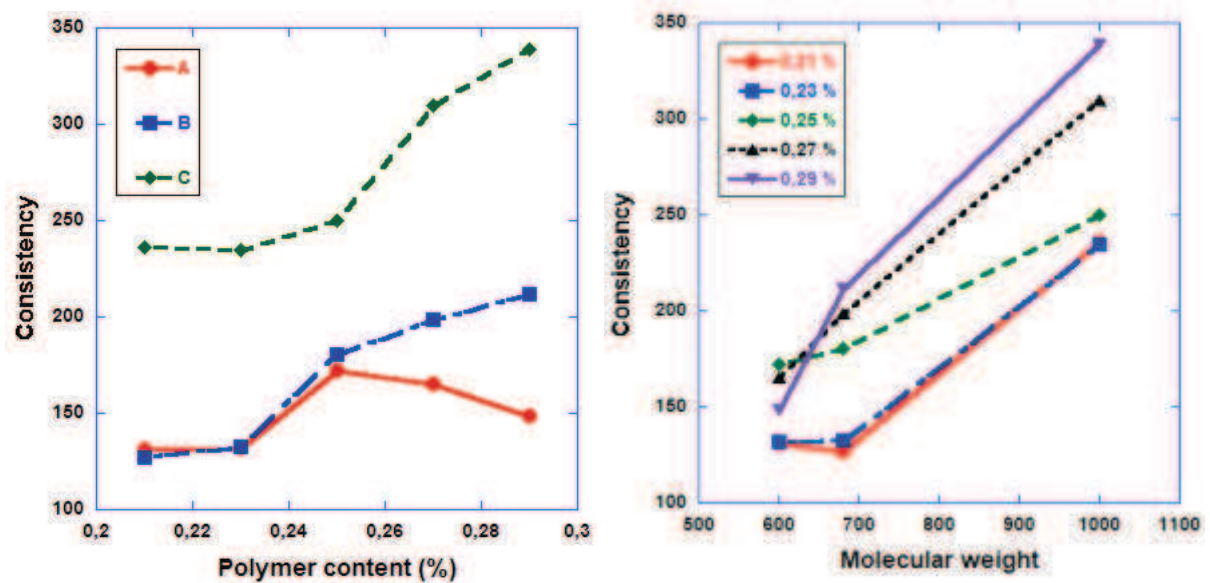


Figure 5. 43. Evolution of the consistency of mortar pastes as a function of polymer content and molecular weight

## 5.5. Conclusion

Adhesive and rheological properties of mortars in the fresh state have been investigated by varying the content of three types of hydroxyethyl methyl cellulose denominated A, B and C. These polymers differ from each other mainly in their molecular weights.

The sensitivity of the paste adhesive properties relative to the variation of polymer concentration increases successively from case of A, B and C. In case of A, the paste adhesion is almost unchanged with polymer concentration, and significantly increases with the increase of polymer content in case of C. Our tack tests measurements are in line with the practical facts that cellulose ether type C is used in adhesive mortars while A and B are rather used in render mortar mixes. The latter are generally applied using a pumping procedure. The product must have only moderate stickiness in order to get high enough pumping rates. Moreover, during the finishing stage the product must present low stickiness to the tool in order to obtain plane surfaces. Some stickiness is however needed in order for the mortar to stay on the support on which it is applied. In the case of adhesive mortars high tackiness is not an issue since it is usually applied handily.

At low shear rates, all the mortar mixes behaved as a shear-thinning fluid. However at high shear rates, we observed a difference between the mixes corresponding to the different cellulose ethers. In case of A, the mortar pastes behave as shear-thinning fluids for all investigated concentrations. In case of B, the rheological behavior of mortar is shear thinning at low concentrations, while it behaves as Bingham fluids at high contents. In case of C, the

mortars behaved much like Bingham fluids through the entire shear-rate interval investigated.

A comparison between the resistance of mortar in tension and in shearing condition has been performed. The results show that for the three types of polymers, the resistance of mortar in tension is much lower than that in shearing condition.

The evolution of the paste cohesion with molecular weight of polymer displays a difference between the low and high-investigated polymer concentrations. At low contents, the cohesive stress decreases with the increase of polymer concentration. This decrease has been reported in literature by *L. Patural 2011*. However, at high contents, an inverse phenomenon was obtained. We observed a plateau of the cohesive stress at low molecular weight, and a significantly increase at high molecular weight.

The investigation of the influence of molecular weight on the properties of fresh mortars has shown a similar observation to the reported research in literature [*Patural 2011*]. The yield stress of the mortar decreases with the increase of molecular weight. This decrease is not significant at low molecular weights, and becomes much more significant at high molecular weights. Inversely, the mortar consistency is found to increase with the increase of molecular weight.

*Redispersible polymer*  
*powder*

Contents

6.1. Effect of Vinnapas on the adhesive properties ..... 133

6.1.1. Tack test results ..... 133

6.1.2. Adhesive strength ..... 136

6.1.3. Cohesion force ..... 136

6.1.4. Adherence force..... 137

6.1.5. Adhesive failure energy..... 138

6.2. Effect of Vinnapas on the rheological behavior ..... 139

6.3. Comparing the adhesive properties to the rheological behavior ..... 142

6.4. Conclusion ..... 143

In this chapter, a study on the effect of a commercial water-soluble dispersible polymer powder on the properties of mortars in fresh state is presented. The mortar formulation used in this study was presented in chapter 2, section 'Mortar formulation'. The fresh state properties have been investigated using the tack test and shear rheology. The test procedures are performed similarly to previous studies. The applied pulling velocity in the tack test was varied between 10 and 500  $\mu\text{m/s}$ . The initial gap between two plane plates was fixed to 3mm. The relaxation time was set 2 minutes.

In this research, a commercial re-dispersible powder has been used. Its trade name is Vinnapas® and invented by Wacker Chemie. It is used in adhesive mortars because it expected to improve the adhesive strength of the bonding of mortar in *the hardened state* with all kind of substrates, the flexibility and deformability of the mortars, the flexural strength, the cohesion and impermeability, the water retention and the workability characteristics of the mortar. However their influences on the properties of the material in fresh state have not been fully investigated, in particular adhesive properties.

We considered the grade Vinnapas 5010N of Wacker Polymer Company to investigate the adhesive and rheological properties of mortar in fresh state. It has been noted by the producer that this type of polymer is ideal for use in combination with other mortar additives intend to enhance specific properties because it has no effect on rheological properties. So, it is interesting to investigate the influence of Vinnapas 5010n in combination with one type of cellulose ether which has found to enhance the mortar consistency, good workability, increase the adhesive properties of mortar in chapter 4, case of Methocel. The dosage rate of cellulose ether-based polymer is fixed and the content of Vinnapas will be varied among 1-5 %.

In the following, the results obtained in tack tests and rheology tests for various polymer contents will be presented.

## 6.1. Effect of Vinnapas on the adhesive properties

### 6.1.1. Tack test results

Figure 6.1 represents in semi-logarithmic scale the evolution of the recorded normal force versus time for different pulling velocities at 3 different polymer concentrations. Additional results corresponding to other Vinnapas content are reported in appendix D.1.

The tack curves seem be independent of the variation of resin content. For example, when the applied pulling velocity is 300  $\mu\text{m/s}$ , the peak value of flow curves obtained in the tack tests remains around 1 (N). This value is not affect by the variation of polymer content although the increment in the content of polymer is 1% each variation. At highest pulling velocity

applied in this study, 500  $\mu\text{m/s}$ , we can distinguish a small difference at the polymer content of 2%. The peak value of flow curves at 2% is higher (around 1.4N) compared with that in case of other polymer content (around 1.2 N). We will discuss this in more details when considering the different adhesive properties, which can be inferred straightforwardly from these curves, in following sections.

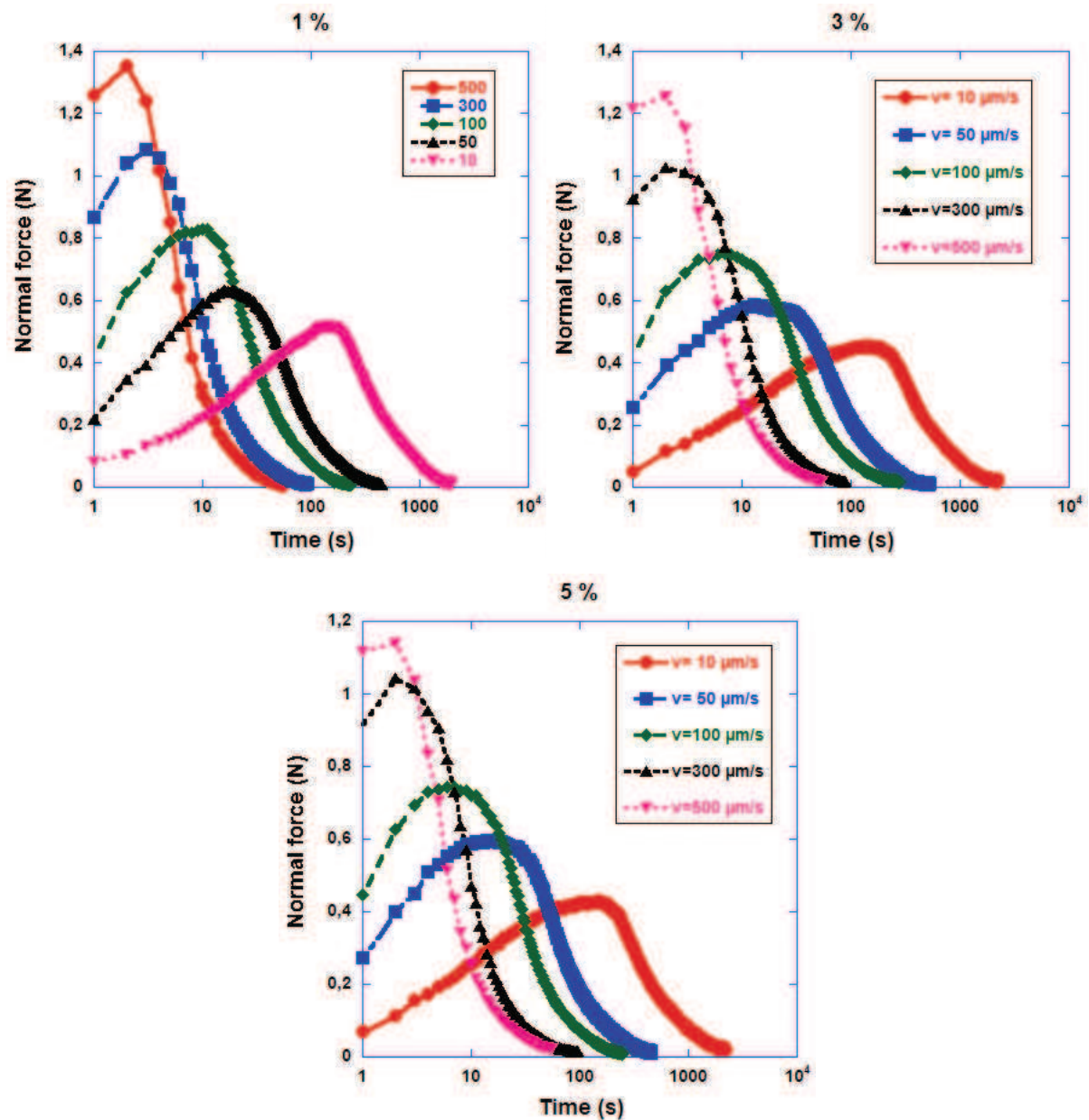


Figure 6. 1. Force versus time curves obtained in the Tack test for different polymer content, influence of Vinnapas content.



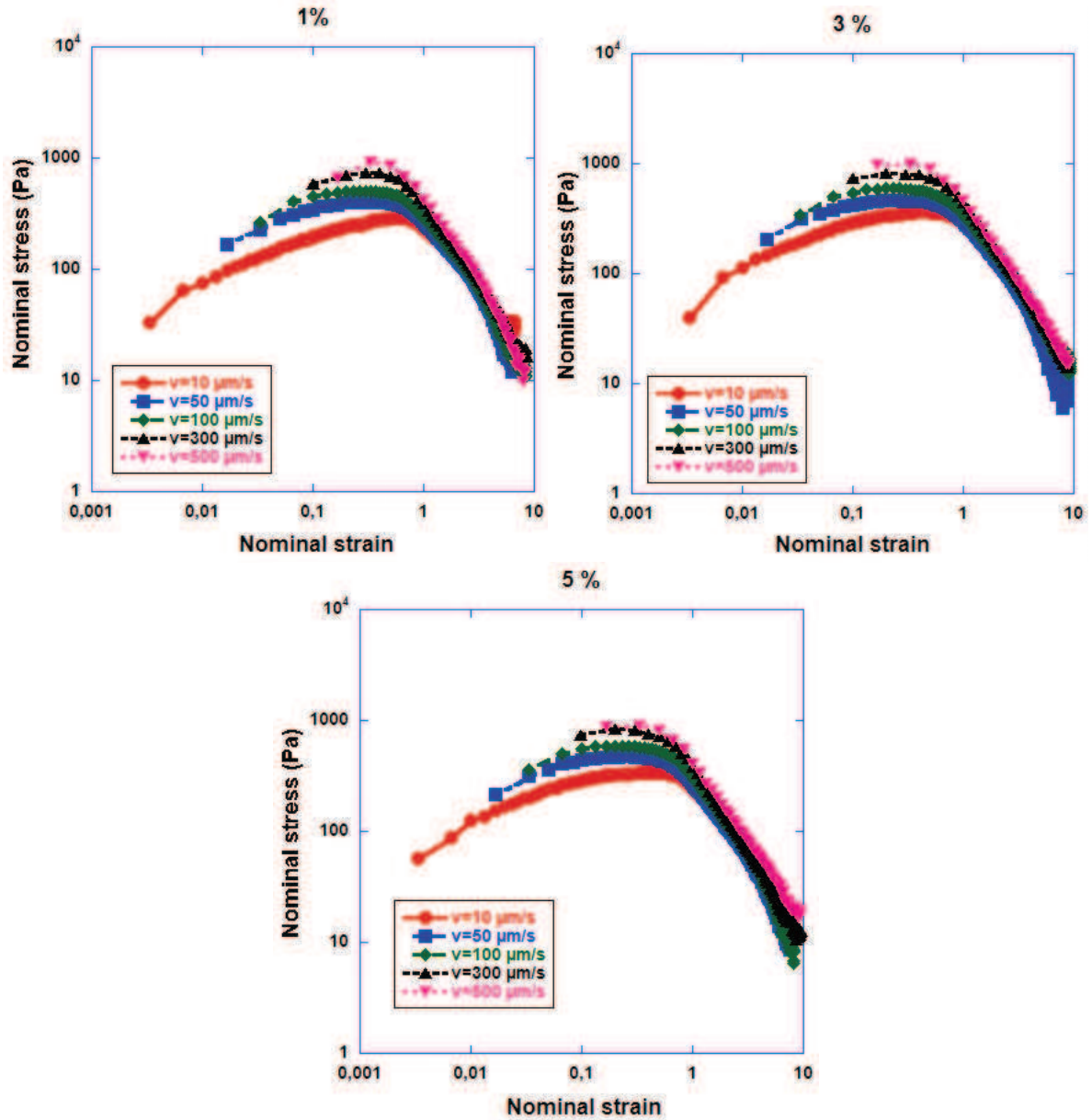


Figure 6. 2. Nominal stress vs. nominal strain curves obtained in the Tack test for different Vinnapas content

We also represented in figure 6.1 the nominal stress evolution with the nominal strain for 3 different polymer contents, in order to investigate further the dependency on the pulling velocity. It can be seen that the variation of Vinnapas content does not affect the form of the curves. Two other tack curves for 2 polymer concentrations of 2% and 4% are represented in appendix D.2. Figure 6.2 indicates that the peak stress (around 1000 Pa), and the peak strain (around 0.5) do not depend on the variation of Vinnapas content. Besides, the peak strain does not depend on the pulling velocity.

From these above results, it can be suspected that the variation of Vinnapas content does not have much effect on the adhesive properties of the fresh mortars. In order to check this more

carefully we will consider the influence of Vinnapas on the adhesive force, cohesive and the adherence force of the test mortars.

### 6.1.2. Adhesive strength

The maximum normal force, referred to as the adhesive force, as a function of Vinnapas contents determined from the tack curves is represented in figure 6.3 (left). The effect of the resin on the peak force is quite small, in particular at small pulling velocities. However the effect is similar to that of low molecular weight cellulose ethers. Overall the peak force decreases slightly with resin content. The decrease becomes more distinguishable at high pulling velocities. Water redispersible polymers are known to increase air-entrainment. The decrease of the peak force may be attributed then to the decrease of the viscosity of the mortar due entrained air. However it is not clear why the peak force decrease is higher at high pulling velocities.

The adhesion force increases with pulling velocity (see left of figure 6.3). However the curves almost superpose, indicating low effect of resin content. The increase of the peak force with velocity is expected and reflects viscous dissipation effects.

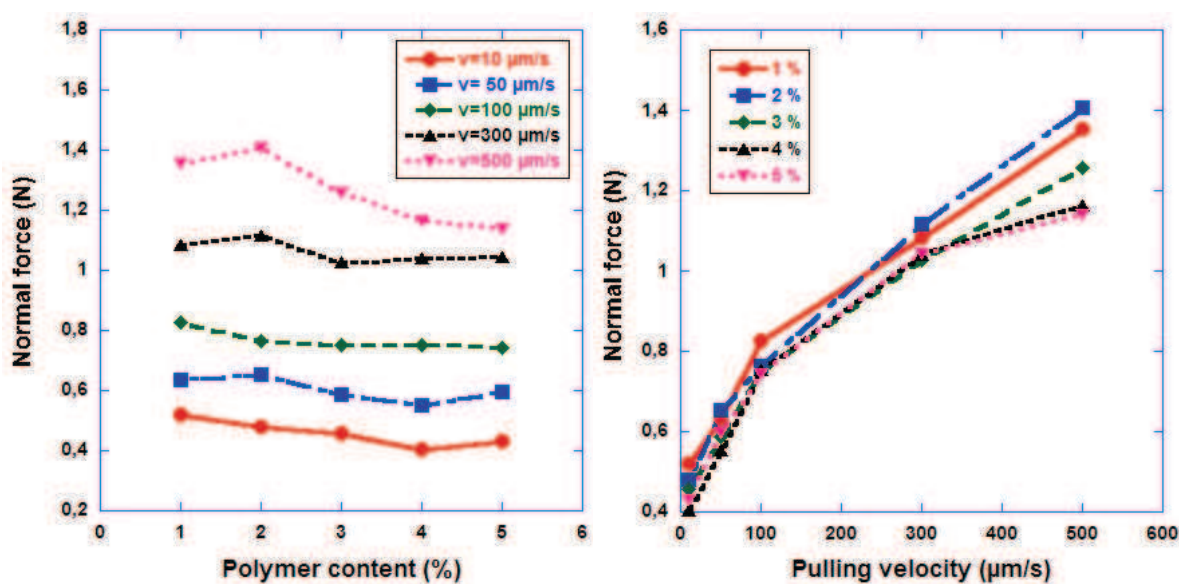


Figure 6. 3. Evolution of the maximum normal force versus Vinnapas resin content,

### 6.1.3. Cohesion force

The cohesion force, which is related to the strength of the interaction between the material constituents at rest, is determined from the adhesive force at zero-velocity (here we take 10μm/s). The evolution of cohesion force for different Vinnapas concentrations is represented

in figure 6.4.

The influence of polymer concentration on the paste cohesion depends qualitatively on the concentration interval considered. Increase the polymer content first leads to the decrease of the paste cohesion. For a polymer concentration of 4 %, we can observe a minimum of the cohesion force, before increasing again at higher concentrations. However the depth of the minimum is quite small. Even though the tests were repeated 3 times, we are wondering if this minimum is physical or this rather corresponds to a plateau.

The decrease of the cohesion force may also be attributed to air-entrainment. The presence of air bubbles may represent leak points for rupture growth and leading to the decrease of the peak force.

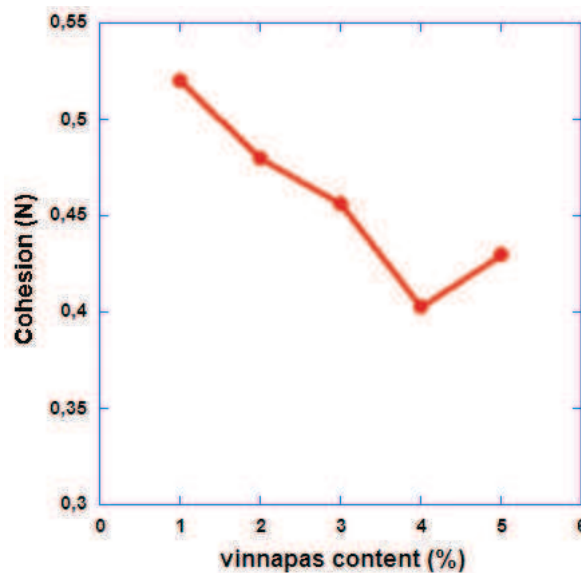


Figure 6. 4. Evolution of the cohesion force versus Vinnapas content.

#### 6.1.4. Adherence force

The evolution of the adherence force as function of resin content for different pulling velocities is represented in figure 6.5. Overall the adherence strength decreases with Vinnapas content, in particular at low velocity. This may also be attributed to increase of the quantity of entrained air.

The adherence force is represented as a function of pulling velocity for different Vinnapas contents in right of figure 6.5. The adherence force decreases with pulling velocity, and then reaches a plateau.

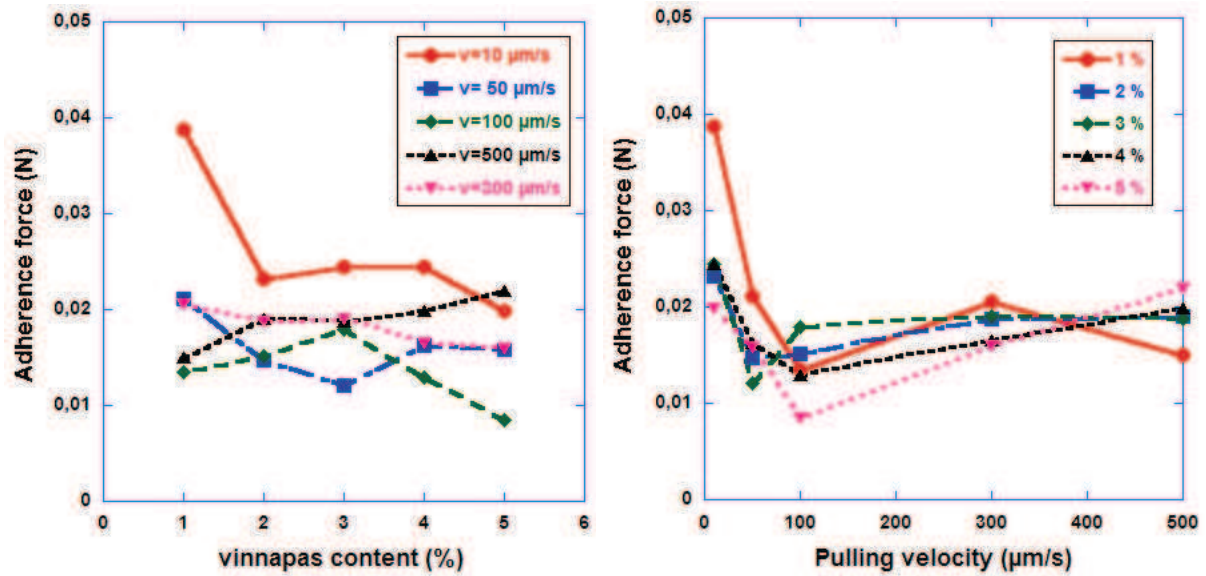


Figure 6. 5. Evolution of the adherence force versus the polymer content, case of Vinnapas

#### 6.1.5. Adhesive failure energy

The adhesive failure energy of the mortars as a function of polymer content and for the different separation velocities is represented in figure 6.6. On right of this figure we also represent the evolution of the adhesive energy as a function of pulling velocity for different resin contents. For each polymer content, there is a significant decrease of the adhesion energy when the pulling velocity increases, similarly to the previous mixes. There is almost not resin effect on adhesive energy. Yet one can observe a small decrease at low velocity. The decrease of the tack energy with velocity suggests that the contribution of the viscous dissipation to this energy (that should increase with velocity) is not significant. This indicates that the capillary forces (due to the presence of air bubbles) may be dominant in resistance to the tack process.

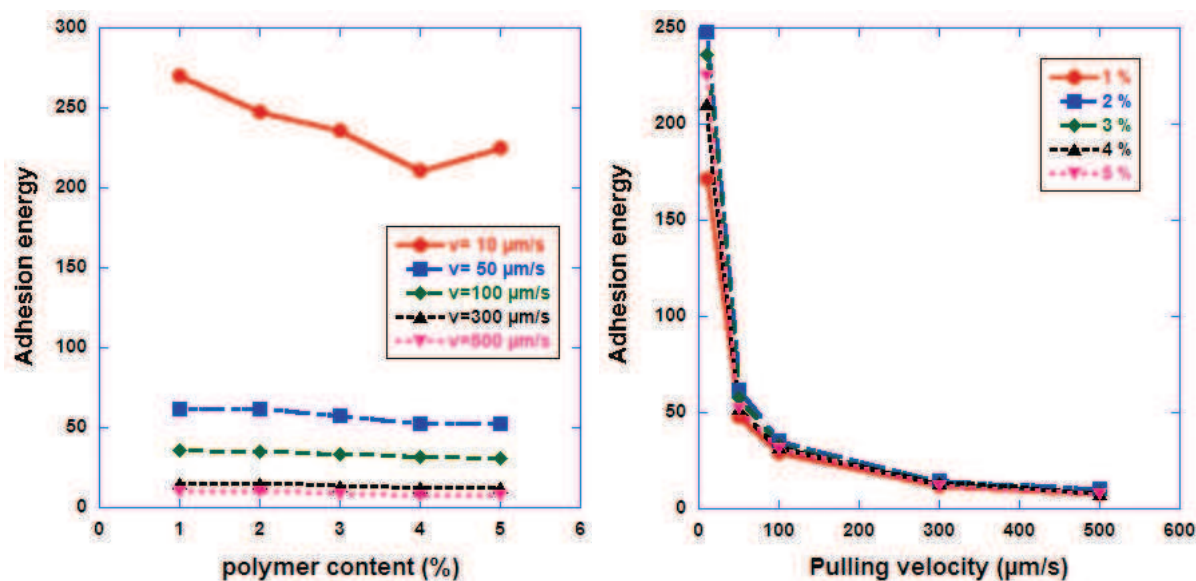


Figure 6. 6. Evolution of the adhesive failure energy versus polymer content, case of Vinnapas and pulling velocity

## 6.2. Effect of Vinnapas on the rheological behavior

Figure 6.7 represents the flow curves obtained in the rheology tests including both loading and unloading curves. The flow curves were determined at controlled stress.

The flow curves are those of shear thinning fluids for all investigated concentrations. The last graph in figure 6.7 represents the uploading curves at different Vinnapas concentrations. The curves indicate that the apparent viscosity (stress divided by corresponding shear rate) decreases with increasing polymer resin content. This is rather surprising since addition of the powder means increase of solid concentration. It is to be noted that the rheological properties (and also the tack properties) are determined while latex film is not formed yet. We will resume this discussion below when considering the evolution of the rheological parameters.

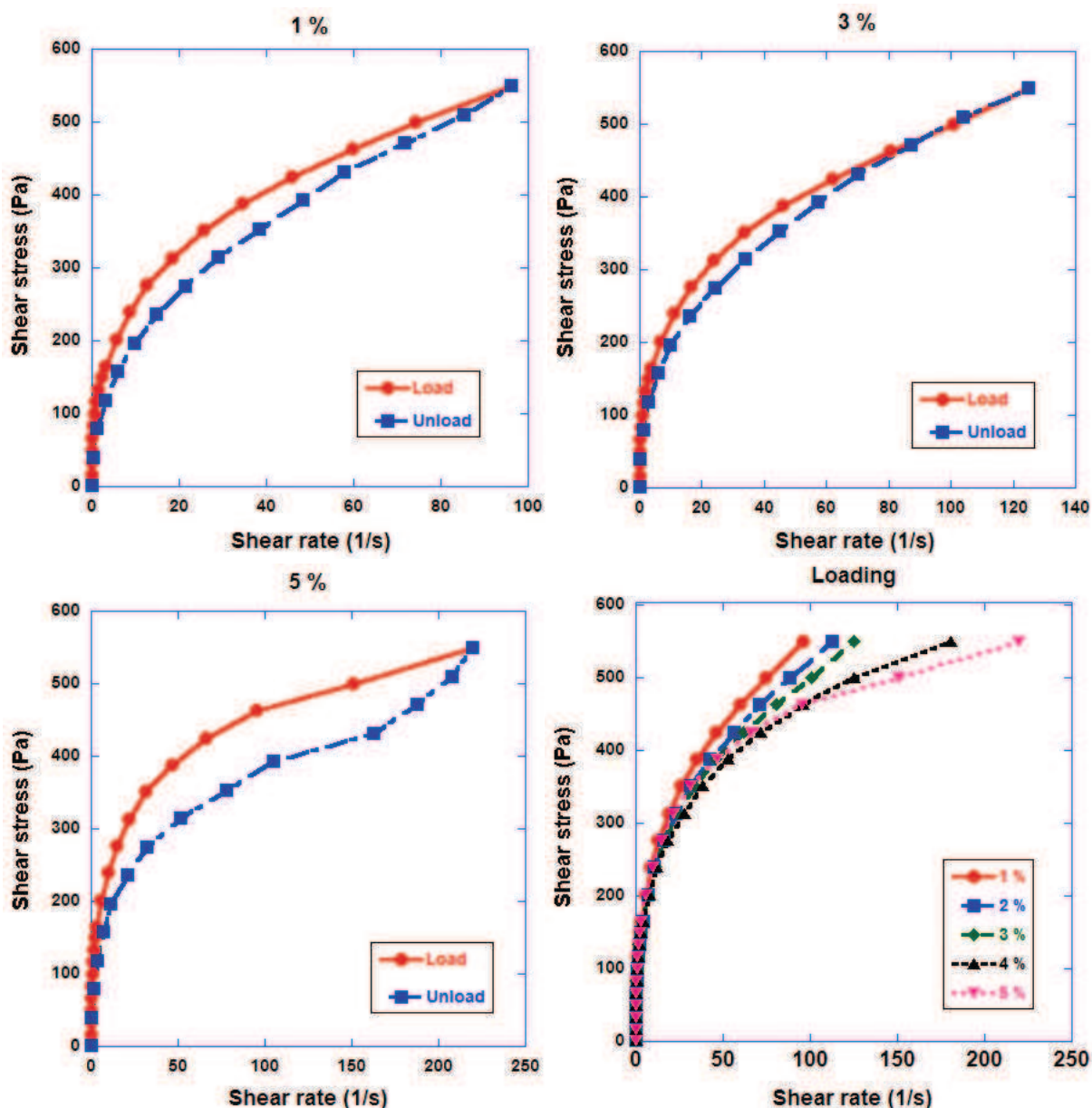


Figure 6. 7. Loading and unloading curves of different content of Vinnapas

The yield stress is measured directly by determining the applied stress for which we have a finite shear-rate. The evolution of the yield stress with varying resin content represented in figure 6.8. It can be seen that the effect of Vinnapas on the paste resistance to shear initiation is not significant. We observe a constant yield stress up to a dosage rate of 4 %. A small increase of the yield stress at 5 % of polymer can be observed.

The two others rheological parameters, including the consistency coefficient and fluidity index, are determined by performing the best fit of Herschel-Bulkley model with the experimental results. The evolution of the consistency coefficient with the polymer concentration is represented in figure 6.9. The evolution is non-monotonic. Increasing the



polymer content first leads to a decrease of the mortar consistency. At high resin contents the consistency seems to start increasing. Figure 6.9 represents also the evolution of the fluidity index as a function of polymer content. We can observe a slight decrease of the shear thinning aspect of the mortar with addition of Vinnapas.

Overall the effect of the polymer powder on the rheological properties of the mortars is significantly smaller than those of cellulose ethers, in particular those with high molecular weight. It seems that we have only indirect effect of the resin on the rheological properties. Their influence should be due mainly to the increase of air content. Increasing air content may have two consequences: On one hand we will have a decrease of the viscosity of the mortar and on the other air bubbles will increase cohesion due to capillary forces. This may depend on the shear rate interval considered. At low shear-rates capillary effects may dominate, this may explain the slight increase of the yield stress (figure 6.8). At high shear rates, viscous effects are dominant and the viscosity of the mortar should decrease with air content. This may explain the decrease of the apparent viscosity at high shear rates that can be observed in the last graph of figure 6.7. The consistency parameter comprises a mixture of both high and low shear effects, which may explain its non-monotonic behavior.

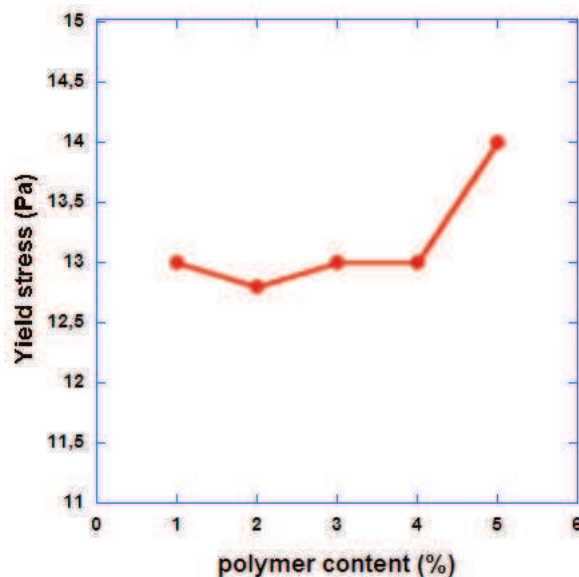


Figure 6. 8. Yield stress obtained in shearing condition of mortar in case of adding Vinnapas

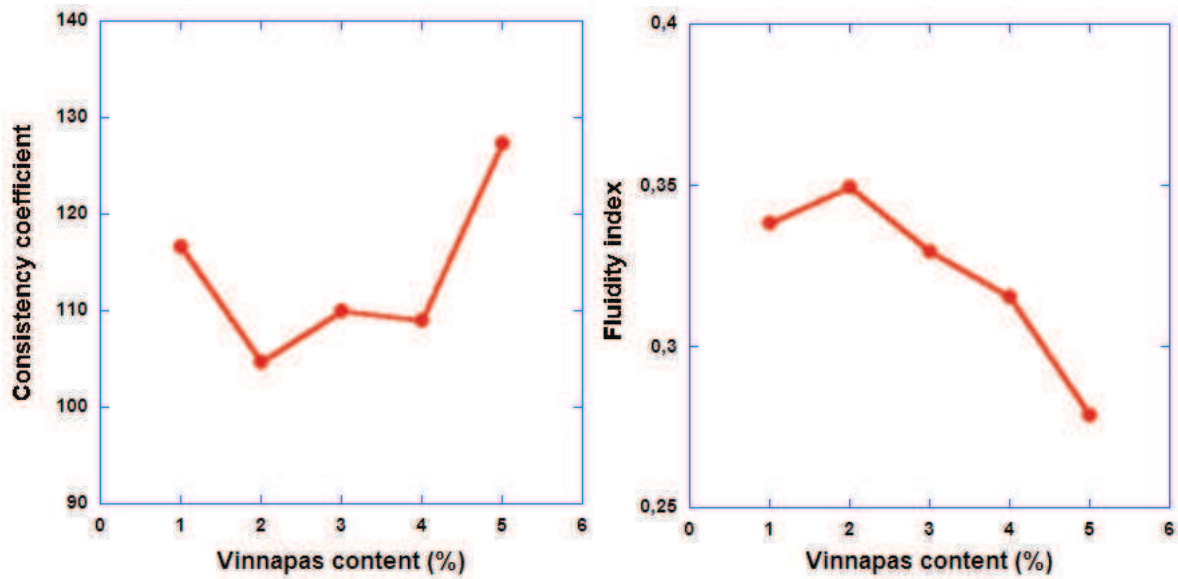


Figure 6. 9. Consistency coefficient and fluidity index of mortar

### 6.3. Comparing the adhesive properties to the rheological behavior

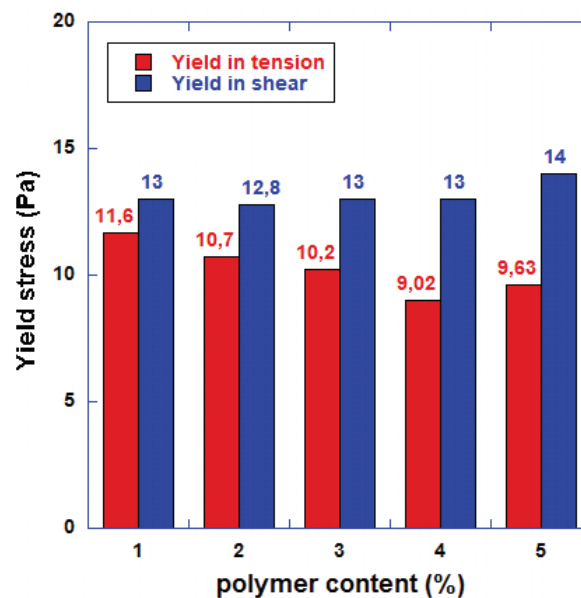


Figure 6. 10. Comparison between the yield stress in tension and in shear for different polymer content, case of Vinnapas

The yield stress in tension condition is calculated using the equation 3.3. The results, which are plotted in figure 6.10, indicate that the resistance of the mortar with varying Vinnapas content is slightly lower in tension than in shear. However, this difference is not significant (figure 6.11), in contrast with mortars formulated with varying cellulose ether contents. The fact that the yield stress in extension (cohesion) and that under shear are close to each other can also be understood if we assume that these two properties are controlled by capillarity.

Indeed, under the measurement conditions of these properties (very small deformation rate) the deformation of the bubbles should be negligible and there is no difference between extension and shear when dealing with capillary forces.

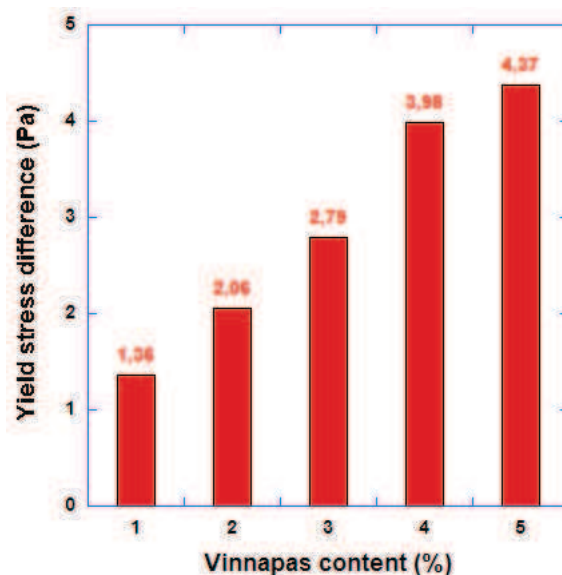


Figure 6. 11. Difference between the yield stress in tension and in shear for varying Vinnapas content

#### 6.4. Conclusion

The adhesive properties and rheological behavior of mortars in fresh state containing different amounts of a water redispersible polymer powder Vinnapas 5010n in combination with a cellulose ether-based polymer have been investigated.

In general, the effect of Vinnapas on the fresh properties of the mortar, including adhesive and shear rheological properties is not significant. In particular the effects are much lower than those of high molecular weight cellulose ethers. The main point is that the powder resin seems to have only indirect and minor effects on the fresh properties through increase of air content. These results are in agreement with the recommendation of the producer indicating that Vinnapas do not change the rheological properties. Actually latex powders are mainly used to improve mechanical properties of mortars and adherence in the hardened state. Our investigation indicates that the change in mortar properties should be significant only when the latex film is fully formed and spans all the material. This investigation should be completed by considering the evolution of the mortar properties with varying resin content from the fresh state through the early age and in the hardened state.

# *General Conclusions*

## *and Perspectives*

In this thesis, the adhesive and rheological properties of mortars in fresh state have been investigated. The influences of different additives/admixtures, including a cellulose fiber, organic versus mineral thickeners, three types of hydroxyethyl methyl celluloses and a combination between a redispersible polymer powder and a cellulose ether-based polymer, had been studied .

Adhesive properties of the mortars were studied using the probe tack test. From the measured tack force curves, various adhesive quantities were determined, including adhesion, cohesion, adherence and adhesive failure energy. A comparison between adhesive and rheological properties was presented for all the mixes. The tack properties were generally very different from the shear rheological ones. This indicates the two measurements methods are far to be redundant, but they are rather complementary.

We first presented the influence for cellulosic fibers on the fresh properties of the mortars, including adhesive and rheological properties. It was found that the evolution of these properties versus fiber content was in general non-monotonous, comprising low and high increase regimes. Such behavior was attributed to a probable transition to fiber entanglement and interlocking when increasing fiber content. More investigation, in particular by taking into account the fiber geometry, is needed in order to achieve quantitative interpretation of the tack test results. The adhesive energy was found to be independent on the fiber dosage rate, and decreases with tack velocity. A comparison between adhesive and rheological properties showed that the resistance of the mortars with varying fiber contents was significantly larger in extension than in shear. This was attributed to the difference between the induced orientation of the fibers in extension compared to that in shear.

We then compared the influence on the mortar fresh properties of a cellulose ether based

thickening admixture (Methocel) to that of mineral thickening additive (bentonite). With Methocel addition we observed a marked dependence of the adhesive properties, in particular adhesion strength, on pulling velocity, reflecting the increase of the viscosity due to the polymer. With bentonite addition, the dependence of the adhesion force with respect to pulling velocity was much less significant. On the other hand bentonite increased significantly the cohesion component of the mortar. Similarly, cellulose ether was found to increase the consistency with much less effects on the yield stress, while the clay was found to increase the yield stress but decreases the consistency. This suggests that cellulose-ether and bentonite may play complementary roles in mix-design of mortars.

Different cellulose ethers of type hydroxyethyl methyl cellulose denominated A, B and C with different molecular weights were then considered. The sensitivity of the adhesive properties to the variation of polymer contents increased successively from A, B and C. In case of A, the paste adhesion is almost unchanged with polymer concentration, and significantly increases with the increase of polymer content in case of C. Our tack tests results are in line with the practical fact that the cellulose ether type C is used in adhesive mortars while A and B are used in render mortars. The latter are generally applied with a pumping procedure. The product must have only moderate stickiness in order to obtain high enough pumping rates. Moreover, during the finishing stage the product must present low stickiness to the tool in order to obtain plane surfaces. Some stickiness is however needed in order for the mortar to stay on the substrate on which it is applied. In the case of adhesive mortars high tackiness is not an issue since it is usually applied handily.

The last study was devoted to the influence of a water redispersible powder latex (Vinnapas). The effect of Vinnapas on the fresh properties of the mortar, including adhesive and shear rheological properties was found to be quite small. In particular the effects are much lower than those of high molecular weight cellulose ethers. The main point is that the powder resin seems to have only indirect and minor effects on the fresh properties through increase of air content. Actually latex powders are mainly used to improve mechanical properties of mortars and its adherence to the substrate in the hardened state. Our investigation indicates that the change in mortar properties should be significant only when the latex film is fully formed and spans all the material. This investigation should be completed by considering the evolution of the mortar properties with varying resin content from in the fresh state, through the early age, and in the hardened state.

# *Appendix*



# Fiber-reinforced mortar

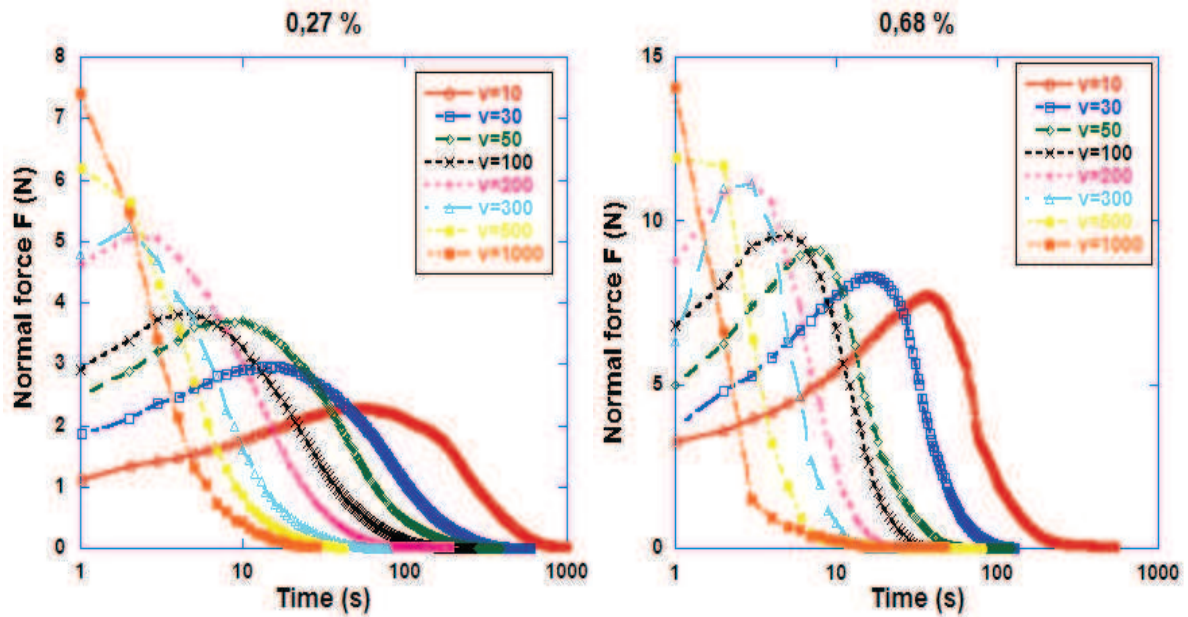


Figure A. 1. Evolution of the stretching force versus time as a function of pulling velocities (in  $\mu\text{m/s}$ ) for different contents of fibers

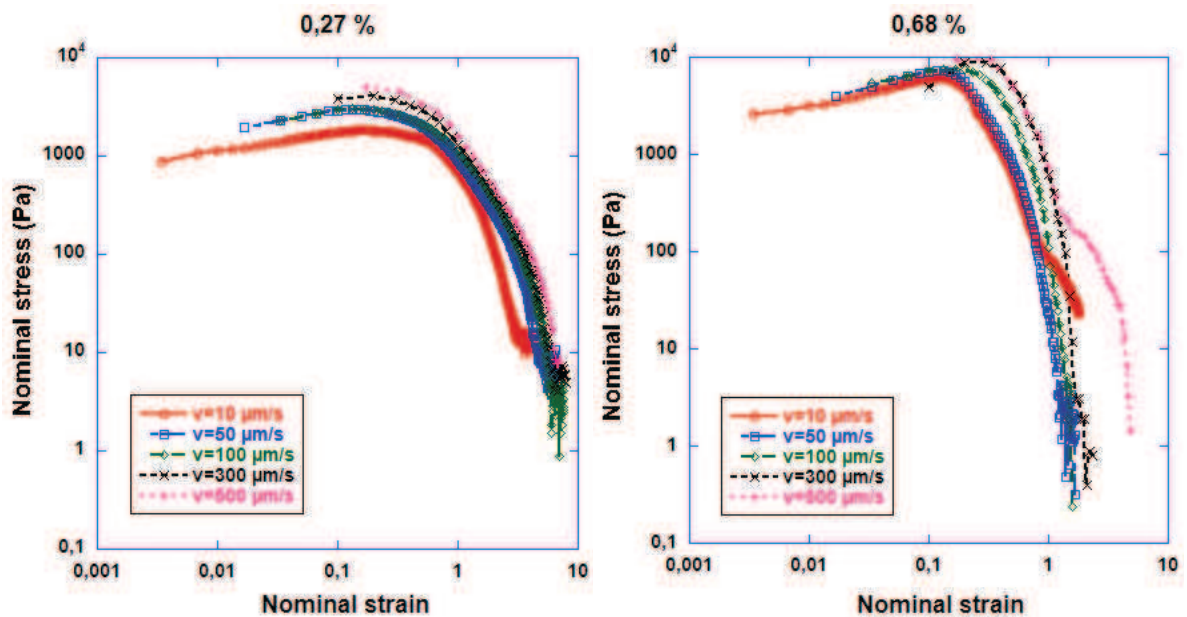


Figure A. 2. Nominal stress versus nominal strain for varying pulling velocity at certain contents of fiber

# Mortar formulated with bentonite

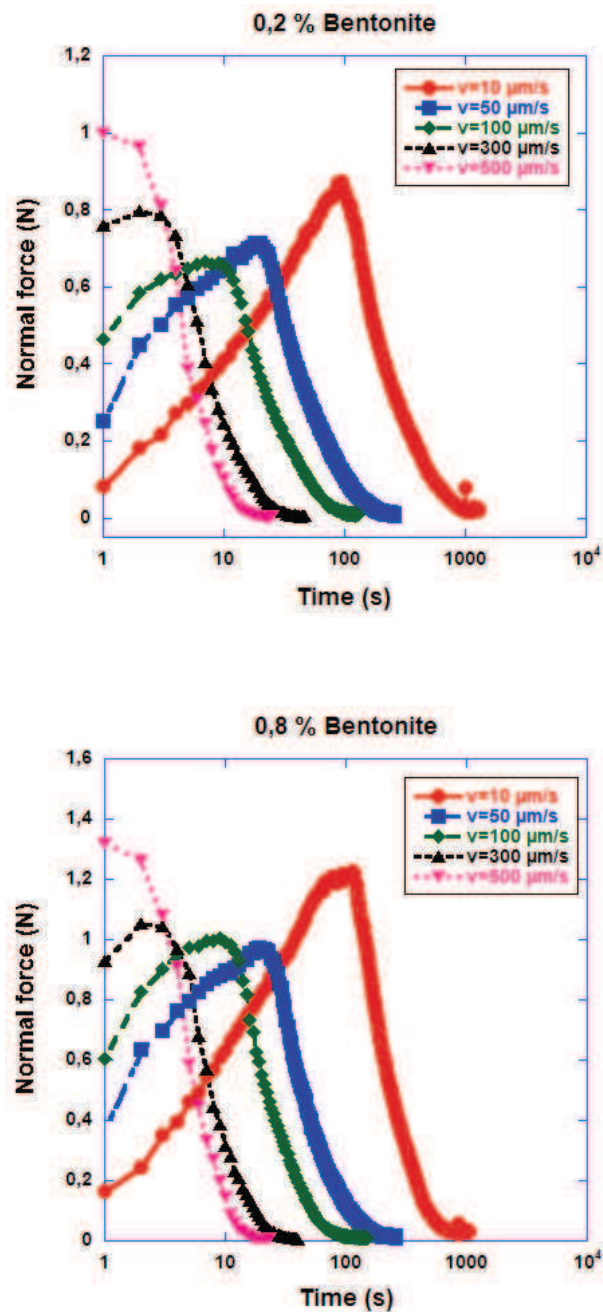


Figure B. 1. Force versus time curves obtained in the Tack test for different bentonite contents

# Mortar formulated with HEMCs

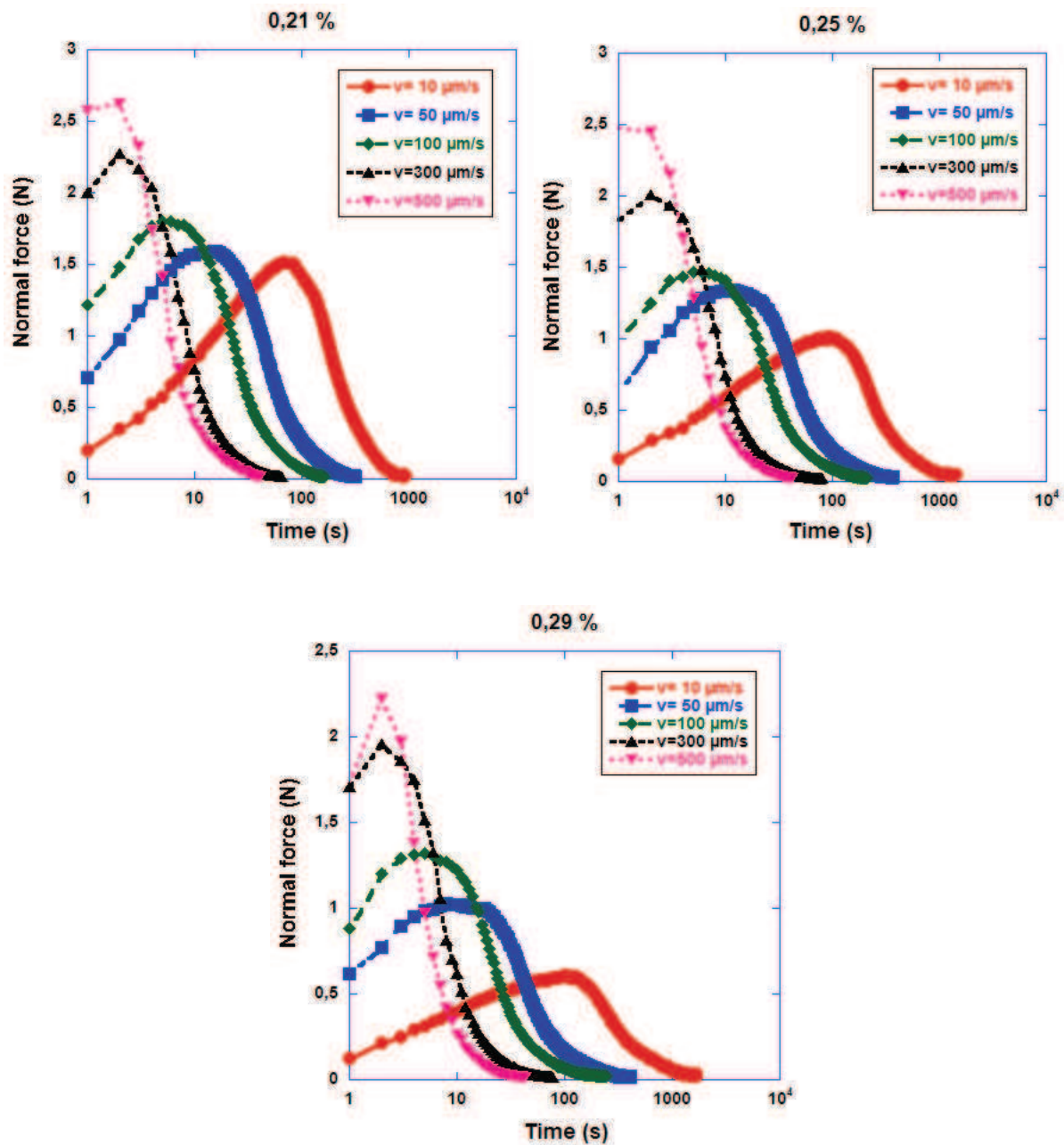


Figure C. 1. Force versus time curves obtained in Probe tack test for different content of A

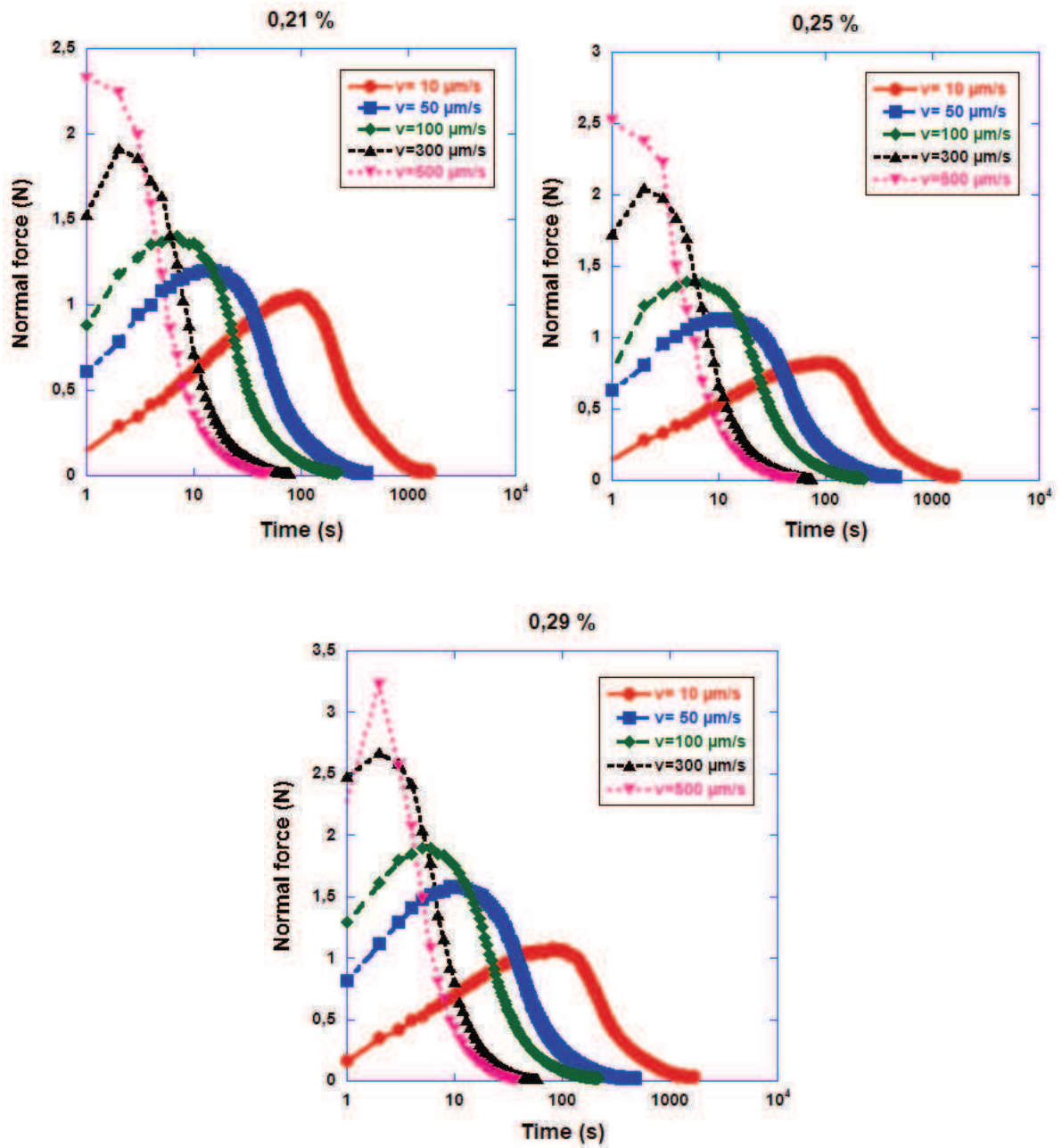


Figure C. 2. Force versus time curves obtained in Probe tack test for different content of B

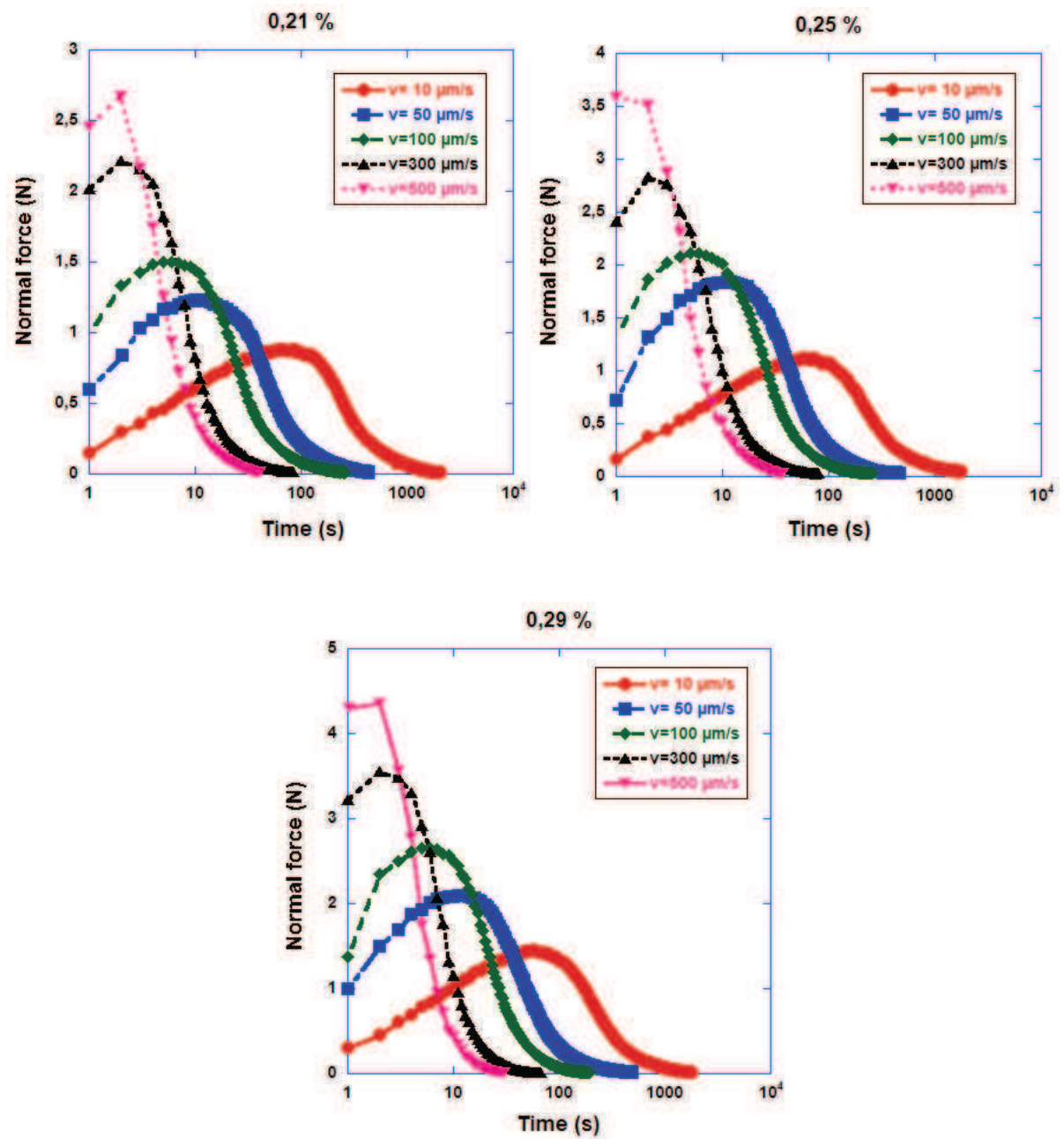


Figure C. 3. Force versus time curves obtained in Probe tack test for different content of C



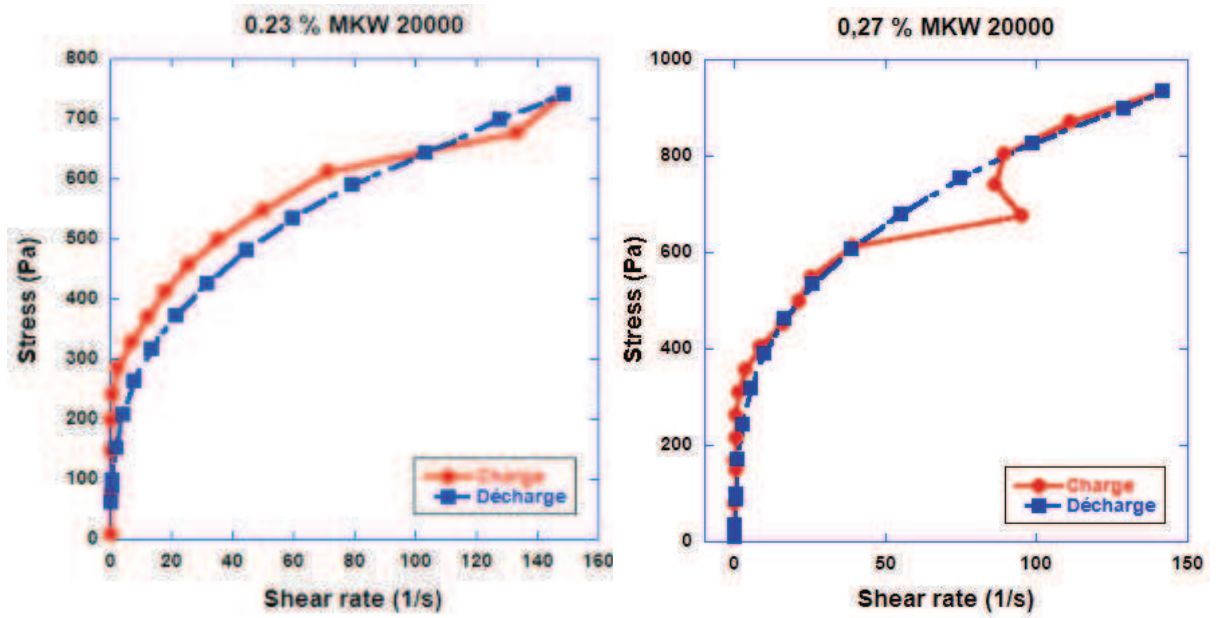


Figure C. 4. Flow curves obtained in rheology measurement with the variation contents of A

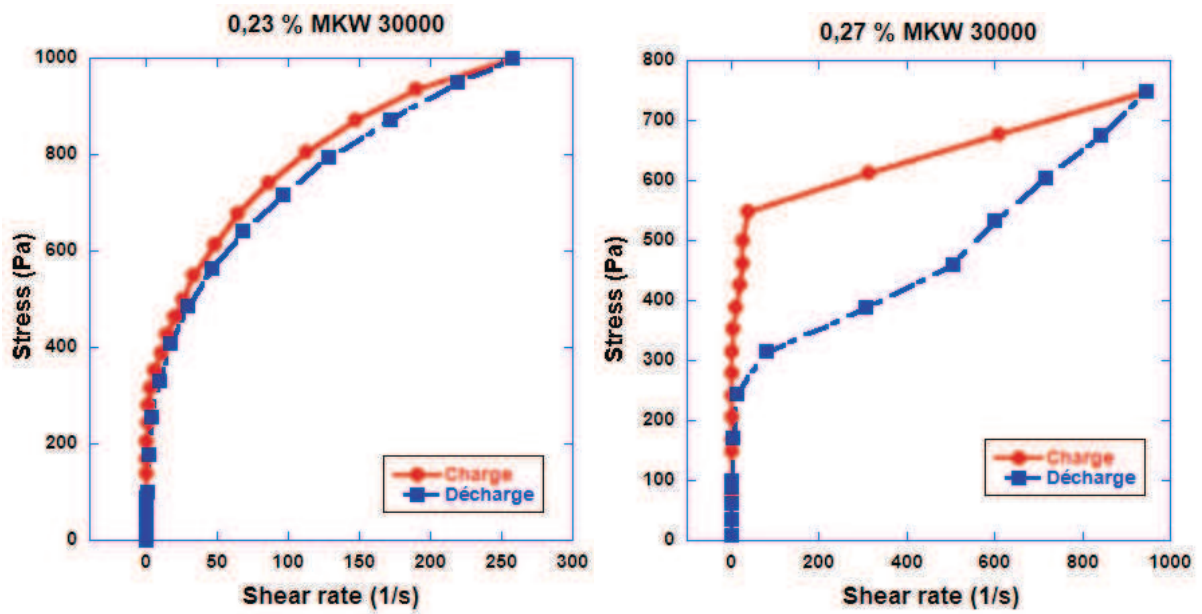


Figure C. 5. Flow curves obtained in rheology measurement with the variation contents of B



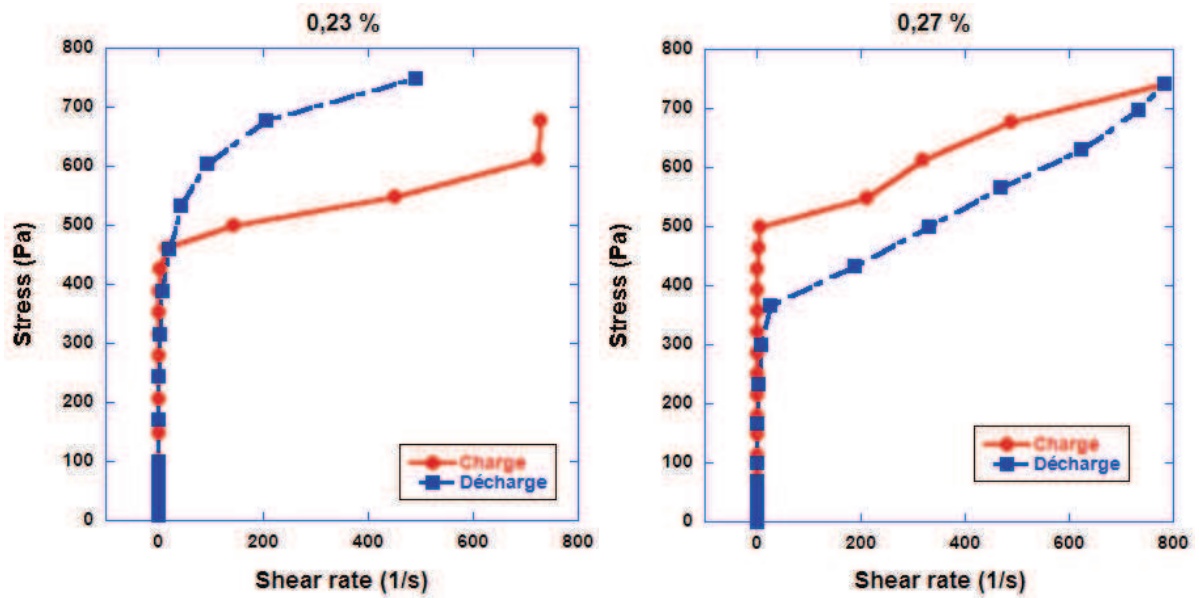


Figure C. 6. Flow curves obtained in rheology measurement with the variation contents of C

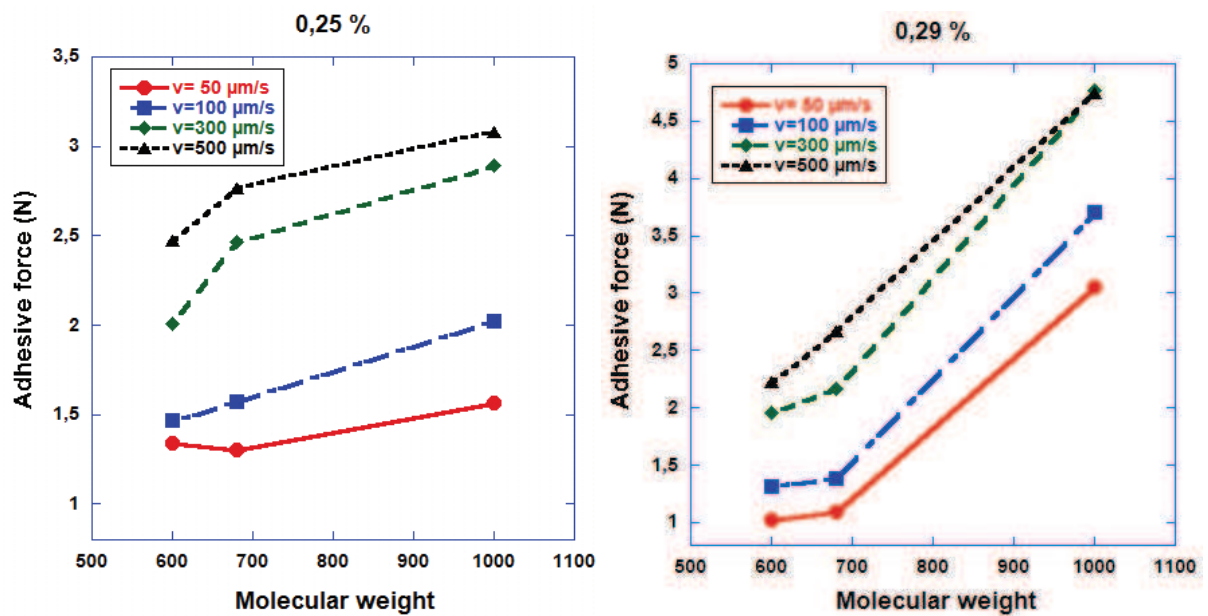


Figure C. 7. Evolution of the adhesive force as a function of molecular weight at high polymer contents for different tack speeds.

# Mortar formulated with Vinnapas

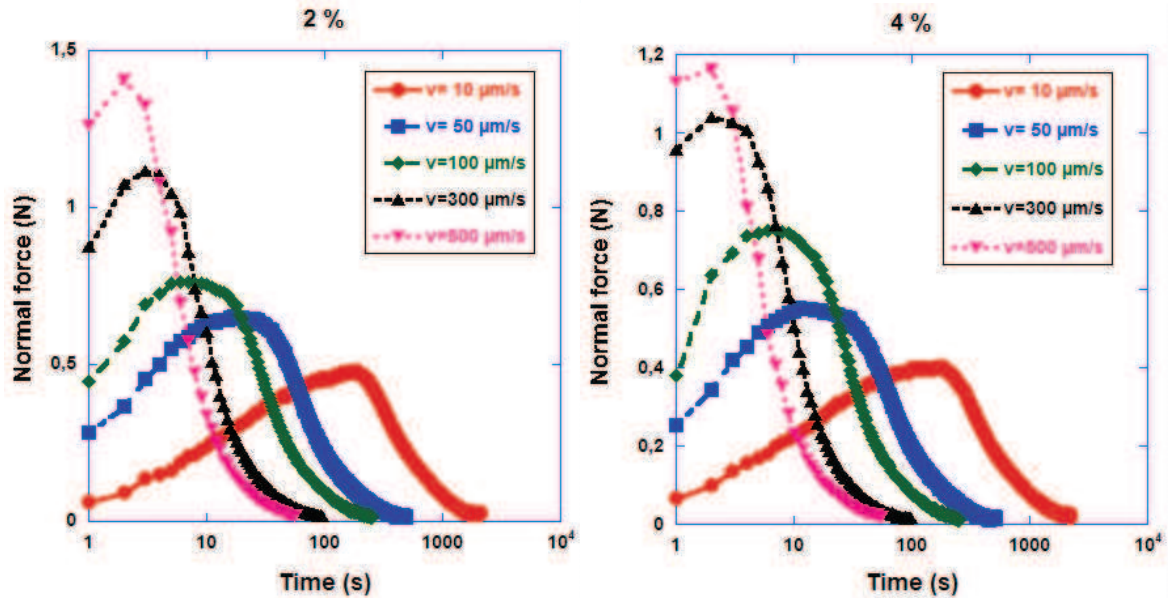


Figure D. 1. Force versus time curves obtained in the Tack test for different contents of Vinnapas

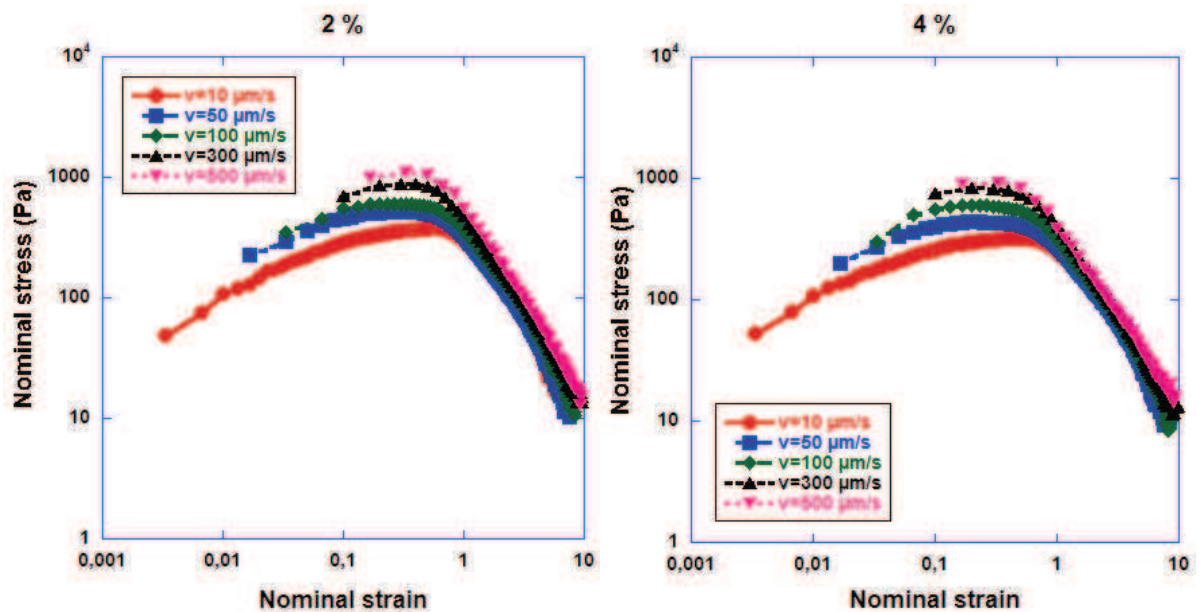


Figure D. 2. Nominal stress vs. nominal strain curves obtained in the Tack test for different Vinnapas content

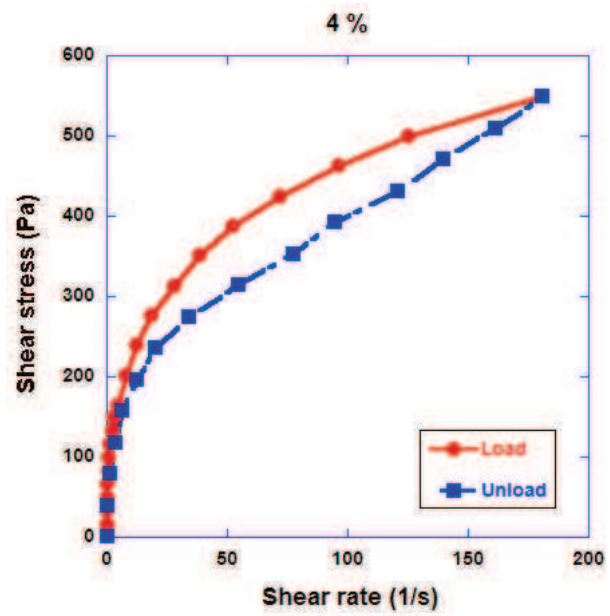
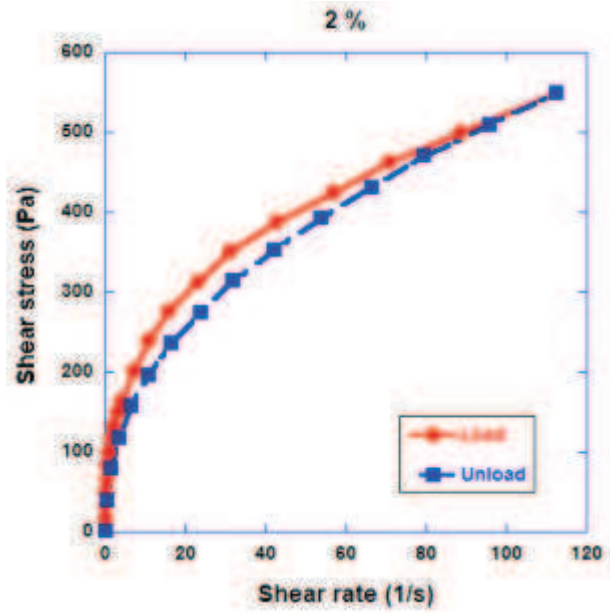


Figure D. 3. Loading and unloading curves of different content of Vinnapas

# References

- [Afridi 2003] M.U.K. Afridi, Ohama Y., K. Demura, M.Z. Iqbal. **Development of polymer films by the coalescence of polymer particles in powdered and aqueous polymer-modified mortars.** *Cement and Concrete Research*, 33:1715-1721,2003
- [Ambroise 1999] J. Ambroise, S. Rols and J. Pera. **Effect of different viscosity agents on the properties of self-leveling concrete.** *Cement and Concrete Research*, 29:261-266,1999
- [Angadi 2010] Angadi S.C., Manieshwar L.S., Aminabhavi T.M. **Interpenetrating polymer network blend microspheres of chitosan and hydroxyethyl cellulose for controlled release of isoniazid.** *International Journal of Biological Macromolecules*, 47(2):171-179, 2010
- [Atzeni 1991] C. Atzeni, A. Marcialis, L. Massidda, U. Sanna. **Mechanical and thermohygroscopic properties of adhesion between PCMs and cement supports.** *Cement and Concrete Research*, 21(2-3):251-256,1991
- [Banfill 1994] P.F.G. Banfill. **Rheological methods for assessing the flow properties of mortar and related materials.** *Construction and Building Materials*, 8(1):43-50, 1994
- [Banfill 2003] P.F.G. Banfill. **The rheology of fresh cement and concrete.** *Paper accepted for publication in Proc 11<sup>th</sup> International Cement Chemistry Congress, Durban, May 2003*
- [Banfill 2006] P.F.G Banfill, G. Starrs, G. Derruau, W.J. McCarter, T.M. Chrisp. **Rheology of low carbon fiber content reinforced cement mortar.** *Cement and Concrete Composites*, 28:773-780,2006
- [Barbosa 1994] Silvia E. Barbosa, Daniel R. Ercoli. **Rheology of short-fiber composites. A systematic approach.** *Composite structures*, 27:83-91,1994
- [Barral 2010] Q. Barral, X. Chateau, J. Boujel, B. Rabideau, G. Ovarlez and P. Coussot. **Adhesion of yield stress fluids.** *The Royal Society of Chemistry*, 6 :1343-1351,2010
- [Batchelor 1970] G. Batchelor. **The stress generated in a non dilute suspension of elongated particles by pure training motion.** *Journal of Fluid Mechanics*, 46:813-829,1970
- [Bauer 2007] E. Bauer, E.A. Guimaraes, J.G.G. de Sousa and F.G.S. Silva. **Study of the laboratory vane test on mortars.** *Building and Environment*, 42(1):86-92, 2007
- [Bayer 2003] Bayer, R., Lutz H. **Dry mortar.** *Ullmann's Encyclopedia of Industrial Chemistry, Sixth Edition 2003 Electronic Release, Wiley-VCH Weinheim, 2003*
- [Bouras 2008] R. Bouras, M. Chaouche, S. Kaci. **Influence of viscosity-modifying**

**admixture on the thixotropic behaviour of cement pastes.** *Applied Rheology*, 18(4):1-8,2008

[Bousmina 1999] A. Ait-Kadi Bousmina M. and J.B. Faisant. **Determination of shear rate and viscosity from batch mixer data.** *Journal of Rheology*, 45:415-433, 1999

[Burgers 1938] J.M. Burgers. **On the motion of small particles of elongated form suspended in a viscous liquid, second report of viscosity and plasticity, chapter 3n** *Amsterdam: north Holland publ.co.* 16(4):113-184,1938

[Chaouche 2001] M. Chaouche, D. Koch. **Rheology of non-brownian rigid fiber suspensions with adhesive contacts.** *Jal of Rheology*, 45:369-382, 2001

[Chaouche 2008] M. Chaouche, Y.O. Mohamed Abdelhay and H. Van Damme. **The tackiness of smectite muds.** *Applied Clay Science*, 42:163-167,2008

[Chen 2010] Rong Chen, Chuanbin Yi, Hong Wu, Shaoyun Guo. **Degradation kinetics and molecular structure development of hydroxyethyl cellulose under the solid state mechanochemical treatment.** *Carbohydrate Polymers*, 81(2):188-195: 2010

[Comyn 1997] John Comyn. **Adhesion science.** 1997

[Cox 1971] R.G. Cox. **The motion of long slender bodies in a viscous liquid, part 2. Shear flow.** *Journal Fluid Mechanics*, 45:625-657,1971

[Creton 1996] C. Creton, L. Leibler. **How does tack depend on time of contact and contact pressure?** *Journal of Polymer Science: Part B: Polymer Physics*, 34:545-554,1996

[Dhonde 2007] H.B. Dhonde, Y.L. Mo, T.T.C. Hsu, J. Vogel. **Fresh and hardened properties of self-consolidating fiber-reinforced concretes.,** *ACT.Mater.J.*,104-M54:491-500,2007

[Diamantonis 2010] N. Diamantonis, M.S. Katsiotis, A. Sakellariou, A. Papathanasiou, V. Kaloidas, J. Marinos and M. Katsioti. **Investigation about the influence of fine additives on the viscosity of cement paste for self-compacting concrete.** *Construction and Building Materials*, 01:1518-1522,2010

[Dinh 1984] Dinh S.M., Armstrong RC. **A rheological equation of state for semi-concentrated fiber suspensions.** *Journal of Rheology*, 28:207-227,1984

[Dzuy 1985] NGUYEN Q. Dzuy and D.V. Boger. **Direct yield stress measurement with the vane method.** *Journal of Rheology*, 29(3):335-347, 1985

[Ferraris 2001] C.F. Ferraris, K.H. Obla and R. Hill: **The influence of mineral admixtures on the rheology of cement paste and concrete.** *Cement and Concrete Research*, 31:245-255,2001

[Glatthor 1994] A. Glatthor, D. Schweizer. **Rheological lab testing of building formulations.** *Construction chemistry*, 1994

[Goncalves 2007] J.P.Goncalves, L.M.Tavares, R.D.Toledo Filho, E.M.R. Fairbairn, E.R.Cunha. **Comparison of natural and manufactured fine aggregates in cement mortars.** *Cement and Concrete Research*, 37, 924-932, 2007.



- [Grim 1978] R.E. Grim, N. Guven. **Bentonites : Geology, mineralogy, properties and uses** (development in sedimentary), Elsevier, 1978
- [Grunewald 2004] S. Grunewald. **Performance-based design of self-compacting fiber reinforced concrete**. *PhD thesis, Section of structural and building engineering. Delf University of Technology, Netherland*, 2004
- [Iso 1996] Yoichi Iso, Donald L. Koch, Claude Cohen. **Orientation in simple shear flow in semi-dilute fiber suspensions. 1. Weakly elastic fluids**. *Journal of Non-Newtonian Fluid Mechanics*, 62:115-134,1996
- [Izaguire 2009] A. Izaguirre, J.I. Alvarez, J. Lanás. **Effect of water-repellent admixtures on the behavior of aerial lime-based mortars**. *Cement and concrete research*, 39(11):1095-1104, 2009
- [Izaguire 2010] A. Izaguire, J.I. Alvarez, J. Lanás: **Ageing of lime mortars with admixtures: Durability and strength assessment**. *Cement and Concrete Research*, 40(7):1081-1095,2010
- [Izaguire 2011] A. Izaguirre, J.I. Alvarez, J. Lanás. **Effect of a polypropylene fiber on the behavior of aerial lime-based mortars**. *Construction and Building Materials*, 25(2):992-1000, 2011
- [Jeffery 1922] F. Jeffery. **The motion of ellipsoidal immersed particles in a viscous fluid**. *Proceeding Royal Society of London*, A102:161-179,1922
- [Jenni 2005] A. Jenni, L. Holzer, R. Zurbiggen, M. Herwegh. **Influence of polymer on microstructure and adhesive strength of cementitious tile adhesive mortars**. *Cement and Concrete Research*, 35(1):35-50, January 2005
- [Jenni 2006] A. Jenni, R. Zurbiggen, L. Holzer, M. Herwegh. **Changes in microstructure and physical properties of polymer-modified mortars during wet storage**. *Cement and Concrete Research*, 36(1), 79-90, 2006
- [Jiang 2011] Y.C. Jiang, X. Wang, P.S. Cheng. **Synthetic and solution behavior of polycaprolactone grafted hydroxyethyl cellulose copolymers**. *International Journal of Biological Macromolecules*, 48(1): 210-214, 2011
- [Kaci 2009] A. Kaci, R. Bouras, M. Chaouche, P-A. Andréani, H. Bouras. **Adhesive and rheological properties of mortar joints**. *Appl. Rheol.*, 19:51-71,2009
- [Kaci 2010] A. Kaci, P-A. Andreani, M. Chaouche. **Influence of bentonite clay on the rheological behavior of fresh mortars**. *Cement and Concrete Research*, 41:373-379, 2010
- [Kaci 2011] A. Kaci, R. Bouras, V.T. Phan, P.A. Andréani, M. Chaouche, H. Brossas. **Adhesive and rheological properties of fresh fiber-reinforced mortars**. *Cement and Concrete Composites*, 33(2), 218-224, 2011.
- [Khayat 1997] K.H. Khayat and Z. Guizani. **Use of the viscosity-modifying admixture to enhance stability of fluid concrete**. *ACI Materials Journal*, 94:332-340,1997
- [Khayat 1998] K.H. Khayat. **Viscosity-enhancing admixtures for cement-based materials**. *Cement and Concrete Composites*, 20:171-188,1998



[Kinloch 1987] A.J. Kinloch. **Adhesion and adhesives: Science and technology.** *Chapman and Hall, London, 1987*

[Klemm 1998] D. Klemm, B. Philipp, T. Heinze, U. Heinze, W. Wagenknecht. **Comprehensive cellulose chemistry.** 1998

[Kuder 2007] Katherine G. Kuder, Nilufer Ozyurt, Edward B. Mu, Surendra P. Shah. **Rheology of fiber reinforced cementitious materials.** *Cement and Concrete Research*, 37:191-199, 2007

[Lachemi 2003] Lachemi, M., Hossain, K.M.A., Nkinamubanzi, P.C. and Bouzoubaa, N., **Performance of new viscosity modifying admixtures in enhancing the rheological properties of cement past.** *Cement and Concrete Research*, 33, 1229-1234, 2003.

[Lachemi 2004] M. Lachemi, K.M.A Houssain and N. Bouzoubaa, V. Lambros P., C. Nkinamubanzi. **Performance of new viscosity modifying admixtures in enhancing the rheological properties behavior of cement pastes.** *Cement and Concrete Research*, 34:185-193, 2004

[Lamure] Alain Lamure. **Adhesion et adherence des materiaux**, [http://www.inp-toulouse.fr/tice/pdf/01extrait\\_at\\_adherence.pdf](http://www.inp-toulouse.fr/tice/pdf/01extrait_at_adherence.pdf). 2007

[Laribi 2005] S. Laribi, J.M. Fleureau, J.L. Grossiord, N. Kbir-Ariguib. **Comparative yield stress determination for pure and interstratified smectite clays.** *Rheologica Acta*, 44:262-269, 2005

[Leeman 2007] A. Leeman and F. Winnefeld. **The effect of viscosity modifying agents on mortar and concrete.** *Cement and Concrete Composites*, 29:341-349, 2007

[Lombois-Burger 2008] H. Lombois-Burger, J.L. Halary, P. Colombet and H. Van Damme. **On the frictional contribution to the viscosity of cement and silica pastes in the presence of adsorbing and non adsorbing polymers.** *Cement and Concrete Research*, 38:1306-1314, 2008

[Maranhao 2011] Flávio L. Maranhão, Kai Loh, Vanderley M. John. **The influence of moisture on the deformability of cement-polymer adhesive mortar.** *Cement and Building Materials*, 25(6), 2948-2954, 2011.

[Martinie 2010] Laetia Martinie, Pierre Rossi, Nicolas Roussel. **Rheology of fiber reinforced cementitious materials: classification and prediction.** *Cement and Concrete Research*, 40:226-234, 2010

[Mason 1951] S.G. Mason, B.J. Trevelyan. **Particle motions in sheared suspension i. rotations.** *J. Colloid Science*, 6:354-367, 1951

[Mason 1957] S.G. Mason, R.St.J. Manley. **Particle motions in sheared suspension: orientations and interactions of rigid rods.** *Proc. R. Soc. London*, A238:117-131, 1957

[Meeten 2002] G.H. Meeten. **Constant-force squeeze flow of soft solids.** *Rheo. Acta.*, 41:557-566, 2002

[Menezes 2010] R.R. Menezes et al. **Use of statistical design to study the influence of cmc on the rheological properties of bentonite dispersion for water-based drilling fluids.**

[Nehdi 2004] M. Nehdi, M.-A. Rahman. **Estimating rheological properties of cement pastes using various rheological models for different test geometry, gap and surface friction.** *Cement and Concrete Research*, 34:1993-2007,2004

[Noh 2005] M.H. Noh, C.K. Park and T.H. Park. **Rheological properties of cementitious materials containing mineral admixtures.** *Cement and Concrete Research*, 35:842-849,2005

[Ohama 1998] Y. Ohama. **Polymer-based admixtures.** *Cement and Concrete Composites*, 20:189-212,1998

[Ozyurt 2007] Nilufer Ozyurt, Thomas O. Mason, Surendra P. Shah. **Correlation of fiber dispersion, rheology and mechanical performance of FRCs.** *Cement and Concrete Composites*, 29:63-158,2007

[Paiva 2009] H. Paiva, L.P. Esteves, P.B. Cachim, V.M. Ferreira. **Rheology and hardened properties of single-coat render mortars with different types of water retaining agents.** *Construction and Building Materials*, 23:1141-1146,2009

[Paiva 2009] H. Paiva, J.A. Labrincha, L.M. Silva and V.M. Ferreira. **Effects of a water-retaining agent on the rheological behavior of a single-coat render mortar.** *Cement and Concrete Research*, 36:1257-1262,2009

[Pareek 1993] S.N Pareek. **Movement in adhesion of polymeric repair and finish materials for reinforced concrete structures.** *Nihon university, College of Engineering, Doctoral thesis*, 1993

[Pareek 1995] S.N. Pareek, Y. Ohama, K. Demura. **Evaluation method for adhesion test results of bonded mortars to concrete substrates by square optimization method.** *Materials Journal*, 92:355-360,1995

[Patural 2011] L. Patural, P. Marchal, A. Govin, P. Grosseau, B. Ruot, O. Devès. **Cellulose ethers influence on water retention and consistency in cement-based mortars.** *Cement and Concrete Research*, 41(1):46-55, 2011

[Percin 2011] Percin I., Saglar E., Yavuz H., Aksoz E., Denizli A. **Poly(hydroxyethyl methacrylate) based affinity cryogel for plasmid dna purification.** *International Journal of Biological Macromolecules*, 48(4):577-582, 2011

[Perez-Pena 1994] M. Perez-Pena, B. Mobasher. **Mechanical properties of fiber reinforced lightweight concrete composites.** *Cement and Concrete Research*, 24:1121-1132,1994

[Petrich 2000] Petrich M.PM, Chaouche M., Koch D.L., Cohen C. **Oscillatory shear alignment of a non-Brownian fiber in a weakly elastic fluid.** *Journal of non-Newtonian Fluid Mechanics*, 9:1-14,2000

[Petrie 1999] C.J.S. Petrie. **The rheology of fiber suspensions.** *Journal of Non-Newtonian Fluid Mechanics*, 87:369-402,1999

[Pourchez 2006] J. Pourchez, A. Peschard, P. Grousseau, R. Guyonnet, B. Guilhot, F. Vallée. **HPMC and HEMC influence on cement hydration.** *Cement and Concrete*

*Research*, 36(2) :288-294,2006

[Ramazani 1997] A. Ramazani, A. Ait-Kadi, M. Grmela . **Rheological modeling of short fiber thermoplastic composites**, *J.Non-Newtonian Fluid Mechanics*, 73:241-260,1997

[Ray 1994] Indrajit Ray, A.P. Gupta, M. Biswas. **Effect of latex and superplasticiser on Portland cement mortar in the fresh state**. *Cement and Concrete Composites*, 16 (4), 309-316, 1994

[Rossi 1992] P. Rossi. **Mechanical behaviors of metal-fiber reinforce concretes**. *Cement and Concrete Composite*, 14(1):3-6,1992

[Said 2006] G.S. Said, F.H.A. Kader, M.M.E. Naggar, B.A. Anees. **Differential scanning calorimetry and dielectric properties of methyl-2-hydroxyethyl cellulose doped with erbium nitrate salt**. *Carbohydrate Polymers*, 65(2):253-262, 2006

[Seabra 2007] M.P. Seabra, J.A. Labrincha, V.M. Ferreira. **Rheological behavior of hydraulic lime-based mortars**. *Journal of the European Ceramic Society*, 27, 1735-1741, 2007.

[Sigh 2003] N.K. Sigh, P.C. Mishra, V.K. Singh, K.K. Narang. **Effect of hyfroxyethyl cellulose and oxalic acid on the properties of cement**. *Cement and Concrete Research*, 33(9):1319-1329, 2003

[Sivrikaya 2011] O. Sivrikaya, A.I. Arol. **Pelletization of magnetite ore with colemanite added organic binders**. *Powder Technology*, 210(1):23-28, 2011

[Song 2005] P.S. Song, S. Hwang, B.C. Sheu. **Strength properties of nylon- and polypropylene-fiber reinforced concretes**. *Cement and Concrete Research*, 35:1546-1550,2005

[Stefan 2005] Stefan, Erkselius, Ola J. Karlsoon. **Free radical degradation of hydroxyethyl cellulose**. *Carbohydrate Polymers*, 62(4):344-356, 2005

[Stokes 2004] J.R. Stokes and J.H. Telford. **Measuring the yield behavior of structured fluids**. *Journal of Non-Newtonian Fluid Mechanics*, 124:137-146, 2004

[Su 1991] Z. Su, JMM.J.M. Bien, J.A. Larbi. **The influence of polymer modification on the adhesion of cement pastes to aggregates**. *Cement and Concrete Research*, 21(5):727-736,1991

[TAinstrument 2011] [tainstrument.co.uk](http://tainstrument.co.uk) **Rheometer AR2000ex descriptions from TA instruments company**, 2011

[Tregger 2010] N.A. Tregger, M.E. Pakula, S.P. Shah. **Influence of clays on the rheology of cement pastes**. *Cement and Concrete Research*, 40:384-391,2010

[Ventola 2011] L. Ventola, M. Vendrell, P. Giraldez, L. Merino. **Traditional organic additives improve old mortars: New old materials for restoration and building natural stone fabrics**. *Construction and Building Materials*, 25(8):3313-3318,2011

[Wang 1990] Youjiang Wang. **Tensile properties of synthetic fiber reinforced mortars**. *Cement and Concrete Composites*, 12:29-40,1990

**[Winnefeld 2012]** Frank Winnefeld, Josef Kaufmann, Erwin Hack, Sandy Harzer, Alexander Wetzel, Roger Zurbriggen. **Moisture induced length changes of tile adhesive mortars and their impact on adhesion strength**, *Construction and Building Materials*, 30, 426-438, 2012

**[Zosel 1985]** A. Zosel. **Adhesion and tack of polymers: influence of mechanical properties and surface tensions**. *Colloid and Polymer Science*, 263:541-553, 1985